GEORGIA INSTITUTE OF TECHNOLOGY
OFFICE OF RESEARCH ADMINISTRATION

RESEARCH PROJECT INITIATION

Date: June 6, 1972

Project Title: Combustion Generated Noise in Turbopropulsion Systems

Project No: E-16-624

Principal Investigator: Dr. Warren C. Strahle

Sponsor: Air Force Office of Scientific Research; Arlington, Virginia

Agreement Period: From June 1, 1972 Until May 31, 1973

Type Agreement: Grant No. AFOSR-72-2365

Amount: $24,200.00 AFOSR Funds (E-16-624)
3,150.00 GIT Contribution (E-16-324)
$27,350.00 Total

Reports Required: Final Scientific Report; Interim (Annual) Report if extended beyond one year.

Sponsor Contact Person (s):

Technical Matters
Bernard T. Wolfson
Program Manager
AFOSR (NAE)
1400 Wilson Boulevard
Arlington, Va. 22209

Contractual Matters
(Via O.R.A.)
Marvin L. Roberts
Contracting Officer
AFOSR (PMD)
1400 Wilson Boulevard
Arlington, Va. 22209

Assigned to: School of Aerospace Engineering

COPIES TO:

- Principal Investigator
- School Director
- Dean of the College
- Director, Research Administration
- Director, Financial Affairs (2)
- Security-Reports-Property Office
- Patent Coordinator
- Library
- Rich Electronic Computer Center
- Photographic Laboratory
- Project File
- Other

RA-3 (6-71)

GEORGIA INSTITUTE OF TECHNOLOGY
OFFICE OF CONTRACT ADMINISTRATION

SPONSORED PROJECT TERMINATION

Date: August 18, 1976

Project Title: Combustion Generated Noise in Turbopropulsion System

Project No: E-16-624

Cont. A FOSR-72-2365

Project Director: Dr. W. C. Strahle

Sponsor: Air Force Office of Scientific Research

Effective Termination Date: 5/31/75

Clearance of Accounting Charges: all clear

Grant/Contract Closeout Actions Remaining:

- _ Final Invoice and Closing Documents
- x Final Fiscal Report
- _ Final Report of Inventions
- _ Govt. Property Inventory & Related Certificate
- _ Classified Material Certificate
- _ Other _____

Assigned to: Aerospace Engineering (School/Laboratory)

COPIES TO:

Project Director
Division Chief (EES)
School/Laboratory Director
Dean/Director–EES
Accounting Office
Procurement Office
Security Coordinator (OCA) ✓
Reports Coordinator (OCA)
Library, Technical Reports Section
Office of Computing Services
Director, Physical Plant
EES Information Office
Project File (OCA)
Project Code (GTRI)
Other _____

CA–4 (3/76)

COMBUSTION GENERATED NOISE IN TURBOPROPULSION SYSTEMS

Interim Technical Report

for

Air Force Office of Scientific Research

Grant No. AFOSR-72-2365

July 24,1973

Prepared by:

B. N. Shivashankara

J. C. Handley

Approved by:

W. C. Strahle
Principal Investigator

School of Aerospace Engineering
Georgia Institute of Technology

ABSTRACT

Experiments on noise radiation by open turbulent premixed flames are described. Detailed directionality distributions, scaling rules for acoustic power radiated, thermo-acoustic efficiency and spectral content are presented and discussed. Scaling rules for reacting volume are generated by a direct flame photography technique. These experiments are shown to be quite useful in decomposing combustion noise scaling laws. The acoustic power is shown to scale as $U^{2.7}\ D^{2.8}\ S_L^{1.4}\ F^{0.4}$, and combustion noise spectra peak in the 250-700 Hz range. The directionality is quite weak for noise from open turbulent flames. The experimental results are critically examined in the light of the theoretical predictions from Strahle's theory of combustion noise.

TABLE OF CONTENTS

LIST OF TABLES

LIST OF ILLUSTRATIONS

Figure Page

SUMMARY

Combustion noise has been recognized as a possible major contributor to the overall noise from aircraft turbopropulsion systems and industrial furnaces. A review of the literature shows that combustion noise generation is little understood. All the theoretical analyses have been inadequate due to lack of clear understanding of the mechanism of the turbulent combustion process itself. The body of experimental data available does not cover the range of flow velocities typical of turbopropulsion systems. Further, in most cases, scaling laws for acoustic power radiated have been based on the assumption of spherically symmetric noise emission, although, combustion noise is known to be weakly directional.

This report describes experiments conducted on open turbulent premixed flames designed to overcome the above shortcomings. A simple burner configuration is used to enable rational interpretation of the experimental results and thus provide useful information toward a systematic approach to noise reduction problems.

Experiments are conducted in an anechoic chamber on pilot-flame stabilized, turbulent flames at the end of burner tubes of diameters 0.402" - 0.96". Flow velocities up to 600 ft/sec and fuels propane, propylene, and ethylene with air as the oxidizer are employed. Mixture ratios ranging from fuel lean to stoichiometric are used. The study of noise generation is done primarily through acoustic measurements where scaling laws for acoustic power radiated, thermo-acoustic efficiency, spectral content and directionality are deduced from sound pressure

measurements made by an array of condenser microphones. The acoustic experiments are supplemented by the scaling laws on reacting volume generated by a direct flame photography method.

Combustion noise is shown to be weakly directional. Comparison with Strahle's theory shows refraction of sound at temperature discontinuities to be the possible explanation of the directionality results. The spectra of combustion noise show a broad band noise radiation with a single peak in the 250-700 Hz frequency range. The scaling law for peak frequency is obtained in the form $f_c \propto U^{0.18} D^{0.08} S_L^{0.53} F^{-0.69}$ where U is the flow velocity, D is the burner diameter, S_L is the laminar flame speed and F is the fuel mass fraction.

Acoustic power radiated is shown to scale as $P \propto U^{2.7} D^{2.8} S_L^{1.4} F^{0.4}$. Errors involved in obtaining the scaling law are discussed. A thermo-acoustic efficiency as high as 10^{-6} is observed for the 600 ft/sec flame, indicating that noise generation from high speed flames can be appreciable.

Detailed scaling laws on flame volume obtained by a direct flame photography method are shown to be quite useful in decomposing combustion noise scaling laws. Flame volume studies show that turbulence structure in the flame is primarily decided by the pipe flow process and not by the flame. The results of the overall program are compared with existing theories and other experimental results. The comparisons with Strahle's theory show that the theoretical solution of the noise problem is reasonable but that some of the order of magnitude estimates need modification before satisfactory scaling laws can be obtained from the theory.

CHAPTER I

INTRODUCTION

General

"Noise is unwanted sound." Noise produces annoyance, decreases efficiency and can impair hearing. With increasing population density around airports and military airfields, aircraft noise has become a problem of primary concern. The problem is further enhanced by the expected increases in both number and size of aircraft in military as well as commercial applications.

It is a well known fact that turbulent combustion generates noise and that most of the combustion processes in practice are turbulent. A substantial portion of the noise, in aircraft using turbo-propulsion systems, could be due to combustion in primary combustors and afterburners. In the case of afterburning turbojets and turbofans a substantial portion of the basic engine noise could originate from the afterburner combustion process, and for "quiet" lifting fans a large contributor to the noise could be the primary gas turbine combustors. In industrial furnaces combustion roar is a primary source of noise.

Noise suppression could be achieved either at the source or by some treatment of the medium separating the source and the environment. The merits of decreasing the noise at the source are easily recognized. In order to attempt reduction of combustion noise at its source a detailed study of the mechanism of noise generation is essential. Also, radiation characteristics from the source would be essential to devise methods to control the noise by the use of acoustic baffles and sound absorbent

liners.

Literature Review

The subject of combustion noise has received very little attention in the literature. The mechanisms of generation and radiation have not been understood to any appreciable extent. Although combustion generated noise itself is nothing new, the study of it is of a recent nature.

At the outset, it can be seen that all the theoretical studies were restricted by the lack of a clear understanding of the mechanism of turbulent combustion. On the experimental side, a serious limitation has been noticed as regards acoustic power calculations. Except in a very few cases, the scaling laws for acoustic power radiated were obtained from a single microphone sound pressure measurement and the assumption of spherical symmetry. This could lead to incorrect power scaling laws since the combustion noise, in almost all the experiments, was found to be directional, although weakly so. Also, a substantial amount of experimental data available in the literature is for particular burner configurations, thus tending to make the task of deriving general scaling rules almost impossible.

In a theoretical study of the interaction of a free flame with a turbulence field Tucker[1] showed that appreciable noise generation could result in the region of interaction. He also showed that the intensity of noise generated would be a strong function of the laminar flame speed. No expression for acoustic power radiated was derived in this work.

Bragg[2] developed a theory based on the wrinkled flame concept of turbulent flames. The theory predicted the mechanism of turbulent com-

bustion noise generation to be due to a distribution of monopole-like sources in the reaction zone. Thermo-acoustic efficiency, a measure of the total energy of the flame converted into acoustic radiation, was shown to vary as the square of the flow velocity.

At about the same time, Smith and Kilham[3] presented experimental data on noise produced by open premixed turbulent flames. The burner sizes varied from $\frac{1}{4}$" to $\frac{1}{2}$" in diameter with flow velocities up to 350 ft/sec. Gaseous fuels ethylene, methane, propane, and propylene were used with air as the oxidizer. It was observed that the acoustic power radiated was proportional to $(UDS_L)^2$ where U is the flow velocity, D the burner diameter and S_L the laminar flame speed. A more detailed work[4] showed that the scaling with S_L could vary between 0.6 and 3.4 while the scaling with respect to D and U was quite precise. However, except for scaling with respect to U, the scaling laws were inferred from sound pressures measured at the 90° microphone. The results of the experiments for directionality showed that the noise generated was weakly directional ($\sim$ 3 db) and that the directionality pattern systematically changed with the flow velocity. The maximum sound pressure was found to occur at angles of 50° to 80° to the flow direction.

Smith and Kilham observed the combustion noise to be a broad band noise with a single peak in the range of 250-500 Hz. The peak frequency, in general, was found to increase with the flow velocity. The rate of increase with velocity, however, was different for different fuels. The thermo-acoustic efficiency, the ratio of acoustic power radiated to the total energy per unit time released by combustion, varied between 10^{-8} and 10^{-7} (thermal inputs of 1-7 kw) and was found to increase linearly

with flow velocity. Since ethylene flames showed higher efficiencies almost twice those for propylene, it was concluded that fuels with higher S_L were more efficient sound generators.

A study of the noise of diffusion flames was reported by Kotake and Hatta[5]. Based on an analysis using the conservation equations and upon examination of diffusion flames structure an acoustic model containing a distribution of monopole and dipole sources in the reaction zone was postulated. The theoretical analysis would allow an acoustic power scaling of U^2D^3 in low velocity flames and a scaling of U^4D^3 in high velocity flames. Experiments conducted with equivalence ratios of 1, 2, and 3, over a rather narrow velocity range of 9 m/sec to 23 m/sec, were shown to substantiate both the scaling laws. The frequency spectra were flat at lower frequencies and dropped off at higher frequencies. These frequency spectra were quite unlike the spectra reported by other investigators which always exhibited a recognizable peak and amplitude fall off on both sides of the peak frequency. Once again, scaling rules depended on the measurements at a single microphone location. No details are available as to the acoustic environment for these experiments. The burner sizes were 6.8 mm to 21.8 mm. The flames were stabilized at the end of convergent nozzles in contrast with those of Reference 3 where fully developed pipe flow existed at the burner exit.

Bolinger *et al*[6] could recognize the presence of combustion noise in rocket motor exhaust noise when operating fuel rich. They experimented upon a 500 lb-thrust RP1-LOX motor and noticed a predominant component of noise in the low frequency range ($\sim$ 500 Hz) when the rocket motor was

fired with excess fuel. The authors concluded that the combustion of the unburned fuel in the atmosphere outside the nozzle is the most likely source of this noise.

An entirely new line of approach to the study of combustion noise resulted due to the experiments of Thomas et al[7]. They found a one to one correspondence between the instantaneous rate of change of the radius of the flame front and the pressure for spark ignited combustible gases contained in spherical soap bubbles. Hurle et al[8] showed that the rate of change of emission intensity of CH and C_2 radicals in the reaction zone can be used to derive the instantaneous sound pressure generated by the flame for the spherically expanding flame fronts as well as for open turbulent flames. Such a correlation implies a direct relation between the sound pressure and the volume integral of the first time derivative of the global reaction rate. A good correlation was obtained in Reference 8 when the bandwidth of the signals was limited to 50 Hz-1kHz. Due to increased noise in the optical system, correlation was poor when higher frequencies were included. In the computation of the frequency spectrum from the optical measurements the signal to noise ratio was very low and hence the comparison between the optically and acoustically obtained spectra should be viewed with reservations. Hurle et al concluded that the mechanism of combustion noise conforms to the monopole behavior.

The work of Hurle et al was extended by Price et al[9] to include diffusion flames and liquid spray combustion. A good correlation between the first time derivative of the emission intensity of the C_2 radical and the instantaneous sound pressure was demonstrated in all these cases of turbulent combustion. The only limitation to this technique was that

there should be no continuum radiation in the flame. The acoustic radiation from premixed, diffusion and liquid spray combustion was shown by this study to conform to a monopole source distribution. Experiments using turbulence grids showed that both r.m.s. sound pressures and r.m.s. values of the time derivative of the emission intensity increase with turbulence intensity.

Smithson and Foster[10], in a short paper, reported a thermo-acoustic efficiency variation with U^2 for a Meker burner using town's gas. Flow rates of town's gas varied from 0.092 to 0.12 litres/sec with air/gas ratios from 1 to 6. The microphone distance quoted would be in the near field for laboratory Meker burners (1 to 2 cm in diameter) and hence the scaling rules may be in error. The lowest value of acoustic efficiency ($\sim 3 \times 10^{-9}$) was reported by Powell[11] for a gasoline vapor primus stove flame. The burner size was about 0.2" in diameter. The frequency peaked in the 300-600 Hz range.

Giammar and Putnam[12] have studied the noise generated by pure diffusion flames. Two burner configurations, axially impinging jets and an "octopus" burner, were used. Flow rates were as high as 12 SCFM in the case of the octopus burner. The only drawback of this extensive body of data on pure diffusion flames is the complicated burner configuration. Sound power scaled with firing rate to an exponent of 1 to 2; a thermo-acoustic efficiency as high as 6×10^{-7} was obtained for the impinging jets. In all the experiments the peak frequency was found to be in the range 300-500 Hz. In a recent paper[13], Giammar and Putnam have presented the results of some experiments on premixed fuel rich flames on commercial burners of sizes $1\frac{1}{4}$", $1\frac{1}{2}$" and 2". Heat inputs were of the order of 0.25

to 0.69 million BTU/hr (75-200 kw). Both single burners and burners in pairs showed that sound power varies, in general, as the square of the firing rate. The experimental data showed a tendency to follow an exponent slightly lower than 2.

Further experiments on diffusion flames were reported by Knott[14]. Hydrogen and ethylene were burned with air and oxygen. Co-flowing jets and impinging jets configurations were studied. A volume of experimental data has been presented but in a manner very difficult to interpret. Flow velocities were 250 fps to 1000 fps. The thermo-acoustic efficiency was found to be in the range 10^{-8} - 10^{-5} and it varied as $\dot{m}_f$ for co-flowing jets, $1/\dot{m}_f$ for impinging jets and as $\dot{m}_f^3$ for the premixed case. Here, $\dot{m}_f$ is the mass flux of fuel. The highest value of thermo-acoustic efficiency of 2×10^{-5} was reported for the ethylene-oxygen flame. The hydrogen-oxygen system had a cold flow peak frequency of 6000 Hz and the corresponding combustion noise peaked around 2000-4000 Hz. For the ethylene-air system (Re. No. 50,000) the combustion noise had a peak in the 600-900 Hz frequency range. The burner sizes for co-flowing jets were 1.835 cm diameter for the outer tube and 0.813 cm and 0.391 cm for the inner tube. For the impinging jet burner both the tubes had the same diameter, 1.303 cm, 0.8079 cm or 0.4981 cm.

Seebold[15] has reported noise data obtained from a full scale test furnace as well as from process plant furnaces. The heat release varied from 1-10 million BTU/hr. The corresponding fuel flow rates would be roughly 10-100 SCFM. Power output was found to scale with the square of the heat release. The frequency spectra were found to peak in the 125-500 Hz range.

The three papers by Strahle[16,17,18] perhaps form the most extensive theoretical analysis on combustion noise. A rather detailed description of this work is given here because of the particular significance of the prediction from Strahle's theory of combustion noise to the experimental program described in this report.

Following the classical method of Lighthill[19,20] in his work on aerodynamic noise, Strahle's theory starts with (Reference 16)

$$\rho_{tt} - a_o^2 \rho_{x_i x_i} = F_s \tag{1}$$

as the wave equation describing the noise generated from a region undergoing turbulent fluctuations. Physical arguments were presented to show that the appropriate source term F_s for the case of combustion noise is given by $-a_o^2 \rho_{T_{x_i x_i}}$. With this source term the solution to the wave equation was shown to be

$$\rho = \frac{1}{4\pi a_o^2 r} \frac{\partial^2}{\partial t^2} \int_V \rho_{T_t} \left(\underset{\sim}{r}_o, t - \frac{r}{a_o}\right) dV \left(\underset{\sim}{r}_o\right) \tag{2}$$

where V corresponds to the volume undergoing turbulent combustion where ρ is dominated by turbulent fluctuations and not by the acoustics. Further developments of the solution gave the important result (Reference 17)

$$\rho = \frac{\gamma - 1}{\gamma} \frac{H\bar{\rho}_1}{4\pi \bar{a}_o r \bar{p}} \int_V \omega_t \left(\underset{\sim}{\gamma}_o, t - \frac{\gamma}{c_o}\right) dV \left(\underset{\sim}{\gamma}_o\right) \tag{3}$$

where ω_t is the time derivative of the global reaction rate. This showed that regardless of the turbulence structure and whether or not the flame is of premixed or of diffusion type, the far field acoustic density (or pressure) is proportional to the volume integral over the reacting volume V of the time derivative of the global reaction rate. With this result Strahle's theory could explain the one to one correspondence established between the optical and acoustic emissions by the experiments of References 8 and 9.

In Reference 17, considering the particular case of premixed, fuel lean flames, an expression was developed for the acoustic power P radiated from a region undergoing turbulent combustion in the form

$$P = \frac{(\Delta\rho/\rho_o)^2}{\bar{\rho}_o \bar{a}_o 4\pi F^2} \int_V dV\,(\underset{\sim}{r}_o) \int_{V_d} C(\underset{\sim}{r}_o, \underset{\sim}{d})\, dV\,(\underset{\sim}{d}) \qquad (4)$$

where $\Delta\rho$ represented the density change across the flame, F the fuel mass fraction, C an autocorrelation of the time derivative of the reaction rate, V the reacting volume and V_d a correlation volume.

Strahle has shown that scaling laws for acoustic power can be obtained from the above equation by making order of magnitude estimates for the quantities involved. Since the order of magnitude estimates would very heavily depend on the model of turbulent combustion used in Reference 17 the scaling laws were deduced for three possible phenomenological models of turbulent combustion, namely, a) wrinkled flame, b) slow distributed reaction and c) fast distributed reaction. A similar analysis

was made in Reference 18 for the scaling laws for diffusion flames. Strahle's theory recognized flow velocity U, laminar flame speed S_L, burner dimension D, fuel mass fraction F, scale of turbulence ℓ_t, and intensity of turbulence $\mathcal{I}$ as the important parameters in the study of combustion noise. Further, it was predicted that acoustic power radiated could be expressed by a law of the type

$$P = K\, U^{a_1}\, S_L^{a_2}\, F^{a_3}\, D^{a_4}\, \ell_t^{a_5}\, \mathcal{I}^{a_6} \tag{5}$$

where the prefactor K and the exponents $a_1, \ldots, a_6$ are constants. Reference 18 studied the effects of convection and refraction on the directionality of combustion noise and showed that the observed directionality of combustion noise could be explained qualitatively by these effects but the quantitative agreement with existing experiments is poor.

Kushida and Rupe[21], in an investigation of the effect on supersonic jet noise of nozzle plenum pressure fluctuations, observed that pressure fluctuations in the plenum chamber of a supersonic nozzle can strongly increase the noise radiated from the jet plume. Since some appreciable pressure fluctuations do exist in turbojet engines, the authors conclude that the reduction or elimination of plenum chamber pressure fluctuations may be an important method of reducing the total noise from jet engines.

A similar result was obtained by Abdelhamid *et al*[22]. They found a good cross correlation between the pressure oscillations in the combustor and the far field sound pressure. A 3-inch combustor with a 2-inch nozzle was used in this study. The major conclusion reached was that a large

portion of the far field noise due to jet aircraft could be from the combustors.

The literature survey leads to the following conclusions:

1. Combustion noise exists as an identifiable phenomenon in many practical systems.

2. In almost all the configurations, combustion noise occupies the lower range of the frequency spectrum; a typical range is between 150-500 Hz.

3. The acoustic power radiated is found to scale with U to an exponent between 1 and 4, with D to an exponent between 2 and 3 and with S_L to an exponent between 0.6 and 3.4. This represents a very wide variation in the scaling rules, thus making them virtually useless. Furthermore, many of the power scalings in the literature were based on single microphone measurements and the assumption of spherical symmetry. This could give misleading results because of the weak directionality of the combustion noise. Also, only a few of the reported experiments were conducted in an anechoic enclosure. Finally, the choice of independent variables with which to derive scaling laws has been insufficient.

4. Very little work has been done on the directionality of the acoustic radiation. A systematic correlation of the spectral content with the flow variables and the chemistry has not been attempted in any of the existing experimental results.

5. The theories of References 16, 17 and 18 can, with experimental support and verification at various stages of the theoretical solution, yield useful scaling rules for the acoustic power, spectral content and directionality of the combustion generated noise.

6. Without firm scaling laws it is impossible at this point to quan-

titatively estimate the true importance of combustion noise to the total turbopropulsion noise problem.

Objectives of Research

The literature survey points out a need for further experimentation in the area of combustion noise. The experimental results, in order to be applicable to turbopropulsion systems of aircraft, should be obtained at velocities comparable to those found in afterburners ($\approx$ 600 ft/sec). Also, in order to get a true indication of the acoustic radiation from the flames all the experiments should be conducted in an anechoic chamber so that free field conditions can be closely approximated. The sound pressures should be measured at various azimuthal positions around the flame and then integrated for power radiated. A detailed directionality study should be made. The scaling laws for spectral content should be generated.

The objectives of the experimental program were decided by the needs expressed above. However, only the case of open turbulent flames would be considered because of the simplicity of the burner configuration. The objectives can be listed as follows:

1. to conduct noise experiments on three burners in an anechoic chamber to flow velocities of 600 ft/sec using both fuel lean and fuel rich mixtures. These experiments will be called "Acoustic Experiments" and are designed to yield scaling laws for acoustic power, thermoacoustic efficiency, and spectral content. Detailed directionality information will also be obtained.
2. to analyze the scaling rules for the volume of the reaction zone.

These experiments will be entitled "Direct Flame Photography" since direct flame photography techniques will be employed in reducing the scaling laws. The analysis of the reacting volume will provide an independent diagnostic check for Strahle's theory of combustion noise.

3. to compare the experimental findings with the theories of References 15, 16 and 17, and

4. to present the results of the investigation in a form useful to the practicing engineers.

Thus, it is believed that this study would lead to a better understanding of the mechanism of generation of combustion noise and provide useful scaling rules for the noise generated by open turbulent flames.

CHAPTER II

ACOUSTIC EXPERIMENTS

The experiments conducted, to determine the scaling rules for acoustic power, thermo-acoustic efficiency, spectral content and directionality of combustion noise generated by open turbulent flames established at the end of burner tubes, are described in this chapter. The measurements are made in the far field since near field information would be too complicated by the phase relationships to be of any real value. Also, theories exist, e.g., References 16, 17 and 18, which enable a study of the mechanism of noise generation based on experimental far field information. In addition, the far field measurements are of practical significance in evaluating the noise radiation from sources.

Based on an analysis of the literature, the parameters that affect the noise generation from turbulent flames can be recognized as: U, the flow velocity, D, the burner size, S_L, the laminar flame speed, F, the fuel mass fraction, ℓ_t, the scale of turbulence, and $\mathcal{I}$, the intensity of turbulence. In this chapter only U, D, S_L and F are considered since no effort is made to devise methods to vary the turbulence intensity independently. The experiments are designed so that only one parameter is varied at a time. However, S_L and F can not be varied independently of each other using the same fuel, but combinations of mixture ratios and fuel can be worked out so as to vary either S_L or F independent of the other. Since the scaling rules sought for can be obtained by regression

analysis even when both the parameters vary at the same time, equivalence ratio ϕ was used as one of the parameters. Equivalence ratio is defined as the ratio of $(\text{fuel/air})_{\text{actual}}$ to $(\text{fuel/air})_{\text{stoichiometric}}$. In order to identify the various tests conducted the following notation is used.

P	—	100	—	0.8	—	1
Fuel						Burner Diameter
P = Propane		Flow Velocity In Ft/Sec		Equivalence Ratio		1 = 0.402"
E = Ethylene						2 = 0.652"
Py = Propylene						3 = 0.96"

In this report results of only premixed flames are presented.

Anechoic Chamber

A 13' x 10' x 6' - 6" (working space) anechoic chamber was built in the Aerospace Propulsion Laboratory in order that acoustic measurements be made in conditions close to free field. The chamber would also serve the secondary purpose of preventing drafts around the flame. Figures 1(a) and (b) show the basic construction details of the anechoic chamber. The two walls of the room formed two outer walls of the chamber. The other two walls were constructed with 8" dry gypsum wall stuffed with fiberglas. The basic acoustic insulation was provided by 18" thick fiberglas and a 3" air space between the walls and the fiberglas insulation. The density of fiberglas used was roughly 0.6 lb/cft. The floor and the ceiling were also covered with 18" thick fiberglas although no air gap was provided. A grating floor, provided in the chamber, was

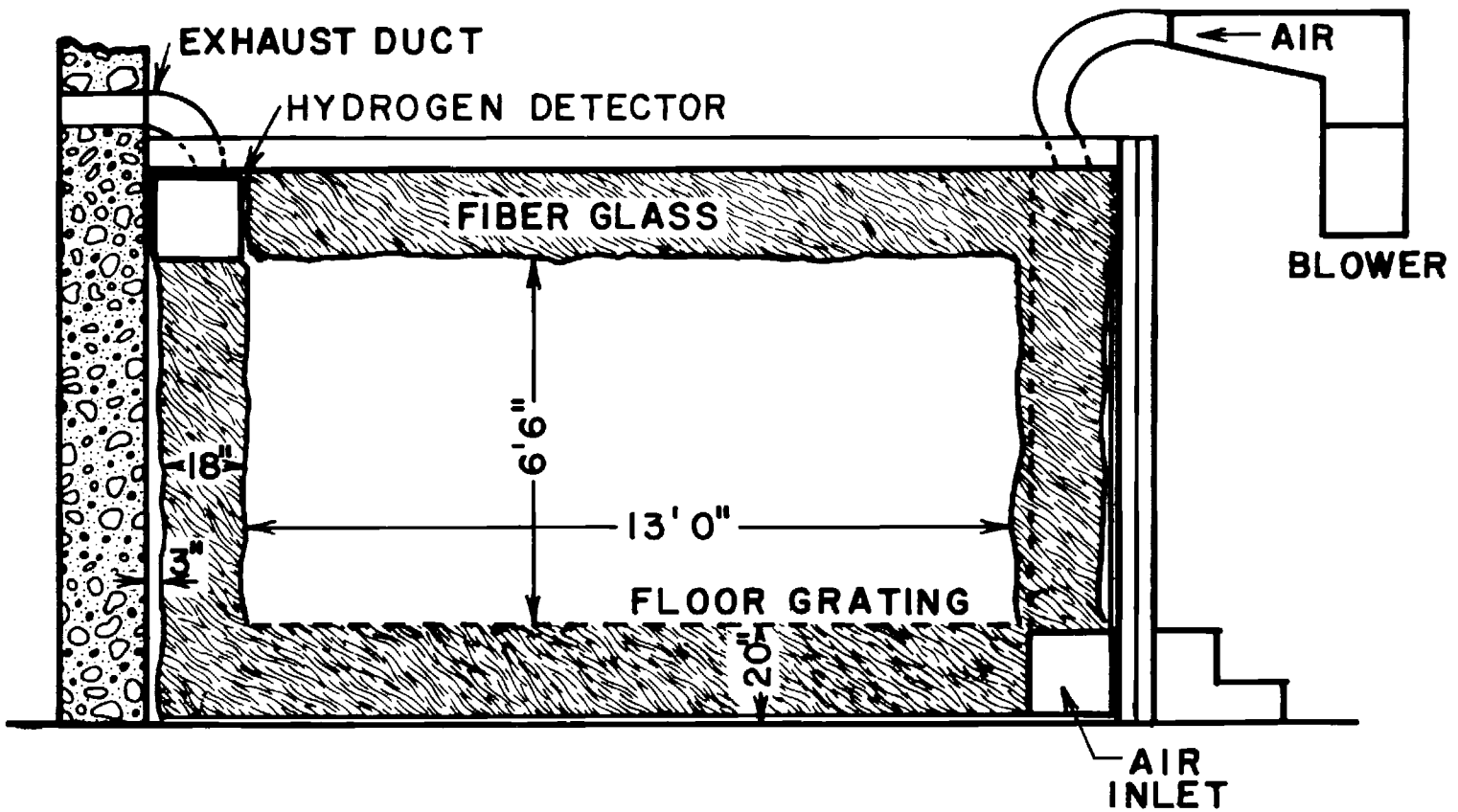

Figure 1(a). Cross-Sectional Elevation of Anechoic Chamber.

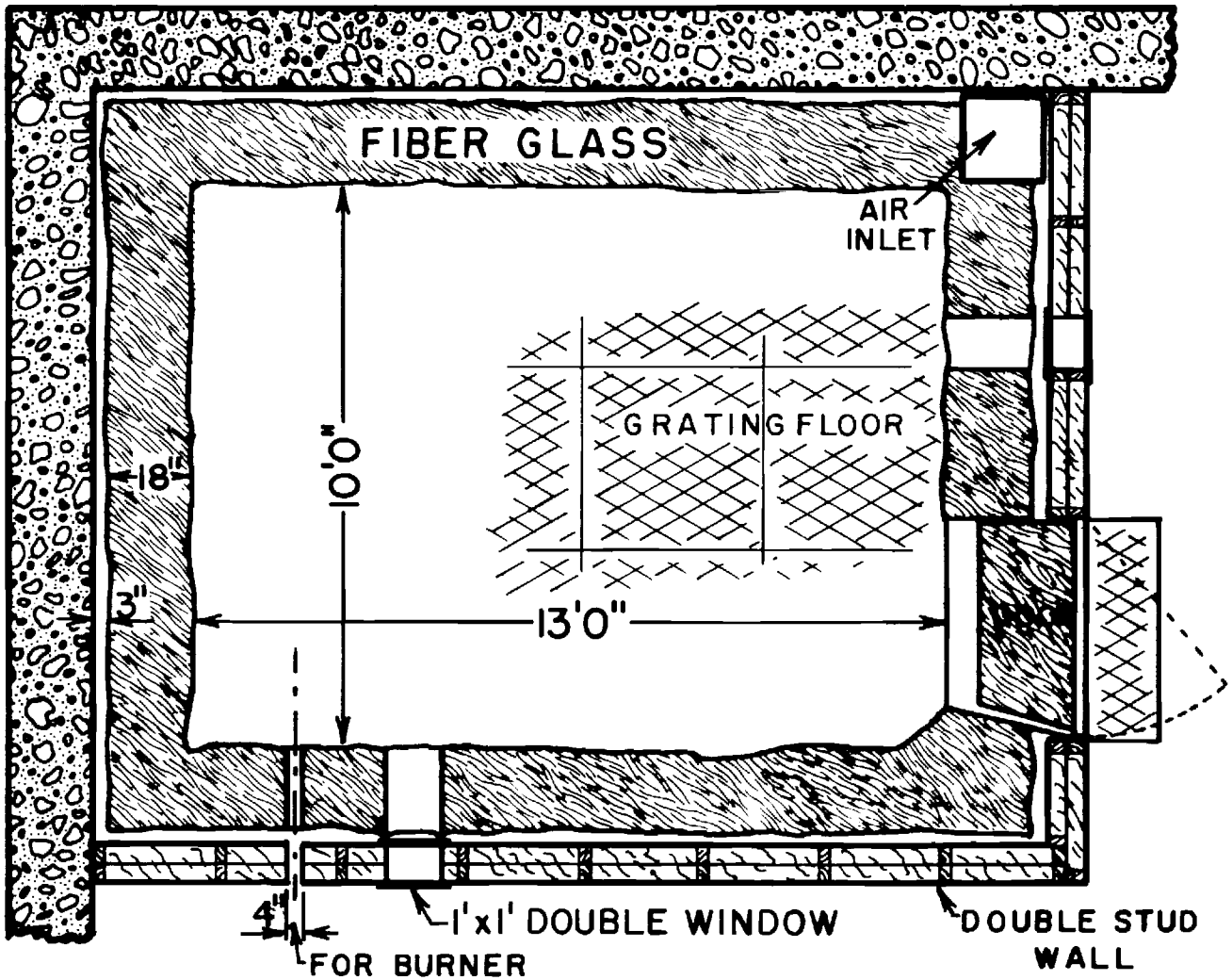

CROSS-SECTIONAL PLAN

Figure 1(b). Cross-Sectional Plan of Anechoic Chamber.

supported on a metal structure. The supporting structure was mounted on $\frac{1}{2}$" rubber pads to isolate structurally carried vibrations to some extent.

The chamber has two windows (1' x 1') so as to keep a close watch on the flame. A hinged door, also with the same thickness of insulation as the walls, provides an entry into the working area. A hydrogen detector has been installed in the ceiling.

The ventilation to the chamber is provided by a blower. The air from the blower passes through a long acoustic duct work and enters the chamber at one of the lower edges. Exhaust ducting with a long and tortuous passage is provided at the opposite edge of the chamber.

The anechoic chamber was tested with an acoustic driver as the source at various discrete frequencies and was found to be reasonably anechoic, in the frequency range of 125 Hz to 5000 Hz, for source to microphone distances of up to 5 ft (Figure 2). However, the ventilation blower was observed to produce low frequency oscillations in the sound meter readings, especially when the sound pressure levels being measured were of the order of 60 db re.0.0002 μ bar (20-20,000 Hz linear). Also, at this level, it was noticed that the external disturbances, such as the laboratory compressors, the air conditioning system, and the noise due to the flourescent tube ballast could add up to 0.5 to 2 db to the measured sound levels inside the anechoic chamber. This suggests that the experiments should be done when all these external disturbances are not operating. The reasons for the appreciable influence of the external disturbances in the anechoic chamber are 1) the chamber is not structurally isolated from other parts of the building, and 2) the walls are made of

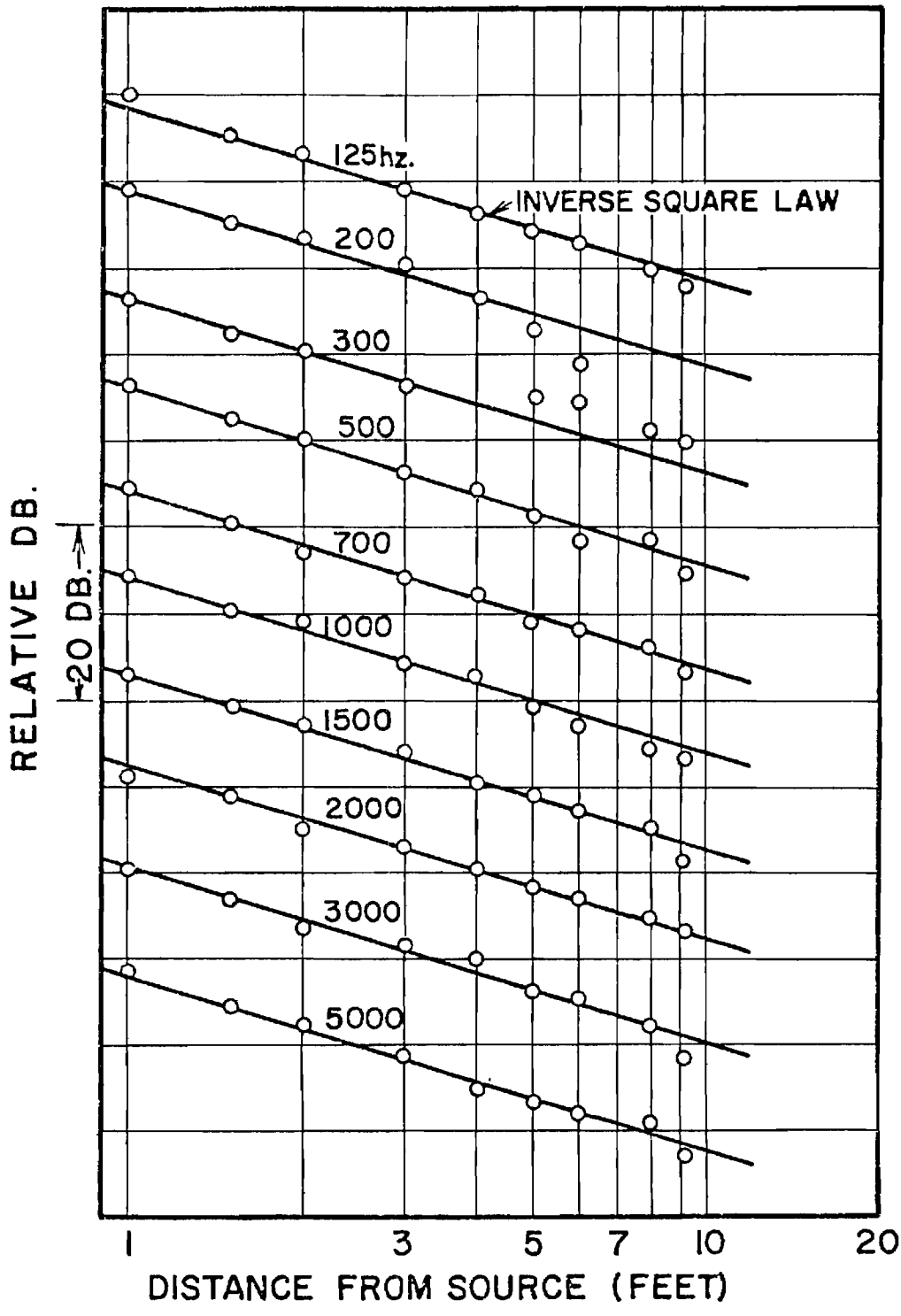

Figure 2. Anechoic Chamber Characteristics .

light-weight construction and are thus fairly inefficient in the prevention of sound transmission through them. In any case, the chamber was designed to have inner walls which are efficient in absorbing the incident sound waves and tests have shown that the purpose has been achieved.

The anechoic chamber has a typical background noise of 52 db re. 0.0002 μ bar (20-20,000 Hz linear). The spectrum of the background noise was nearly flat from 100-10,000 Hz.

Burners and Flow Systems

The burners used in this study have been constructed from coaxial tubing of circular cross section held together by 'Swagelok' heat exchanger T-joints as shown in Figure 3. The mixture of reactants flows through the inner tube and hydrogen for the stabilizing diffusion flames flows through the annular space between the tubes. The burner sizes are 0.402", 0.652" and 0.96" in diameter. The sizes quoted here are the inner diameters of the central tube which determines the size of the flame. The size of the annular gap is less than 1/32 inch in all the three cases. The two smaller burners are built out of copper tubing while the largest burner has a stainless steel inner tube and a copper outer tube. A straight length of 50 diameters is provided for the flow of reactants preceding the burner port. This ensures fully developed turbulent pipe flow conditions at the burner exit. A mixing chamber filled with 4 mm glass balls is introduced in the main burner tube just before the 50 D straight length to aid proper mixing of fuel and air. This mixing chamber, in addition, serves as a flash-back suppressor. The burners are mounted in the anechoic chamber with their axes horizontal at

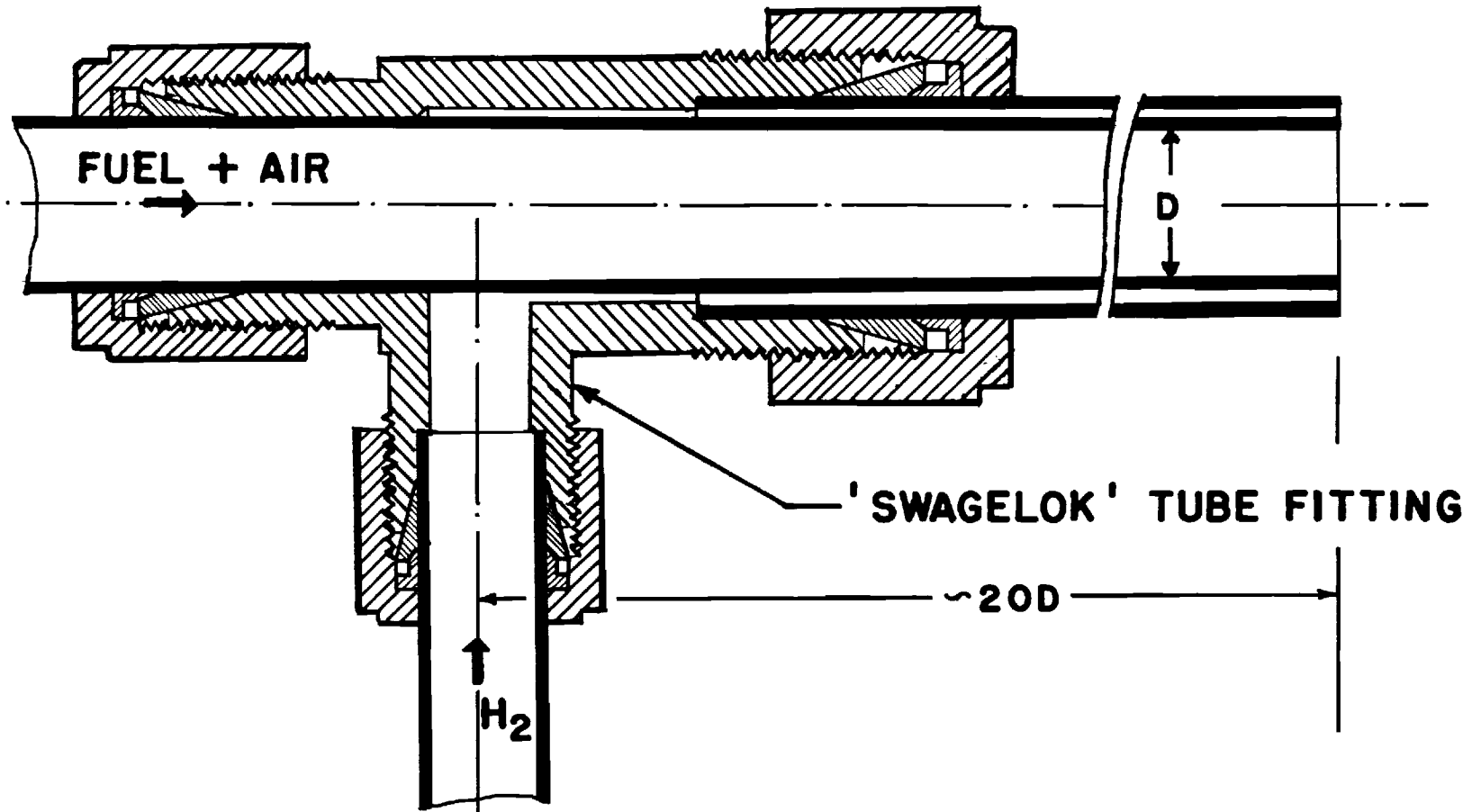

Figure 3. Burner Assembly.

3 ft above the floor grating and at least 2 ft from the walls.

Figure 4 shows the flow system. Air for the experiments is supplied by the 1000 ft^3 125 PSI Air resorvoir. The flow of air is measured by two rotameters with overlapping flow ranges. Fuels and hydrogen are metered by orifice meters; two orifice plates with different orifice dimensions are used on the fuel metering system to cover the entire flow range. The control valve downstream of each flow meter is used to introduce the pressure drop required to maintain a desired upstream pressure at the meter, thus vastly increasing the metering range of each flow meter. Fuels, hydrogen and nitrogen are supplied from gas bottles which are stored outside the room in a separate gas storage area. A muffler is provided in the air line to reduce the flow noises. Also, air leaving the muffler flows through flexible rubber hoses thereby preventing abrupt flow turns which generate flow noises.

The fuel and air are mixed at a T-joint. The hydrogen line entering the anechoic chamber is shrouded by nitrogen. Also, both fuel and hydrogen lines are provided with nitrogen purge.

Instrumentation

Sound pressures are measured by Brüel and Kjaer type 4134 half-inch condensor microphones. Five such microphones mounted on stands in the same horizontal plane as the burner are used. The microphones are placed at constant radius with respect to burner port and at angular locations between 15 and 120° to the flow direction; closer than 15° to the flow direction would be likely to produce flow noises at the microphone. The outputs of the microphones are directly read out as sound

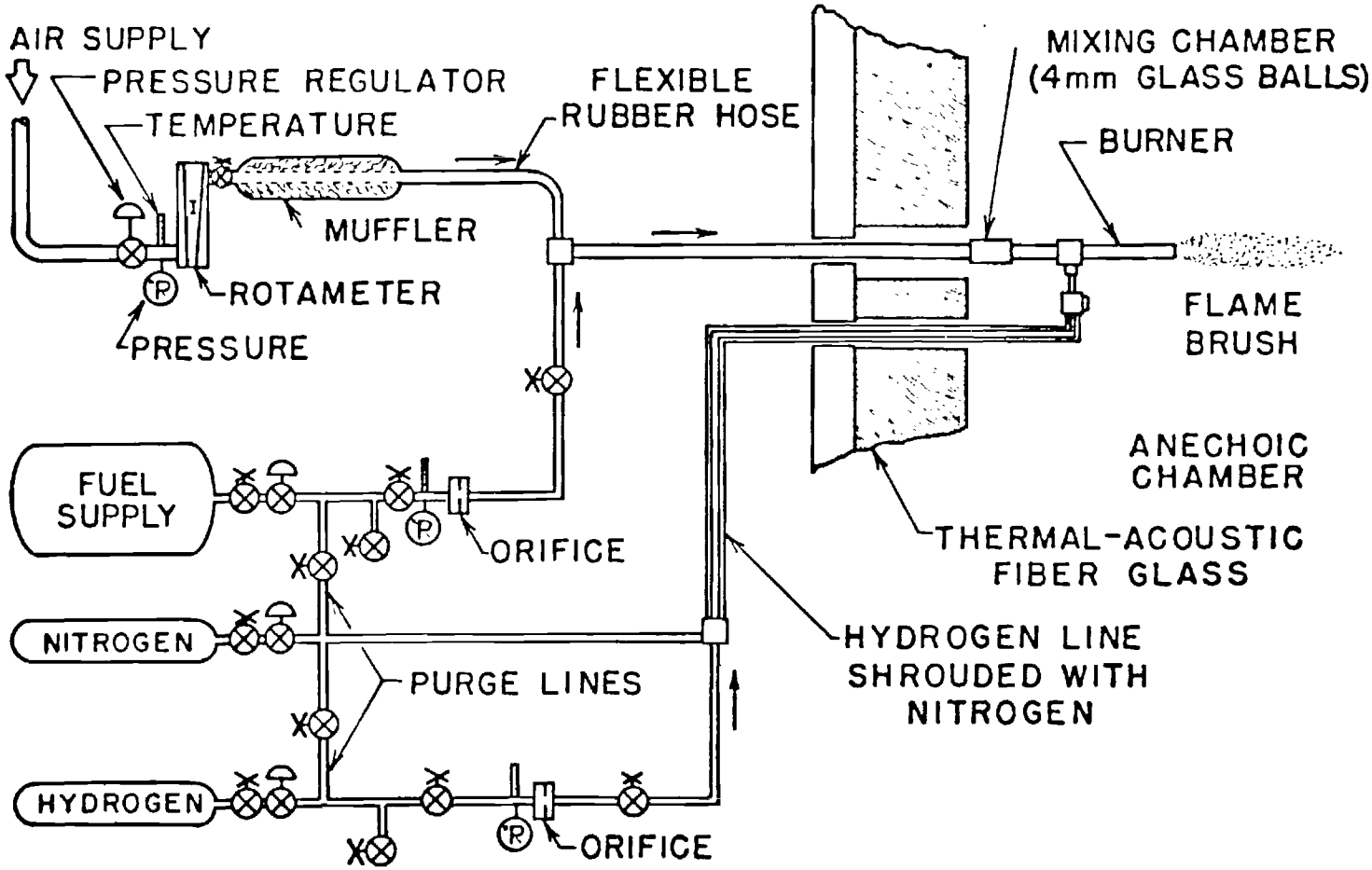

Figure 4. Flow System Schematic.

pressure levels (db re. 0.0002 μbar) on a Brüel and Kjaer type 2604 microphone amplifier, one at a time. They are also amplified by an array of five NEFF type 122 amplifiers and recorded on five channels of an AMPEX FR 1300, 14 channel magnetic tape recorder, usually at 30 ips tape speed. The direct calibration of microphones is done by a Whittaker type PC-125 acoustic calibrator. In order to provide a calibration reference for data analysis the sound output from an acoustic driver, producing a 1000 Hz sound and placed under the burner port, is also recorded on the tape. The sound pressure level at each microphone due to the acoustic driver is read on the microphone amplifier and noted. This procedure enables the calibration of the entire system directly.

The data acquisition and reduction schematic is shown in Figure 5. It can be noticed that only microphones are placed inside the anechoic chamber. The microphone signal carrying cables are brought out of the anechoic chamber through a conduit and connected to the appropriate instruments. The spectral analysis of the noise is performed on a Hewlett Packard type 5645 Fourier analyzer and associated hardware. The spectra are computed digitally using a fast Fourier transform by the machine. A multi-sample averaging technique is used to obtain stable results and eliminate spurious noise from the signal. The output from the Fourier analyzer could be observed on the oscilloscope, plotted on an x-y plotter or printed out on a teletype. In this study x-y plots were preferred over the other modes of output.

Flame Stabilization

The flames were stabilized at the end of burner tubes by an annular

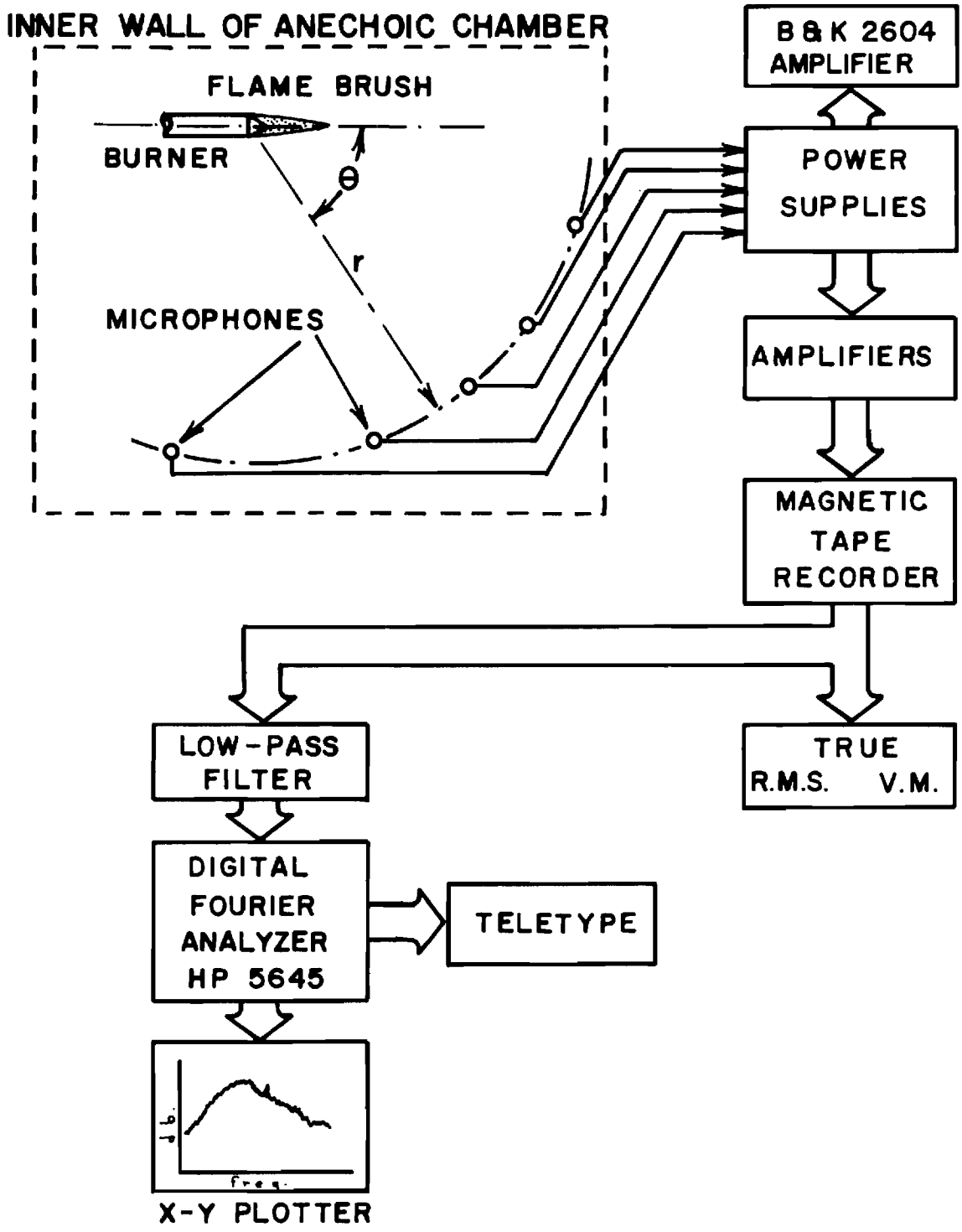

Figure 5. Data Acquisition and Reduction Schematic for Acoustic Experiments.

diffusion flame of hydrogen. Smith and Kilham[3] have studied the effect of various amounts of hydrogen flow on the noise generated. According to their study the optimum amount of hydrogen was found to be between about $2\frac{1}{2}$ to $3\frac{1}{2}$ percent by volume of the main flow. Before using the values for the H_2 required for stabilization from Reference 3, a test measurement was made on one of the typical cases. The result of this experiment is shown in Figure 6. This result is in essential agreement with the results of Reference 3 and, therefore, in all the experiments $2\frac{1}{2}$ percent hydrogen has been used since this would contribute the least to the overall noise output. Although this quantity of hydrogen was found satisfactory in most of the experiments, the flames of velocity greater than 300 ft/sec on a 0.402" burner required 5 percent for satisfactory stabilization of the flame.

Combustion Noise and Jet Noise

The relative importance of combustion noise in comparison with the noise from a pure jet of the same velocity, and also the air jet plus pilot flame combination, is presented in Figure 7. The microphone azimuth of 55° to the flow direction was chosen so as to be somewhat close to the direction of predominant radiation for all three cases. Combustion noise dominates over the entire velocity range from 50 ft/sec to 600 ft/sec. An interesting observation made during these experiments was that the hydrogen diffusion flame was by itself very quiet. However, when the main stream of air was turned on the flame would interact with the outer boundaries of the turbulent jet close to the burner exit and enhance the noise output from the air jet.

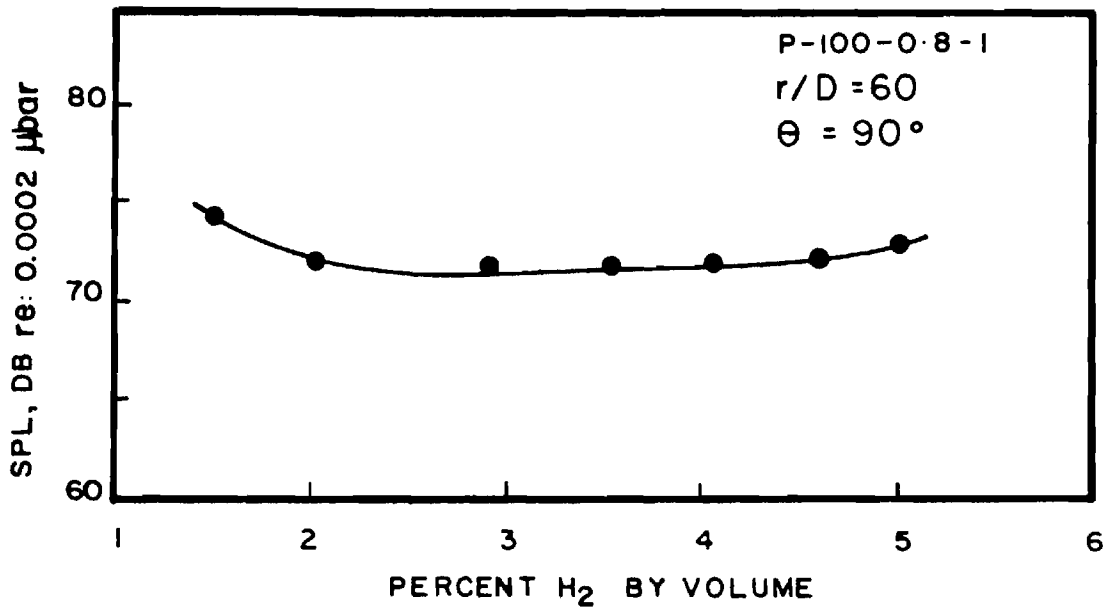

Figure 6. Effect of the Quantity of Hydrogen Used for Flame Stabilization on Overall Noise Level.

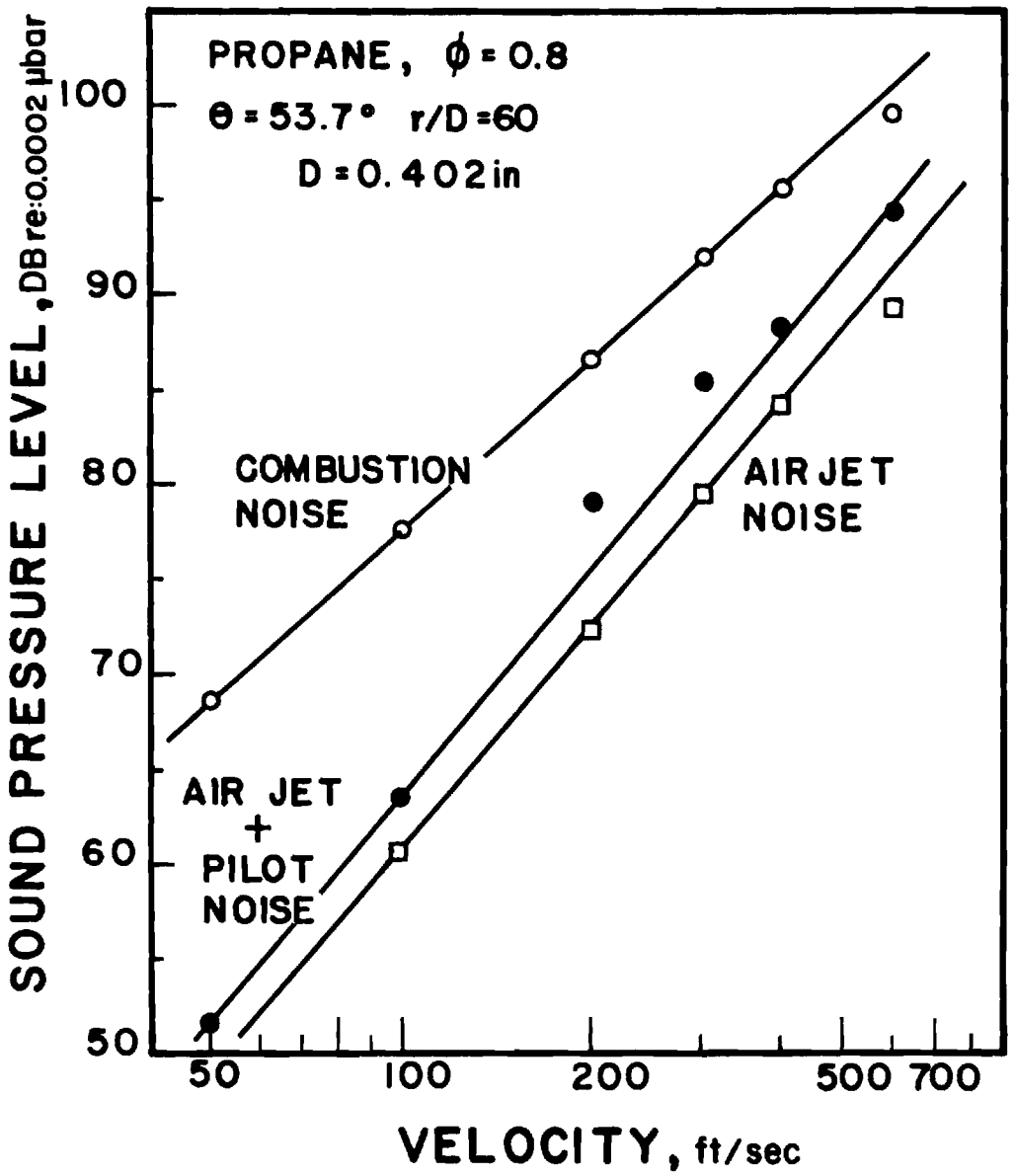

Figure 7. Jet Noise, Combustion Noise and Air Jet plus Pilot Flame Noise at Various Flow Velocities.

The results shown in Figure 7 can be used to determine the approximate scaling laws for power radiated if, for the present, directionality is neglected. The jet noise appears to follow a U^4 law for acoustic power while combustion noise favors an exponent of 2.8. Because of the higher exponent on U the difference between the combustion noise and the jet noise decreases with velocity. Nevertheless, even at 600 ft/sec combustion noise is predominant.

Sound Pressure Measurement

The sound pressures were measured by a B & K type 2604 microphone amplifier using 20-20,000 Hz linear response with the meter set to slow response. In most cases, the meter excursions were less than a db and, in accordance with standard practice[23], the arithmetic mean between the maximum and minimum readings was taken as the sound pressure level. In doing this any occasional highs and lows of the meter readings should be neglected.

As explained earlier, the locations of the microphones are determined with respect to the burner port and the flow direction. For computation of the acoustic power radiated and the directionality it is necessary to reference the sound pressures measured to the acoustic center in the flame. Acoustic center is a point within the noise generating region from which the noise would appear to originate to a far field observer. There is both experimental[8,9] and theoretical[17] evidence to show that the noise emitters in the case of combustion noise are confined to the visible region of the flame. Thus, it can be considered reasonable to state that the acoustic center in the flame would be located at the

point of maximum volume per unit length as determined by direct photographic flame volume measurements. These measurements are explained in detail in the next chapter.

Figure 8 shows sound pressure level distributions along a line parallel to the flow direction, i.e., parallel to the length of the flame. The distance between the microphone and the axis of the burner was kept constant at 9-7/8". If the noise radiation from the flame were spherically symmetric the location of maximum sound pressure level would correspond to the acoustic center. However, since the acoustic radiation from the flame is weakly directional in the forward 90°, the observed maximum will get shifted towards the flame tip. This shift will depend upon the distance between the burner axis and the microphone as well. In the light of these facts the location of the acoustic center cannot be obtained from Figure 8. The acoustic center locations as decided by direct flame photography have been indicated on the sound pressure level traces. It can be noticed that the acoustic center locations do consistently fall below the maximum sound pressure level location.

In order to determine whether the calculation of acoustic power radiated from the flame is very sensitive to the inaccuracies in locating the acoustic center, certain calculations have been made for three typical cases. The acoustic power radiated was evaluated assuming that the acoustic center lay at a) the location of maximum flame volume per unit length and b) the tip of the flame. Table 1 presents the results of these calculations. Even with a rather drastic shift of the acoustic center to the flame tip the error introduced is less than 0.4 db.

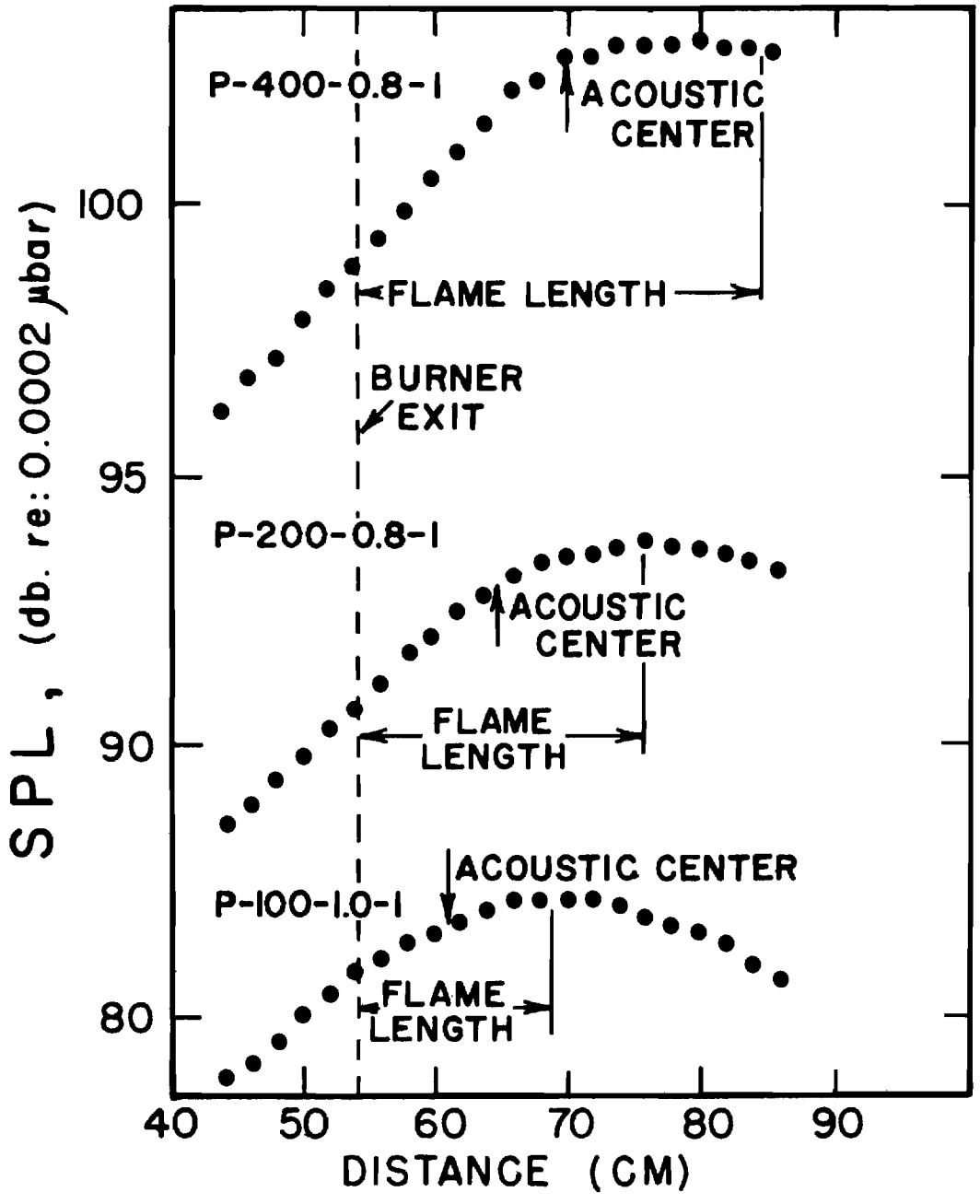

Figure 8. Sound Pressure Levels Along a Line Parallel to the Flame Length 9.875" Below the Burner Axis.

Table 1. Errors in Acoustic Power Due to Inaccuracy in Locating Acoustic Center

Test	Acoustic Power, Watts W_1 Acoustic Center at Max Flame Volume Per Unit Length Location	Acoustic Power, Watts W_2 Acoustic Center at Flame Tip	Difference DB $(= 10 \log_{10} \frac{W_2}{W_1})$
P-100-1.0-1	0.3650×10^{-3}	0.3564×10^{-3}	-0.1
P-200-0.8-1	0.1700×10^{-2}	0.1624×10^{-2}	-0.2
P-400-0.8-1	0.1121×10^{-1}	0.1030×10^{-1}	-0.38

After having established the location of the acoustic center from flame photography experiments, the measured sound pressures were corrected for both geometry and magnitude to account for the change in origin. In the process of calculating the altered values of sound pressures, spherical divergence was assumed since the measurements are in the far field. To the corrected sound pressures a polynomial relation,

$$p^2 = \frac{1}{r^2} \sum_{n=0}^{3} a_n \cos^n \theta \qquad (6)$$

suggested by the theory in Reference 18, was fitted by the method of least squares using all the five sound pressure readings. This polynomial in cos θ was found to fit the data very closely. The maximum error was ± 1 db which is of the same order of magnitude as the accuracy of the instrumentation itself.

Calculation of Acoustic Power Radiated

The acoustic power radiated from the flame is calculated, from the polynomial relation for sound pressure with θ, by integration over a sphere of some radius r assuming axial symmetry. For values of sound pressures beyond the last microphone angular location the value obtained for the last location was used. To determine the order of magnitudes of the errors involved due to such an extrapolation, three representative experiments were conducted in which a single microphone was traversed around the flame up to 170° with the flow direction. The sound pressures measured were corrected for the acoustic center and a polynomial in cos θ was fitted to these readings. Figure 9 shows a comparison between the single microphone directionality pattern and the one from five fixed microphones. The comparison is quite favorable and is within the accuracy of ± 2 db. More important, however, is the error involved in calculating acoustic power based on 5 microphone data. The power calculated from one microphone covering up to 170° does not involve any appreciable extrapolation and hence is considered to be the true estimate. Table 2 presents a comparison of the acoustic power values due to both cases. It can be seen that the error due to the extrapolation is not excessive. The use of five fixed microphones is preferred from a practical standpoint since the time required for sound pressure measurement is drastically reduced compared to the time it would take to traverse one microphone around the flame. On quite a few tests, the heat input was so high ($\sim$ 100 kw) that the duration of the tests had to be restricted to a fraction of a minute to keep the anechoic chamber from getting overheated.

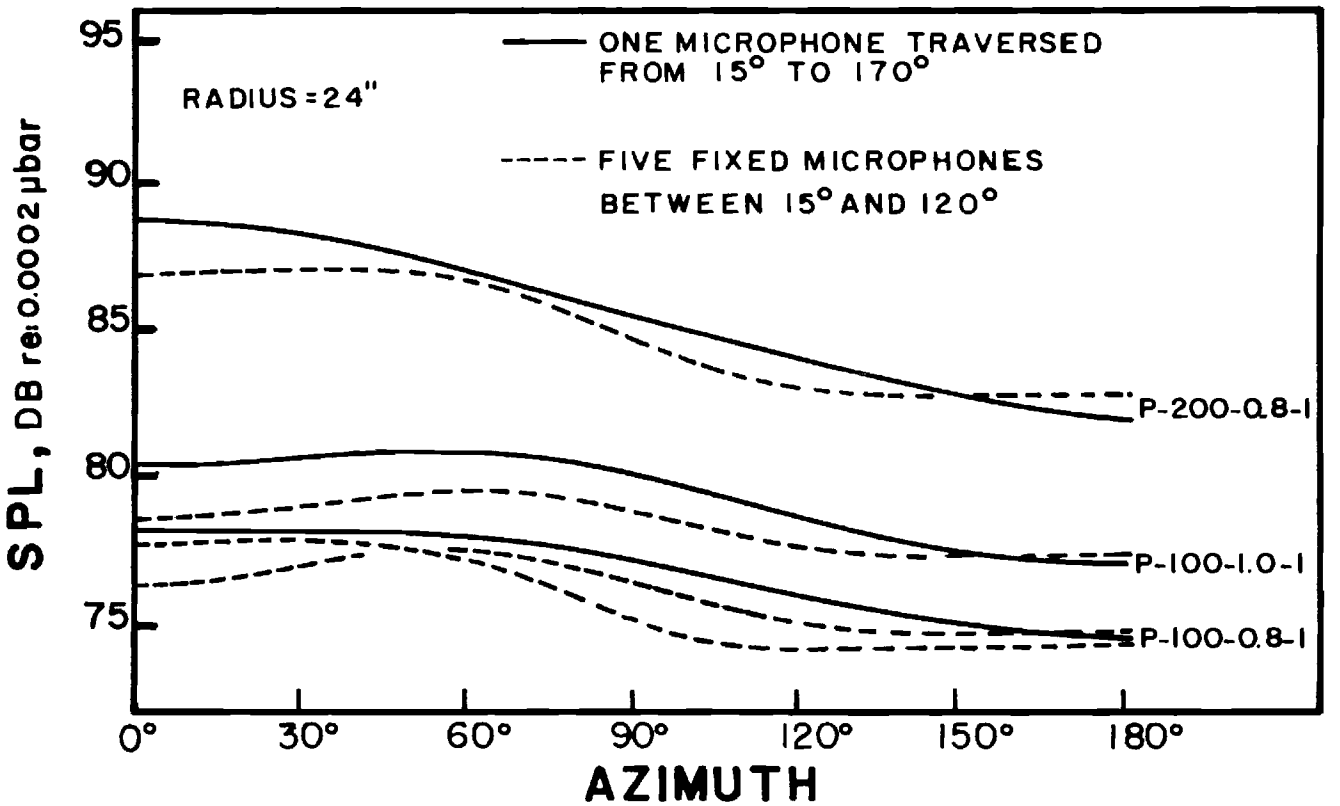

Figure 9. Comparison Between Directionality Patterns Obtained by Using Five Fixed Microphones and by Traversing a Single Microphone.

Table 2. Error in Acoustic Power Due to Using Only Five Microphones to Measure the Sound Field Around the Flame

Test	Acoustic Power, Watts W_1 One Microphone Covering 15° - 170°	Acoustic Power, Watts W_2 Five Fixed Microphones Covering 15° - 120°	Difference DB $(= 10 \log_{10} \frac{W_1}{W_2})$
P-100-0.8-1	0.2266×10^{-3}	0.1826×10^{-3}	0.94
P-100-1.0-1	0.4286×10^{-3}	0.3199×10^{-3}	1.28
P-200-0.8-1	0.1790×10^{-2}	0.1536×10^{-2}	0.66

Referring back to Figure 9, two traces (corresponding to 5 fixed microphone data) are presented for the P-100-0.8-1 case. These are from the same experiment repeated on two different days. The difference in the power calculated between the two traces is about 0.3 db which shows good repeatability of data. However, the tests of equivalence ratio of 0.6 had a tendency to be rather unstable and, consequently, the repeatability in such instances was not as good. Some experiments of $\phi = 0.6$ case could reproduce only within a ± 2 db limit.

Experimental Results for Fuel Lean Flames

Directionality of Noise Radiation

The directionality of the far field radiation from a source can give some indications regarding the nature of the source. At the same time, the directional information is required for deciding the most effective locations for acoustic liners. The directionality results

presented here are the polynomials in cos θ fitted to experimental measurements. The origin of reference is the acoustic center in the flame and the azimuthal positions are measured from the flow direction. The difference between the maximum sound pressure level observed (any θ) and the value at the axis (θ = 0) when one makes a constant radius traverse in the plane of the flame can be considered as a quantitative measure of the directionality of the source.

Figure 10 shows the directionality patterns at various flow velocities for propane-air flames of equivalence ratio 0.8. It can be seen that the effect of velocity on the directionality is to shift the maximum sound pressure location closer to the axis of the flame. The convection of sources by the flow causes this shift towards the axis with an increase in flow velocity.

The effect of burner diameter on the direction of maximum sound radiation can be seen in Figure 11. Results are obtained for all the three fuels, propane, propylene and ethylene. The sound pressure levels have been converted to refer to a radius of 57" and are plotted on the graph instead of quoting all the results at a certain r/D distance. This was done so as to be able to observe the amplitudes of noise from the three burners at the same distance from the source. Figure 11 shows that there is a distinct effect of diameter on the directionality pattern. With an increase in diameter the peak in the directionality curve shifts away from the burner axis, an effect opposite to the velocity influence. Another effect due to an increase in burner diameter appears to be increased directionality. Furthermore, comparing traces from various fuels, ethylene-air flames exhibit a stronger directionality than either

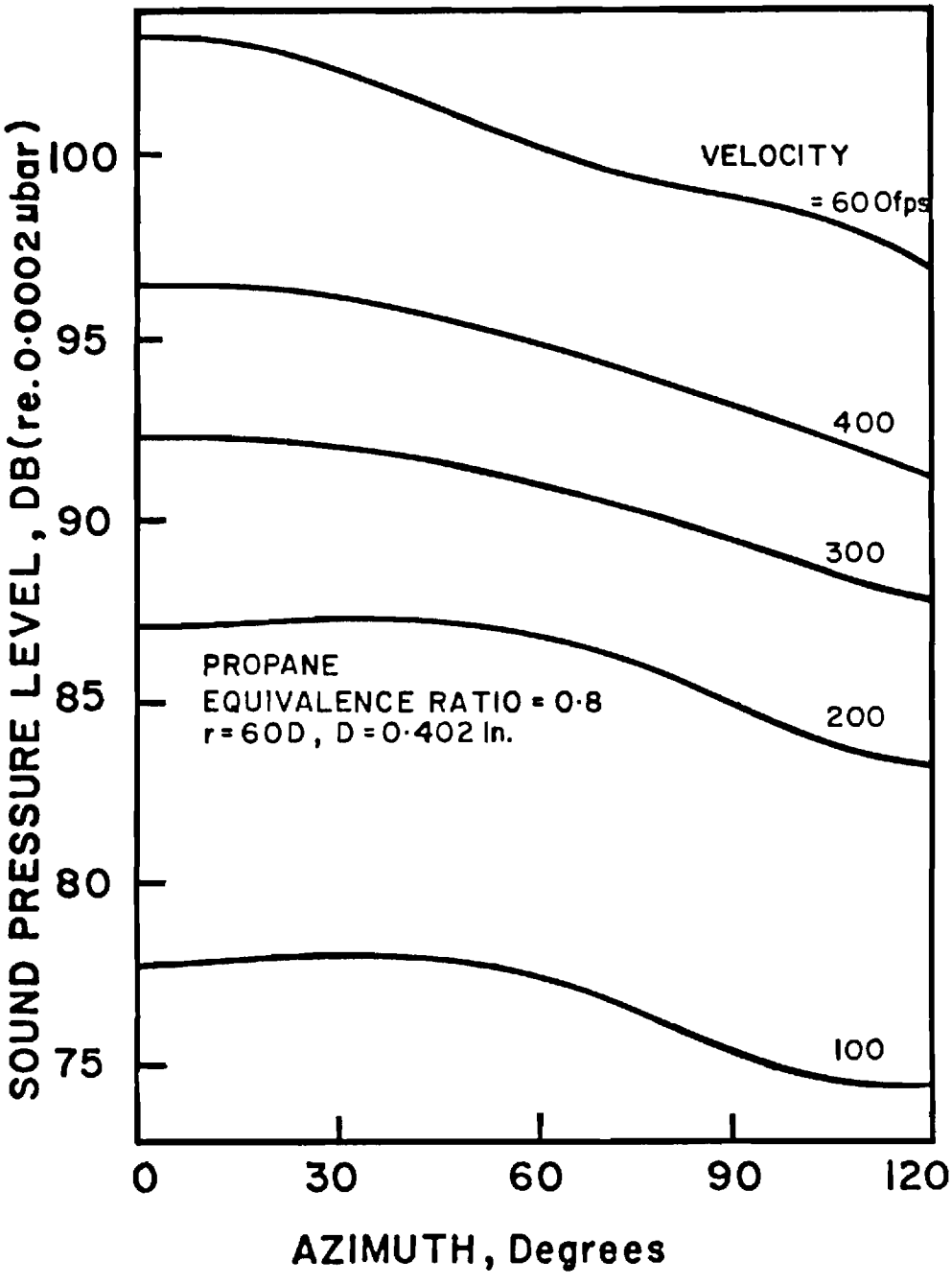

Figure 10. Directionality as a Function of Flow Velocity.

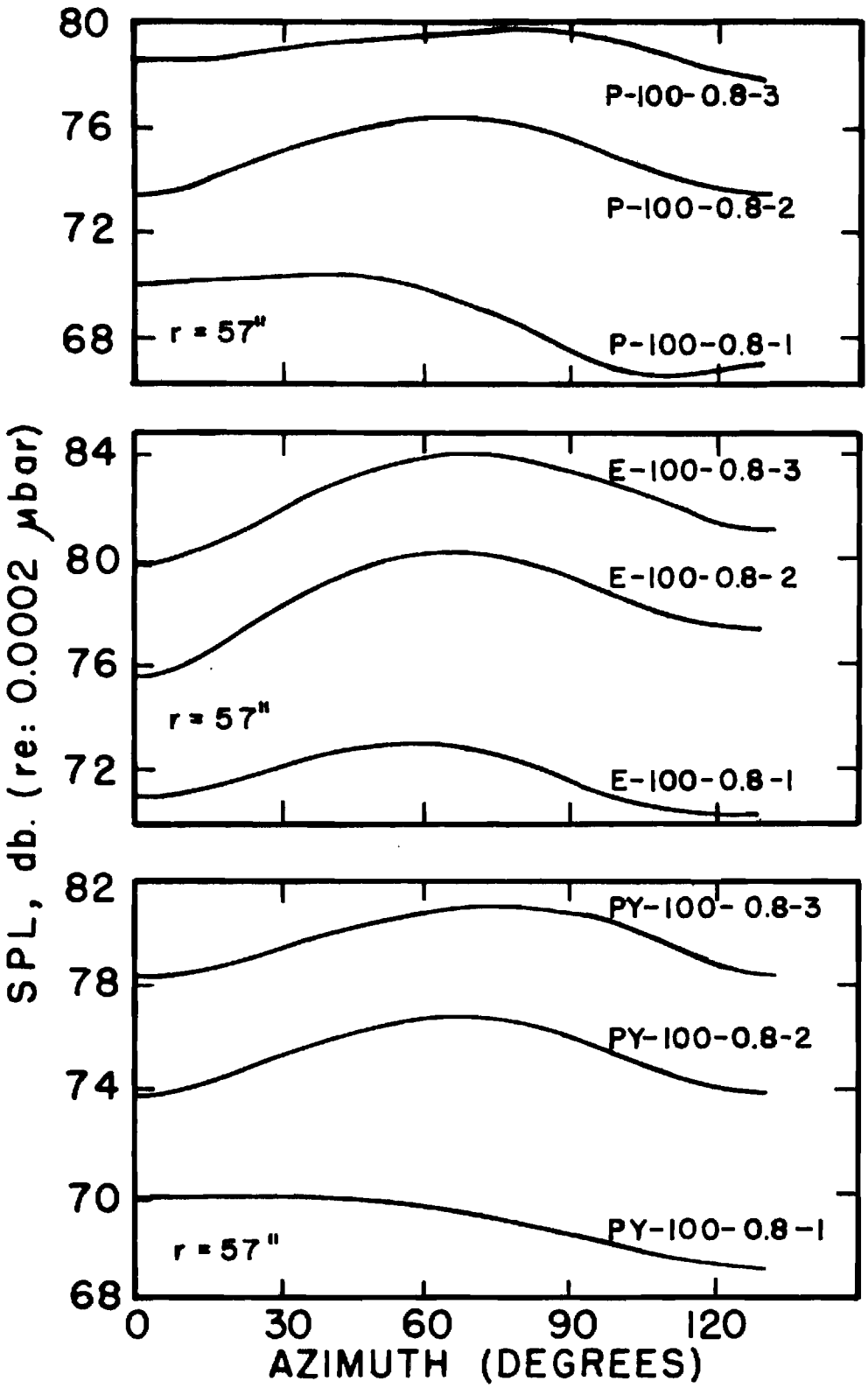

Figure 11. Directionality as a Function of Burner Diameter.

the propane-air or propylene-air flames. This could be the effect due to laminar flame speed since ethylene-air has the highest laminar flame speed.

Directionality curves as a function of equivalence ratio are plotted in Figure 12. The range of ϕ included is between 0.6 and 1.0; that is, from fuel lean to stoichiometric. The effect of equivalence ratio on directionality can be seen to be very minor. Again, ethylene cases show maximum directionality.

Scaling Laws on Acoustic Power Radiated

Velocity Scaling. Velocity of the reactants is one of the primary parameters that influence noise radiation from regions undergoing turbulent combustion. Here, the behavior of acoustic power as a function of velocity is presented in Figures 13 and 14. In Figure 13 the acoustic power radiated is plotted as a function of mean velocity of reactants at the burner exit for all the three fuels, propane, propylene and ethylene. The equivalence ratio is 0.8 and the burner diameter is 0.402". Over a 12:1 velocity range, a $U^{2.9}$ law is seen to be appropriate for acoustic power radiated. The ethylene flames appear noisier which will be seen to be a laminar flame speed effect in the succeeding paragraphs. Also, ethylene data points appear to prefer an exponent on mean flow velocity slightly lower than 2.9. Figure 14 shows the results obtained for 0.652" and 0.96" burners. There is a good agreement with the scaling law obtained for a 0.402" burner, although in this case, a $U^{2.6}$ law fits the data better. This result is in agreement with the results of Reference 17 which predicted a velocity scaling exponent to be greater than 2. Also, this velocity exponent is much lower than the velocity scaling for jet noise[19,20].

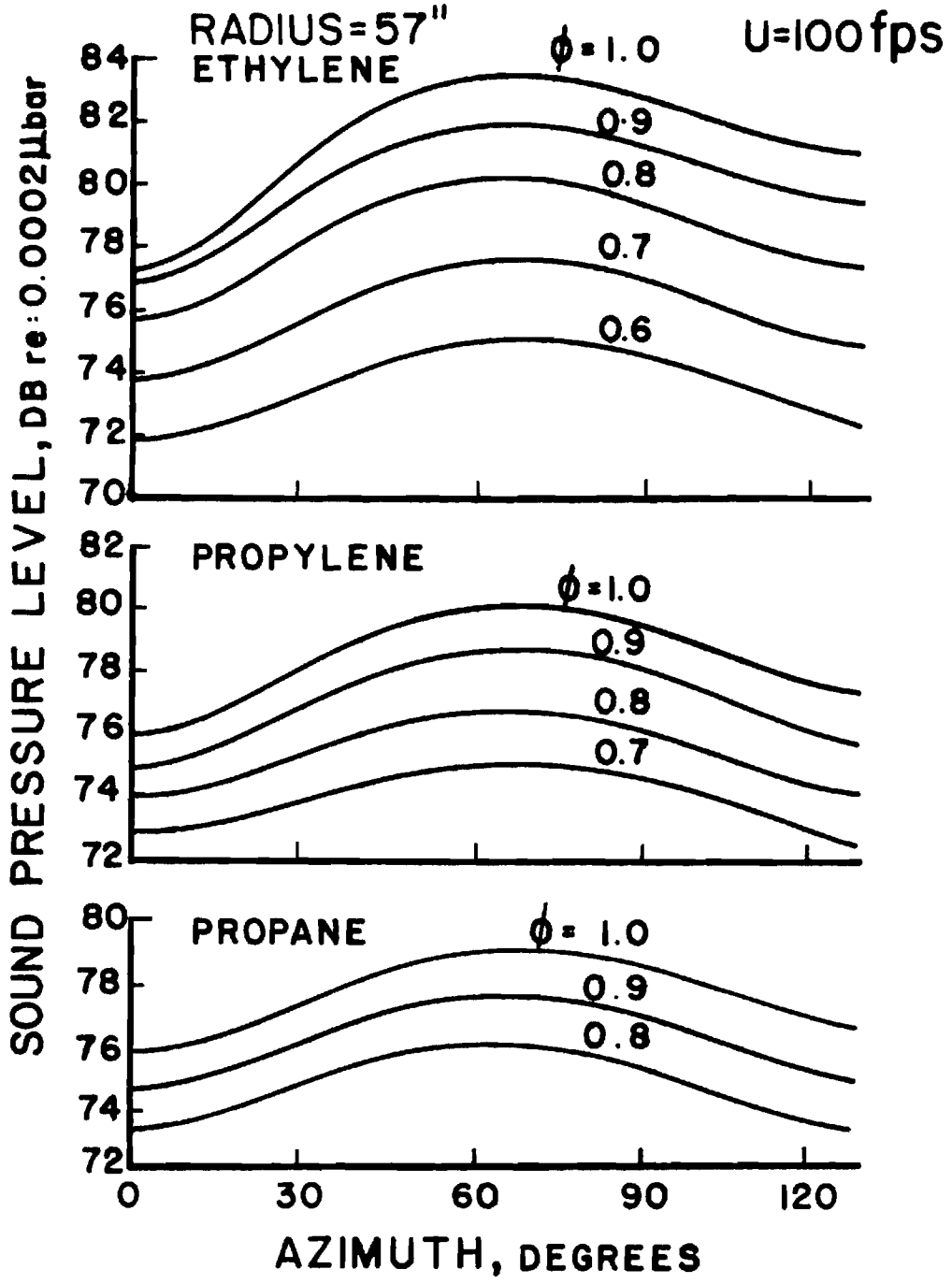

Figure 12. Effect of Equivalence Ratio on Directionality for a Burner of Diameter 0.652".

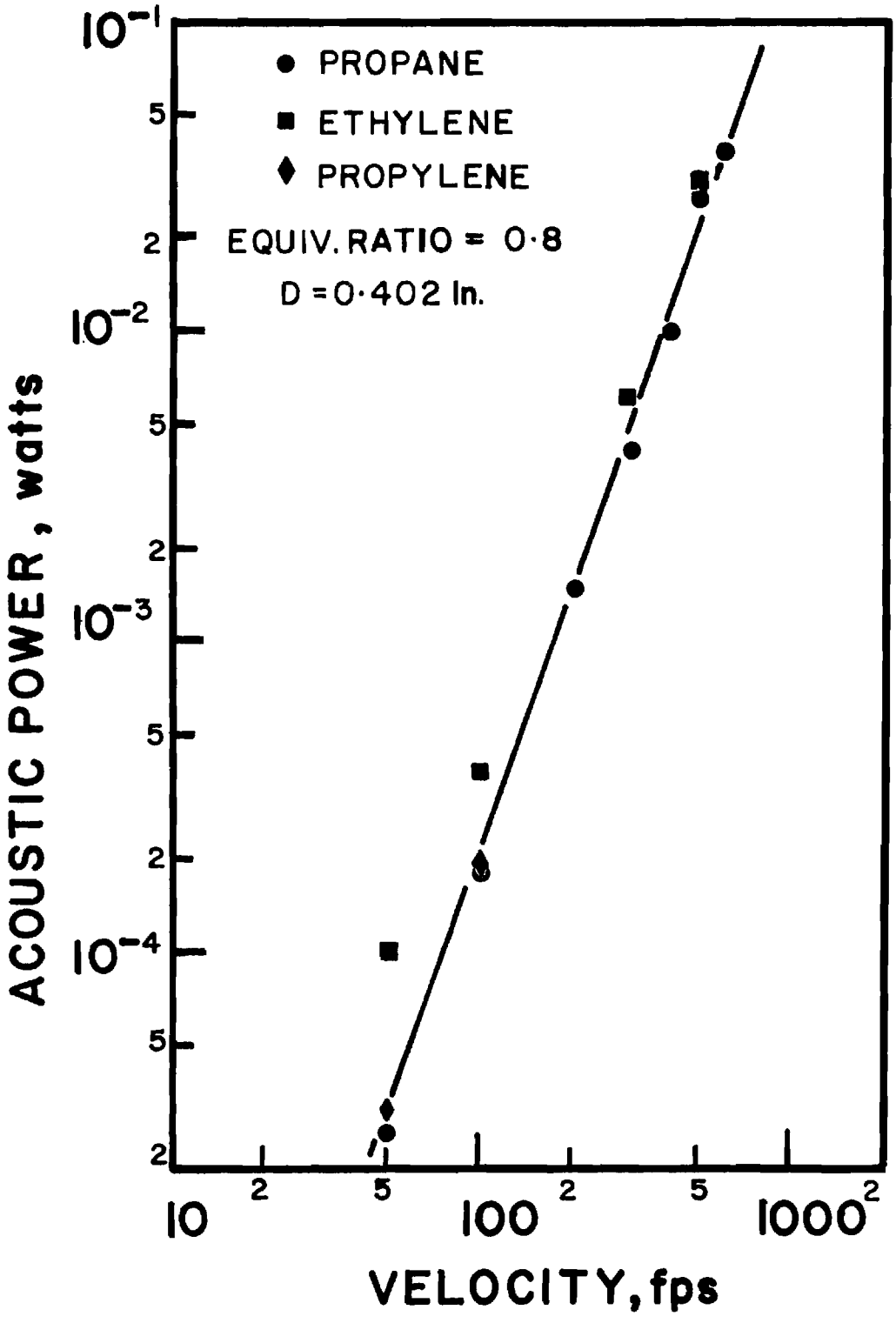

Figure 13. Acoustic Power as a Function of Velocity for a Burner of Diameter 0.402".

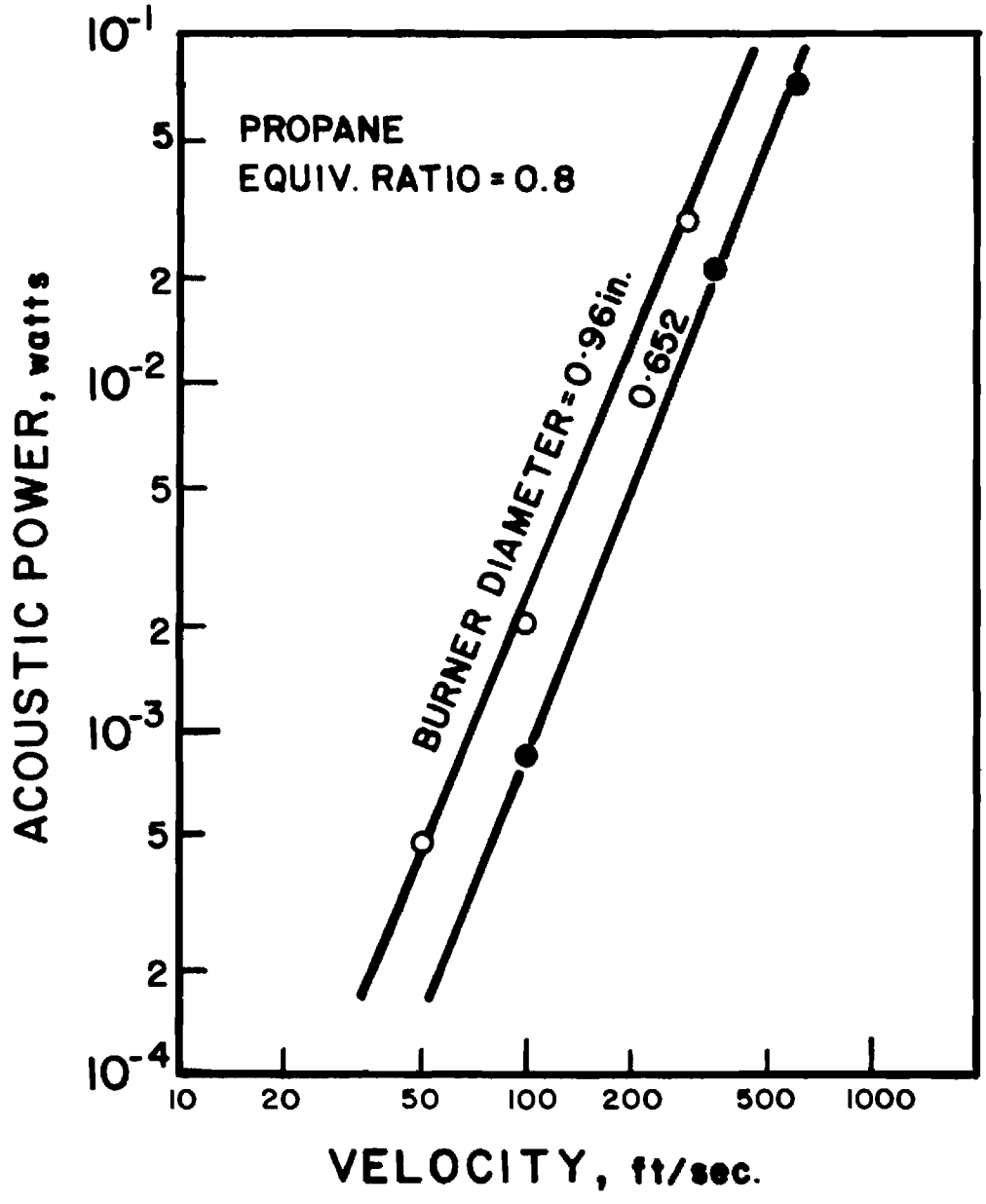

Figure 14. Acoustic Power as a Function of Velocity for Burners of Diameters 0.96" and 0.652".

Diameter Scaling. The diameter of the burner is yet another parameter of interest in noise radiation from flames. A positive exponent of U obtained in the preceding paragraph would suggest lowering of flow velocity to decrease noise output. This would imply that burner size would have to be increased to maintain the same mass flow. The effect of diameter, therefore, becomes quite important. Primarily, the knowledge of the diameter effect is required in order to predict the noise output from larger burners.

Figure 15 shows the results of the experiments conducted to determine the diameter effect. An acoustic power scaling of $D^{3.0}$ is obtained in the case of all the three fuels. The effect of decreasing flow velocity can now be considered. For a burner of circular cross section the mass flow is given by

$$\dot{m} \propto \rho_o U D^2 \tag{7}$$

Thus, reducing the velocity by a factor of 4, say, would mean increasing diameter by a factor of 2 to maintain constant $\dot{m}$. Since the noise exponents on U and D are almost equal to each other, there seems to be a definite advantage in choosing the lowest value of the flow velocity possible within the other design restrictions.

Laminar Flame Speed Scaling. Laminar flame speed, S_L, is a measure of the reactivity of the fuel. It represents the velocity of propagation of a laminar flame through a reactive mixture. For turbulent flames, a turbulent flame speed, S_t, could be defined. There is sufficient

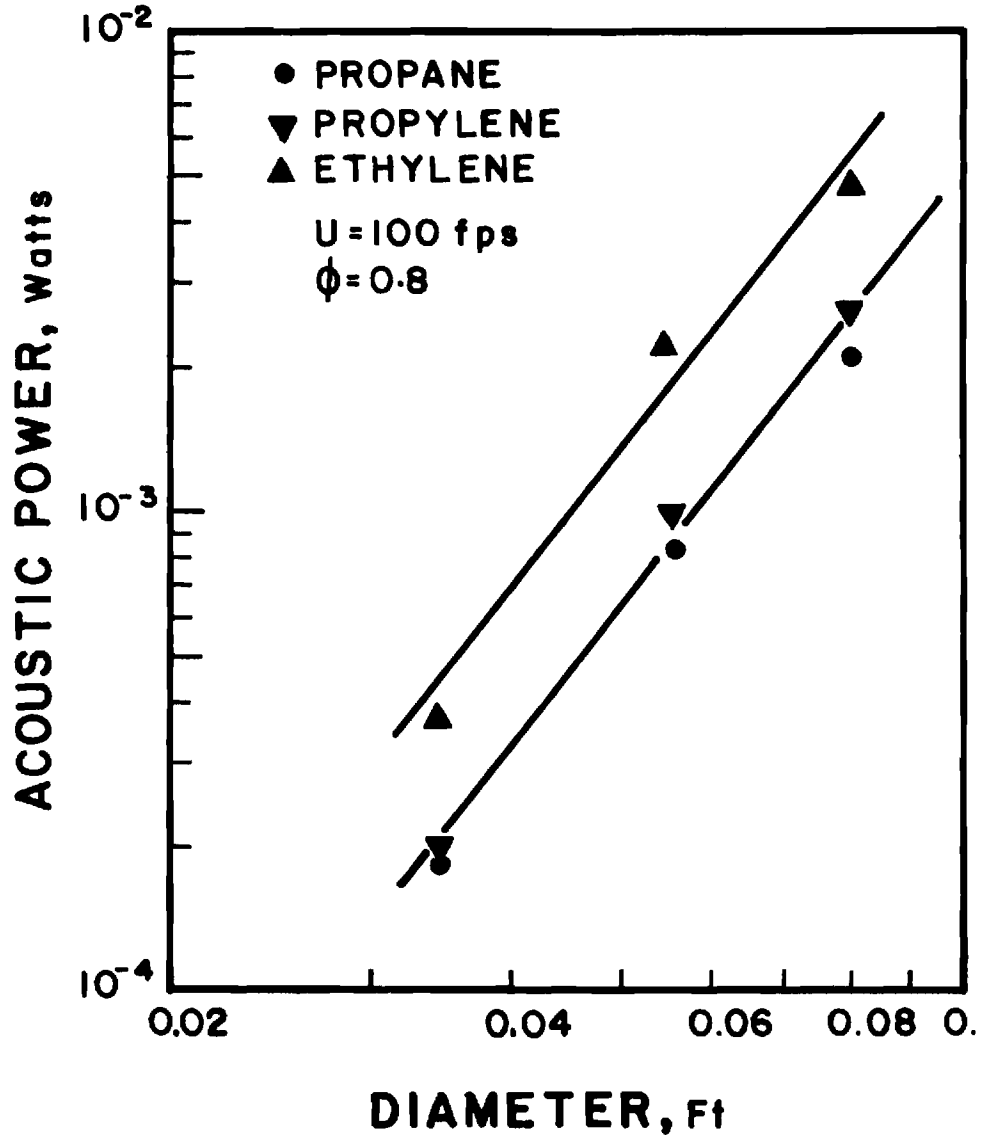

Figure 15. Acoustic Power as a Function of Burner Diameter for Fuel-Lean Flames.

evidence[24] to show that turbulent flame speed is proportional to laminar flame speed; S_t is always higher due to faster transport processes in a turbulent flame. Further, S_t is dependent on flow conditions as well. Thus, if flow conditions like mean flow velocity, turbulence intensity and scale are being considered independently, laminar flame speed would appear to be the correct parameter to choose. In this analysis, therefore, laminar flame speed has been chosen to represent the chemistry effects due to changes in fuel and mixture ratio. The values used in this analysis for S_L are calculated from the equation

$$\frac{S_L}{S_{L_{max}}} = 2.6 \log_{10} \phi + 0.94 \qquad (8)$$

$$(\phi \leq 1.0)$$

from Reference 25. The values of $S_{L_{max}}$ were also chosen from Reference 25. Table 3 shows the values of $S_{L_{max}}$ used.

Table 3. Values of Laminar Flame Speed from Reference 25 for Combustion with Air at Atmospheric Pressure and Room Temperature

Fuel	$\frac{S_{L_{Max}}}{S_{L_{Max,\ Propane}}}$	$S_{L_{Max}}$ Ft/Sec
Propane	1.00	1.41
Ethylene	1.75	2.32
Propylene	1.12	1.58

Figure 16 shows the variation of acoustic power with laminar flame speed. The independent variation of S_L is obtained by changing fuels with all other parameters held constant. But, there is a certain variation in fuel mass fraction F even when ϕ is constant because

$$F = \frac{\phi\left(\frac{F}{1 - F}\right)_{Stoic}}{1 + \phi\left(\frac{F}{1 - F}\right)_{Stoic}} \tag{9}$$

and $\left(\frac{F}{1 - F}\right)_{Stoic}$ for propane, propylene and ethylene are 0.064, 0.625 and 0.0677 respectively. However, this variation in F is small in comparison with the S_L variation and it will be shown later that the exponent on F is smaller, also. Figure 16 should, therefore, yield estimates of the scaling on S_L. Acoustic power appears to scale to an exponent of 1.4 - 1.6 with S_L for fuel lean to stoichiometric mixtures. This confirms the belief that noise reduction can be achieved by reducing the reactivity of the fuel. The extent of reduction possible, however, cannot be appreciable due to a rather low value of the exponent.

Combined Scaling Law. Although the study of a phenomenon dependent on many parameters can be made by varying them one at a time and this results in ease and clarity of analysis, it is not without disadvantages. The most serious disadvantage is that a large number of experiments would have to be performed, this number increasing rapidly with the number of independent parameters. Also, such an analysis using one variable at a time does not utilize all the information that can be obtained from the

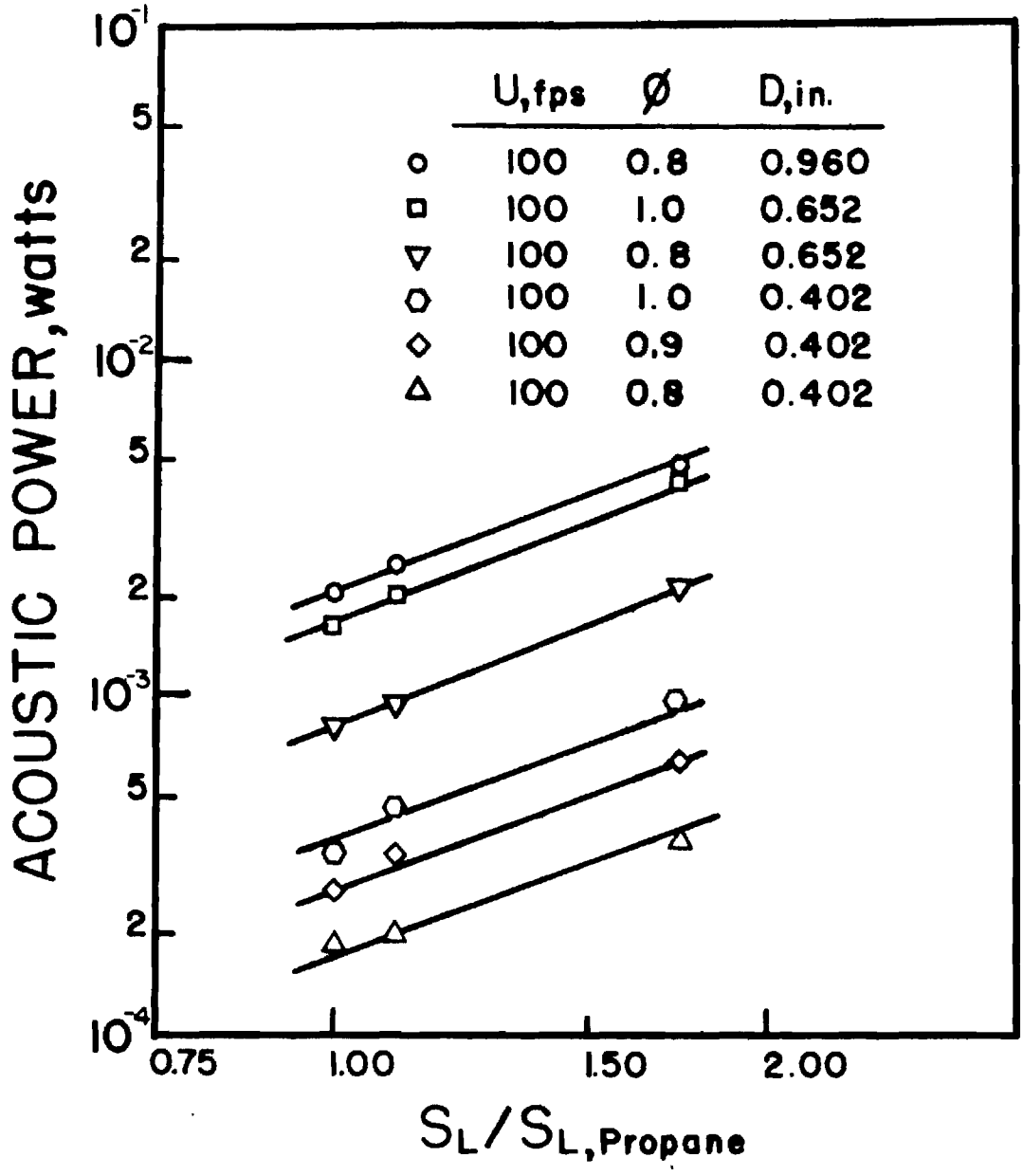

Figure 16. Acoustic Power as a Function of Laminar Flame Speed.

test results. At certain times, it is possible that two dependent parameters be considered independent without ever suspecting otherwise. If such a coupling exists there is a possibility that the process of obtaining a combined law would give some indications to that effect.

An effective means of examining the experimental data is by regression analysis in which a theoretically derived law is fitted to the experimental data. In this case, the possible law would be of the type

$$y = K \prod_{i=1}^{N} x_i^{c_i} \tag{10}$$

where K and the c_i's are constants and the x_i's are parameters affecting a quantity y. By taking logarithms on both sides of Equation (10), it is possible to curve fit as a linear problem by the method of least squares.

For the case of acoustic power P scaling, Strahle has suggested that the parameters are U, D, S_L and F. Using 57 different tests the following expression was obtained for the acoustic power radiated from open turbulent premixed flames:

$$P = 4.89 \times 10^{-5} \, U^{2.68} \, D^{2.84} \, S_L^{1.35} \, F^{0.41} \text{ watts} \tag{11}$$

where

$$50 \leq U(\text{fps}) \leq 600$$

$$0.0335 \leq D(\text{ft}) \leq 0.08$$

$$0.6 \leq \phi \leq 1.0$$

U and S_L are in fps and D is in ft

An analysis of errors due to the regression fit showed a mean error of 5.7% with 124% and -55% as the maximum and minimum errors respectively The standard deviation was 37%. These errors appear at first sight to be rather large. However, they can be considered very reasonable because of the following reasons:

a) A very wide range of acoustic powers (from 10^{-1} to 10^{-5} watts) are included in Equation (11).

b) The instrumentation accuracies are of the order of a db (if power P_1 is 1 db larger than P_2, then P_1/P_2 will be as large as 1.25), and

c) The flow measurement accuracy was no better than 3% of full flow rates. The flow inaccuracies can affect U and mixture ratio. The error in mixture ratio will introduce errors in both F and S_L.

In order to graphically observe the significance of the regression fit, the calculated values of acoustic power ($P_{regression}$) were cross plotted against the measured values ($P_{measurement}$) in Figure 17. Without doubt it can be said that Equation (11) fits the experimental data very well. Thus, it can be stated that acoustic power can, in fact, be represented by a power type law with respect to the parameters U, S_L, D and F. Further, laminar flame speed S_L appears to be quite adequate to represent the chemistry effect due to various fuels.

It is interesting to note that some of the Smith and Kilham[3] data plotted on Figure 17 show that the measurements of Smith and Kilham can be reproduced satisfactorily by Equation (11). Reference 3 deduced a $(US_LD)^2$ law for acoustic power. Equation (11) can explain the results of Reference 3 and has been obtained over a much wider range of acoustic

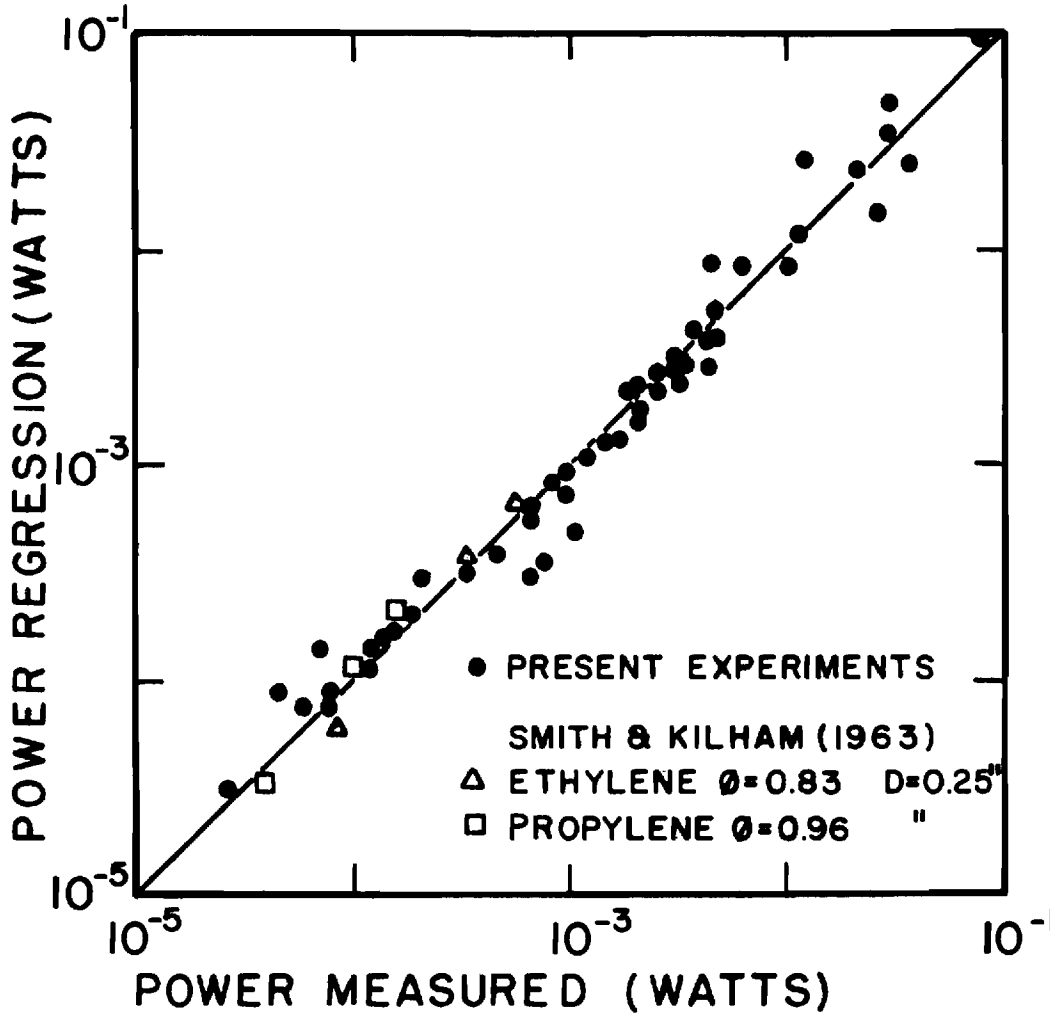

Figure 17. Significance of the Regression Fit for Acoustic Power.

powers, thus establishing a clear preference over the $(US_L D)^2$ law. Surprising as it may seem, Equation (11) is the first empirical relation published from which acoustic power can be calculated directly for noise from hydrocarbon-air turbulent flames. Equation (11) should prove quite useful to anyone interested in determining noise output from combustion zones.

Thermo-Acoustic Efficiency

Thermo-acoustic efficiency is a measure of the portion of total thermal input to the flame converted into noise radiation. Thermo-acoustic efficiency η_{ta} is defined as

$$\eta_{ta} = \frac{\text{Acoustic Power Radiated}}{\text{Thermal Input}} \tag{12}$$

If $\dot{m}$ is the mass flow rate of reactants, and H is the heating value per unit mass of fuel, then

$$\text{Thermal input} = \dot{m}FH$$

where as before F is the fuel mass fraction,

$$\dot{m} = \rho_o \frac{\pi}{4} D^2 U$$

and ρ_o is the density of mixture of reactants. Thus,

$$\eta_{ta} = \frac{P}{\frac{\pi}{4} \rho_o U D^2 F H} \tag{13}$$

Therefore, the scaling laws for η_{ta} can be obtained from scaling laws for acoustic power radiated. For the premixed open turbulent flames of this study, $\eta_{ta} \propto U^{0.7} D^{0.8} F^{-0.6} S_L^{1.4}$ would represent the behavior of η_{ta}. Some representative values of thermo-acoustic efficiency are presented in Table 4. The results for a burner of diameter 0.402" and equivalence ratio of 0.8 are shown over the entire velocity range. The maximum η_{ta} is of the order of 10^{-6}. This indicates that for high velocity flames combustion noise could in fact be quite substantial.

Table 4. Thermo-Acoustic Efficiency

Test	Power Watts	$\eta_{ta} = \frac{\text{Power Radiated}}{\text{Thermal Input}}$
P- 50-0.8-1	0.264×10^{-4}	8.36×10^{-9}
P-100-0.8-1	0.183×10^{-3}	2.89×10^{-8}
P-200-0.8-1	0.154×10^{-2}	1.22×10^{-7}
P-300-0.8-1	0.423×10^{-2}	2.23×10^{-7}
P-400-0.8-1	0.103×10^{-1}	4.01×10^{-7}
P-500-0.8-1	0.271×10^{-1}	8.57×10^{-7}
P-600-0.8-1	0.382×10^{-1}	1.01×10^{-6}

Spectral Content of Combustion Noise

The acoustic emission from regions of turbulent combustion has

been recognized in the literature as a broad-band noise with a single peak in the 250 Hz - 1500 Hz range. Discrete frequency components appear when the combustion is confined by enclosures[22,26]. This is not of interest to the present study of open turbulent flames. The frequency spectra will clearly indicate the type of acoustic material that will be needed for noise reduction treatments. Furthermore, the peak frequency will establish the characteristic time in the flame and comparison with the theories in References 17 and 18 will assist in determining the most plausible mechanism of noise generation.

Procedure. The frequency spectra of noise were obtained from the tape recording of sound pressure signals. A Hewlett Packard Fourier analyzer was used. The analyzer was programmed to produce power spectra by the following process. First the analog signal is digitized. Then, the Fourier transform is taken. This is multiplied by its own complex conjugate. The process is repeated a set number of times to obtain a stable average. The number of samples required depends on the particular signal being analyzed. Also, the number of digital bits of information used in each sample decides the maximum frequency and the frequency resolution.

A low-pass filter was inserted between the Fourier analyzer and the tape-recorder (Figure 5) to eliminate all frequency components above a preselected maximum. If this is not done the high frequency components will fold over and appear as spurious low frequency components due to the inherent quality of all A to D converters called aliasing. After a preliminary study, the maximum frequency was selected at 8 kHz for the noise spectra. Since the filter frequency response is not flat

beyond 0.8 $f_{cut\text{-}off}$ only spectra up to 5 kHz are presented in this report. The initial spectra were obtained with the number of samples used in averaging between 15 and 200. The 15 sample averaging was found to be adequate to obtain all the information required while the 200 sample averaging resulted in smoother spectra with less scatter. Thus a majority of the combustion noise spectra were obtained with 15 to 50 sample averaging.

The frequency spectra depend on U, D, S_L and F. Also, if combustion noise radiation directionality is frequency dependent, then the spectra depend on the microphone location as well. The spectra shown in the figures that follow are smooth lines drawn through the spectra plotted on the x-y plotter. Figure 18 shows both the actual x-y plot and the smooth line drawn through the mid-points for a typical case. The smooth line is found to be quite satisfactory for representing the spectrum.

Results. The frequency dependence of directionality is studied in Figures 19(a) and (b). Very similar spectra were obtained in all the tests conducted. The azimuth and radius are referenced to the burner exit in these figures. Thus, amplitude comparisons cannot be made directly without correcting the results for the acoustic center. The information regarding directionality can, of course, be obtained from Figures 19(a and b) without any corrections. If the directionality patterns were independent of frequency the spectra at various azimuthal locations would be parallel to each other. An examination of the spectra reveals that directionality of noise generated is almost independent of frequency except for the locations near the axis of the flame which

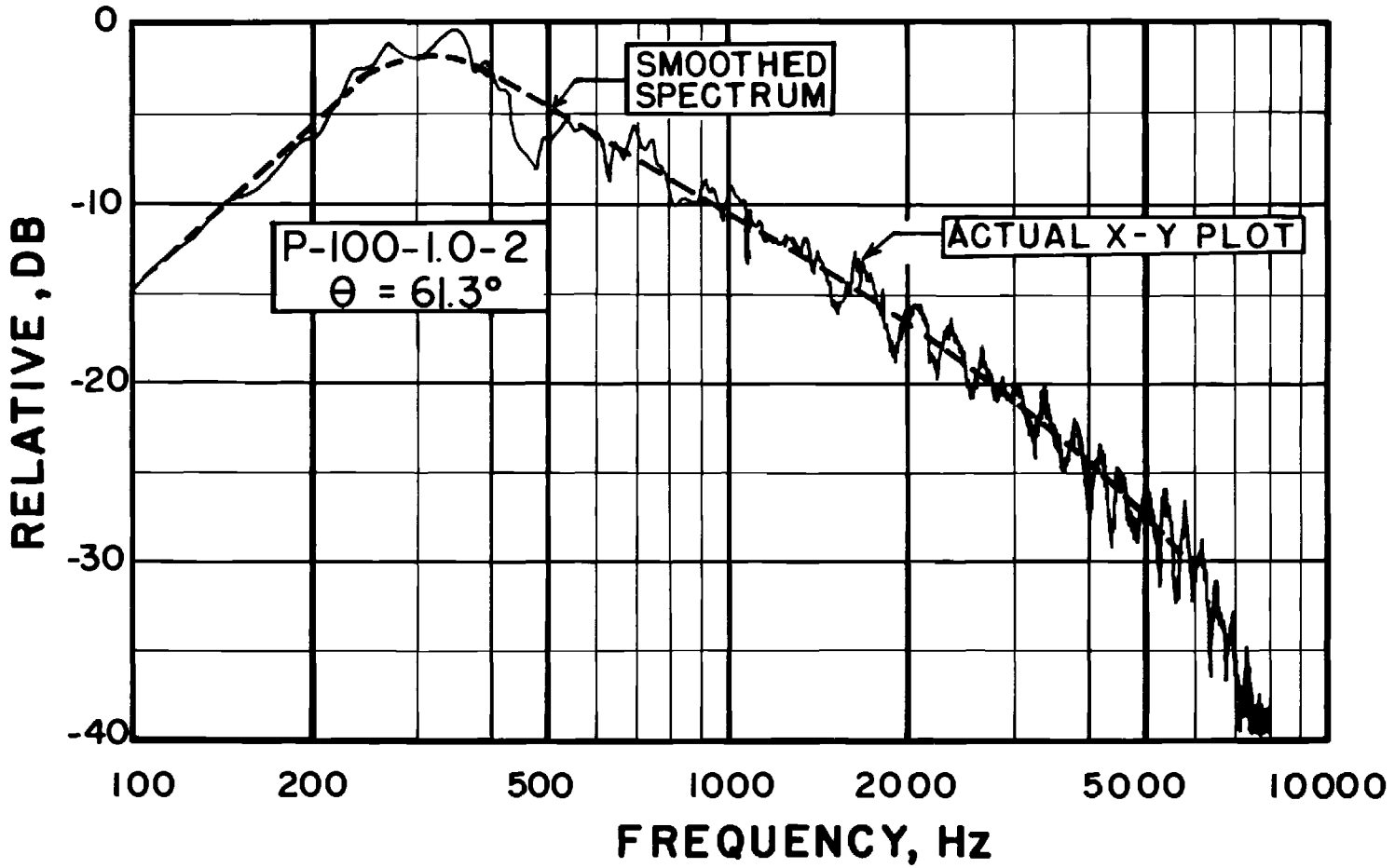

Figure 18. Actual X-Y Plot and Smoothed Spectrum.

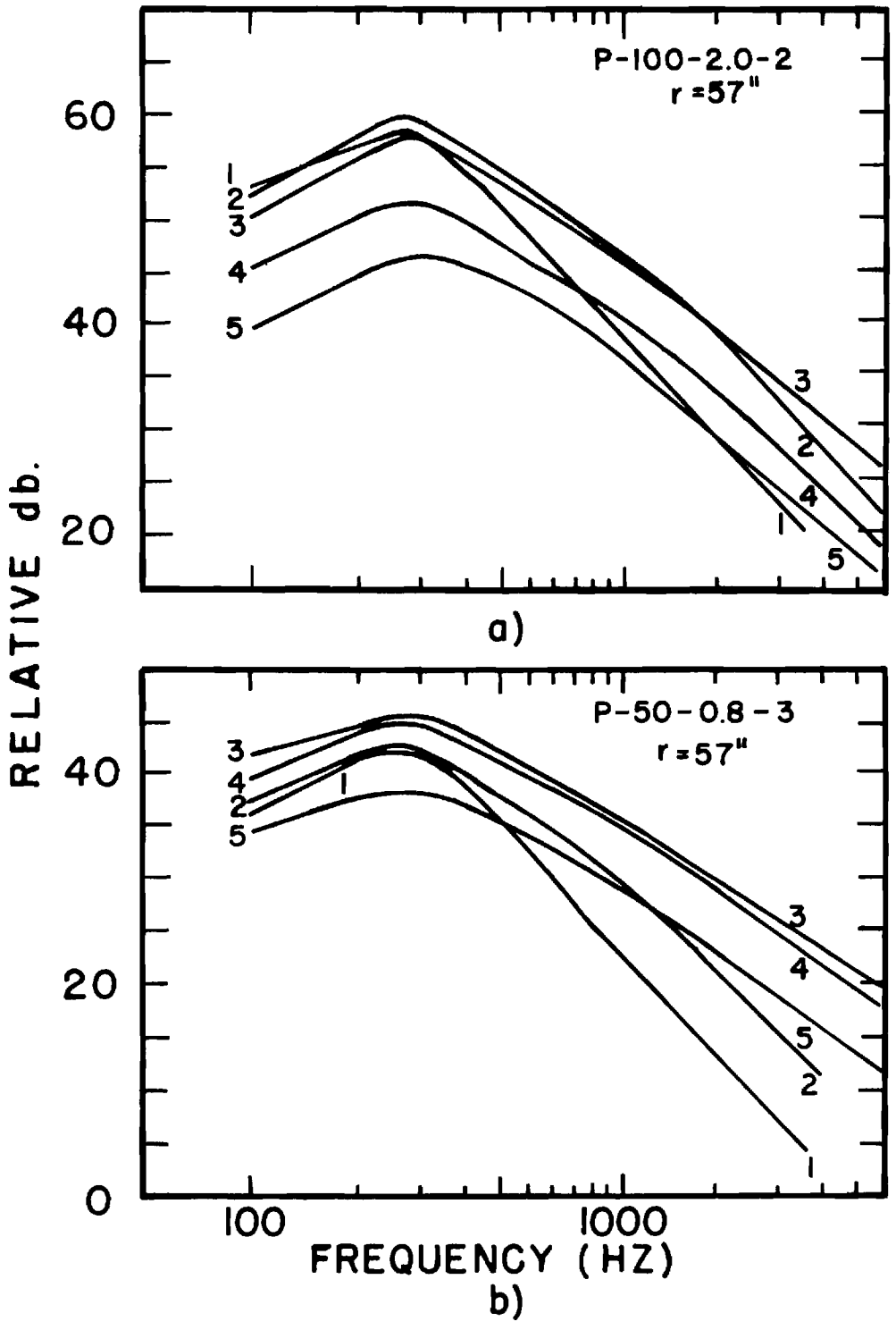

Figure 19. Frequency Dependence of Directionality. The Numbers 1 to 5 Indicate Microphone Locations between 15° and 120°.

exhibit a strong reduction in the high frequency components. Reference 9 observed a much stronger dependence for pure diffusion flames of CH_4 and H_2 burning in air.

Figure 20 presents the effects of flow velocity and laminar flame speed on the frequency spectra. There is clearly a tendency for the peak frequency (frequency corresponding to maximum amplitude on the spectrum) to increase with flow velocity. However, the rate of increase is small. For propane over a 12:1 velocity range the peak changes from 350-270 Hz while for ethylene over a 10:1 velocity range the peak frequency varies between 650 and 350 Hz. The increase in peak frequency is a little more marked for ethylene-air mixtures in comparison with propane-air mixtures. In any case, the peak frequency is a very weak function of flow velocity and it appears doubtful if using Strouhal number (f D/U) as a non-dimensional parameter as suggested in References 3 and 5 would serve any useful purpose. Use of Strouhal number has been found appropriate for jet noise in Reference 20, where the peak frequency is found to scale inversely with D and directly with U. The experiments for fuel rich flames also showed a similar velocity behavior. Further, Figure 20 shows that the peak frequency for ethylene is higher than that for propane. Since ethylene has higher S_L values this is clearly an effect due to S_L. It appears, therefore, that the characteristic time in the flame is considerably influenced by the chemical time.

Combustion noise can be seen to peak at lower frequencies with an increase in burner diameter in Figures 21(a), (b) and (c). This diameter effect, however, is quite small when compared with a 1/D dependence for jet noise. Again, Strouhal number appears to be inappropriate for

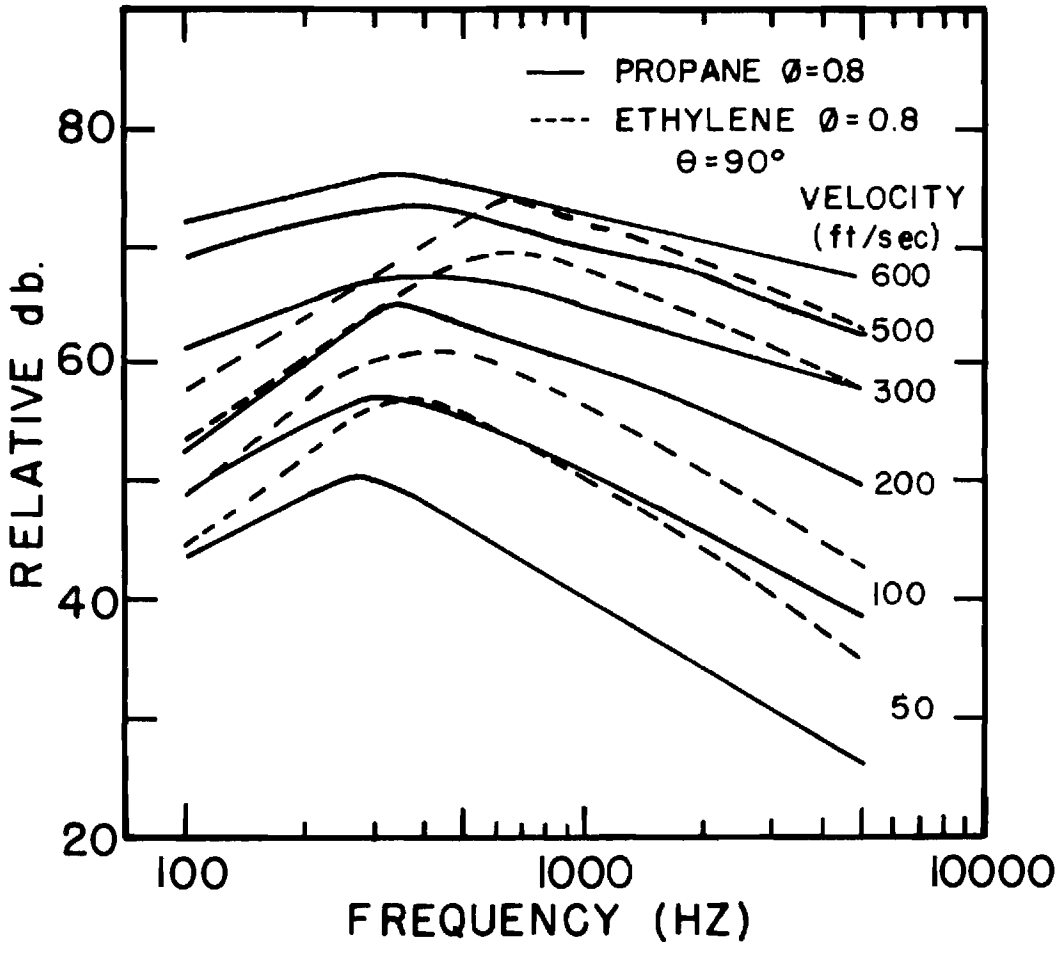

Figure 20. Effects of Velocity and Laminar Flame Speed on the Frequency Spectra.

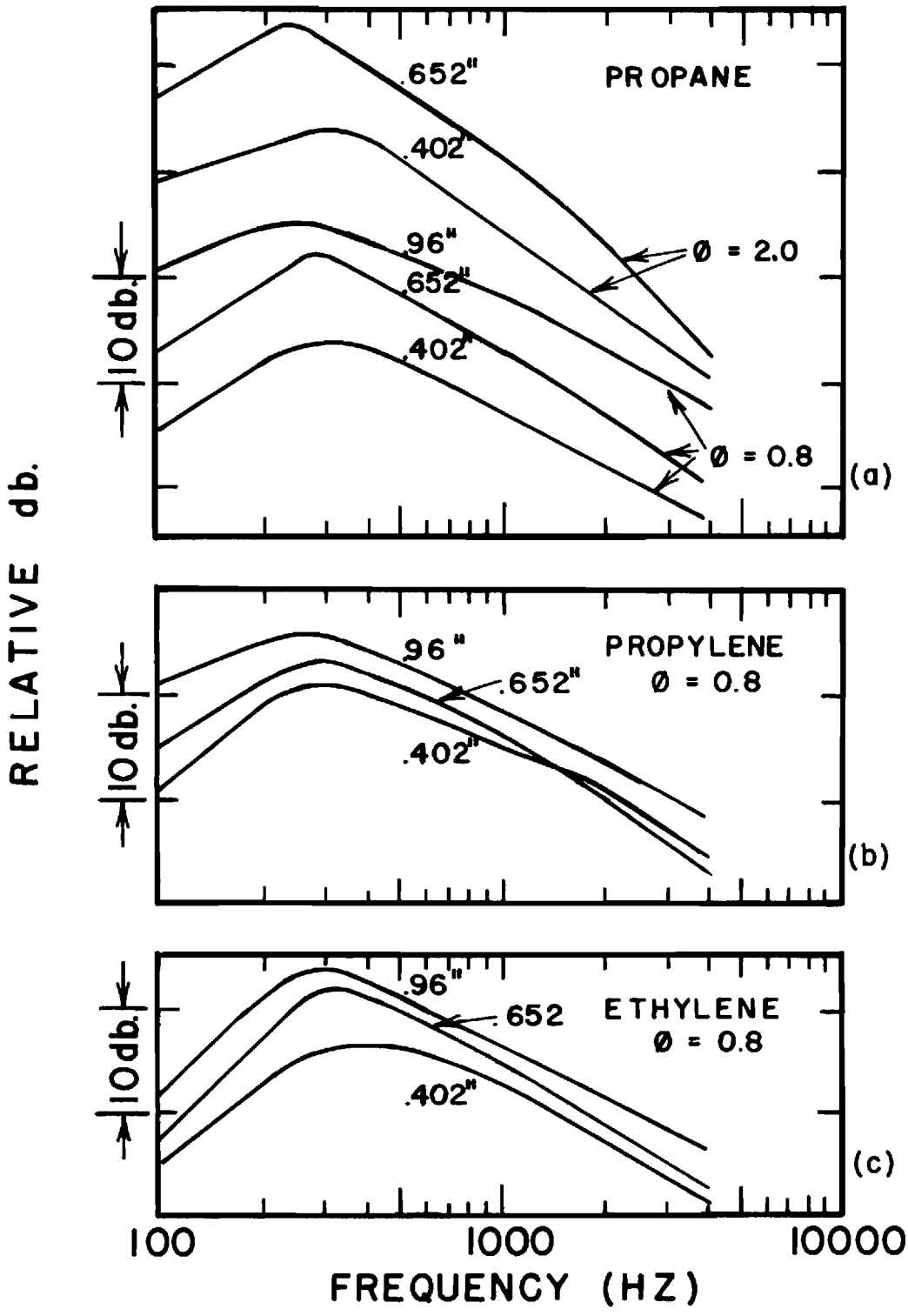

Figure 21. Effect of Burner Diameter on the Frequency Spectra.

combustion noise.

Figure 22 shows the effect of equivalence ratio on frequency spectra. While propane and propylene flames show negligible effects the ethylene flames show some effect due to equivalence ratio.

Peak Frequency. A power type law (Equation (10)) was fitted by regression analysis to the peak frequencies measured. The procedure followed was identical to the one used for obtaining acoustic power law (Equation (11)). If f_c is the peak frequency then the regression analysis gives

$$f_c = 11.83\ U^{0.19}\ D^{-0.082}\ S_L^{0.53}\ F^{-0.69}\ \text{Hz} \qquad (14)$$

where U and S_L are in fps and D is in ft.

$$0.6 \leq \phi \leq 1.0$$

$$50 \leq U(\text{fps}) \leq 600$$

$$0.0335 \leq D(\text{ft}) \leq 0.08$$

The number of tests was 56, the mean error was 0.85% and the standard deviation was 13.4%. Equation (14) shows that S_L and F have the most effect on peak frequency and U and D effects are negligible. An inverse S_L and F scaling would explain the negligible ϕ dependence of propane and propylene flames shown on Figure 22. The behavior of f_c of ethylene flames with ϕ is somewhat anomalous.

Discussion of Results

A discussion of the experimental results of this study in the light of the theories of Strahle[16,17,18] and other experimental results

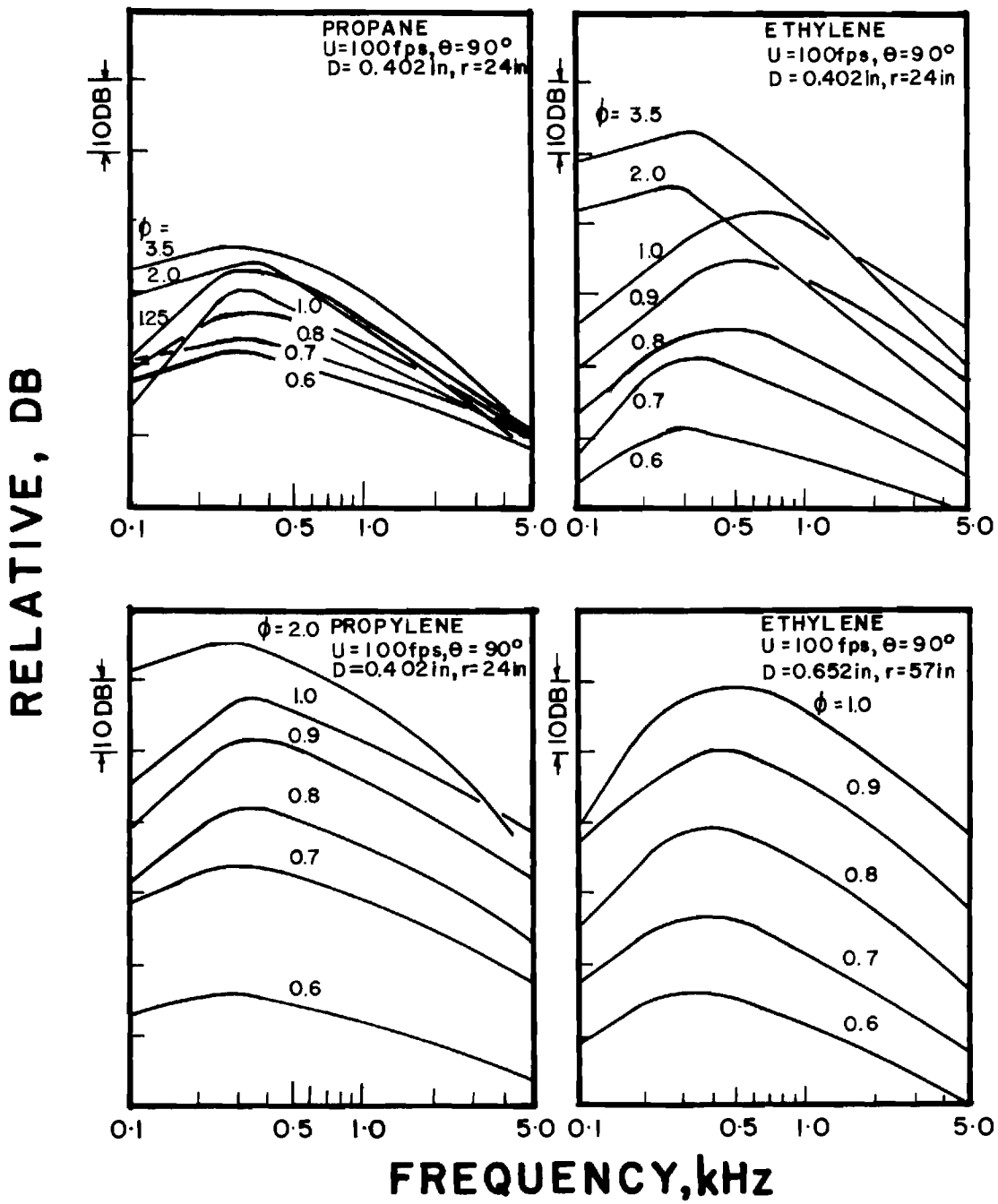

Figure 22. Effect of Equivalence Ratio on Frequency Spectra.

that are available will be presented in the succeeding paragraphs.

The directionality of combustion noise is seen to be rather weak. In this study the maximum difference, between the maximum sound pressure level and the minimum (observed at the $\theta = 0^{\circ}$ location) sound pressure level over a constant radius path around the flame in a plane containing the flame axis, was about 4 db. The general lack of strong directionality would support the monopole theory of noise generation. Further, there is some similarity between the experimental results for directionality and the directionality patterns deduced in Reference 18 considering refraction at temperature discontinuities. Thus, the directionality patterns can qualitatively be explained by the refraction theory. The general tendency for the location of peak sound pressure to shift towards the axis with an increase in velocity is a result of the convection effect. The spectra of the sound pressures as measured by the five microphones at various aximuthal positions have shown that directionality is frequency dependent to the extent that the high frequency components drop off rather rapidly towards the burner axis. The results of Reference 18 considering refraction effects showed a similar effect with increasing frequencies. Thus, the high frequency fall-off near the axis could be at least qualitatively explained by the refraction effect. The directionality patterns of Reference 3 have general similarity with the patterns presented in this work. Price et al saw a more marked effect of frequency on directionality for a pure diffusion flame of H_2-CH_4 burning in air. Except for some results with the 0.402" burner all other results show maximum noise radiation at 50° - 80° to flow direction. An off-axis maximum is very important for noise reduction efforts using acoustic liners.

The spectra of combustion noise show a predominantly low frequency nature. They show a broad-band noise with a single peak and a gradual amplitude fall-off on either side of the peak. The rate of fall-off on the high velocity cases was observed to be rather slow. This could be due to the fact that the difference between jet noise and combustion noise decreases with flow velocity as shown in Figure 7. Thus, the higher velocity flames show a slight increase in higher frequency components. The noise spectrum, however, is decided by the predominant combustion noise. The peak frequency does not seem to be strongly influenced by any parameter. F and S_L appear to have the most effect. For all practical purposes one could summarize the experimental findings by stating that combustion noise peaks in the 250-700 Hz range for hydrocarbon-air flames. The values of peak frequencies obtained here are in excellent agreement with the values obtained by References 3, 11 and 15 for premixed flames. Even diffusion flames of Reference 12 seem to support the above statement. Hurle et al report a peak frequency of 1200Hz for a stoichiometric ethylene-air flame on a 0.175" diameter burner. This value is slightly higher than what would be obtained from the peak frequency relation deduced in this work (Equation (14)). However, the spectra of Kotake and Hatta[5], which show for stoichiometric natural gas-air flames a flat low-frequency spectra, look improbable in view of the extensive analysis of our study which always showed a recognizable low frequency fall-off. Also, it appears quite improper to try to use Strouhal number to non-dimensionalize combustion noise peak-frequencies as suggested by References 3 and 5.

The results shown in Equation (14) emphasize that chemical time is an important characteristic time in the flame. Referring to Strahle's[17]

theories, all the three models of turbulent combustion can explain the values of peak frequencies reported.

The scaling laws for acoustic power and thermo-acoustic efficiency generated in this work are considered to be a major contribution to the noise data on open turbulent flames. The scaling laws have been obtained over a much wider range of values of the parameters compared to those of the only other similar work[3]. Also, Smith and Kilham[3] deduced the scaling laws on only U by actual sound pressure measurement around the flame while obtaining those on S_L and D by a single microphone sound pressure measurement. Further, the important parameter F was not considered in their work. In addition, the experimentally measured acoustic powers of Reference 3 could be reproduced by the experimental regression equation, Equation (11), of this study as shown on Figure 17. Thus, it is felt that the scaling laws for acoustic power presented in Equation (11) are more representative of noise radiation than the $(US_LD)^2$ scaling of Reference 3.

The scaling laws for acoustic power deduced by Strahle[17] showed that for premixed flames, Equation (5)

$$P = K\, U^{a_1}\, S_L^{a_2}\, F^{a_3}\, D^{a_4}\, \ell_t^{a_5}\, \mathcal{I}^{a_6}$$

would allow: $a_1 = 2 - 3.5$, $a_2 = 2 - 5$, $a_3 = -1.8$, $a_4 = 2$, $a_5 = 1.5 - 3$ and $a_6 = 0 - 2.5$, depending upon the model of turbulent combustion considered. Notice that with reference to a_3, a relation $(\Delta\rho/\rho F)^2 \propto F^{-1.8}$ has been used. This relation was obtained for premixed hydrocarbon-

air flames at room temperature and atmospheric pressure using the data available in Reference 27. Comparing the scaling laws above with Equation (11), it can be seen that the exponent on U is within the values of a_1 specified by the theory. In view of the facts that only D is considered in Equation (11) and the result $\ell_t \propto D$ from Chapter III, the theory would allow a D exponent between 3.5 and 8 as compared with the experimental value of 2.8. For S_L, the theoretical expectation allows an exponent between 2 and 5 and experimentally 1.4 is observed. As far as F scaling is concerned, an error of F^2 has been noticed in the autocorrelation estimation of Reference 17. If this is taken into account, a $F^{0.2}$ law would result against the experimental $F^{0.4}$ law. Thus, the theoretical estimates of Reference 17 do not fall completely in line with the experimentally generated scaling laws. The basic differences may be attributed to incorrect order of magnitude estimates made in the theory of Reference 17 with extremely limited knowledge available at that time. The experimental results of this study should prove very useful in clarifying the differences between the theoretical and experimental scaling laws.

CHAPTER III

DIRECT FLAME PHOTOGRAPHY

The decomposition of combustion noise scaling rules can be in part achieved by a direct flame photographic technique. From Equation (4),

$$P \propto \int_V dV\ (\underset{\sim}{r}_o) \int_{V_d} C(\underset{\sim}{r}_o, \underset{\sim}{d})\ dV\ (\underset{\sim}{d}) \tag{15}$$

where C is an autocorrelation of the reaction rate and V_d is a correlation volume. The second integral is over V, the reacting volume, which is of interest to this study. It is furthermore shown that the order of magnitude of Equation (15) may be expected to be given by

$$P \propto V\ V_d\ \bar{C} \tag{16}$$

where $\bar{C}$ is an order of magnitude estimate of C. The reacting volume is, therefore, a fundamental quantity in establishing the scaling laws for combustion noise. The scaling laws on reaction volume directly affect the scaling rules for combustion noise. An investigation of the parametric behavior of the flame volume is, therefore, a useful step in understanding the origin of combustion noise. A theoretical evaluation in Reference 17 deduced an analytical expression for the order of magnitude of the reacting volume based on physical reasoning. Three different models of

turbulent combustion were considered. The analytical expression developed was

$$V = K\, U^{a}\, D^{b}\, S_L^{c}\, F^{d}\, \ell_t^{e}\, \mathcal{I}^{f} \tag{17}$$

where V is the flame volume, U is the mean flow velocity, D the burner diameter, S_L the laminar flame speed, F the fuel mass fraction, ℓ_t the turbulence length scale and $\mathcal{I}$ the relative intensity of turbulence. K, a, b, c, d, e and f are constants. Depending upon the model of turbulence chosen the exponents would take the values as shown in Table 5.

Table 5. Scaling Laws on Reacting Volume from Strahle's Theory

	Exponents on					
	U	D	S_L	F	ℓ_t	$\mathcal{I}$
Model of Turbulent Combustion	a	b	c	d	e	f
Wrinkled Flame (WF)	1	2	-1	0	1	0
Slow Distributed Reaction (SDR)	$\frac{1}{2}$	2	-2	0	$\frac{1}{2}$	$\frac{1}{2}$
Fast Distributed Reaction (FDR)	1	2	-1	0	1	0

Thus having established the importance of analyzing the flame volume in the development of the theory of combustion noise a need of an experimental study of the subject became evident. If the scaling laws could be experimentally determined for the turbulent flame volume and compared with the theoretical predictions of Reference 17 a substantial improvement in the understanding of scaling laws for combustion generated

noise would result. Also, an investigation of this kind would answer, at least partially, questions on the turbulence structure in the reaction zone.

An experimental program was therefore developed to decompose the scaling rules for the flame volume. Spectroscopic studies[28] of hydrocarbon flames have shown that the luminosity of the flame brush is due to the emission of active radicals like CH, C_2 and OH in the reaction zone. Since these active radicals are present only in the active reaction zone, the volume of the combustion region can be obtained by direct photography viewing the flame through an optical filter centered on the radiation of a particular radical. The volumes could be measured by tracing out the density curves on a microdensitometer.

The technique of direct photography is fast, direct and simple compared to methods where thermocouples are used to estimate the extent of the reaction zone. In fact, the direct photography method is free from the errors due to the presence of the probe in the flame and the positional inaccuracy of the probe caused by vibrations and deflections due to aerodynamic forces[29]. An evaluation of the accuracy of the photographic method will be done at a later stage in this chapter.

Dimensional Analysis

Dimensional analysis is based on the fundamental requirement of dimensional homogeneity in a physical equation. If it is possible to recognize all the parameters that affect a physical quantity, dimensional analysis can provide an insight into the parametric behavior. The functional form, however, cannot be determined by the dimensional analysis.

Following the arguments of Reference 17 it is reasonable that the parameters that can affect the reacting volume V are: flow velocity, U, burner diameter, D, laminar flame speed, S_L, turbulence velocity in the axial direction, u', turbulence length scale, ℓ_t, and finally the fuel mass fraction, F, which is already nondimensional. Thus over a limited range of the independent variables it is fair to assume

$$V = K\, U^{\ell}\, D^{m}\, S_L^{n}\, u'^{p}\, \ell_t^{q}\, F \tag{18}$$

Here, since the fundamental dimensions involved are only length and time and there are six unknowns to determine, there will be four nondimensional groups. By dimensional reasoning the following V dependence is obtained

$$\frac{V}{D^3} = \text{fn}\left\{\left(\frac{u'}{U}\right),\ \left(\frac{U}{S_L}\right),\ \left(\frac{\ell_t}{D}\right),\ F\right\} \tag{19}$$

Any further explanation based on Equation (19) will be deferred until after the experimental results are presented.

Experimental Procedure

The burners and flow systems used have already been explained in Chapter II. The flame is photographed using a Graflex Speed Graphic Camera and 4" x 5" black-and-white panchromatic film. An optical filter centered on the CH radiation (4315Å) is used in this work since CH is one of the predominant components in the emission spectra of these flames. More importantly, however, it is found from Reference 30 that the spectral

intensity of CH emission is much more pronounced than any other in fuel lean flames of propane-air. Thus, CH emission is more appropriate for determining the reaction volume since a majority of the experiments were planned using this fuel.

The filter used in this investigation has a half peak transmittance bandwidth of about 500 Å and a peak in the vicinity of 4300 Å. The flames are photographed inside an anechoic chamber since these experiments are done parallel with the acoustic measurements. As far as optical studies are concerned the anechoic chamber serves to prevent extraneous drafts around the flame and also eliminates stray light when photographs are being taken. A microdensitometer is used to measure the image of the flame recorded on the photographic negative.

Measurement of the Flame Volume

A turbulent premixed flame stabilized at the end of a burner tube has a luminous zone contained between fairly well-defined inner and outer cones. Although the inner and the outer cones of the flame are qualitatively simple to visualize, a quantitative study requires that certain criteria be adopted for the flame volume computation. In this study, it was decided to fix the outer boundary of the flame by defining it as the surface which has an intensity 0.1 I_{max}, where I_{max} is the maximum intensity recorded on the photograph. The definition of the inner cone presents additional difficulty since it is viewed through a part of the flame brush by the camera lens. A reasonable estimate is obtained, however, by considering the inner cone to be defined by the peaks in the densitometer trace. Figure 23 clearly explains the procedure adopted. In order to obtain the volume of the flame the densitometer traces were

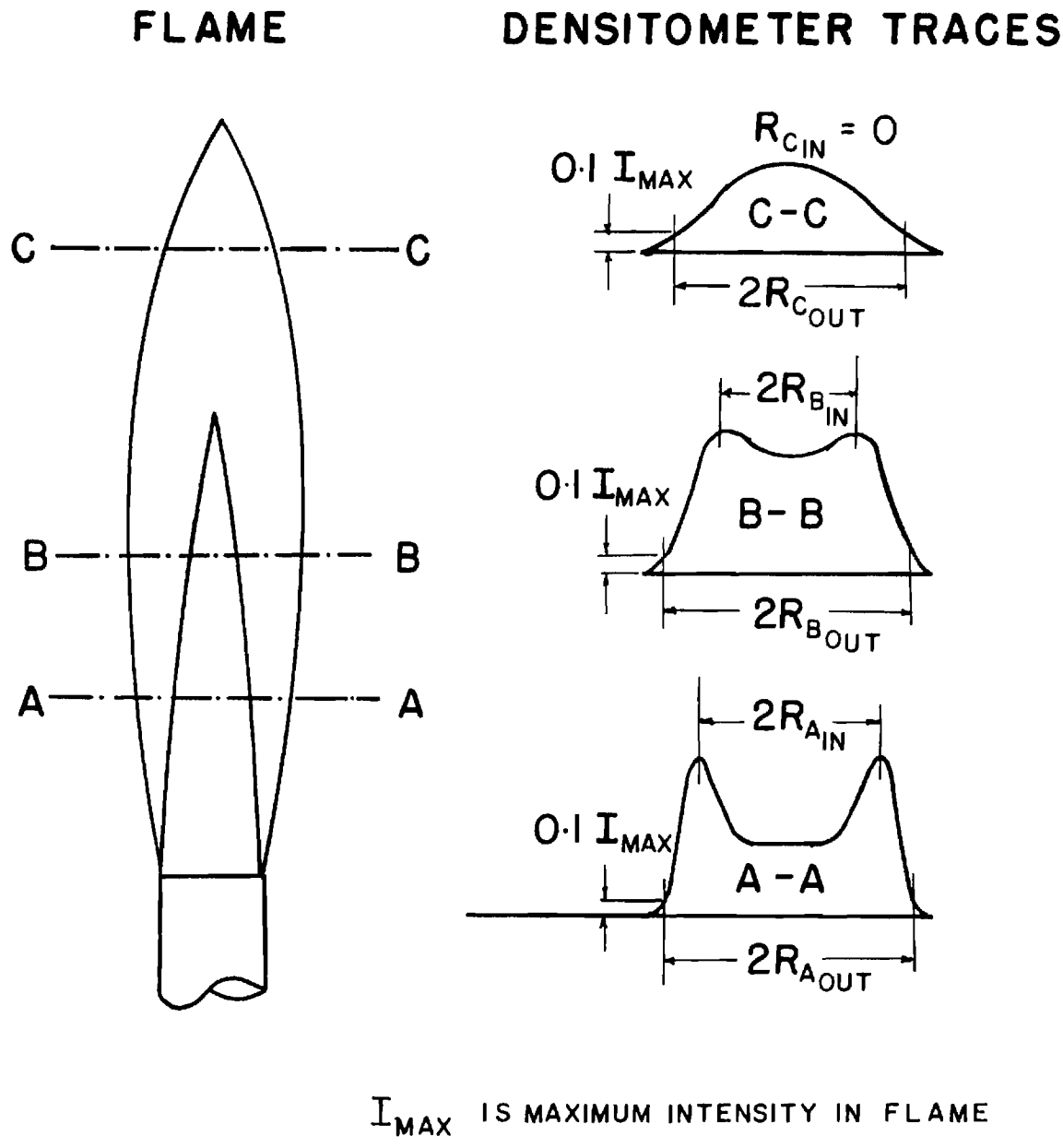

Figure 23. Flame Volume Measurement - Location of Inner and Outer Cones.

taken at various short distances along the length of the flame. From the traces the inner and outer radii were measured as shown in Figure 23. The volumes of the outer and inner cones between the adjacent sections were computed as truncated cones. The difference between their volumes gives the reaction volume between the two measurement sections. The total flame volume is then obtained as a simple sum of all such elemental volumes.

At this stage, it should be realized that an analysis of this kind does not yield the true volume of the reaction zone in a strict sense; but such an analysis is capable of furnishing acceptable scaling laws when the criteria set forth are consistently adhered to in all the tests.

Experimental Results

Acoustic Center Location

The determination of the location of the acoustic center was one of the important contributions to the acoustic measurements. Earlier it has been stated that the volume of the flame was computed as a simple arithmetical sum of the elemental volumes between various longitudinal sections. These elemental volumes were divided by the corresponding elemental length of the flame to obtain the volume per unit length which is plotted as a function of the flame length. Figure 24 shows two such plots. The acoustic center corresponds to the location of the maximum volume per unit length in the flame. The results of many experiments showed that the fraction of flame length at which the maximum volume per unit length occurred could be expressed as a function of equivalence ratio ϕ alone. This result simplified the task of determining the acoustic center to one of measuring the length of the flame. The relationship

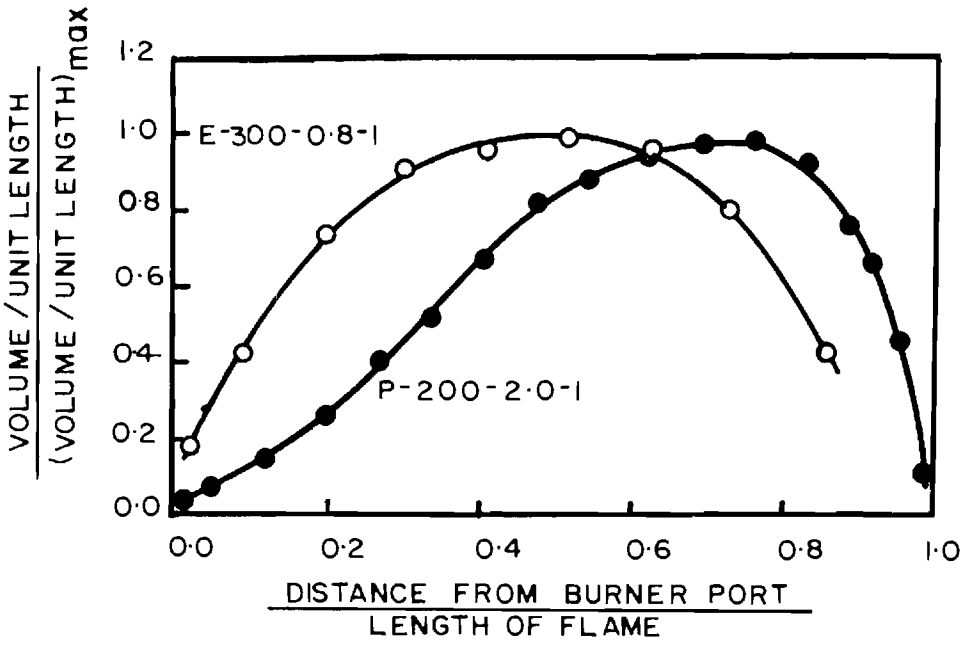

Figure 24. Flame Volume Distribution.

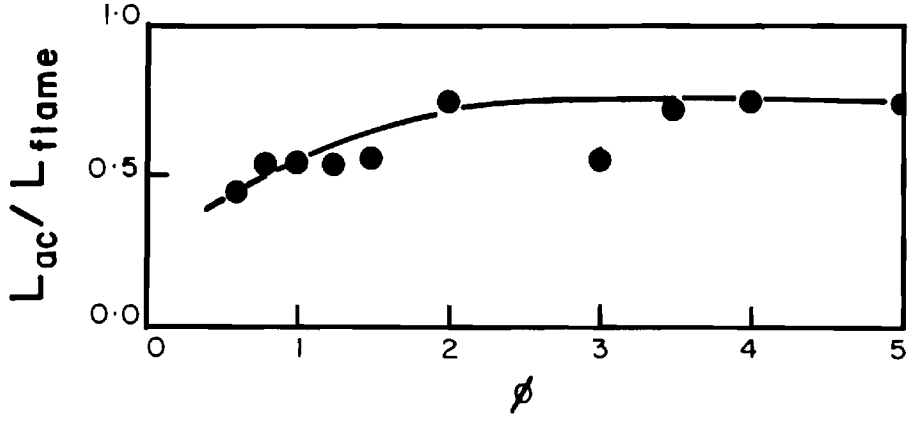

Figure 25. Distance L_{ac} from Burner Port at which Acoustic Center is Located as a Function of Equivalence Ratio.

between ϕ and fraction of flame length measured from burner port at which the acoustic center is located is shown in Figure 25. Figures 26(a), (b) and (c) present some data on the length of the flame which could be used in the determination of acoustic center. It is interesting to note that the flame length increases as only $U^{\frac{1}{2}}$ (Figure 26(a)) and as $D^{0.64}$ (Figure 26(b)). Further, the flame length achieves a minimum near stoichiometric mixtures as seen on Figure 26(c). This is simply a reflection of the fact that maximum laminar flame speed (and hence the turbulent flame speed) is obtained for conditions near stoichiometry.

Flame Volume Scaling Laws

The behavior of the flame volume with burner diameter is shown in Figure 27. It can be seen that the flame volume increases as the cube of the burner diameter. Table 5 (page 67) shows that both WF and FDR models of Strahle's theory can explain this result if the turbulence length scale ℓ_t is proportional to D. In cold jet flows it is known that the turbulence length scale is proportional to the jet diameter[31]. The result $V \propto D^3$ therefore presents a strong possibility that the turbulence length scale in the reaction zone is also proportional to the burner diameter. In Figure 27 the effect of S_L has not been eliminated from the data points.

Figure 28 presents the flame volume as a function of the mean flow velocity of the reactants in the burner tube. Based on the result of Figure 27 a D^3 correction has been applied to the flame volume so as to take care of the diameter effect and allow a simple graphical correlation. The flame volume is seen to scale linearly with flow velocity, which is in accord with the theories of Reference 17. Again on this plot the effects of S_L and F have not been considered. The tendency of the ethylene

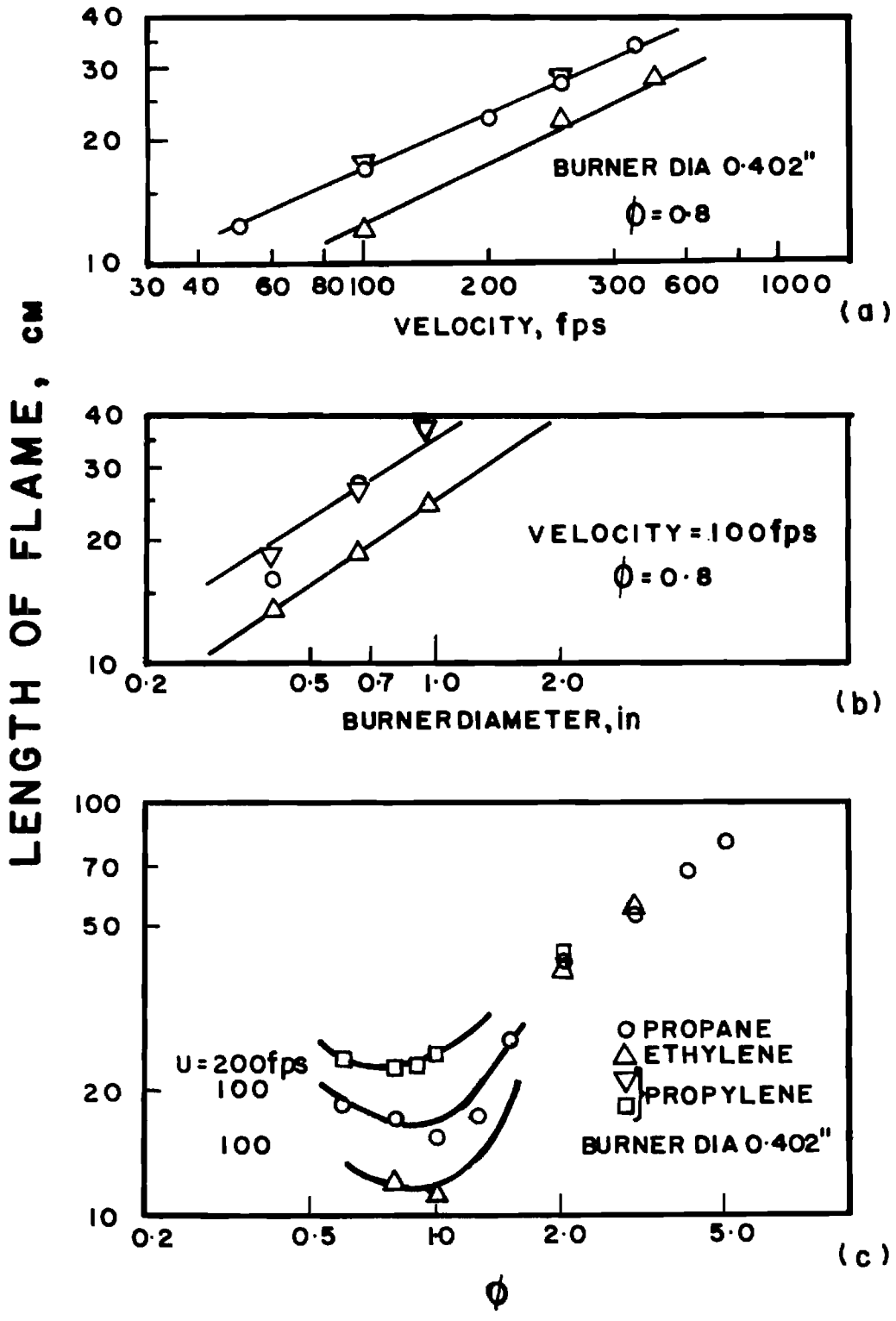

Figure 26. Length of Flame as a Function of a) Velocity, b) Burner Diameter, and c) Equivalence Ratio.

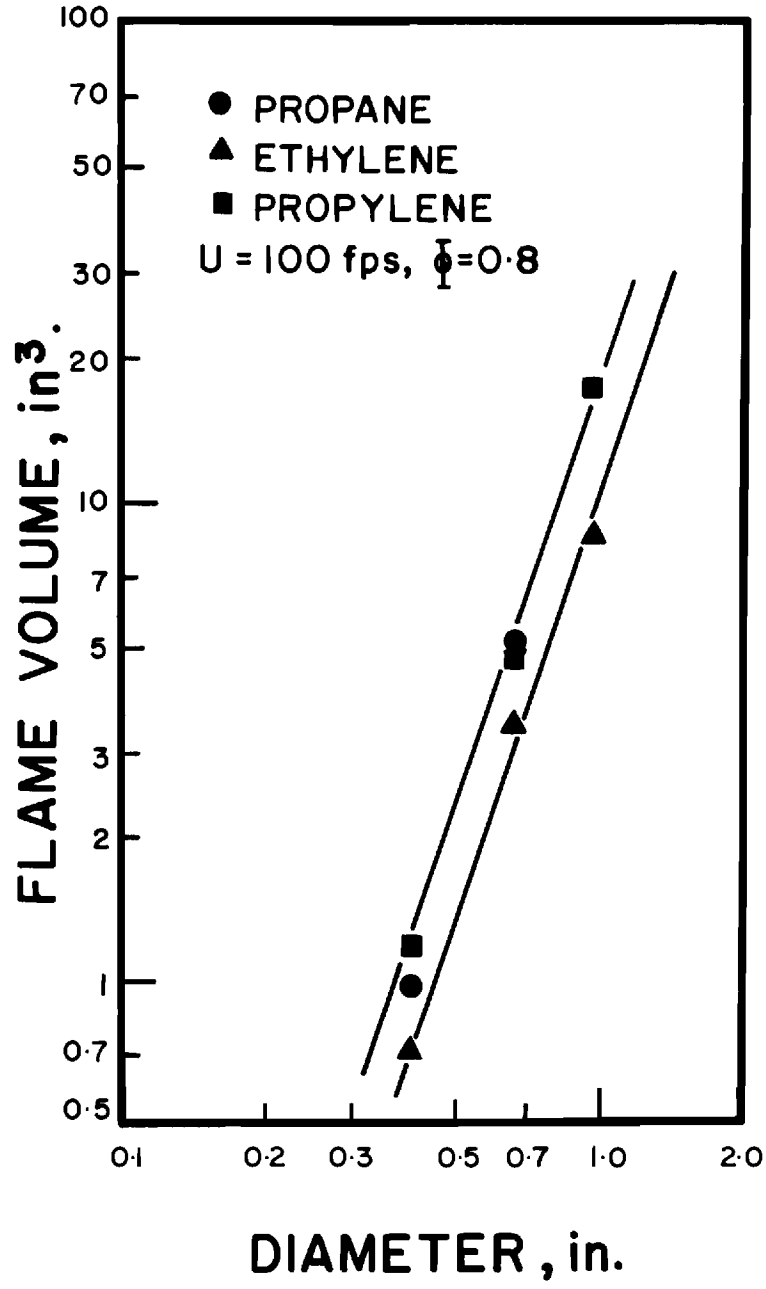

Figure 27. Flame Volume as a Function of Burner Diameter.

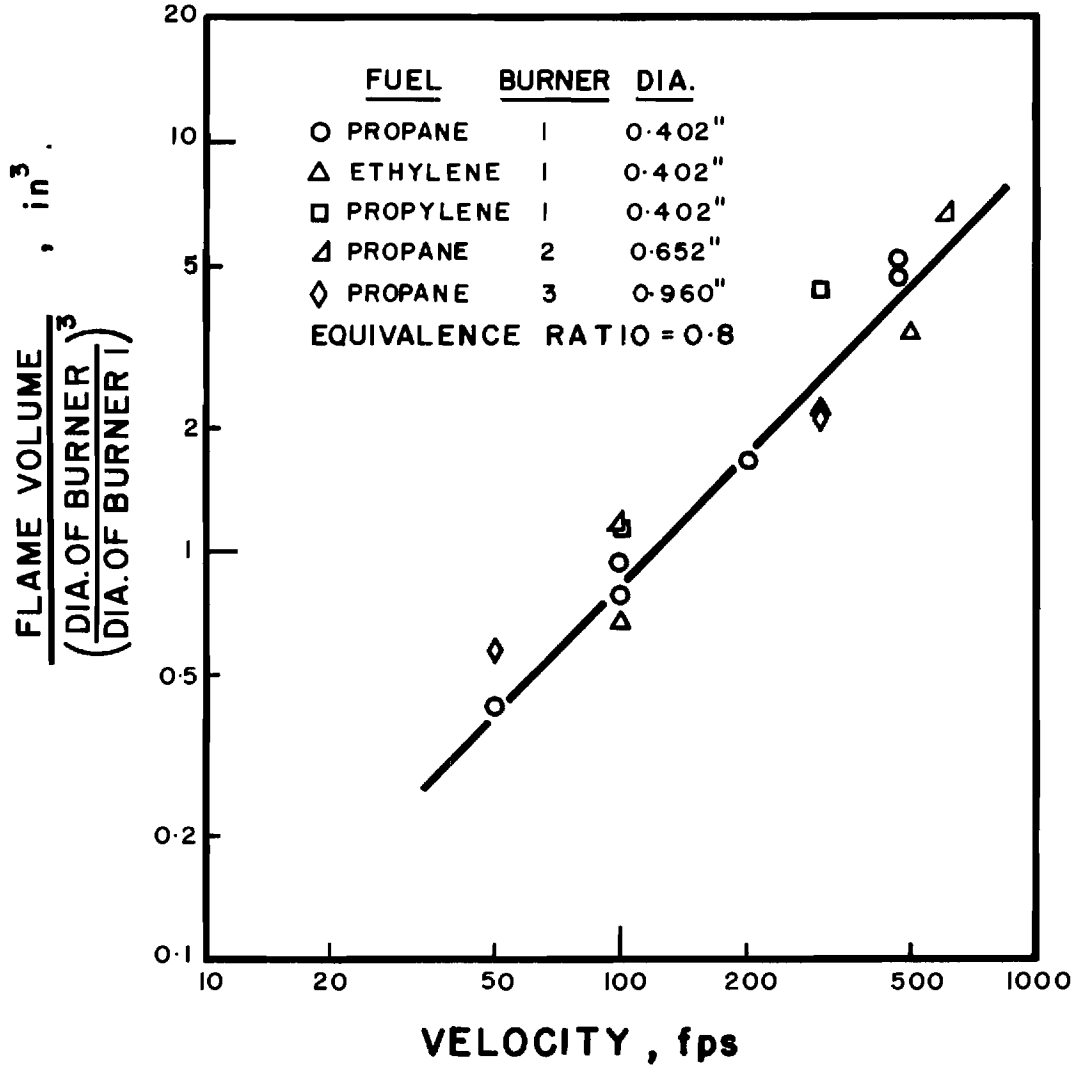

Figure 28. Flame Volume as a Function of Mean Flow Velocity of Reactants.

data points to remain below those for propane is an indication of the inverse scaling of V with S_L. Following the procedure adopted to get scaling laws for acoustic power and peak frequency by regression analysis the volume scaling laws were also deduced.

Using 39 different tests on the three burners and the three fuels at various equivalence ratios between 0.6 and 1.0 and velocities from 50 fps to 600 fps the following relation is obtained:

$$V = 3.4 \times 10^3 \, U^{0.87} \, D^{3.2} \, S_L^{-0.85} \, F^{2.8} \qquad (20)$$

where V is in ft^3, U is in ft/sec, D is in ft and S_L is in ft/sec. The analysis of the errors due to the fit obtained in Equation (18) gave a mean error of 3.2% with a standard deviation of 29%. The maximum error was 82%. The rather high standard deviation of the error distribution was not unexpected. Any linear inaccuracy in linear dimensions on the photograph shows up cubed in volume computations. The important aspect of this analysis, however, is not the accuracy of measuring the reaction volume but rather obtaining the scaling laws. It has been noticed that the exponents on U, D, S_L and F obtained from the regression fit are quite stable in as much as the exponents varied very little when the number of tests used for the fit was varied from 14 to 39, the tests being picked at random. Thus, it is reasonable to assume that good statistical stability is attained for the results of the correlation of interest.

The scaling laws obtained from Equation (20) fall in line with

those deduced from Figures 28 and 29. The scaling on S_L is in favorable agreement with the estimates of Reference 17.

However, Reference 17 does not allow for any dependence on F while experimentally there is quite a strong cubic dependence. It is as if each linear dimension were being increased in proportion to the temperature difference across the flame, since the temperature difference is roughly proportional to F (Reference 27). There is no apparent reason for this dependence. Although a dependence upon F to the first power might be reasoned through a temperature (density) effect upon ℓ_t, the cubic law is puzzling. Since only relative photographic intensity and not absolute intensity is being measured, this cannot be a radiation intensity effect.

Referring back to Equation (17) from the dimensional analysis a comparison of the experimental data with the nondimensional equation can be made. An experimental D^3 dependence can only be explained if $\ell_t \propto D$. This independently confirms the earlier deduction that the turbulent length scale should be proportional to the burner diameter. Further, the exponents on U and S_L obtained in Equation (20) are 0.87 and -0.85, respectively. This shows that the U and the S_L effects mutually balance in Equation (19). Thus, a dimensional homogeneity can only be achieved when u'/U is a constant. This result implies that the turbulence intensity in the flame is relatively independent of the other scaling parameters. Since it is known for fully developed pipe flow that u'/U is a constant[30], this analysis tends to support the statement that the turbulent intensity is not affected by the flame. The conclusion to be reached on the turbulence structure in the reaction zone is therefore that there is no major modification to the turbulence structure due to the flame.

Comparison With Acoustic Power Scaling Laws

It is now possible to compare the flame volume scaling law of $V \propto U^{0.87} D^{3.2} S_L^{-0.85} F^{2.8}$ with the acoustic power scaling law of Equation (11). As was expected in the theory, the flame volume does partially explain the scaling laws on acoustic power. Both flame volume and the acoustic power scale to about D^3 with burner diameter. This shows that almost all the diameter effect perhaps comes from the scaling of reacting volume. The reacting volume accounts only partially for the velocity scaling. This is in accord with the expectations of Reference 17. The scaling law on S_L in flame volume tends to lower the S_L exponent for acoustic power radiated. As has been discussed earlier the F scaling remains unexplained at this time.

Summarizing the comparison with Strahle's theory[17], it can be observed that the expression deduced for far field acoustic radiation in the term of Equation (3) appears to be satisfactory, considering the experimental results of References 8 and 9. Further, estimates of reaction volume are quite satisfactory except for the F scaling. Thus, the order of magnitude estimates of autocorrelation function of the time derivative of the reaction rate and the correlation volume can be suspected to be incorrect.

Concluding Remarks

A comparison of the predictions of the combustion noise theory of Strahle with the experimental results has shown that the theoretical estimates are reasonable. Summarizing the findings, the following conclusions can be drawn:

1. The direct photography technique has been shown to be a useful tool in decomposing the scaling rules of combustion noise.

2. The turbulence length scale in the reaction zone has been shown to be proportional to the burner diameter.

3. The preference for WF and FDR models has been established. Since both these theoretical models yield the same scaling laws for the flame volume, it is not possible to judge the superiority of either of the two models by this method.

4. An evaluation of the experimental findings with the results of dimensional analysis has demonstrated that the turbulence structure is determined primarily by the pipe flow process and not by the flame.

CHAPTER IV

CONCLUSIONS

A comprehensive study of the radiation of noise from open turbulent flames has been made. The study has shown that combustion noise predominates over the range of experimental results obtained and that it differs from jet noise in terms of scaling laws, directionality and spectral content. Summarizing the results of this investigation it can be concluded that:

1. Combustion noise predominates over jet noise even for flow velocities as high as 600 fps.

2. The combustion noise from open turbulent flames is weakly directional. The directionality behavior can be qualitatively explained by refraction and convection effects of Strahle's theory.

3. Combustion noise is a low frequency broad band radiation with a single peak. The peak frequency for premixed flames was obtained in the form $f_c \propto U^{0.18} S_L^{0.53} D^{0.08} F^{-0.69}$. However, for all practical purposes it may be sufficient to consider combustion noise to peak in the 250-700 Hz range for hydrocarbon fuels burning with air as the oxidizer.

4. Acoustic power has been found to follow the law $P \propto U^{2.7} D^{2.8} S_L^{1.4} F^{0.4}$. An empirical expression from which acoustic power can be directly obtained has been generated by regression analysis of the experimental data.

5. Thermo-acoustic efficiency has been shown to follow a $\eta_{ta} \propto U^{1.7} D^{0.8}$

$S_L^{1.4} F^{-0.6}$ law. For a 600 fps flame an η_{ta} as high as 10^{-6} has been obtained showing that noise output from high velocity flames could be appreciable.

6. A direct flame photography technique has been shown to be a useful tool in analyzing combustion noise scaling laws. The flame volume has been shown to scale as $V \propto (U/S_L) D^3$. This study has shown that turbulence in the flame is primarily decided by the pipe flow process.

7. Comparison of experimental results with Strahle's theory has shown that the theoretical solution to the noise problem is reasonably good. The order of magnitude estimates for flame volume are satisfactory. However, the order of magnitude estimates for the autocorrelation function of the time derivative of the reaction rate and the correlation volume appear to be incorrect leading to poor overall scaling laws.

BIBLIOGRAPHY

1. Tucker, M., "Interaction of a Free Flame with Turbulence Field," NACA Report No. 1277 (1956).

2. Bragg, S. L., "Combustion noise," Journal of the Institute of Fuel, 36, p. 12 (1963).

3. Smith, T. B. J., and Kilham, J. K., "Noise generated by open turbulent flames," Journal of the Acoustic Society of America, 35, p. 715 (1963).

4. Smith, T. B. J., "Combustion Noise," Ph.D. Thesis, University of Leeds (1961).

5. Kotake, S., and Hatta, K., "On the noise of diffusion flames," Bulletin of JSME, 8 (30), p. 211 (1965).

6. Bollinger, L. E., Fishbruke, E. S., and Edse, R., "Contribution of Combustion Noise to Overall Rocket Exhaust Jet Noise," NACA CR-463 (May 1966).

7. Thomas, A., and Williams, G. T., "Flame noise: Sound emission from spark ignited bubbles of combustible gas," Proceedings of the Royal Society of London A294, p. 449 (1966).

8. Hurle, I. R., Price, R. B., Sugden, T. M., and Thomas, A., "Sound emission from open turbulent premixed flames," Proceedings of the Royal Society of London A303, p. 409 (1968).

9. Price, R. B., Hurle, I. R., and Sugden, T. M., "Optical studies of the generation of noise in turbulent flames," Twelfth Symposium (International) on Combustion, Pittsburg, the Combustion Institute, p. 1093 (1968).

10. Smithson, R. N., and Foster, P. J., "Combustion noise from a Meker burner," Combustion and Flame, 9, p. 426 (1965).

11. Powell, A., "Noise measurement of a turbulent gasoline vapor flame," Journal of the Acoustic Society of America, 35, p. 405 (1963).

12. Giammar, R. D., and Putnam, A. A., "Combustion roar of turbulent diffusion flames," Journal of Engineering for Power, p. 157 (April 1970).

13. Giammar, R. D., and Putnam, A. A., "Combustion roar of premix burners, singly and in pairs," Combustion and Flame, 18, p. 435 (1972).

14. Knott, P. R., "Noise generated by turbulent non-premixed flames," AIAA Paper no. 71-732 (1971).

15. Seebold, J. G., "Combustion noise and its control in process plant furnaces," ASME Paper no. 71-Pet-6 (1971).

16. Strahle, W. C., "On combustion generated noise," Journal of Fluid Mechanics, 49, p. 399 (1971).

17. Strahle, W. C., "Some results in combustion generated noise," Journal of Sound and Vibration, 23, p. 113 (1972).

18. Strahle, W. C., "Refraction, convection and diffusion flame effects in combustion generated noise," Fourteenth Symposium (International) on Combustion (to be published).

19. Lighthill, M. J., "On sound generated aerodynamically, I. General theory," Proceedings of the Royal Society of London, A211, p. 564 (1952).

20. Lighthill, M. J., "On sound generated aerodynamically, II. Turbulence as a source of sound," Proceedings of the Royal Society of London, A222, p. 1 (1964).

21. Kushida, R., and Rupe, J., "Effect on supersonic jet noise of nozzle plenum pressure fluctuations," AIAA Journal, 10, p. 946 (1972).

22. Abdelhamid, A. N., Harrje, D. T., Plett, E. G., and Summerfield, M., "Noise characteristics of combustion augmented high speed jets," AIAA Paper No. 73-189 (1973).

23. Peterson, A. P. G. and Gross, Jr., E. E., "Handbook of Noise Measurement," Seventh Ed. General Radio, Massachusetts (1972).

24. Williams, F. A., Combustion Theory, Addison-Wesley (1965).

25. "Basic Considerations in the Combustion of Hydrocarbon Fuels with Air," NACA Report No. 1300 (1957).

26. Putnam, A. A., Combustion-Driven Oscillations in Industry, American Elsevier (1971).

27. Steffenson, R. J., Agnew, J. T., and Olson, R. A., "Tables for Adiabatic Flame Temperature and Equilibrium Composition of Six-Hydrocarbon Fuels (With Air and Oxygen)," Engineering Experiment Series No. 122, Purdue University (1966).

28. Gaydon, A. G., and Wolfhard, H. G., Flames: Their Structure, Radiation, and Temperature, 3rd Ed., Rev., Chapman and Hall, London (1970).

29. Fristrom, R. M., and Westenberg, A. A., Flame Structure, McGraw Hill, New York (1965).

30. John, R. R., and Summerfield, M., "Effect of turbulence on radiation intensity from propane-air flames," Jet Propulsion, 27, p. 169 (1957).

31. Schlichting, H., Boundary Layer Theory, 6th Ed., McGraw Hill, New York (1968).

AFOSR Interim Scientific Report

AFOSR-TR- 73 - 1899

COMBUSTION GENERATED NOISE IN TURBOPROPULSION SYSTEMS

Prepared for

Air Force Office of Scientific Research

Aerospace Sciences Directorate

Arlington, Virginia

by

W. C. Strahle
B. N. Shivashankara
J. C. Handley

School of Aerospace Engineering
Georgia Institute of Technology
Atlanta, Georgia 30332

Approved for public release; distribution unlimited

Grant No. AFOSR-72-2365

October 1973

AFOSR Interim Scientific Report

AFOSR-TR- 73 - 1899

COMBUSTION GENERATED NOISE IN TURBOPROPULSION SYSTEMS

Prepared for

Air Force Office of Scientific Research

Aerospace Sciences Directorate

Arlington, Virginia

by

W. C. Strahle
B. N. Shivashankara
J. C. Handley

School of Aerospace Engineering
Georgia Institute of Technology
Atlanta, Georgia 30332

Grant No. AFOSR-72-2365 October 1973

COMBUSTION GENERATED NOISE IN TURBOPROPULSION SYSTEMS

Interim Scientific Report

for

Air Force Office of Scientific Research

Grant No. AFOSR-72-2365

July 24, 1973

Prepared by:

B. N. Shivashankara

J. C. Handley

Approved by:

W. C. Strahle
Principal Investigator

School of Aerospace Engineering
Georgia Institute of Technology

ABSTRACT

Experiments on noise radiation from open turbulent premixed flames are described. Detailed directionality distributions, scaling rules for acoustic power radiated, thermo-acoustic efficiency and spectral content are presented and discussed. Scaling rules for reacting volume are generated by a direct flame photography technique; the reacting volume is shown to be directly related to the sound power output. Combustion noise is shown to be broad band noise with a single spectral peak in the range 250-700 Hz for hydrocarbon-air flames. The directionality is quite weak. The sound power output scales with flow velocity to an exponent of 2.7, with burner diameter to an exponent of 2.9, with laminar flame speed to an exponent of 1.2, and with fuel mass fraction to an exponent of 3.0. The results are examined in the light of the theory of combustion noise.

TABLE OF CONTENTS

LIST OF TABLES

LIST OF ILLUSTRATIONS

Figure Page

SUMMARY

Combustion noise has been recognized as a possible major contributor to the overall noise from aircraft turbopropulsion systems and industrial furnaces. A review of the literature shows that combustion noise generation is little understood. All the theoretical analyses have been inadequate due to lack of clear understanding of the mechanism of the turbulent combustion process itself. The body of experimental data available does not cover the range of flow velocities typical of turbopropulsion systems. Further, in most cases, scaling laws for acoustic power radiated have been based on the assumption of spherically symmetric noise emission, although, combustion noise is known to be weakly directional.

This report describes experiments conducted on open turbulent premixed flames designed to overcome the above shortcomings. A simple burner configuration is used to enable rational interpretation of the experimental results and thus provide useful information toward a systematic approach to noise reduction problems.

Experiments are conducted in an anechoic chamber on pilot-flame stabilized, turbulent flames at the end of burner tubes of diameters 0.402" - 0.96". Flow velocities up to 600 ft/sec and fuels propane, propylene, and ethylene with air as the oxidizer are employed. Mixture ratios ranging from fuel lean to stoichiometric are used. The study of noise generation is done primarily through acoustic measurements where scaling laws for acoustic power radiated, thermo-acoustic efficiency, spectral content and directionality are deduced from sound pressure

measurements made by an array of condenser microphones. The acoustic experiments are supplemented by the scaling laws on reacting volume generated by a direct flame photography method.

Combustion noise is shown to be weakly directional. Comparison with Strahle's theory shows refraction of sound at temperature discontinuities to be the possible explanation of the directionality results. The spectra of combustion noise show a broad band noise radiation with a single peak in the 250-700 Hz frequency range. The scaling law for peak frequency is obtained in the form $f_c \propto U^{0.2} D^{-0.08} S_L^{0.45} F^{0.31}$ where U is the flow velocity, D is the burner diameter, S_L is the laminar flame speed and F is the fuel mass fraction.

Acoustic power radiated is shown to scale as $P \propto U^{2.7} D^{2.9} S_L^{1.2} F^{3.0}$. Errors involved in obtaining the scaling law are discussed. A thermo-acoustic efficiency as high as 10^{-6} is observed for the 600 ft/sec flame, indicating that noise generation from high speed flames can be appreciable.

Detailed scaling laws on flame volume obtained by a direct flame photography method are shown to be quite useful in decomposing combustion noise scaling laws. Flame volume studies show that turbulence structure in the flame is primarily decided by the pipe flow process and not by the flame. The results of the overall program are compared with existing theories and other experimental results. The comparisons with Strahle's theory show that the theoretical solution of the noise problem is reasonable but that some of the order of magnitude estimates need modification before satisfactory scaling laws can be obtained from the theory.

CHAPTER I

INTRODUCTION

General

"Noise is unwanted sound." Noise produces annoyance, decreases efficiency and can impair hearing. With increasing population density around airports and military airfields, aircraft noise has become a problem of primary concern. The problem is further enhanced by the expected increases in both number and size of aircraft in military as well as commercial applications.

It is a well known fact that turbulent combustion generates noise and that most of the combustion processes in practice are turbulent. A substantial portion of the noise, in aircraft using turbo-propulsion systems, could be due to combustion in primary combustors and afterburners. In the case of afterburning turbojets and turbofans a substantial portion of the basic engine noise could originate from the afterburner combustion process, and for "quiet" lifting fans a large contributor to the noise could be the primary gas turbine combustors. In industrial furnaces combustion roar is a primary source of noise.

Noise suppression could be achieved either at the source or by some treatment of the medium separating the source and the environment. The merits of decreasing the noise at the source are easily recognized. In order to attempt reduction of combustion noise at its source a detailed study of the mechanism of noise generation is essential. Also, radiation characteristics from the source would be essential to devise methods to control the noise by the use of acoustic baffles and sound absorbent

liners.

Literature Review

The subject of combustion noise has received very little attention in the literature. The mechanisms of generation and radiation have not been understood to any appreciable extent. Although combustion generated noise itself is nothing new, the study of it is of a recent nature.

At the outset, it can be seen that all the theoretical studies were restricted by the lack of a clear understanding of the mechanism of turbulent combustion. On the experimental side, a serious limitation has been noticed as far as acoustic power calculations. Except in a very few cases, the scaling laws for acoustic power radiated were obtained from a single-microphone sound pressure measurement and the assumption of spherical symmetry. This could lead to incorrect power scaling laws since the combustion noise, in almost all the experiments, was found to be directional, although weakly so. Also, a substantial amount of experimental data available in the literature is for particular burner configurations, thus tending to make the task of deriving general scaling rules almost impossible.

In a theoretical study of the interaction of a free flame with a turbulence field, Tucker[1] showed that appreciable noise generation could result in the region of interaction. He also showed that the intensity of noise generated would be a strong function of the laminar flame speed. No expression for acoustic power radiated was derived in this work.

Bragg[2] developed a theory based on the wrinkled flame concept of turbulent flames. The theory predicted the mechanism of turbulent com-

bustion noise generation to be due to a distribution of monopole-like sources in the reaction zone. Thermo-acoustic efficiency, a measure of the total energy of the flame converted into acoustic radiation, was shown to vary as the square of the flow velocity.

At about the same time, Smith and Kilham[3] presented experimental data on noise produced by open premixed turbulent flames. The burner sizes varied from $\frac{1}{4}$" to $\frac{1}{2}$" in diameter with flow velocities up to 350 ft/sec. Gaseous fuels ethylene, methane, propane, and propylene were used with air as the oxidizer. It was observed that the acoustic power radiated was proportional to $(UDS_L)^2$ where U is the flow velocity, D the burner diameter and S_L the laminar flame speed. A more detailed work[4] showed that the scaling with S_L could vary between 0.6 and 3.4 while the scaling with respect to D and U was quite precise. However, except for scaling with respect to U, the scaling laws were inferred from sound pressures measured at the 90° microphone. The results of the experiments for directionality showed that the noise generated was weakly directional ($\sim$ 3 db) and that the directionality pattern systematically changed with the flow velocity. The maximum sound pressure was found to occur at angles of 50° to 80° to the flow direction.

Smith and Kilham observed the combustion noise to be a broad band noise with a single peak in the range of 250-500 Hz. The peak frequency, in general, was found to increase with the flow velocity. The rate of increase with velocity, however, was different for different fuels. The thermo-acoustic efficiency, the ratio of acoustic power radiated to the total energy per unit time released by combustion, varied between 10^{-8} and 10^{-7} (thermal inputs of 1-7 kw) and was found to increase linearly

with flow velocity. Since ethylene flames showed higher efficiencies almost twice those for propylene, it was concluded that fuels with higher S_L were more efficient sound generators.

A study of the noise of diffusion flames was reported by Kotake and Hatta[5]. Based on an analysis using the conservation equations and upon examination of diffusion flames structure, an acoustic model containing a distribution of monopole and dipole sources in the reaction zone was postulated. The theoretical analysis would allow an acoustic power scaling of U^2D^3 in low velocity flames and a scaling of U^4D^3 in high velocity flames. Experiments conducted with equivalence ratios of 1, 2, and 3, over a rather narrow velocity range of 9 m/sec to 23 m/sec, were shown to substantiate both the scaling laws. The frequency spectra were flat at lower frequencies and dropped off at higher frequencies. These frequency spectra were quite unlike the spectra reported by other investigators which always exhibited a recognizable peak and amplitude fall off on both sides of the peak frequency. Once again, the scaling rules depended on the measurements at a single microphone location. No details are available as to the acoustic environment for these experiments. The burner sizes were 6.8 mm to 21.8 mm. The flames were stabilized at the end of convergent nozzles in contrast with those of Reference 3 where fully developed pipe flow existed at the burner exit.

Bollinger et al[6] could recognize the presence of combustion noise in rocket motor exhaust noise when operating fuel rich. They experimented upon a 500 lb-thrust RP1-LOX motor and noticed a predominant component of noise in the low frequency range ($\sim$ 500 Hz) when the rocket motor was

fired with excess fuel. The authors concluded that the combustion of the unburned fuel in the atmosphere outside the nozzle is the most likely source of this noise.

An entirely new line of approach to the study of combustion noise resulted due to the experiments of Thomas et al[7]. They found a one-to-one correspondence between the instantaneous rate of change of the radius of the flame front and the pressure for spark ignited combustible gases contained in spherical soap bubbles. Hurle et al[8] showed that the rate of change of emission intensity of CH and C_2 radicals in the reaction zone can be used to derive the instantaneous sound pressure generated by the flame for the spherically expanding flame fronts as well as for open turbulent flames. Such a correlation implies a direct relation between the sound pressure and the volume integral of the first time derivative of the global reaction rate. A good correlation was obtained in Reference 8 when the bandwidth of the signals was limited to 50 Hz-1kHz. Due to increased noise in the optical system, correlation was poor when higher frequencies were included. In the computation of the frequency spectrum from the optical measurements the signal to noise ratio was very low and hence the comparison between the optically and acoustically obtained spectra should be viewed with reservations. Hurle et al concluded that the mechanism of combustion noise conforms to the monopole behavior.

The work of Hurle et al was extended by Price et al[9] to include diffusion flames and liquid spray combustion. A good correlation between the first time derivative of the emission intensity of the C_2 radical and the instantaneous sound pressure was demonstrated in all these cases of turbulent combustion. The only limitation to this technique was that

there should be no continuum radiation in the flame. The acoustic radiation from premixed, diffusion and liquid spray combustion was shown by this study to conform to a monopole source distribution. Experiments using turbulence grids showed that both r.m.s. sound pressures and r.m.s. values of the time derivative of the emission intensity increase with turbulence intensity.

Smithson and Foster[10], in a short paper, reported a thermo-acoustic efficiency variation with U^2 for a Meker burner using town's gas. Flow rates of town's gas varied from 0.092 to 0.12 litres/sec with air/gas ratios from 1 to 6. The microphone distance quoted would be in the near field for laboratory Meker burners (1 to 2 cm in diameter) and hence the scaling rules may be in error. The lowest value of acoustic efficiency ($\sim 3 \times 10^{-9}$) was reported by Powell[11] for a gasoline vapor primus stove flame. The burner size was about 0.2" in diameter. The frequency peaked in the 300-600 Hz range.

Giammar and Putnam[12] have studied the noise generated by pure diffusion flames. Two burner configurations, axially impinging jets and an "octopus" burner, were used. Flow rates were as high as 12 SCFM in the case of the octopus burner. The only drawback of this extensive body of data on pure diffusion flames is the complicated burner configuration. Sound power scaled with firing rate to an exponent of 1 to 2; a thermo-acoustic efficiency as high as 6×10^{-7} was obtained for the impinging jets. In all the experiments the peak frequency was found to be in the range 300-500 Hz. In a recent paper[13], Giammar and Putnam have presented the results of some experiments on premixed fuel rich flames on commercial burners of sizes $1\frac{1}{4}$", $1\frac{1}{2}$" and 2". Heat inputs were of the order of 0.25

to 0.69 million BTU/hr (75-200 kw). Both single burners and burners in pairs showed that sound power varies, in general, as the square of the firing rate. The experimental data showed a tendency to follow an exponent slightly lower than 2.

Further experiments on diffusion flames were reported by Knott[14]. Hydrogen and ethylene were burned with air and oxygen. Co-flowing jets and impinging jets configurations were studied. A volume of experimental data has been presented but in a manner very difficult to interpret. Flow velocities were 250 fps to 1000 fps. The thermo-acoustic efficiency was found to be in the range 10^{-8} to 10^{-5} and it varied as $\dot{m}_f$ for co-flowing jets, $1/\dot{m}_f$ for impinging jets and as $\dot{m}_f^3$ for the premixed case. Here, $\dot{m}_f$ is the mass flux of fuel. The highest value of thermo-acoustic efficiency of 2×10^{-5} was reported for the ethylene-oxygen flame. The hydrogen-oxygen system had a cold flow peak frequency of 6000 Hz and the corresponding combustion noise peaked around 2000-4000 Hz. For the ethylene-air system (Re. No. 50,000) the combustion noise had a peak in the 600-900 Hz frequency range. The burner sizes for co-flowing jets were 1.835 cm diameter for the outer tube and 0.813 cm and 0.391 cm for the inner tube. For the impinging jet burner both the tubes had the same diameter, 1.303 cm, 0.8079 cm or 0.4981 cm.

Seebold[15] has reported noise data obtained from a full scale test furnace as well as from process plant furnaces. The heat release varied from 1-10 million BTU/hr. The corresponding fuel flow rates would be roughly 10-100 SCFM. Power output was found to scale with the square of the heat release. The frequency spectra were found to peak in the 125-500 Hz range.

The three papers by Strahle[16,17,18] perhaps form the most extensive theoretical analysis on combustion noise. A rather detailed description of this work is given here because of the particular significance of the prediction from Strahle's theory of combustion noise to the experimental program described in this report.

Following the classical method of Lighthill[19,20] in his work on aerodynamic noise, Strahle's theory starts with (Reference 16)

$$\rho_{tt} - a_o^2 \rho_{x_i x_i} = F_s \tag{1}$$

as the wave equation describing the noise generated from a region undergoing turbulent fluctuations. Physical arguments were presented to show that the appropriate source term F_s for the case of combustion noise is given by $-a_o^2 \rho_{T_{x_i x_i}}$. With this source term the solution to the wave equation was shown to be

$$\rho = \frac{1}{4\pi a_o^2 r} \frac{\partial^2}{\partial t^2} \int_V \rho_T \left(\underset{\sim}{r}_o, t - \frac{r}{a_o}\right) dV \left(\underset{\sim}{r}_o\right) \tag{2}$$

where V corresponds to the volume undergoing turbulent combustion where ρ is dominated by turbulent fluctuations and not by the acoustics. Further developments of the solution gave the important result (Reference 17)

$$\rho = \frac{\gamma - 1}{\gamma} \frac{H\bar{\rho}_1}{4\pi \bar{a}_o^2 r \bar{p}} \int_V \omega_t \left(\underset{\sim}{r}_o, t - \frac{r}{a_o}\right) dV \left(\underset{\sim}{r}_o\right) \tag{3}$$

where ω_t is the time derivative of the global reaction rate. This showed that regardless of the turbulence structure and whether or not the flame is of premixed or of diffusion type, the far field acoustic density (or pressure) is proportional to the volume integral over the reacting volume V of the time derivative of the global reaction rate. With this result Strahle's theory could explain the one-to-one correspondence established between the optical and acoustic emissions by the experiments of References 8 and 9.

In Reference 17, considering the particular case of premixed, fuel lean flames, an expression was developed for the acoustic power P radiated from a region undergoing turbulent combustion in the form

$$P = \frac{(\Delta\rho/\rho_o)^2}{\bar{\rho}_o \bar{a}_o 4\pi F^2} \int_V dV\,(\underset{\sim}{r}_o) \int_{V_d} C(\underset{\sim}{r}_o, \underset{\sim}{d})\, dV\,(\underset{\sim}{d}) \qquad (4)$$

where $\Delta\rho$ represented the density change across the flame, F the fuel mass fraction, C an autocorrelation of the time derivative of the reaction rate, V the reacting volume and V_d a correlation volume.

Strahle has shown that scaling laws for acoustic power can be obtained from the above equation by making order of magnitude estimates for the quantities involved. Since the order of magnitude estimates would very heavily depend on the model of turbulent combustion used in Reference 17 the scaling laws were deduced for three possible phenomenological models of turbulent combustion, namely, a) wrinkled flame, b) slow distributed reaction and c) fast distributed reaction. A similar analysis

was made in Reference 18 for the scaling laws for diffusion flames. Strahle's theory recognized flow velocity U, laminar flame speed S_L, burner dimension D, fuel mass fraction F, scale of turbulence ℓ_t, and intensity of turbulence $\mathcal{I}$ as the important parameters in the study of combustion noise. Further, it was predicted that acoustic power radiated could be expressed by a law of the type

$$P = K\, U^{a_1}\, S_L^{a_2}\, F^{a_3}\, D^{a_4}\, \ell_t^{a_5}\, \mathcal{I}^{a_6} \tag{5}$$

where the prefactor K and the exponents $a_1, \ldots, a_6$ are constants. Reference 18 studied the effects of convection and refraction on the directionality of combustion noise and showed that the observed directionality of combustion noise could be explained qualitatively by these effects but the quantitative agreement with existing experiments is poor.

Kushida and Rupe[21], in an investigation of the effect on supersonic jet noise of nozzle plenum pressure fluctuations, observed that pressure fluctuations in the plenum chamber of a supersonic nozzle can strongly increase the noise radiated from the jet plume. Since some appreciable pressure fluctuations do exist in turbojet engines, the authors conclude that the reduction or elimination of plenum chamber pressure fluctuations may be an important method of reducing the total noise from jet engines.

A similar result was obtained by Abdelhamid *et al*[22]. They found a good cross correlation between the pressure oscillations in the combustor and the far field sound pressure. A 3-inch combustor with a 2-inch nozzle was used in this study. The major conclusion reached was that a large

portion of the far field noise due to jet aircraft could be from the combustors.

The literature survey leads to the following conclusions:

1. Combustion noise exists as an identifiable phenomenon in many practical systems.

2. In almost all the configurations, combustion noise occupies the lower range of the frequency spectrum; a typical range is between 150-500 Hz.

3. The acoustic power radiated is found to scale with U to an exponent between 1 and 4, with D to an exponent between 2 and 3 and with S_L to an exponent between 0.6 and 3.4. This represents a very wide variation in the scaling rules, thus making them virtually useless. Furthermore, many of the power scalings in the literature were based on single microphone measurements and the assumption of spherical symmetry. This could give misleading results because of the weak directionality of the combustion noise. Also, only a few of the reported experiments were conducted in an anechoic enclosure. Finally, the choice of independent variables with which to derive scaling laws has been insufficient.

4. Very little work has been done on the directionality of the acoustic radiation. A systematic correlation of the spectral content with the flow variables and the chemistry has not been attempted in any of the existing experimental results.

5. The theories of References 16, 17 and 18 can, with experimental support and verification at various stages of the theoretical solution, yield useful scaling rules for the acoustic power, spectral content and directionality of the combustion generated noise.

6. Without firm scaling laws it is impossible at this point to quan-

titatively estimate the true importance of combustion noise to the total turbopropulsion noise problem.

Objectives of Research

The literature survey points out a need for further experimentation in the area of combustion noise. The experimental results, in order to be applicable to turbopropulsion systems of aircraft, should be obtained at velocities comparable to those found in afterburners ($\approx$ 600 ft/sec). Also, in order to get a true indication of the acoustic radiation from the flames all the experiments should be conducted in an anechoic chamber so that free field conditions can be closely approximated. The sound pressures should be measured at various azimuthal positions around the flame and then integrated for power radiated. A detailed directionality study should be made. The scaling laws for spectral content should be generated.

The objectives of the experimental program were decided by the needs expressed above. However, only the case of open turbulent flames would be considered because of the simplicity of the burner configuration. The objectives can be listed as follows:

1. to conduct noise experiments on three burners in an anechoic chamber to flow velocities of 600 ft/sec using both fuel lean and fuel rich mixtures. These experiments will be called "Acoustic Experiments" and are designed to yield scaling laws for acoustic power, thermoacoustic efficiency, and spectral content. Detailed directionality information will also be obtained.
2. to analyze the scaling rules for the volume of the reaction zone.

These experiments will be entitled "Direct Flame Photography" since direct flame photography techniques will be employed in reducing the scaling laws. The analysis of the reacting volume will provide an independent diagnostic check for Strahle's theory of combustion noise.

3. to compare the experimental findings with the theories of References 15, 16 and 17, and

4. to present the results of the investigation in a form useful to the practicing engineers.

Thus, it is believed that this study would lead to a better understanding of the mechanism of generation of combustion noise and provide useful scaling rules for the noise generated by open turbulent flames.

CHAPTER II

ACOUSTIC EXPERIMENTS

The experiments conducted, to determine the scaling rules for acoustic power, thermo-acoustic efficiency, spectral content and directionality of combustion noise generated by open turbulent flames established at the end of burner tubes, are described in this chapter. The measurements are made in the far field since near field information would be too complicated by the phase relationships to be of any real value. Also, theories exist, e.g., References 16, 17 and 18, which enable a study of the mechanism of noise generation based on experimental far field information. In addition, the far field measurements are of practical significance in evaluating the noise radiation from sources.

Based on an analysis of the literature, the parameters that affect the noise generation from turbulent flames can be recognized as: U, the flow velocity, D, the burner size, S_L, the laminar flame speed, F, the fuel mass fraction, ℓ_t, the scale of turbulence, and $\mathcal{I}$, the intensity of turbulence. In this chapter only U, D, S_L and F are considered since no effort is made to devise methods to vary the turbulence intensity independently. The experiments are designed so that only one parameter is varied at a time. However, S_L and F can not be varied independently of each other using the same fuel, but combinations of mixture ratios and fuel can be worked out so as to vary either S_L or F independent of the other. Since the scaling rules sought for can be obtained by regression

analysis even when both the parameters vary at the same time, equivalence ratio ϕ was used as one of the parameters. Equivalence ratio is defined as the ratio of $(\text{fuel/air})_{\text{actual}}$ to $(\text{fuel/air})_{\text{stoichiometric}}$. In order to identify the various tests conducted the following notation is used.

P	—	100	—	0.8	—	1
Fuel						Burner Diameter
P = Propane		Flow Velocity In Ft/Sec		Equivalence Ratio		1 = 0.402"
E = Ethylene						2 = 0.652"
Py = Propylene						3 = 0.96"

In this report results of only premixed flames are presented.

Anechoic Chamber

A 13' x 10' x 6' - 6" (working space) anechoic chamber was built in the Aerospace Propulsion Laboratory in order that acoustic measurements be made in conditions close to free field. The chamber would also serve the secondary purpose of preventing drafts around the flame. Figures 1(a) and (b) show the basic construction details of the anechoic chamber. The two walls of the room formed two outer walls of the chamber. The other two walls were constructed with 8" dry gypsum wall stuffed with fiberglas. The basic acoustic insulation was provided by 18" thick fiberglas and a 3" air space between the walls and the fiberglas insulation. The density of fiberglas used was roughly 0.6 lb/cft. The floor and the ceiling were also covered with 18" thick fiberglas although no air gap was provided. A grating floor, provided in the chamber, was

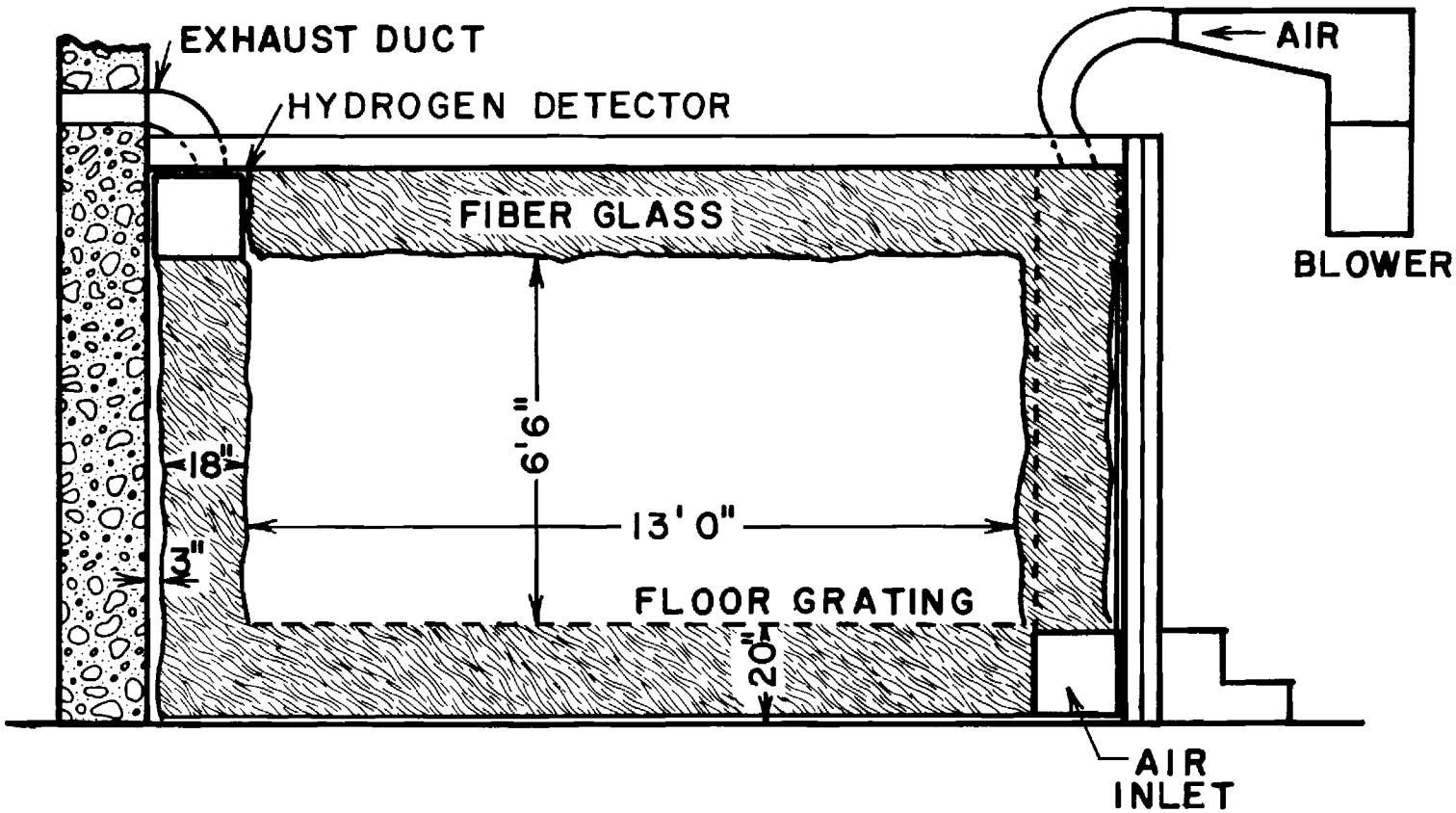

CROSS-SECTIONAL ELEVATION

Figure 1(a). Cross-Sectional Elevation of Anechoic Chamber.

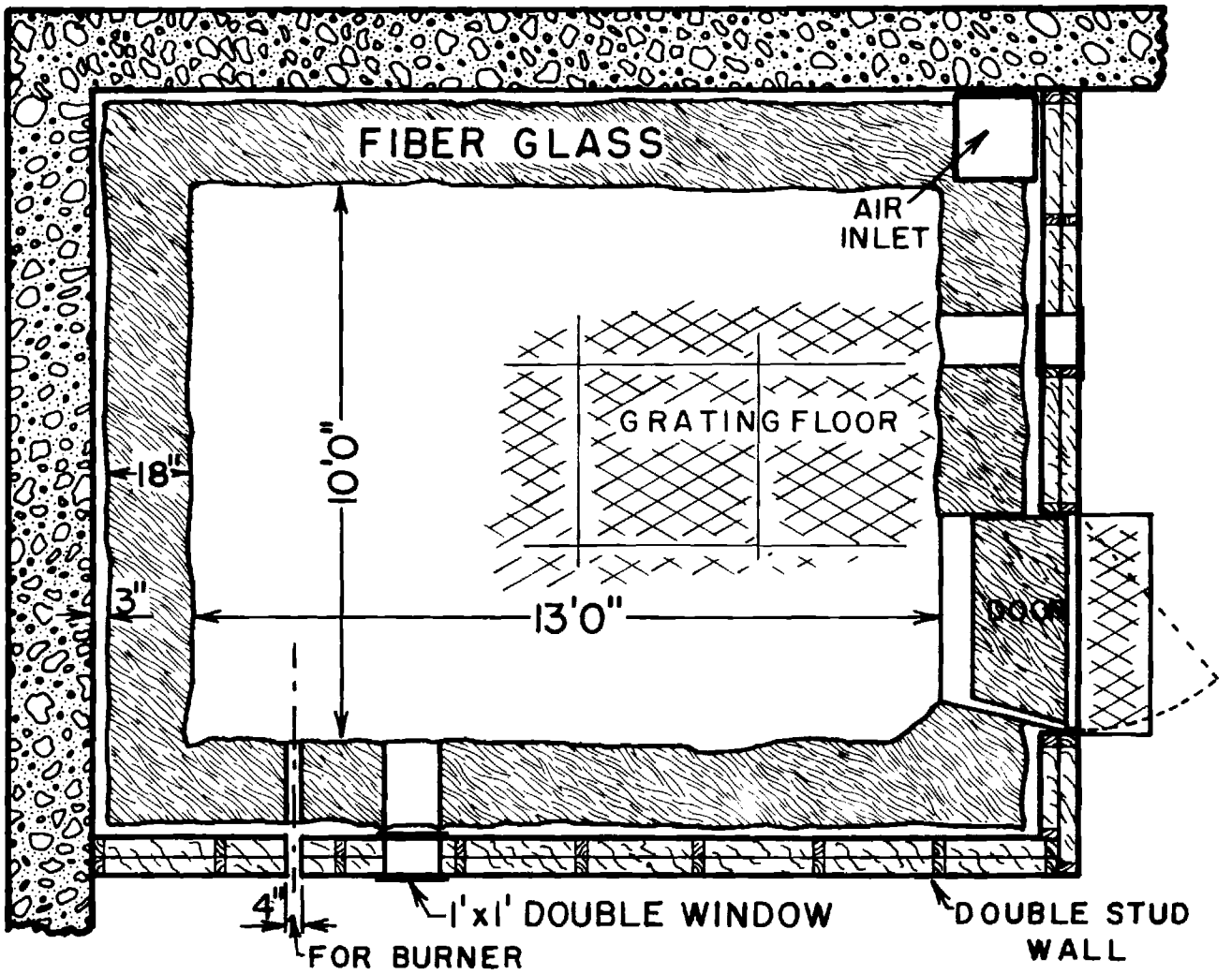

CROSS-SECTIONAL PLAN

Figure 1(b). Cross-Sectional Plan of Anechoic Chamber.

supported on a metal structure. The supporting structure was mounted on $\frac{1}{2}$" rubber pads to isolate structurally carried vibrations to some extent.

The chamber has two windows (1' x 1') so as to keep a close watch on the flame. A hinged door, also with the same thickness of insulation as the walls, provides an entry into the working area. A hydrogen detector has been installed in the ceiling.

The ventilation to the chamber is provided by a blower. The air from the blower passes through a long acoustic duct work and enters the chamber at one of the lower edges. Exhaust ducting with a long and tortuous passage is provided at the opposite edge of the chamber.

The anechoic chamber was tested with an acoustic driver as the source at various discrete frequencies and was found to be reasonably anechoic, in the frequency range of 125 Hz to 5000 Hz, for source to microphone distances of up to 5 ft (Figure 2). However, the ventilation blower was observed to produce low frequency oscillations in the sound meter readings, especially when the sound pressure levels being measured were of the order of 60 db re.0.0002 μ bar (10-200000 Hz linear). Also, at this level, it was noticed that the external disturbances, such as the laboratory compressors, the air conditioning system, and the noise due to the flourescent tube ballast could add up to 0.5 to 2 db to the measured sound levels inside the anechoic chamber. This suggests that the experiments should be done when all these external disturbances are not operating. The reasons for the appreciable influence of the external disturbances in the anechoic chamber are 1) the chamber is not structurally isolated from other parts of the building, and 2) the walls are made of

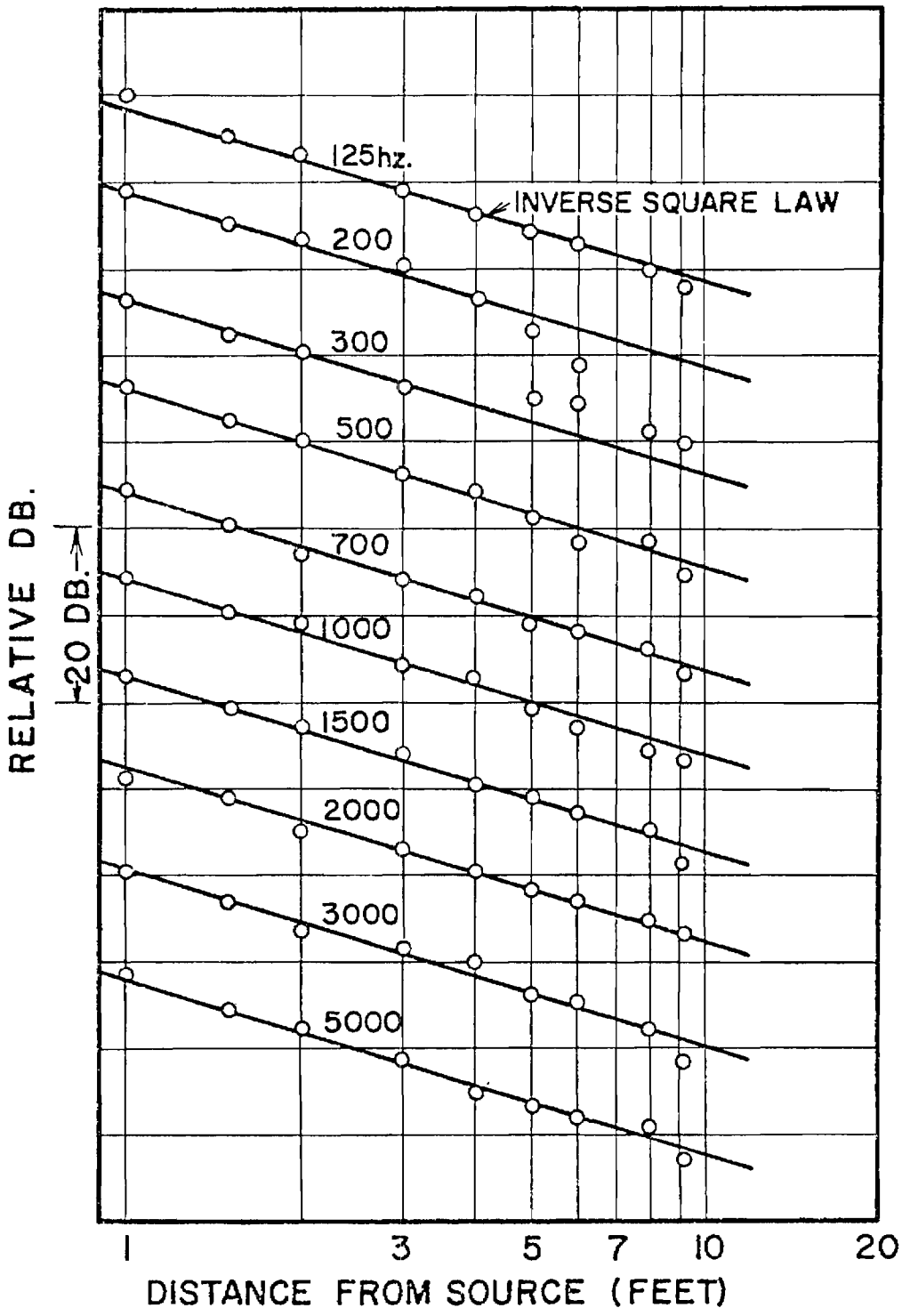

Figure 2. Anechoic Chamber Characteristics .

light-weight construction and are thus fairly inefficient in the prevention of sound transmission through them. In any case, the chamber was designed to have inner walls which are efficient in absorbing the incident sound waves and tests have shown that the purpose has been achieved.

The anechoic chamber has a typical background noise of 52 db re. 0.0002 μ bar (10-200000 Hz linear). The spectrum of the background noise was nearly flat from 100-10,000 Hz.

Burners and Flow Systems

The burners used in this study have been constructed from coaxial tubing of circular cross section held together by 'Swagelok' heat exchanger T-joints as shown in Figure 3. The mixture of reactants flows through the inner tube and hydrogen for the stabilizing diffusion flames flows through the annular space between the tubes. The burner sizes are 0.402", 0.652" and 0.96" in diameter. The sizes quoted here are the inner diameters of the central tube which determines the size of the flame. The size of the annular gap is less than 1/32 inch in all the three cases. The two smaller burners are built out of copper tubing while the largest burner has a stainless steel inner tube and a copper outer tube. A straight length of 50 diameters is provided for the flow of reactants preceding the burner port. This ensures fully developed turbulent pipe flow conditions at the burner exit. A mixing chamber filled with 4 mm glass balls is introduced in the main burner tube just before the 50 D straight length to aid proper mixing of fuel and air. This mixing chamber, in addition, serves as a flash-back suppressor. The burners are mounted in the anechoic chamber with their axes horizontal at

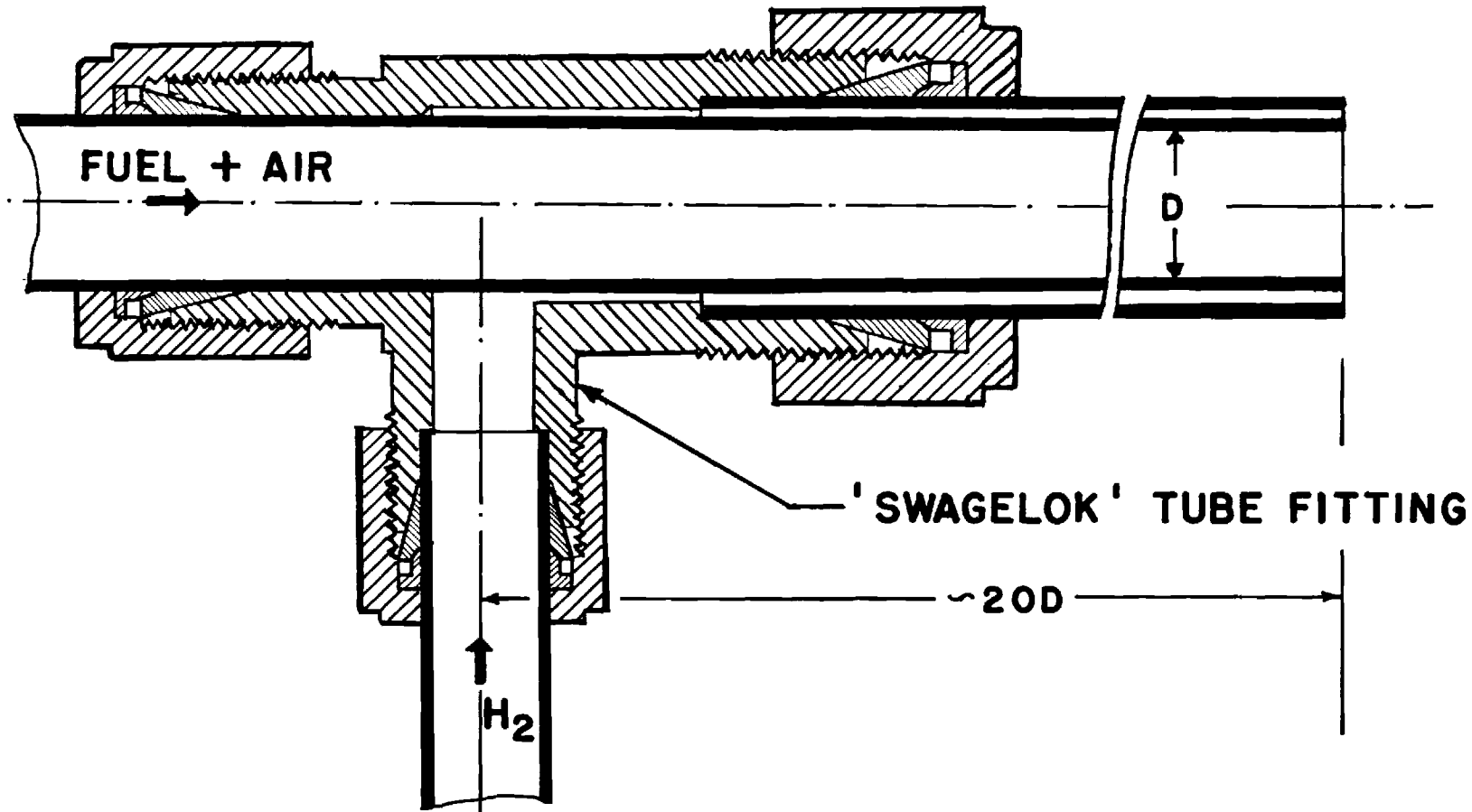

Figure 3. Burner Assembly.

3 ft above the floor grating and at least 2 ft from the walls.

Figure 4 shows the flow system. Air for the experiments is supplied by the 1000 ft^3 125 PSI Air reservoir. The flow of air is measured by two rotameters with overlapping flow ranges. Fuels and hydrogen are metered by orifice meters; two orifice plates with different orifice dimensions are used on the fuel metering system to cover the entire flow range. The control valve downstream of each flow meter is used to introduce the pressure drop required to maintain a desired upstream pressure at the meter, thus vastly increasing the metering range of each flow meter. Fuels, hydrogen and nitrogen are supplied from gas bottles which are stored outside the room in a separate gas storage area. A muffler is provided in the air line to reduce the flow noises. Also, air leaving the muffler flows through flexible rubber hoses thereby preventing abrupt flow turns which generate flow noises.

The fuel and air are mixed at a T-joint. The hydrogen line entering the anechoic chamber is shrouded by nitrogen. Also, both fuel and hydrogen lines are provided with nitrogen purge.

Instrumentation

Sound pressures are measured by Brüel and Kjaer type 4134 half-inch condensor microphones. Five such microphones mounted on stands in the same horizontal plane as the burner are used. The microphones are placed at constant radius with respect to burner port and at angular locations between 15 and 120° to the flow direction; closer than 15° to the flow direction would be likely to introduce flow noises at the microphone. The outputs of the microphones are directly read out as sound

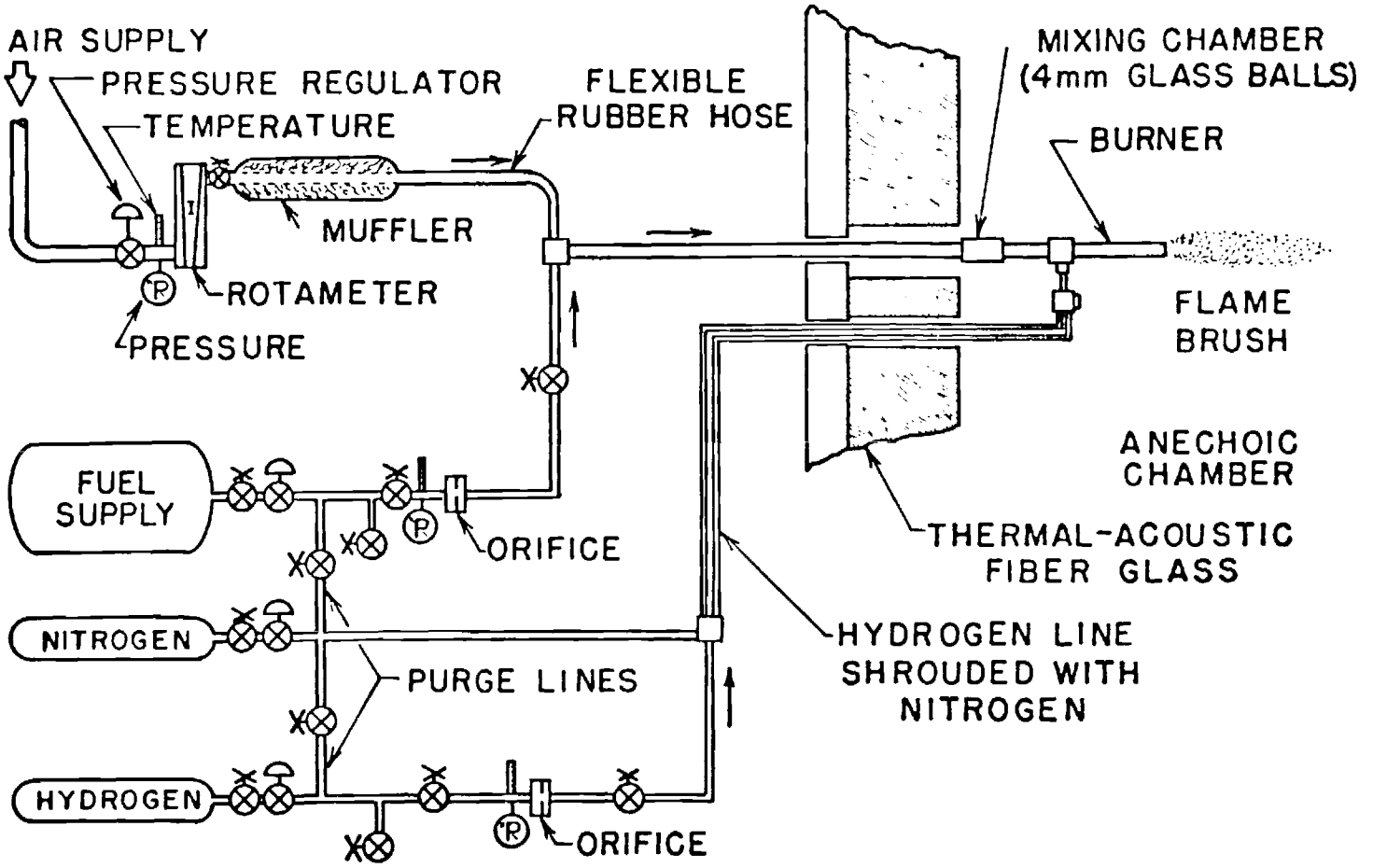

Figure 4. Flow System Schematic.

pressure levels (db re. 0.0002 μbar) on a Brüel and Kjaer type 2604 microphone amplifier, one at a time. They are also amplified by an array of five NEFF type 122 amplifiers and recorded on five channels of an AMPEX FR 1300, 14 channel magnetic tape recorder, usually at 30 ips tape speed. The direct calibration of microphones is done by a Whittaker type PC-125 acoustic calibrator. In order to provide a calibration reference for data analysis the sound output from an acoustic driver, producing a 1000 Hz sound and placed under the burner port, is also recorded on the tape. The sound pressure level at each microphone due to the acoustic driver is read on the microphone amplifier and noted. This procedure enables the calibration of the entire system directly.

The data acquisition and reduction schematic is shown in Figure 5. It can be noticed that only microphones are placed inside the anechoic chamber. The microphone signal carrying cables are brought out of the anechoic chamber through a conduit and connected to the appropriate instruments. The spectral analysis of the noise is performed on a Hewlett Packard type 5645 Fourier analyzer and associated hardware. The spectra are computed digitally using a fast Fourier transform by the machine. A multi-sample averaging technique is used to obtain stable results and eliminate spurious noise from the signal. The output from the Fourier analyzer could be observed on the oscilloscope, plotted on an x-y plotter or printed out on a teletype. In this study x-y plots were preferred over the other modes of output.

Flame Stabilization

The flames were stabilized at the end of burner tubes by an annular

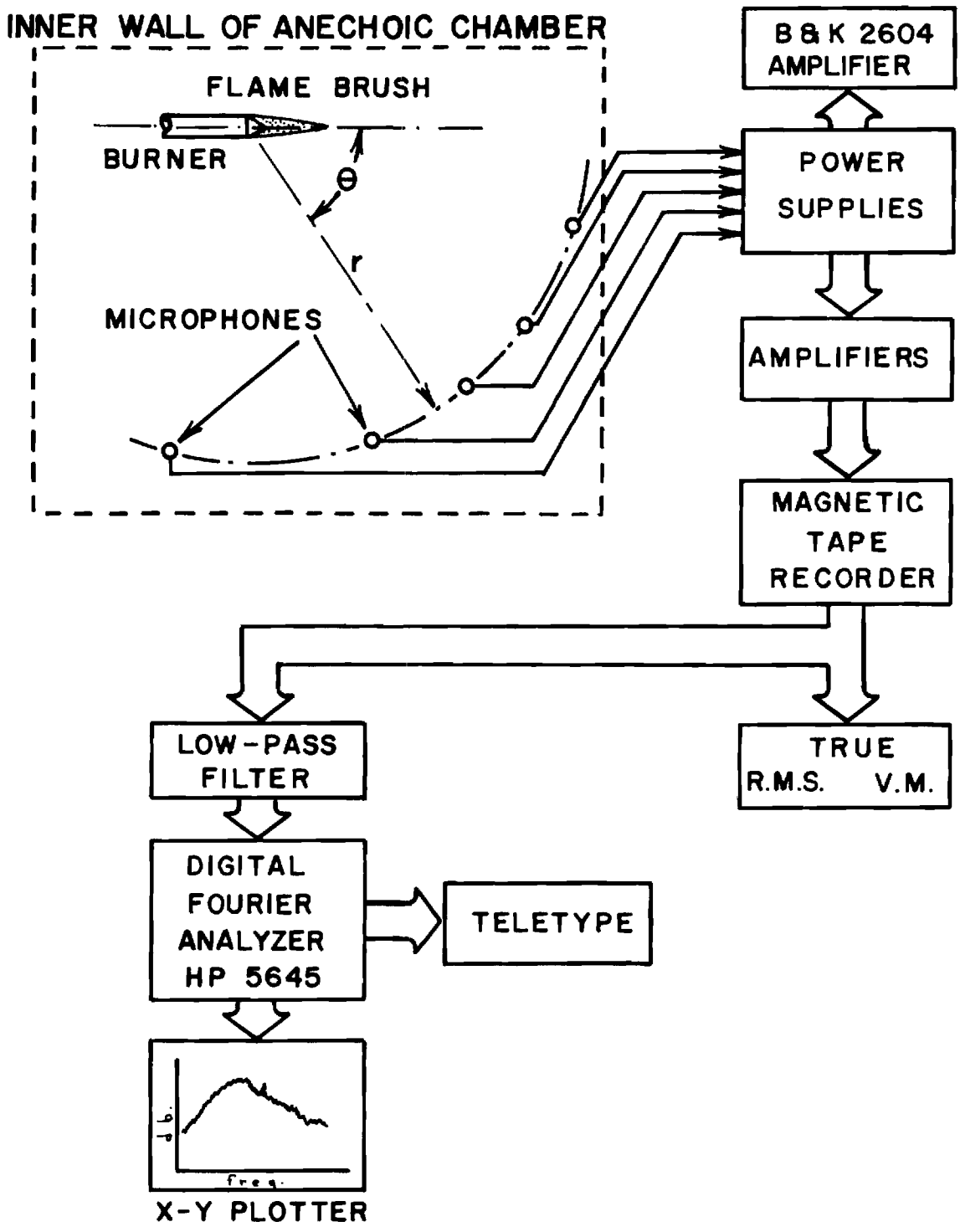

Figure 5. Data Acquisition and Reduction Schematic for Acoustic Experiments.

diffusion flame of hydrogen. Smith and Kilham[3] have studied the effect of various amounts of hydrogen flow on the noise generated. According to their study the optimum amount of hydrogen was found to be between about $2\frac{1}{2}$ to $3\frac{1}{2}$ percent by volume of the main flow. Before using the values for the H_2 required for stabilization from Reference 3, a test measurement was made on one of the typical cases. The result of this experiment is shown in Figure 6. This result is in essential agreement with the results of Reference 3 and, therefore, in all the experiments $2\frac{1}{2}$ percent hydrogen has been used since this would contribute the least to the overall noise output. Although this quantity of hydrogen was found satisfactory in most of the experiments, the flames of velocity greater than 300 ft/sec on a 0.402" burner required 5 percent for satisfactory stabilization of the flame.

Combustion Noise and Jet Noise

The relative importance of combustion noise in comparison with the noise from a pure jet of the same velocity, and also the air jet plus pilot flame combination, is presented in Figure 7. The microphone azimuth of 55° to the flow direction was chosen so as to be somewhat close to the direction of predominant radiation for all three cases. Combustion noise dominates over the entire velocity range from 50 ft/sec to 600 ft/sec. An interesting observation made during these experiments was that the hydrogen diffusion flame was by itself very quiet. However, when the main stream of air was turned on the flame would interact with the outer boundaries of the turbulent jet close to the burner exit and enhance the noise output from the air jet.

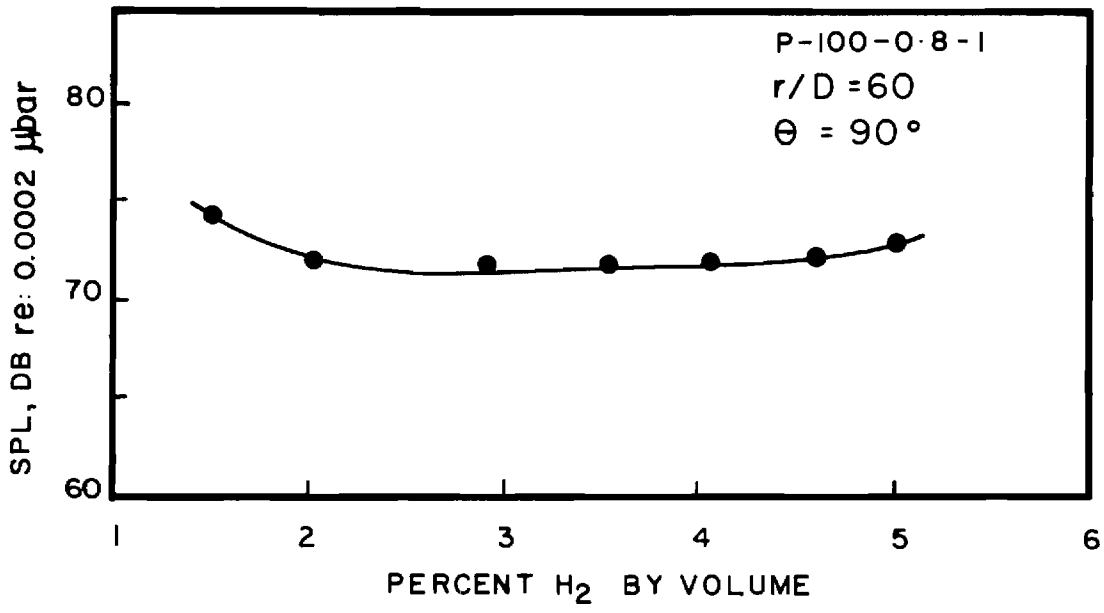

Figure 6. Effect of the Quantity of Hydrogen Used for Flame Stabilization on Overall Noise Level.

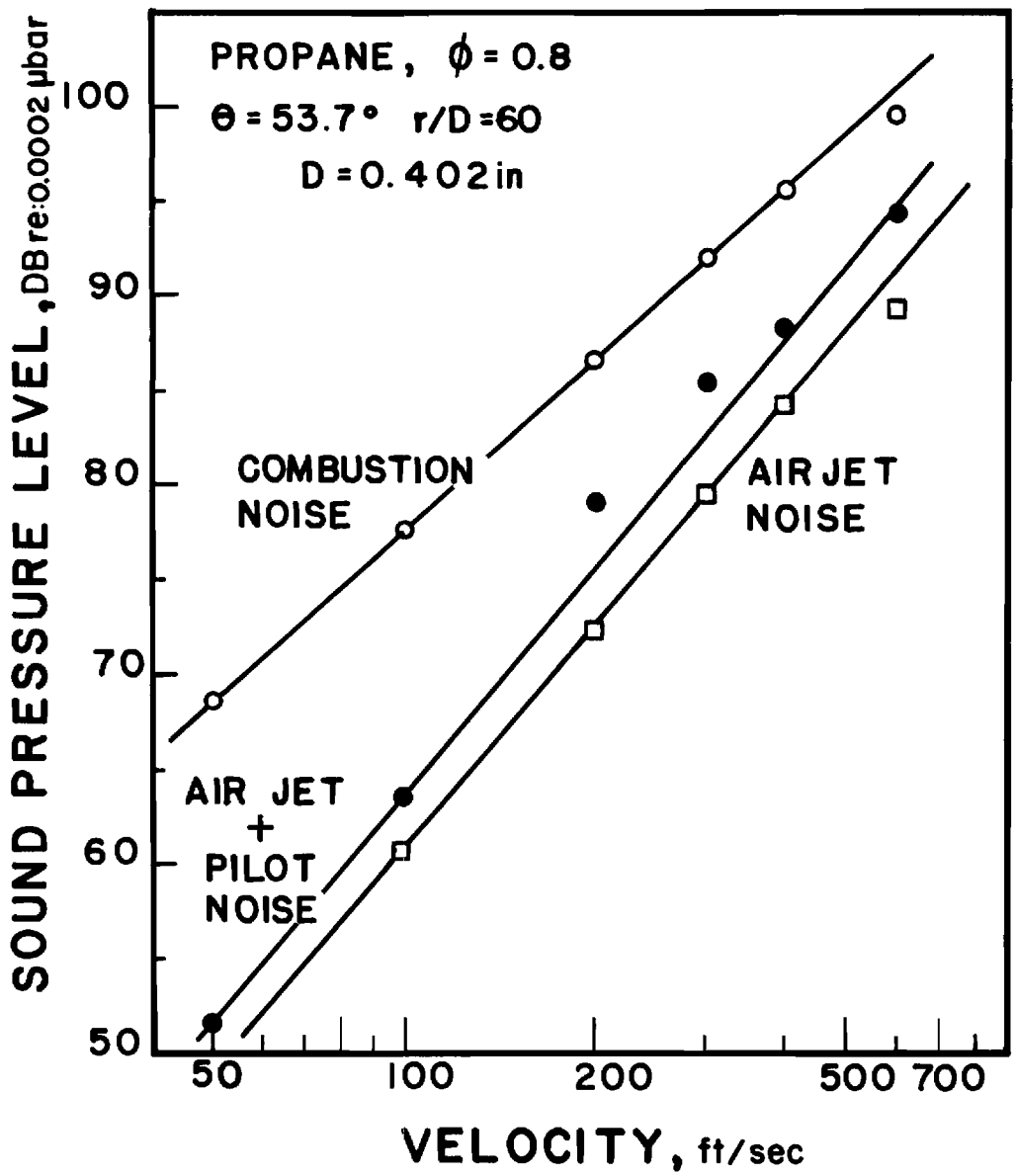

Figure 7. Jet Noise, Combustion Noise and Air Jet plus Pilot Flame Noise at Various Flow Velocities.

The results shown in Figure 7 can be used to determine the approximate scaling laws for power radiated if, for the present, directionality is neglected. The jet noise appears to follow a U^4 law for acoustic power while combustion noise favors an exponent of 2.8. Because of the higher exponent on U the difference between the combustion noise and the jet noise decreases with velocity. Nevertheless, even at 600 ft/sec combustion noise is predominant.

Sound Pressure Measurement

The sound pressures were measured by a B & K type 2604 microphone amplifier using 10-200000 Hz linear response with the meter set to slow response. In most cases, the meter excursions were less than a db and, in accordance with standard practice[23], the arithmetic mean between the maximum and minimum readings was taken as the sound pressure level. In doing this any occasional highs and lows of the meter readings should be neglected.

As explained earlier, the locations of the microphones are determined with respect to the burner port and the flow direction. For computation of the acoustic power radiated and the directionality it is necessary to reference the sound pressures measured to the acoustic center in the flame. Acoustic center is a point within the noise generating region from which the noise would appear to originate to a far field observer. There is both experimental[8,9] and theoretical[17] evidence to show that the noise emitters in the case of combustion noise are confined to the visible region of the flame. Thus, it can be considered reasonable to state that the acoustic center in the flame would be located at the

point of maximum volume per unit length as determined by direct photographic flame volume measurements. These measurements are explained in detail in the next chapter.

Figure 8 shows sound pressure level distributions along a line parallel to the flow direction, i.e., parallel to the length of the flame. The distance between the microphone and the axis of the burner was kept constant at 9-7/8". If the noise radiation from the flame were spherically symmetric the location of maximum sound pressure level would correspond to the acoustic center. However, since the acoustic radiation from the flame is weakly directional in the forward 90°, the observed maximum will get shifted towards the flame tip. This shift will depend upon the distance between the burner axis and the microphone as well. In the light of these facts the location of the acoustic center cannot be obtained from Figure 8. The acoustic center locations as decided by direct flame photography have been indicated on the sound pressure level traces. It can be noticed that the acoustic center locations do consistently fall below the maximum sound pressure level location.

In order to determine whether the calculation of acoustic power radiated from the flame is very sensitive to the inaccuracies in locating the acoustic center, certain calculations have been made for three typical cases. The acoustic power radiated* was evaluated assuming that the acoustic center lay at a) the location of maximum flame volume per unit length and b) the tip of the flame. Table 1 presents the results of these calculations. Even with a rather drastic shift of the acoustic center to the flame tip the error introduced is less than 0.4 db.

* See page 33 for details.

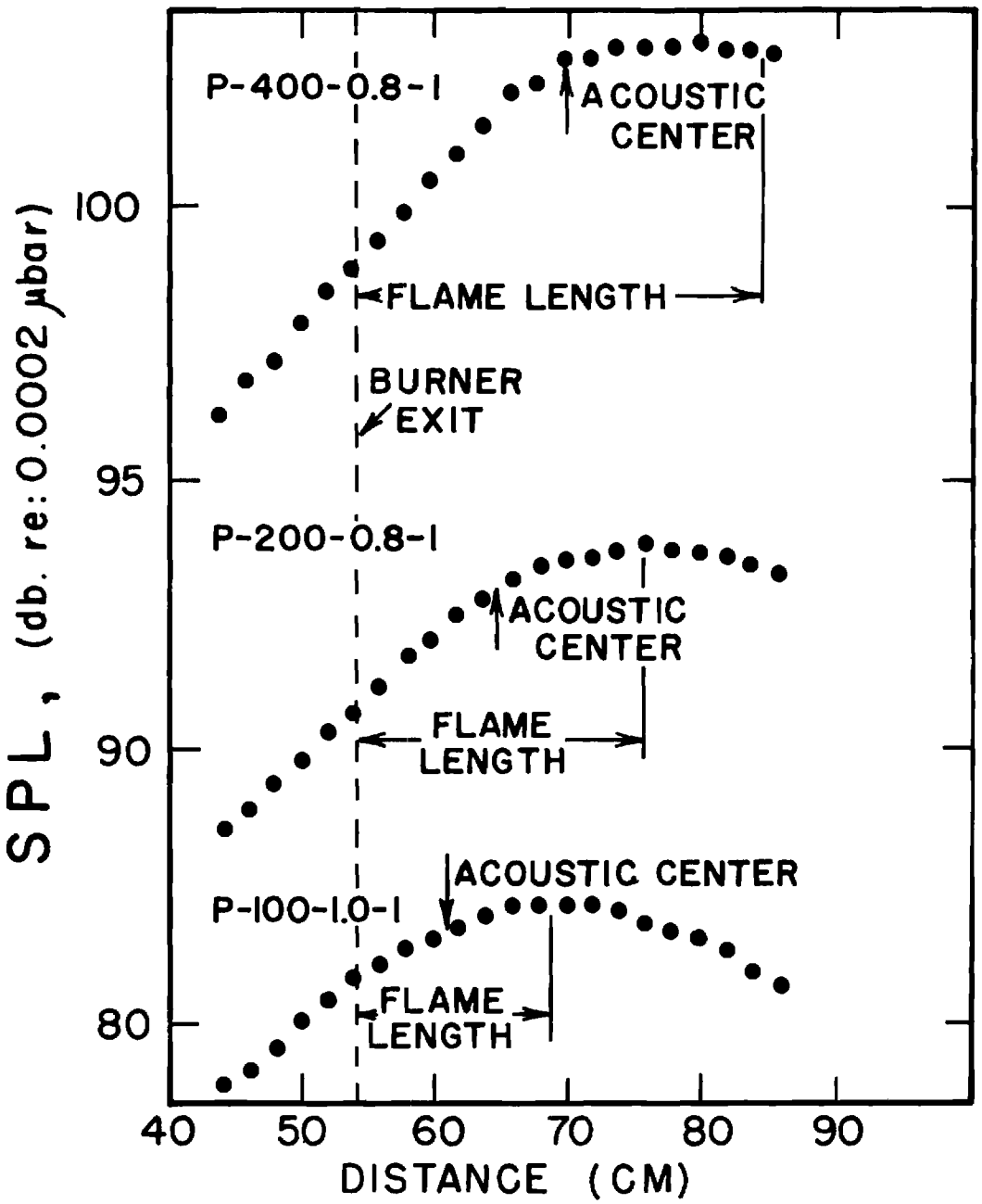

Figure 8. Sound Pressure Levels Along a Line Parallel to the Flame Length 9.875" Below the Burner Axis.

Table 1. Errors in Acoustic Power Due to Inaccuracy in Locating Acoustic Center

Test	Acoustic Power, Watts W_1: Acoustic Center at Max Flame Volume Per Unit Length Location	Acoustic Power, Watts W_2: Acoustic Center at Flame Tip	Difference DB $(= 10 \log_{10} \frac{W_2}{W_1})$
P-100-1.0-1	0.3650×10^{-3}	0.3564×10^{-3}	-0.1
P-200-0.8-1	0.1700×10^{-2}	0.1624×10^{-2}	-0.2
P-400-0.8-1	0.1121×10^{-1}	0.1030×10^{-1}	-0.38

After having established the location of the acoustic center from flame photography experiments, the measured sound pressures were corrected for both geometry and magnitude to account for the change in origin. In the process of calculating the altered values of sound pressures, spherical divergence was assumed since the measurements are in the far field. To the corrected sound pressures a polynomial relation,

$$p^2 = \frac{1}{r^2} \sum_{n=0}^{3} a_n \cos^n \theta \qquad (6)$$

suggested by the theory in Reference 18, was fitted by the method of least squares using all the five sound pressure readings. This polynomial in cos θ was found to fit the data very closely. The maximum error was ± 1 db which is of the same order of magnitude as the accuracy of the instrumentation itself.

Calculation of Acoustic Power Radiated

The acoustic power radiated from the flame is calculated, from the polynomial relation for sound pressure with θ, by integration over a sphere of some radius r assuming axial symmetry. For values of sound pressures beyond the last microphone angular location the value obtained for the last location was used. To determine the order of magnitudes of the errors involved due to such an extrapolation, three representative experiments were conducted in which a single microphone was traversed around the flame up to 170° with the flow direction. The sound pressures measured were corrected for the acoustic center and a polynomial in cos θ was fitted to these readings. Figure 9 shows a comparison between the single microphone directionality pattern and the one from five fixed microphones. The comparison is quite favorable and is within the accuracy of $\pm$ 2 db. More important, however, is the error involved in calculating acoustic power based on 5 microphone data. The power calculated from one microphone covering up to 170° does not involve any appreciable extrapolation and hence is considered to be the true estimate. Table 2 presents a comparison of the acoustic power values due to both cases. It can be seen that the error due to the extrapolation is not excessive. The use of five fixed microphones is preferred from a practical standpoint since the time required for sound pressure measurement is drastically reduced compared to the time it would take to traverse one microphone around the flame. On quite a few tests, the heat input was so high ($\sim$ 100 kw) that the duration of the tests had to be restricted to a fraction of a minute to keep the anechoic chamber from getting overheated.

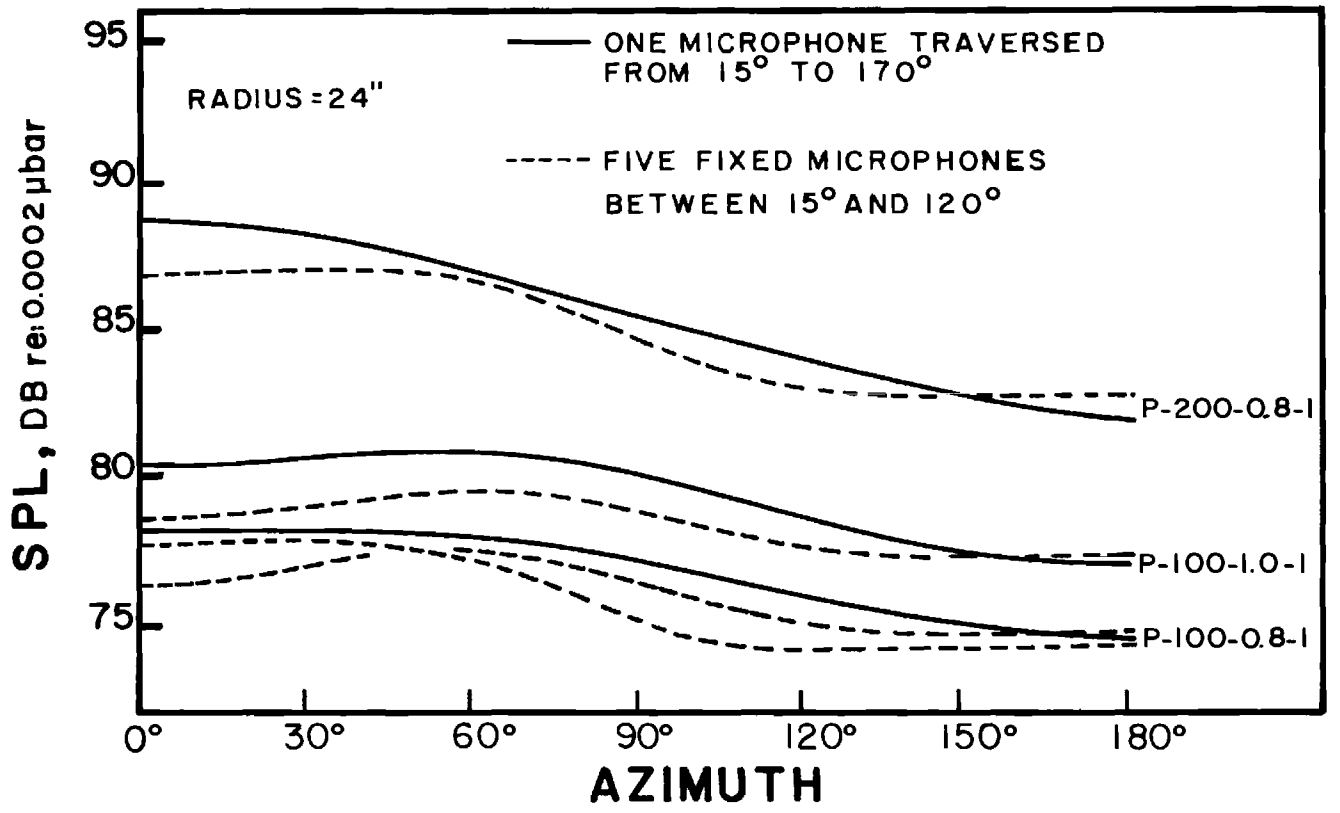

Figure 9. Comparison Between Directionality Patterns Obtained by Using Five Fixed Microphones and by Traversing a Single Microphone.

Table 2. Error in Acoustic Power Due to Using Only Five Microphones to Measure the Sound Field Around the Flame

Test	Acoustic Power, Watts W_1 One Microphone Covering 15° - 170°	Acoustic Power, Watts W_2 Five Fixed Microphones Covering 15° - 120°	Difference DB $(= 10 \log_{10} \frac{W_1}{W_2})$
P-100-0.8-1	0.2266×10^{-3}	0.1826×10^{-3}	0.94
P-100-1.0-1	0.4286×10^{-3}	0.3199×10^{-3}	1.28
P-200-0.8-1	0.1790×10^{-2}	0.1536×10^{-2}	0.66

Referring back to Figure 9, two traces (corresponding to 5 fixed microphone data) are presented for the P-100-0.8-1 case. These are from the same experiment repeated on two different days. The difference in the power calculated between the two traces is about 0.3 db which shows good repeatability of data. However, the tests of equivalence ratio of 0.6 had a tendency to be rather unstable and, consequently, the repeatability in such instances was not as good. Some experiments of $\phi = 0.6$ case could reproduce only within a ± 2 db limit.

Experimental Results for Fuel Lean Flames

Directionality of Noise Radiation

The directionality of the far field radiation from a source can give some indications regarding the nature of the source. At the same time, the directional information is required for deciding the most effective locations for acoustic liners. The directionality results

presented here are the polynomials in cos θ fitted to experimental measurements. The origin of reference is the acoustic center in the flame and the azimuthal positions are measured from the flow direction. The difference between the maximum sound pressure level observed (any θ) and the value at the axis (θ = 0) when one makes a constant radius traverse in the plane of the flame can be considered as a quantitative measure of the directionality of the source.

Figure 10 shows the directionality patterns at various flow velocities for propane-air flames of equivalence ratio 0.8. It can be seen that the effect of velocity on the directionality is to shift the maximum sound pressure location closer to the axis of the flame. The convection of sources by the flow causes this shift towards the axis with an increase in flow velocity.

The effect of burner diameter on the direction of maximum sound radiation can be seen in Figure 11. Results are obtained for all the three fuels, propane, propylene and ethylene. The sound pressure levels have been converted to refer to a radius of 57" and are plotted on the graph instead of quoting all the results at a certain r/D distance. This was done so as to be able to observe the amplitudes of noise from the three burners at the same distance from the source. Figure 11 shows that there is a distinct effect of diameter on the directionality pattern. With an increase in diameter the peak in the directionality curve shifts away from the burner axis, an effect opposite to the velocity influence. Another effect due to an increase in burner diameter appears to be increased directionality. Furthermore, comparing traces from various fuels, ethylene-air flames exhibit a stronger directionality than either

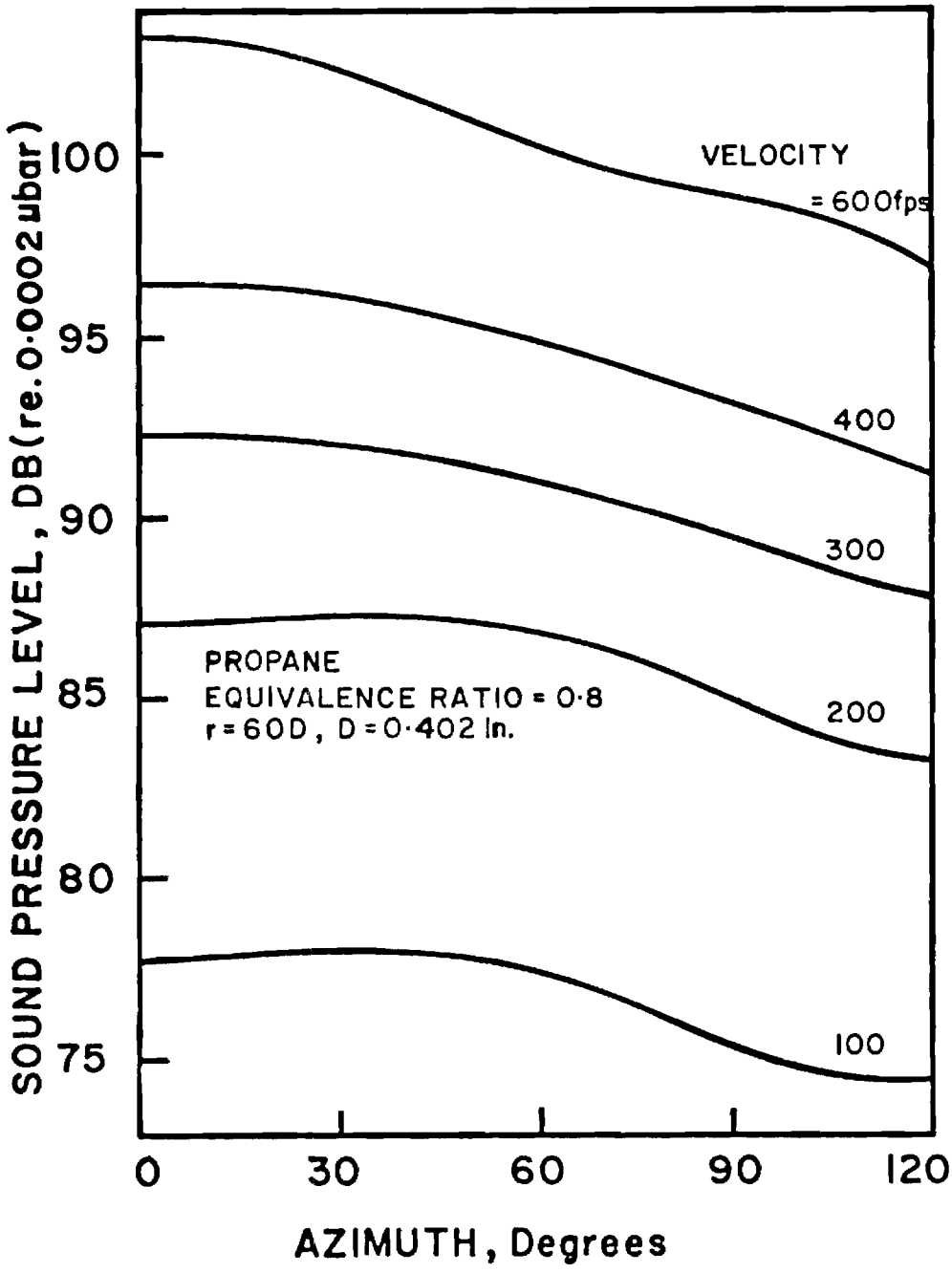

Figure 10. Directionality as a Function of Flow Velocity.

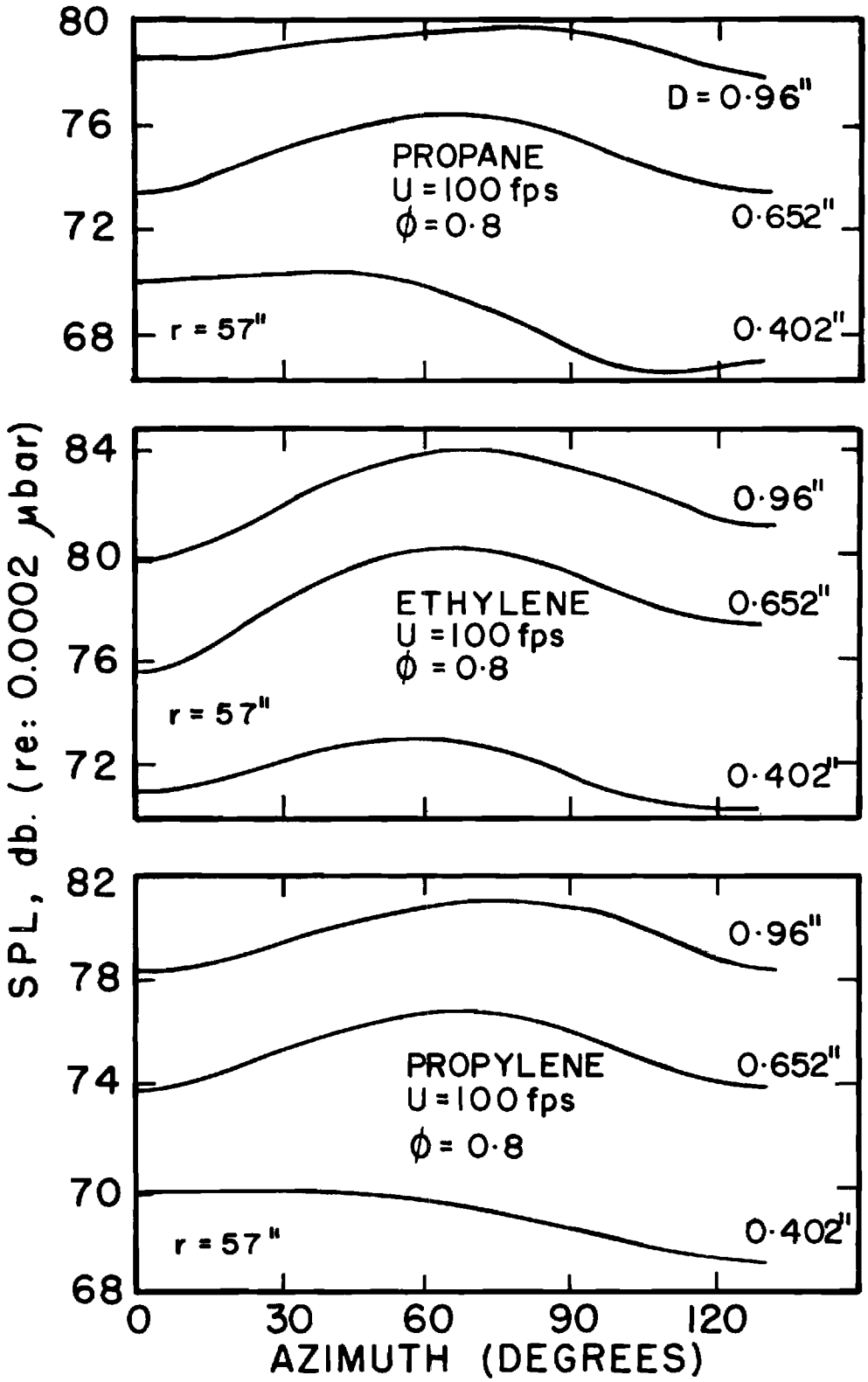

Figure 11. Directionality as a Function of Burner Diameter.

the propane-air or propylene-air flames. This could be the effect due to laminar flame speed since ethylene-air has the highest laminar flame speed.

Directionality curves as a function of equivalence ratio are plotted in Figure 12. The range of ϕ included is between 0.6 and 1.0; that is, from fuel lean to stoichiometric. The effect of equivalence ratio on directionality can be seen to be very minor. Again, ethylene cases show maximum directionality.

Scaling Laws on Acoustic Power Radiated

Velocity Scaling. Velccity of the reactants is one of the primary parameters that influence noise radiation from regions undergoing turbulent combustion. Here, the behavior of acoustic power as a function of velocity is presented in Figures 13 and 14. In Figure 13 the acoustic power radiated is plotted as a function of mean velocity of reactants at the burner exit for all the three fuels, propane, propylene and ethylene. The equivalence ratio is 0.8 and the burner diameter is 0.402". Over a 12:1 velocity range, a $U^{2.9}$ law is seen to be appropriate for acoustic power radiated. The ethylene flames appear noisier which will be seen to be a laminar flame speed effect in the succeeding paragraphs. Also, ethylene data points appear to prefer an exponent on mean flow velocity slightly lower than 2.9. Figure 14 shows the results obtained for 0.652" and 0.96" burners. There is a good agreement with the scaling law obtained for a 0.402" burner, although in this case, a $U^{2.6}$ law fits the data better. This result is in agreement with the results of Reference 17 which predicted a velocity scaling exponent to be greater than 2. Also, this velocity exponent is much lower than the velocity scaling for subsonic jet noise[19,20].

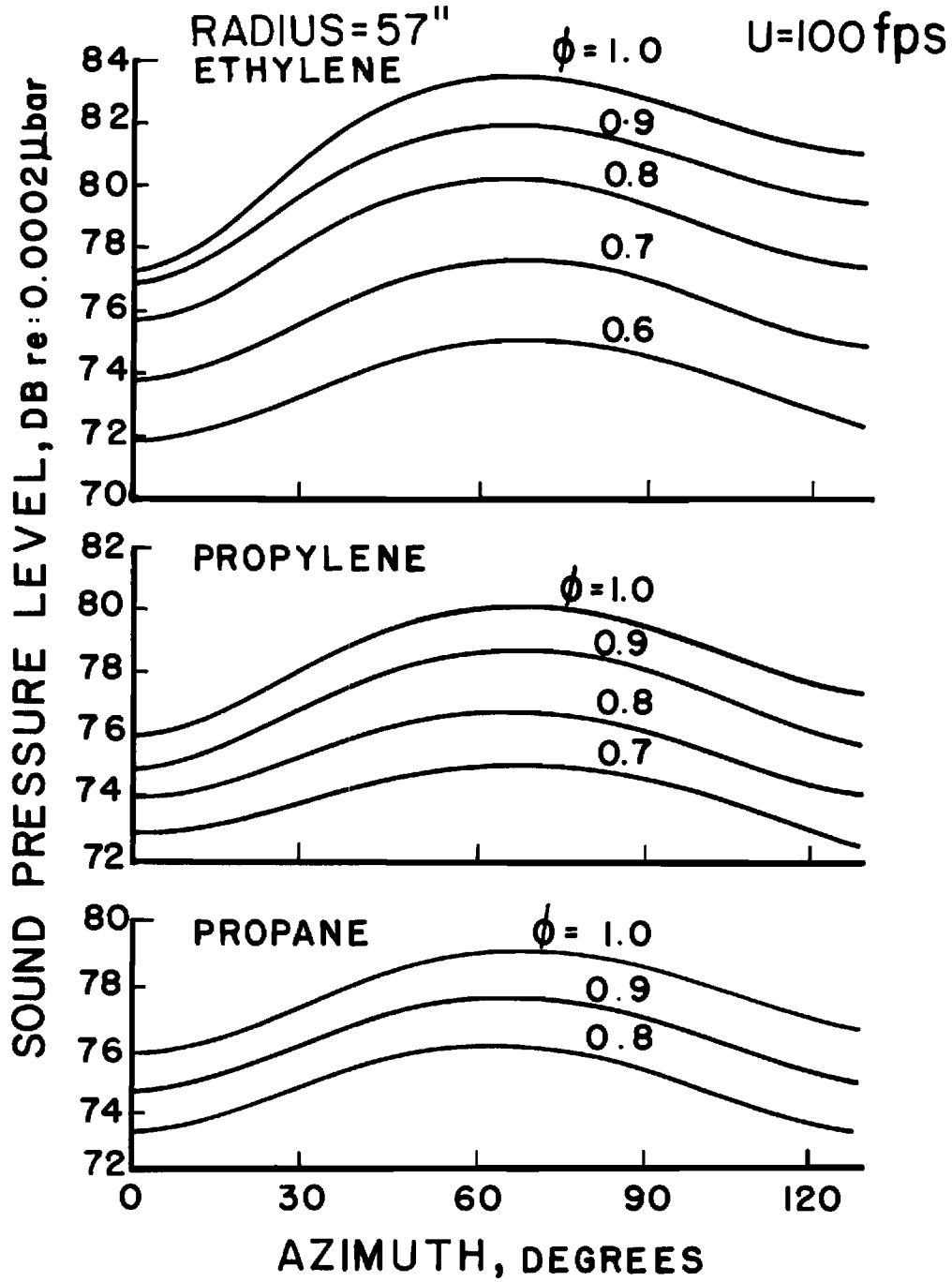

Figure 12. Effect of Equivalence Ratio on Directionality for a Burner of Diameter 0.652".

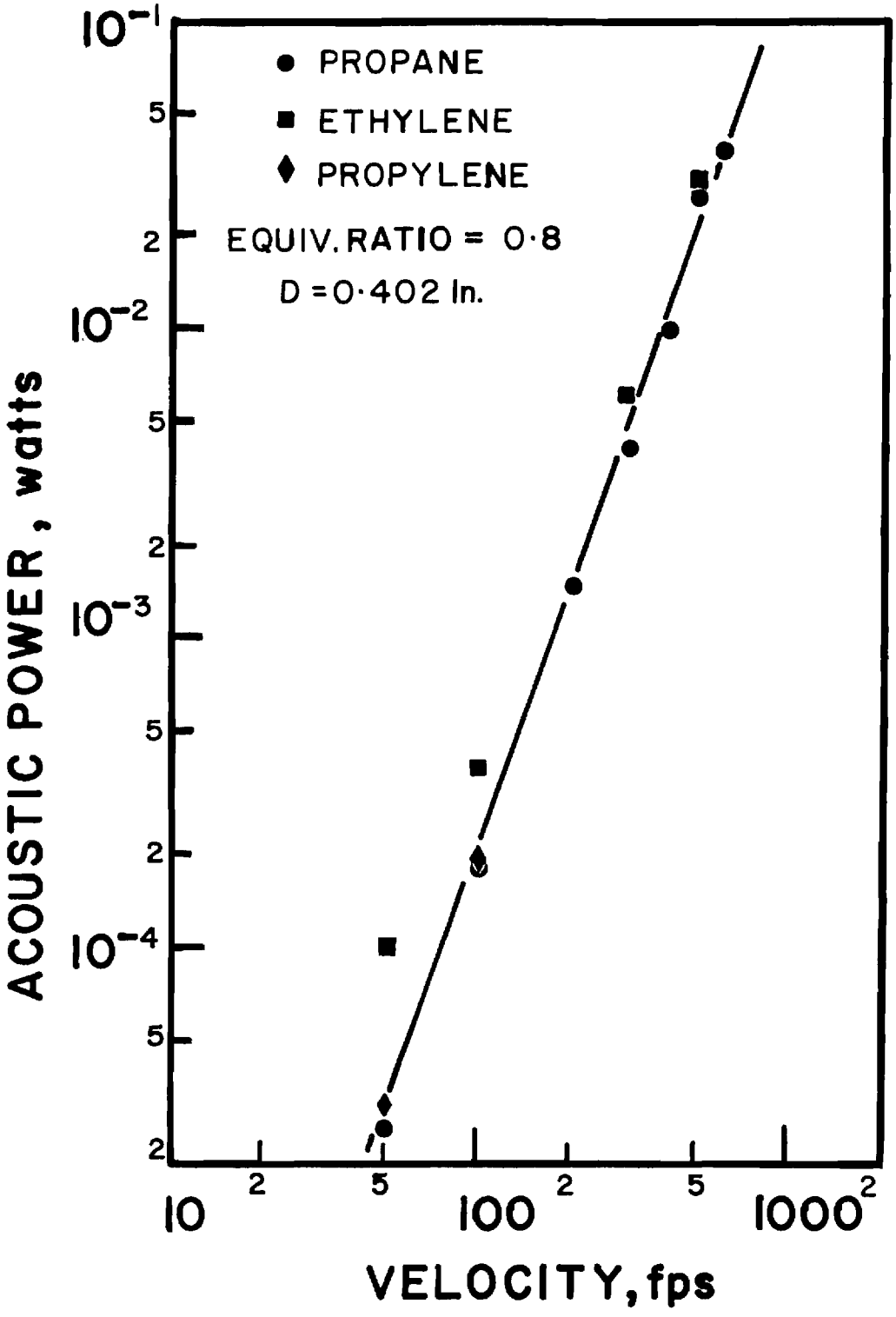

Figure 13. Acoustic Power as a Function of Velocity for a Burner of Diameter 0.402".

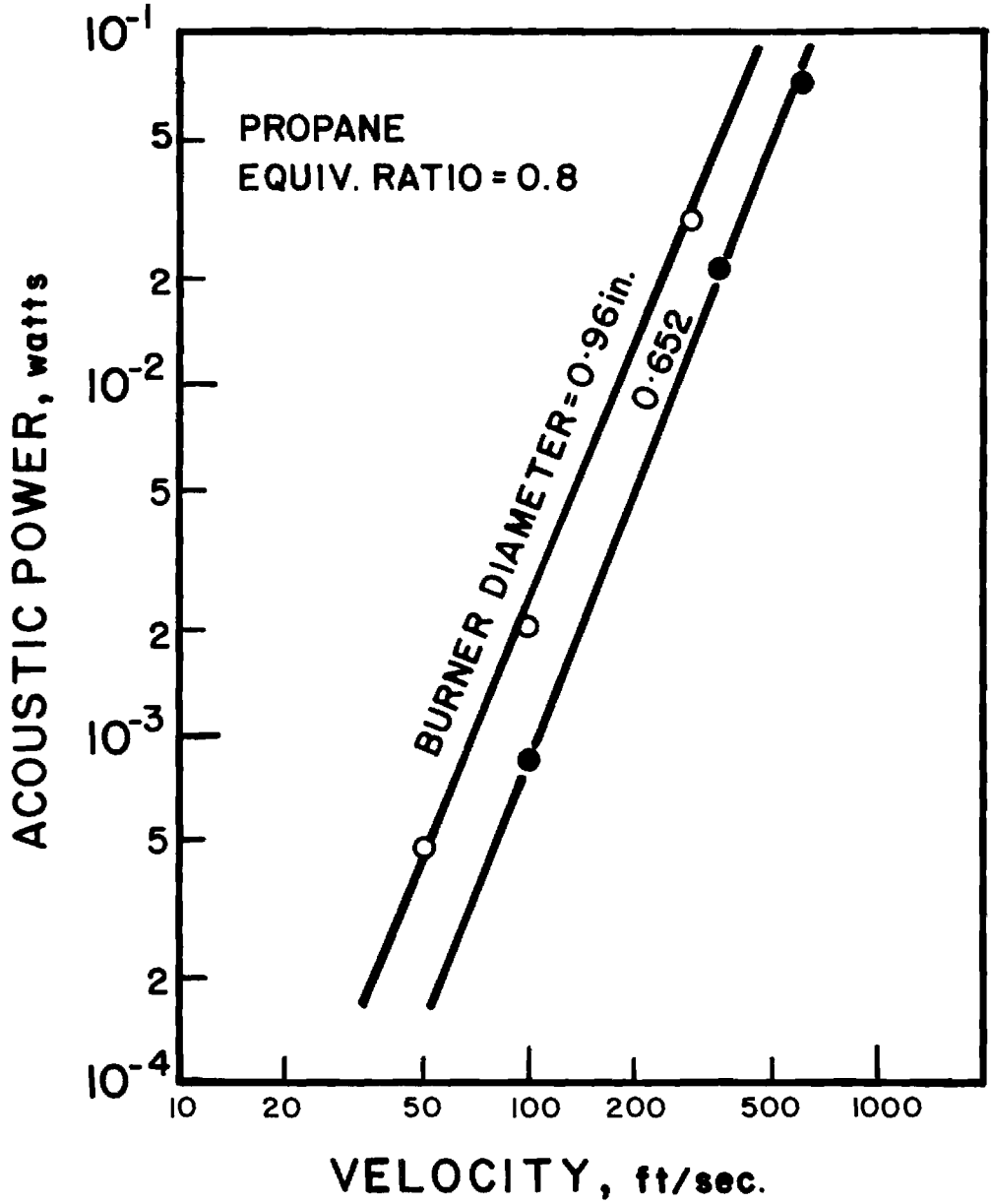

Figure 14. Acoustic Power as a Function of Velocity for Burners of Diameters 0.96" and 0.652".

Diameter Scaling. The diameter of the burner is yet another parameter of interest in noise radiation from flames. A positive exponent of U obtained in the preceding paragraph would suggest lowering of flow velocity to decrease noise output. This would imply that burner size would have to be increased to maintain the same mass flow. The effect of diameter, therefore, becomes quite important. Primarily, the knowledge of the diameter effect is required in order to predict the noise output from larger burners.

Figure 15 shows the results of the experiments conducted to determine the diameter effect. An acoustic power scaling of $D^{3.0}$ is obtained in the case of all the three fuels. The effect of decreasing flow velocity can now be considered. For a burner of circular cross section the mass flow is given by

$$\dot{m} \propto \rho_o U D^2 \tag{7}$$

Thus, reducing the velocity by a factor of 4, say, would mean increasing diameter by a factor of 2 to maintain constant $\dot{m}$. Since the noise exponents on U and D are almost equal to each other, there seems to be a definite advantage in choosing the lowest value of the flow velocity possible within the other design restrictions.

Laminar Flame Speed Scaling. Laminar flame speed, S_L, is a measure of the reactivity of the fuel. It represents the velocity of propagation of a laminar flame through a reactive mixture. For turbulent flames, a turbulent flame speed, S_t, could be defined. There is sufficient

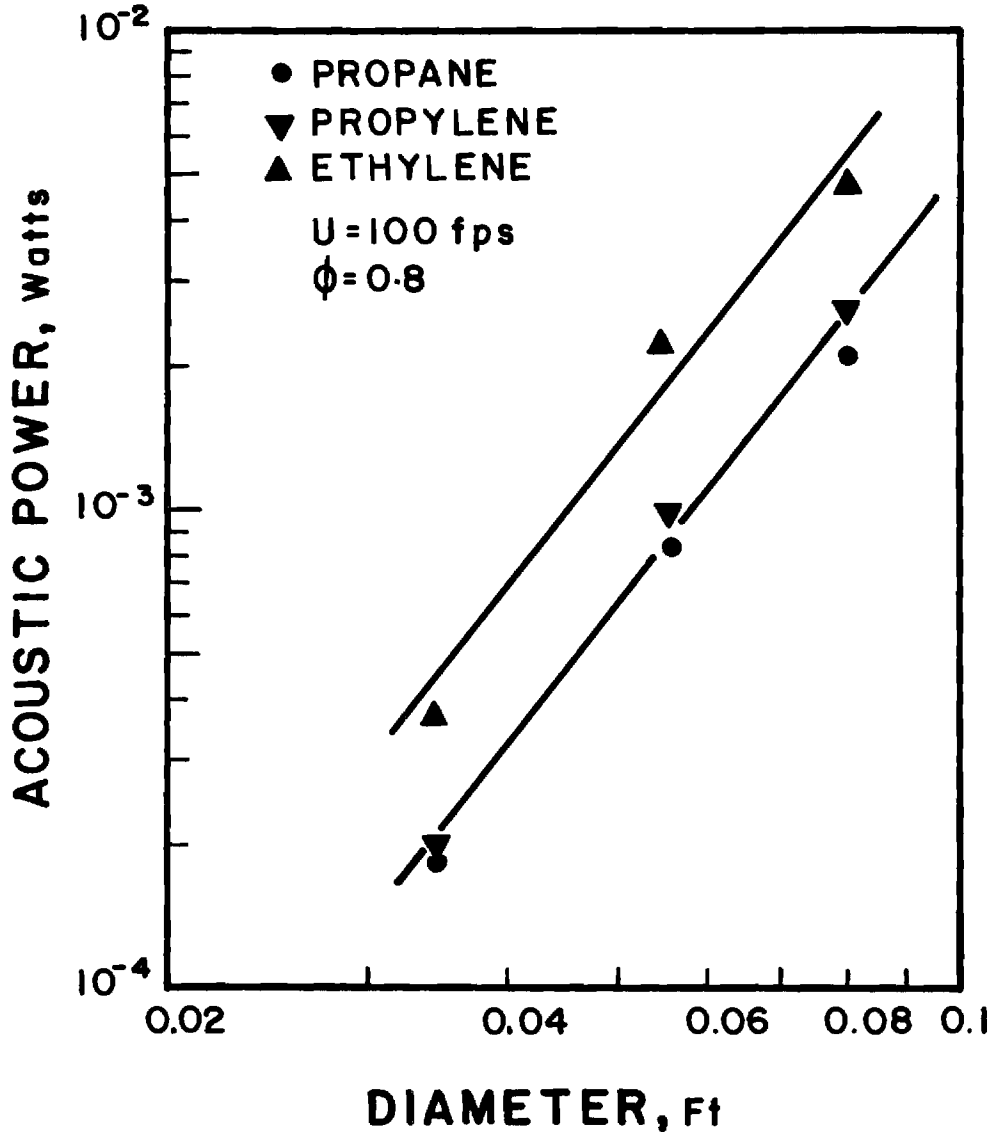

Figure 15. Acoustic Power as a Function of Burner Diameter for Fuel-Lean Flames.

evidence[24] to show that turbulent flame speed is proportional to laminar flame speed; S_t is always higher due to faster transport processes in a turbulent flame. Further, S_t is dependent on flow conditions as well. Thus, if flow conditions like mean flow velocity, turbulence intensity and scale are being considered independently, laminar flame speed would appear to be the correct parameter to choose. In this analysis, therefore, laminar flame speed has been chosen to represent the chemistry effects due to changes in fuel and mixture ratio. The values used in this analysis for S_L are calculated from the equation

$$\frac{S_L}{S_{L_{max}}} = 2.6 \log_{10} \phi + 0.94 \qquad (8)$$

$$(\phi \leq 1.0)$$

from Reference 25. The values of $S_{L_{max}}$ were also chosen from Reference 25. Table 3 shows the values of $S_{L_{max}}$ used.

Table 3. Values of Laminar Flame Speed from Reference 25 for Combustion with Air at Atmospheric Pressure and Room Temperature

Fuel	$\frac{S_{L_{Max}}}{S_{L_{Max,\ Propane}}}$	$S_{L_{Max}}$ Ft/Sec
Propane	1.00	1.41
Ethylene	1.75	2.46
Propylene	1.12	1.58

Figure 16 shows the variation of acoustic power with laminar flame speed. The independent variation of S_L is obtained by changing fuels with all other parameters held constant. But, there is a certain variation in fuel mass fraction F even when ϕ is constant because

$$F = \frac{\phi\left(\frac{F}{1 - F}\right)_{Stoic}}{1 + \phi\left(\frac{F}{1 - F}\right)_{Stoic}} \tag{9}$$

and $\left(\frac{F}{1 - F}\right)_{Stoic}$ for propane, propylene and ethylene are 0.064, 0.0678, and 0.0678 respectively. However, this variation in F is small in comparison with the S_L variation and it will be shown later that the exponent on F is smaller, also. Figure 16 should, therefore, yield estimates of the scaling on S_L. Acoustic power appears to scale to an exponent of 1.4 - 1.6 with S_L for fuel lean to stoichiometric mixtures. This confirms the belief that noise reduction can be achieved by reducing the reactivity of the fuel. The extent of reduction possible, however, cannot be appreciable due to a rather low value of the exponent.

Combined Scaling Law. Although the study of a phenomenon dependent on many parameters can be made by varying them one at a time and this results in ease and clarity of analysis, it is not without disadvantages. The most serious disadvantage is that a large number of experiments would have to be performed, this number increasing rapidly with the number of independent parameters. Also, such an analysis using one variable at a time does not utilize all the information that can be obtained from the

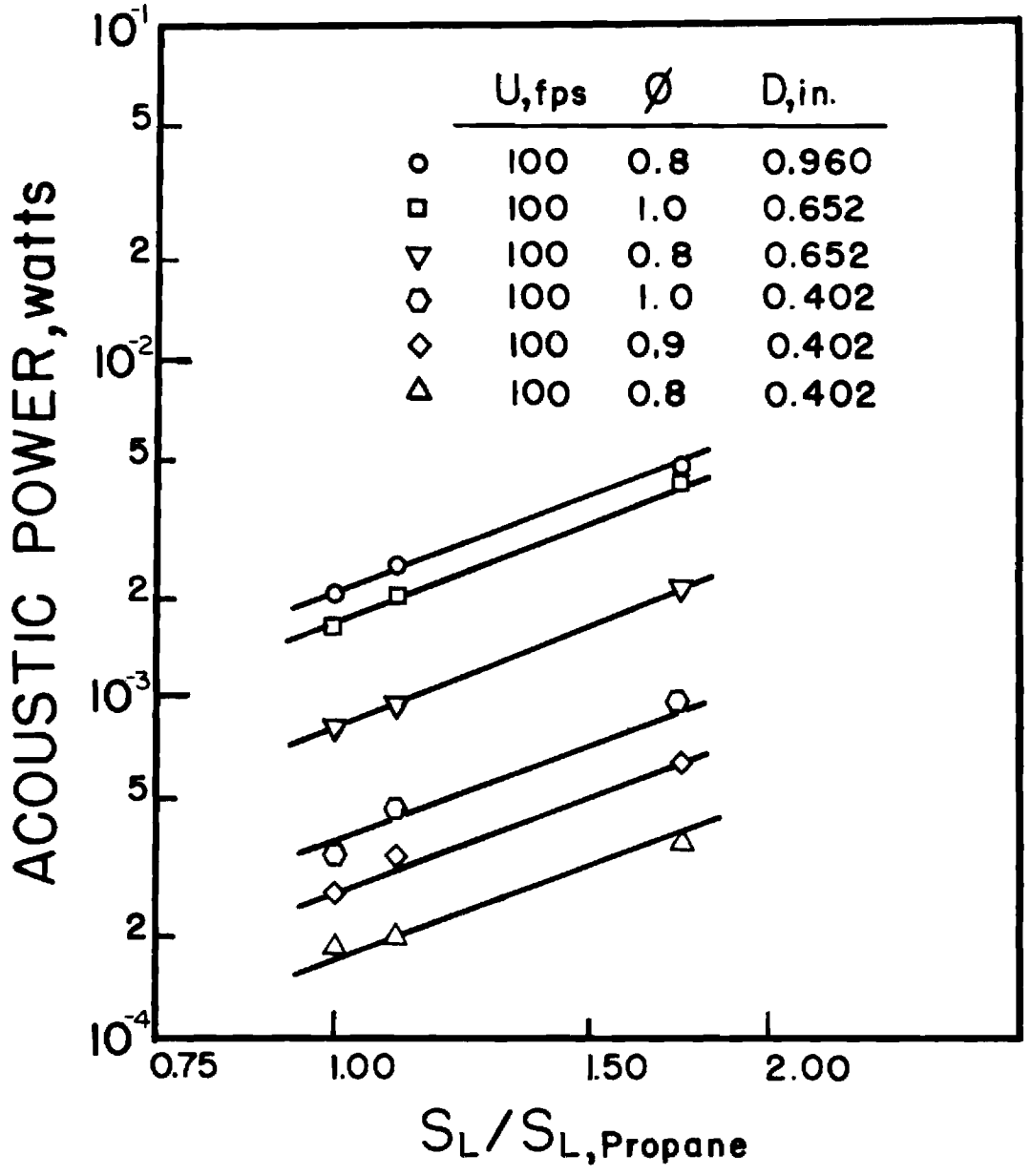

Figure 16. Acoustic Power as a Function of Laminar Flame Speed.

test results. Furthermore, in a real situation, the various parameters vary simultaneously rather than one at a time. Thus it would be meaningful to try to deduce a combined scaling law utilizing all the experimental results generated for the particular quantity.

An effective means of examining the experimental data is by regression analysis in which a theoretically derived law is fitted to the experimental data. In this case, the possible law would be of the type

$$y = K \prod_{i=1}^{N} x_i^{c_i} \tag{10}$$

where K and the c_i's are constants and the x_i's are parameters affecting a quantity y. By taking logarithms on both sides of Equation (10), it is possible to curve fit as a linear problem by the method of least squares.

For the case of acoustic power P scaling, Strahle has suggested that the parameters are U, D, S_L and F. Using 57 different tests the following expression was obtained for the acoustic power radiated from open turbulent premixed flames:

$$P = 6.7 \times 10^{-2}\ U^{2.74}\ D^{2.86}\ S_L^{1.17}\ F^{3.04} \text{ watts} \tag{11}$$

where

$$50 \leq U(\text{fps}) \leq 600$$

$$0.0335 \leq D(\text{ft}) \leq 0.08$$

$$0.6 \leq \phi \leq 1.0$$

and U and S_L are in fps; D is in ft

An analysis of errors due to the regression fit showed a mean error of 5.5% with 117% and -58% as the maximum and minimum errors respectively The standard deviation was 35%. These errors appear at first sight to be rather large. However, they can be considered very reasonable because of the following reasons:

a) A very wide range of acoustic powers (from 10^{-1} to 10^{-5} watts) are included in Equation (11).

b) The instrumentation accuracies are of the order of a db (if power P_1 is 1 db larger than P_2, then P_1/P_2 will be as large as 1.25), and

c) The flow measurement accuracy was no better than 3% of full flow rates. The flow inaccuracies can affect U and mixture ratio. The error in mixture ratio will introduce errors in both F and S_L.

In order to graphically observe the significance of the regression fit, the calculated values of acoustic power ($P_{regression}$) were cross plotted against the measured values ($P_{measurement}$) in Figure 17. Without doubt it can be said that Equation (11) fits the experimental data very well. Thus, it can be stated that acoustic power can, in fact, be represented by a power type law with respect to the parameters U, S_L, D and F. Further, laminar flame speed S_L appears to be quite adequate to represent the chemistry effect due to various fuels.

It is interesting to note that some of the Smith and Kilham[3] data plotted on Figure 17 show that the measurements of Smith and Kilham can be reproduced satisfactorily by Equation (11). Reference 3 deduced a $(US_LD)^2$ law for acoustic power. Equation (11) can explain the results of Reference 3 and has been obtained over a much wider range of acoustic

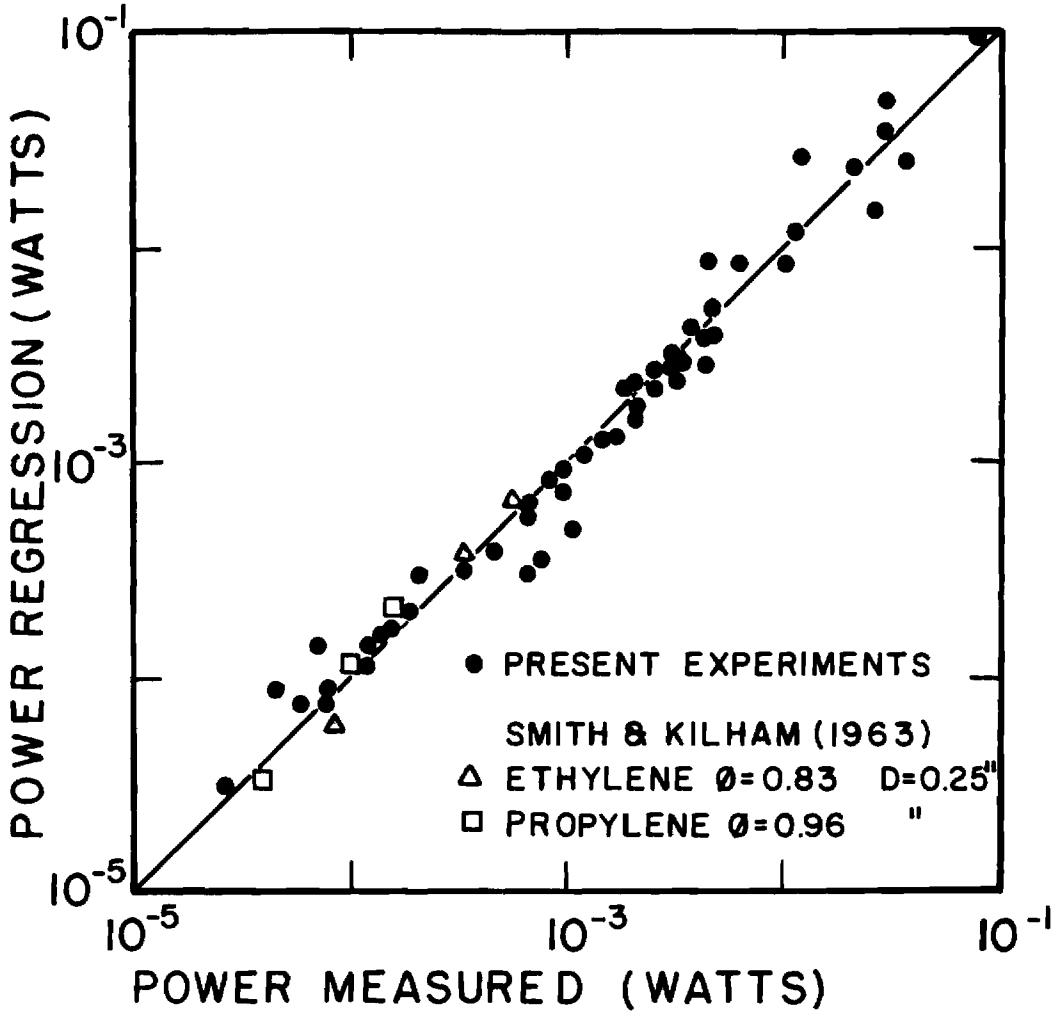

Figure 17. Significance of the Regression Fit for Acoustic Power.

powers, thus establishing a clear preference over the $(US_L D)^2$ law. Surprising as it may seem, Equation (11) is the first empirical relation published from which acoustic power can be calculated directly for noise from hydrocarbon-air turbulent flames. Equation (11) should prove quite useful to anyone interested in determining noise output from combustion zones.

Thermo-Acoustic Efficiency

Thermo-acoustic efficiency is a measure of the portion of total thermal input to the flame converted into noise radiation. Thermo-acoustic efficiency η_{ta} is defined as

$$\eta_{ta} = \frac{\text{Acoustic Power Radiated}}{\text{Thermal Input}} \tag{12}$$

If $\dot{m}$ is the mass flow rate of reactants, and H is the heating value per unit mass of fuel, then

$$\text{Thermal input} = \dot{m}FH$$

where as before F is the fuel mass fraction,

$$\dot{m} = \rho_o \frac{\pi}{4} D^2 U$$

and ρ_o is the density of mixture of reactants. Thus,

$$\eta_{ta} = \frac{P}{\frac{\pi}{4} \rho_o U D^2 F H} \tag{13}$$

Therefore, the scaling laws for η_{ta} can be obtained from scaling laws for acoustic power radiated. For the premixed open turbulent flames of this study, $\eta_{ta} \propto U^{1.7} D^{0.9} F^{2.0} S_L^{1.2}$ would represent the behavior of η_{ta}. Some representative values of thermo-acoustic efficiency are presented in Table 4. The results for a burner of diameter 0.402" and equivalence ratio of 0.8 are shown over the entire velocity range. The maximum η_{ta} is of the order of 10^{-6}. This indicates that for high velocity flames combustion noise could in fact be quite substantial.

Table 4. Thermo-Acoustic Efficiency

Test	Power Watts	$\eta_{ta} = \frac{\text{Power Radiated}}{\text{Thermal Input}}$
P- 50-0.8-1	0.264×10^{-4}	8.36×10^{-9}
P-100-0.8-1	0.183×10^{-3}	2.89×10^{-8}
P-200-0.8-1	0.154×10^{-2}	1.22×10^{-7}
P-300-0.8-1	0.423×10^{-2}	2.23×10^{-7}
P-400-0.8-1	0.104×10^{-1}	4.10×10^{-7}
P-500-0.8-1	0.271×10^{-1}	8.57×10^{-7}
P-600-0.8-1	0.382×10^{-1}	1.01×10^{-6}

Spectral Content of Combustion Noise

The acoustic emission from regions of turbulent combustion has

been recognized in the literature as a broad-band noise with a single peak in the 250 Hz - 1500 Hz range. Discrete frequency components appear when the combustion is confined by enclosures[22,26]. This is not of interest to the present study of open turbulent flames. The frequency spectra will clearly indicate the type of acoustic material that will be needed for noise reduction treatments. Furthermore, the peak frequency will establish the characteristic time in the flame and comparison with the theories in References 17 and 18 will assist in determining the most plausible mechanism of noise generation.

Procedure. The frequency spectra of noise were obtained from the tape recording of sound pressure signals. A Hewlett Packard Fourier analyzer was used. The analyzer was programmed to produce power spectra by the following process. First the analog signal is digitized. Then, the Fourier transform is taken. This is multiplied by its own complex conjugate. The process is repeated a fixed number of times to obtain a stable average. The number of samples required depends on the particular signal being analyzed. Also, the number of digital bits of information used in each sample decides the maximum frequency and the frequency resolution.

A low-pass filter was inserted between the Fourier analyzer and the tape-recorder (Figure 5) to eliminate all frequency components above a preselected maximum. If this is not done the high frequency components will fold over and appear as spurious low frequency components due to the inherent quality of all A to D converters called aliasing. After a preliminary study, the maximum frequency was selected at 8 kHz for the noise spectra. Since the filter frequency response is not flat

beyond 0.8 $f_{cut\text{-}off}$ only spectra up to 5 kHz are presented in this report. The initial spectra were obtained with the number of samples used in averaging between 15 and 200. The 15 sample averaging was found to be adequate to obtain all the information required while the 200 sample averaging resulted in smoother spectra with less scatter. Thus a majority of the combustion noise spectra were obtained with 15 to 50 sample averaging.

The frequency spectra depend on U, D, S_L and F. Also, if combustion noise radiation directionality is frequency dependent, then the spectra depend on the microphone location as well. The spectra shown in the figures that follow are smooth lines drawn through the spectra plotted on the x-y plotter. Figure 18 shows both the actual x-y plot and the smooth line drawn through the mid-points for a typical case. The smooth line is found to be quite satisfactory for representing the spectrum.

Results. The frequency dependence of directionality is studied in Figures 19(a) and (b). Very similar spectra were obtained in all the tests conducted. The azimuth and radius are referenced to the burner exit in these figures. Thus, amplitude comparisons cannot be made directly without correcting the results for the acoustic center. The information regarding directionality can, of course, be obtained from Figures 19(a and b) without any corrections. If the directionality patterns were independent of frequency the spectra at various azimuthal locations would be parallel to each other. An examination of the spectra reveals that directionality of noise generated is almost independent of frequency except for the locations near the axis of the flame which

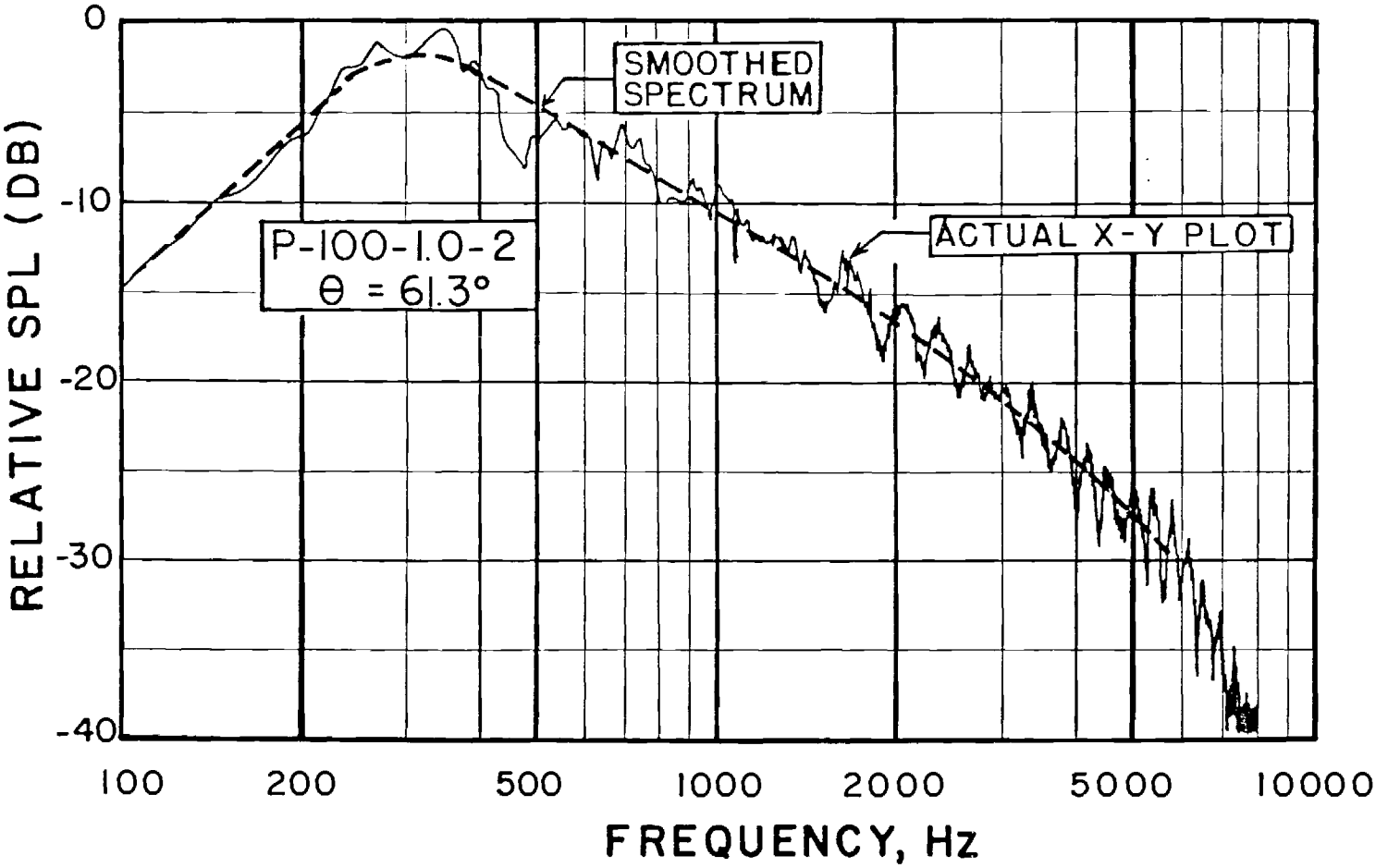

Figure 18. Actual X-Y Plot and Smoothed Spectrum.

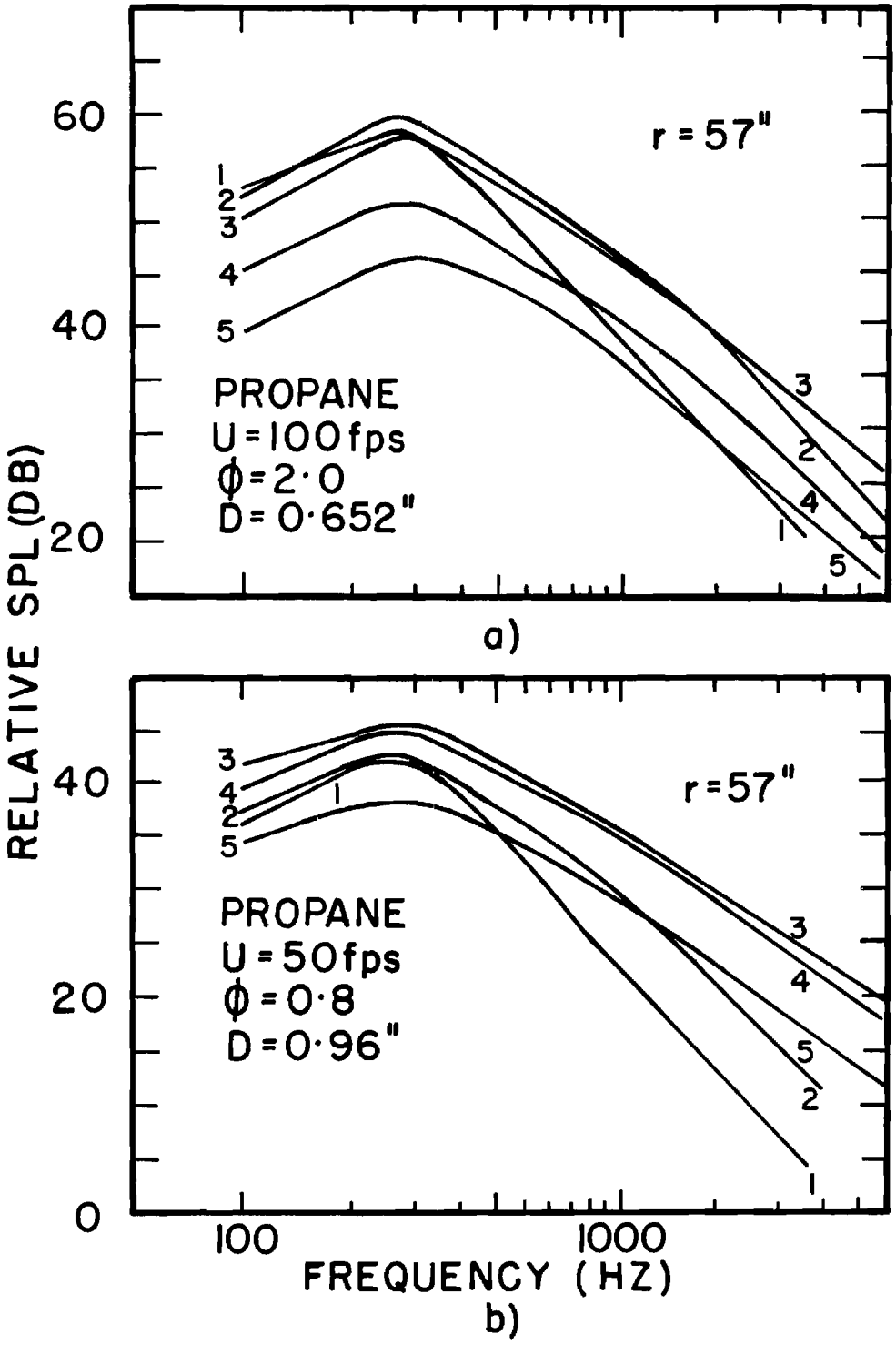

Figure 19. Frequency Dependence of Directionality. The Numbers 1 to 5 Indicate Microphone Locations between 15° and 120°.

exhibit a strong reduction in the high frequency components. Reference 9 observed a much stronger dependence for pure diffusion flames of CH_4 and H_2 burning in air.

Figure 20 presents the effects of flow velocity and laminar flame speed on the frequency spectra. There is clearly a tendency for the peak frequency (frequency corresponding to maximum amplitude on the spectrum) to increase with flow velocity. However, the rate of increase is small. For propane over a 12:1 velocity range the peak changes from 350-270 Hz while for ethylene over a 10:1 velocity range the peak frequency varies between 650 and 350 Hz. The increase in peak frequency is a little more marked for ethylene-air mixtures in comparison with propane-air mixtures. In any case, the peak frequency is a very weak function of flow velocity and it appears doubtful if using Strouhal number (f D/U) as a non-dimensional parameter as suggested in References 3 and 5 would serve any useful purpose. Use of Strouhal number has been found appropriate for jet noise in Reference 20, where the peak frequency is found to scale inversely with D and directly with U. The experiments for fuel rich flames also showed a similar velocity behavior. Further, Figure 20 shows that the peak frequency for ethylene is higher than that for propane. Since ethylene has higher S_L values this is clearly an effect due to S_L. It appears, therefore, that the characteristic time in the flame is considerably influenced by the chemical time.

Combustion noise can be seen to peak at lower frequencies with an increase in burner diameter in Figures 21(a), (b) and (c). This diameter effect, however, is quite small when compared with a 1/D dependence for jet noise. Again, Strouhal number appears to be inappropriate for

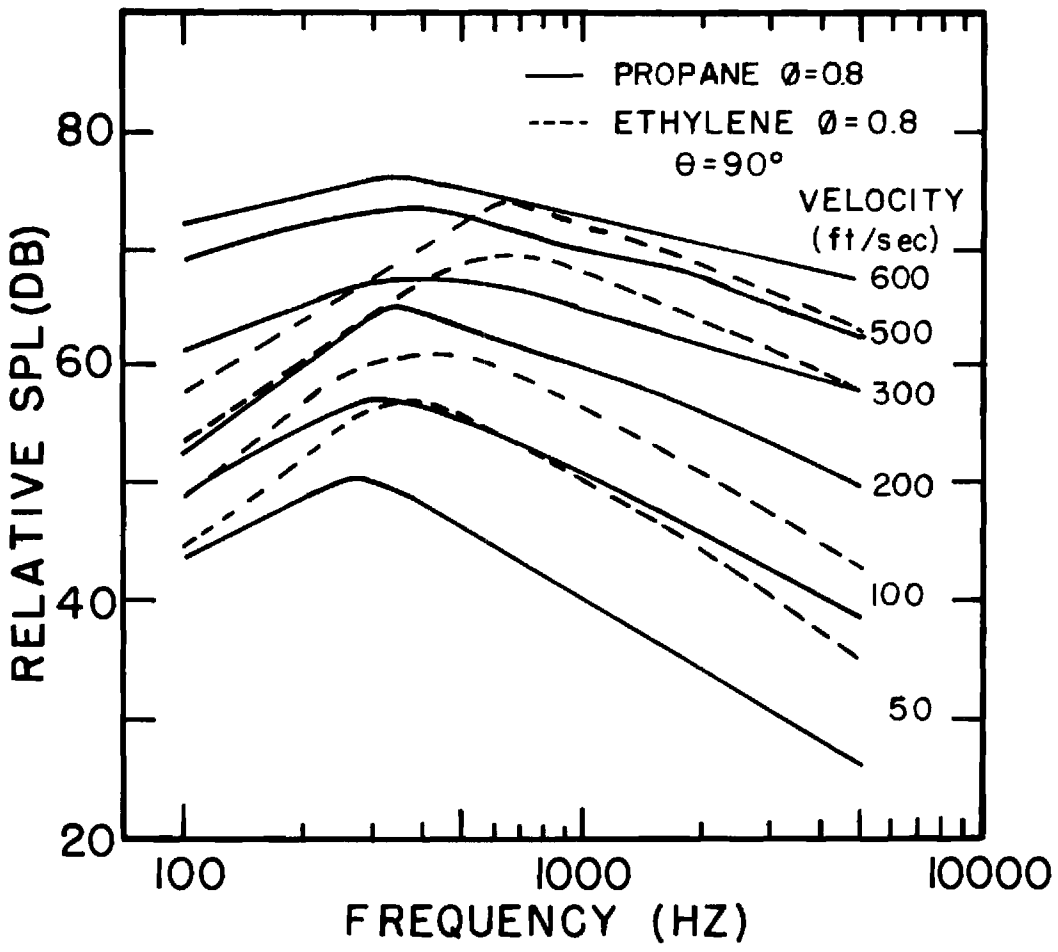

Figure 20. Effects of Velocity and Laminar Flame Speed on the Frequency Spectra.

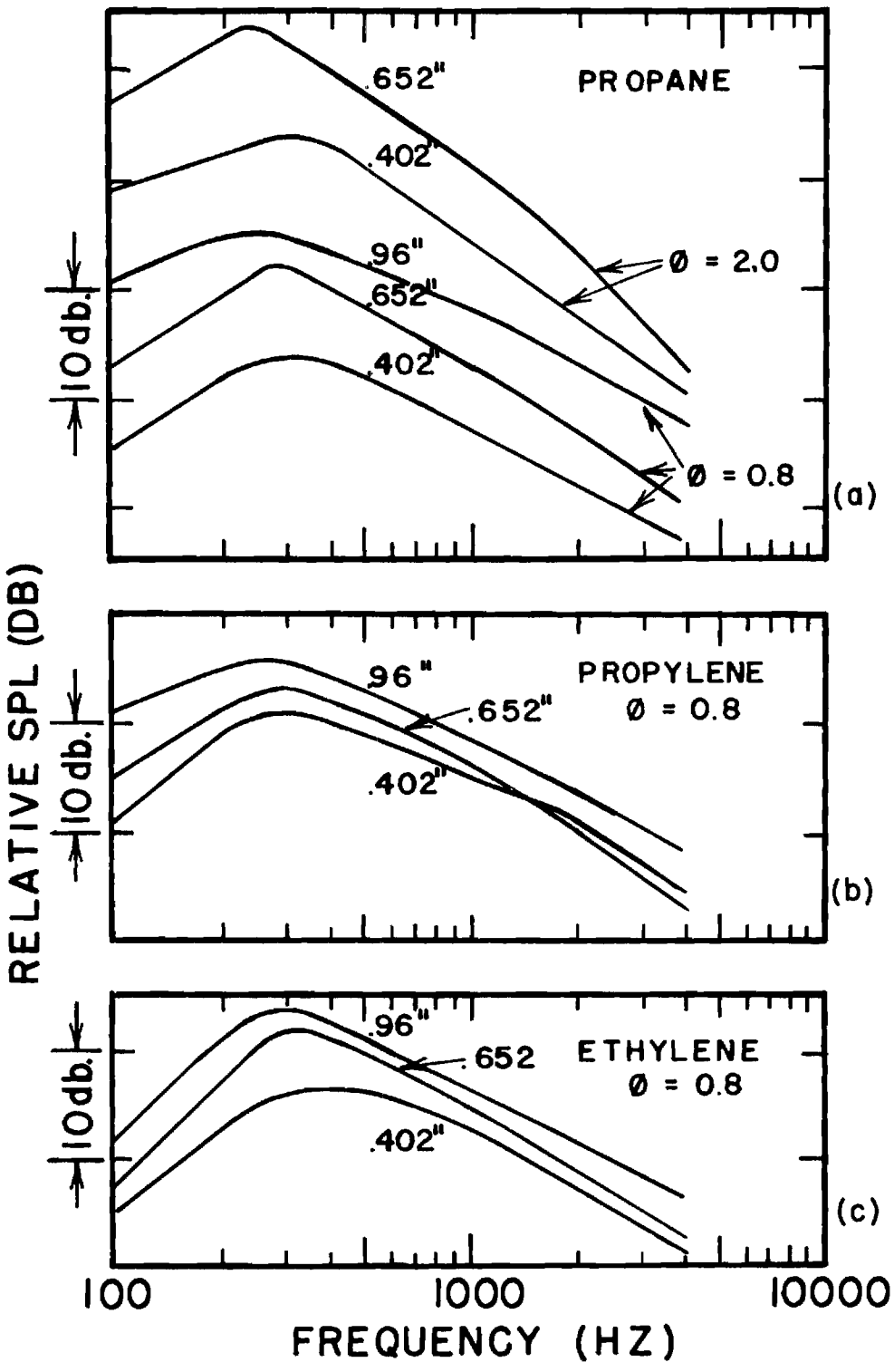

Figure 21. Effect of Burner Diameter on the Frequency Spectra.

combustion noise.

Figure 22 shows the effect of equivalence ratio on frequency spectra. While propane and propylene flames show negligible effects the ethylene flames show some effect due to equivalence ratio.

Peak Frequency. A power type law (Equation (10)) was fitted by regression analysis to the peak frequencies measured. The procedure followed was identical to the one used for obtaining acoustic power law (Equation (11)). If f_c is the peak frequency then the regression analysis gives

$$f_c = 198.9\ U^{0.20}\ D^{-0.08}\ S_L^{0.45}\ F^{0.31}\ \text{Hz} \qquad (14)$$

where U and S_L are in fps and D is in ft.

$$0.6 \leq \phi \leq 1.0$$

$$50 \leq U(\text{fps}) \leq 600$$

$$0.0335 \leq D(\text{ft}) \leq 0.08$$

The number of tests was 56, the mean error was 0.85% and the standard deviation was 13.3%. Equation (12) shows that S_L and F have the most effect on peak frequency and U and D effects are negligible. An inverse S_L and F scaling would explain the negligible ϕ dependence of propane and propylene flames shown on Figure 22. The behavior of f_c of ethylene flames with ϕ is somewhat anomalous.

Discussion of Results

A discussion of the experimental results of this study in the light of the theories of Strahle[16,17,18] and other experimental results

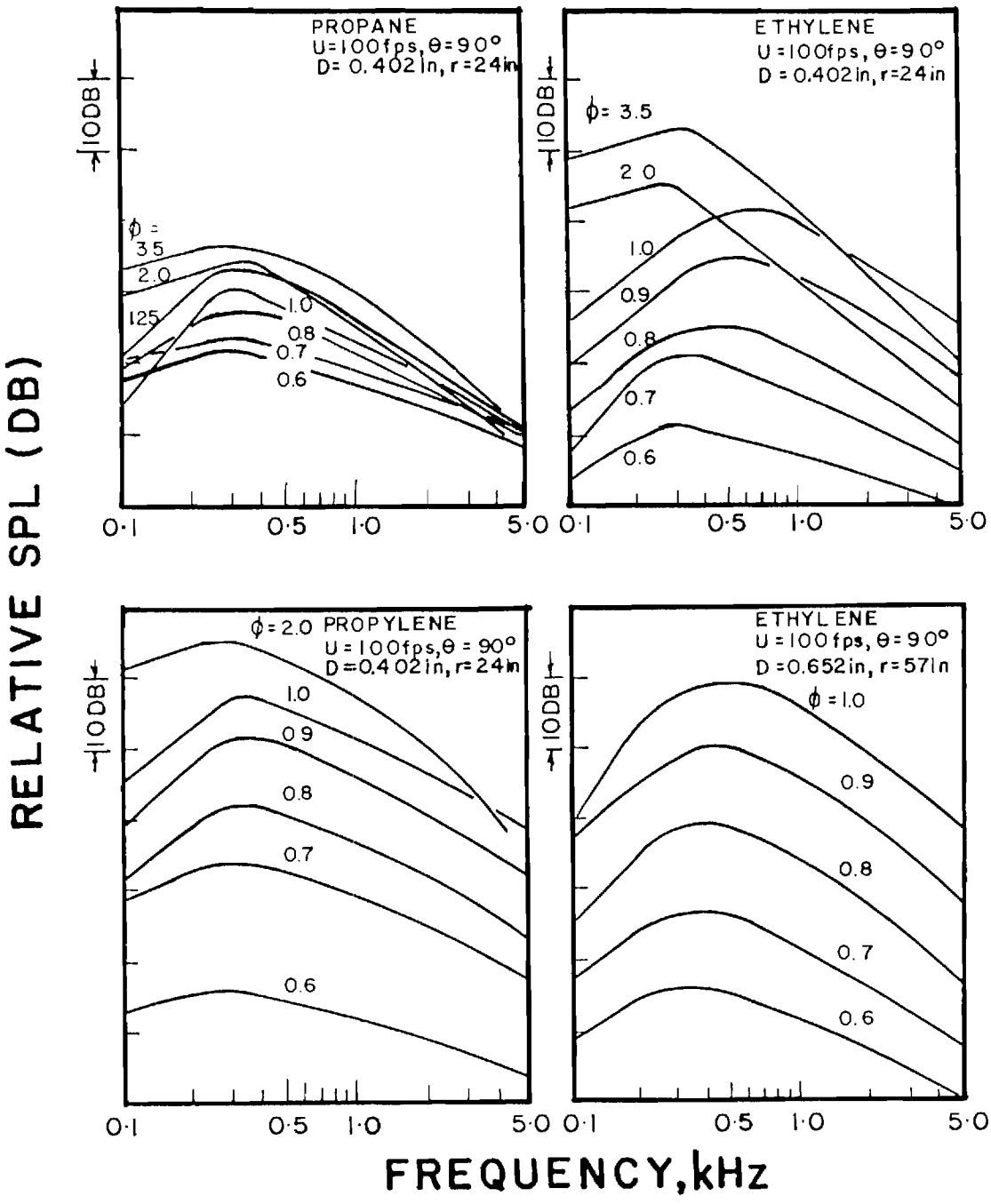

Figure 22. Effect of Equivalence Ratio on Frequency Spectra.

that are available will be presented in the succeeding paragraphs.

The directionality of combustion noise is seen to be rather weak. In this study the maximum difference, between the maximum sound pressure level and the minimum (observed at the $\theta = 0^{\circ}$ location) sound pressure level over a constant radius path around the flame in a plane containing the flame axis, was about 4 db. The general lack of strong directionality would support the monopole theory of noise generation. Further, there is some similarity between the experimental results for directionality and the directionality patterns deduced in Reference 18 considering refraction at temperature discontinuities. Thus, the directionality patterns can qualitatively be explained by the refraction theory. The general tendency for the location of peak sound pressure to shift towards the axis with an increase in velocity is a result of the convection effect. The spectra of the sound pressures as measured by the five microphones at various aximuthal positions have shown that directionality is frequency dependent to the extent that the high frequency components drop off rather rapidly towards the burner axis. The results of Reference 18 considering refraction effects showed a similar effect with increasing frequencies. Thus, the high frequency fall-off near the axis could be at least qualitatively explained by the refraction effect. The directionality patterns of Reference 3 have general similarity with the patterns presented in this work. Price et al saw a more marked effect of frequency on directionality for a pure diffusion flame of H_2-CH_4 burning in air. Except for some results with the 0.402" burner all other results show maximum noise radiation at 50° - 80° to flow direction. An off-axis maximum is very important for noise reduction efforts using acoustic liners.

The spectra of combustion noise show a predominantly low frequency nature. They show a broad-band noise with a single peak and a gradual amplitude fall-off on either side of the peak. The rate of fall-off on the high velocity cases was observed to be rather slow. This could be due to the fact that the difference between jet noise and combustion noise decreases with flow velocity as shown in Figure 7. Thus, the higher velocity flames show a slight increase in higher frequency components. The noise spectrum, however, is decided by the predominant combustion noise. The peak frequency does not seem to be strongly influenced by any parameter. F and S_L appear to have the most effect. For all practical purposes one could summarize the experimental findings by stating that combustion noise peaks in the 250-700 Hz range for hydrocarbon-air flames. The values of peak frequencies obtained here are in excellent agreement with the values obtained by References 3, 11 and 15 for premixed flames. Even diffusion flames of Reference 12 seem to support the above statement. Hurle et al report a peak frequency of 1200Hz for a stoichiometric ethylene-air flame on a 0.175" diameter burner. This value is slightly higher than what would be obtained from the peak frequency relation deduced in this work (Equation (14)). However, the spectra of Kotake and Hatta[5], which show for stoichiometric natural gas-air flames a flat low-frequency spectra, look improbable in view of the extensive analysis of our study which always showed a recognizable low frequency fall-off. Also, it appears quite improper to try to use Strouhal number to non-dimensionalize combustion noise peak-frequencies as suggested by References 3 and 5.

The results shown in Equation (14) emphasize that chemical time is an important characteristic time in the flame. Referring to Strahle's[17]

theories, all the three models of turbulent combustion can explain the values of peak frequencies reported.

The scaling laws for acoustic power and thermo-acoustic efficiency generated in this work are considered to be a major contribution to the noise data on open turbulent flames. The scaling laws have been obtained over a much wider range of values of the parameters compared to those of the only other similar work[3]. Also, Smith and Kilham[3] deduced the scaling laws on only U by actual sound pressure measurement around the flame while obtaining those on S_L and D by a single microphone sound pressure measurement. Further, the important parameter F was not considered in their work. In addition, the experimentally measured acoustic powers of Reference 3 could be reproduced by the experimental regression equation, Equation (11), of this study as shown on Figure 17. Thus, it is felt that the scaling laws for acoustic power presented in Equation (11) are more representative of noise radiation than the $(US_LD)^2$ scaling of Reference 3.

The scaling laws for acoustic power deduced by Strahle[17] showed that for premixed flames, Equation (5)

$$P = K\, U^{a_1}\, S_L^{a_2}\, F^{a_3}\, D^{a_4}\, \ell_t^{a_5}\, \vartheta^{a_6}$$

would allow: $a_1 = 2 - 3.5$, $a_2 = 2 - 5$, $a_3 = -1.8$, $a_4 = 2$, $a_5 = 1.5 - 3$ and $a_6 = 0 - 2.5$, depending upon the model of turbulent combustion considered. Notice that with reference to a_3, a relation $(\Delta\rho/\rho F)^2 \propto F^{-1.8}$ has been used. This relation was obtained for premixed hydrocarbon-

air flames at room temperature and atmospheric pressure using the data available in Reference 27. Comparing the scaling laws above with Equation (11), it can be seen that the exponent on U is within the values of a_1 specified by the theory. In view of the facts that only D is considered in Equation (11) and the result $\ell_t \propto D$ from Chapter III, the theory would allow a D exponent between 3.5 and 5 as compared with the experimental value of 2.9. For S_L, the theoretical expectation allows an exponent between 2 and 5 and experimentally 1.2 is observed. As far as F scaling is concerned, an error of F^2 has been noticed in the autocorrelation estimation of Reference 17. If this is taken into account, a $F^{0.2}$ law would result against the experimental $F^{3.0}$ law. Thus, the theoretical estimates of Reference 17 do not fall completely in line with the experimentally generated scaling laws. The basic differences may be attributed to incorrect order of magnitude estimates made in the theory of Reference 17 with extremely limited knowledge available at that time. The experimental results of this study should prove very useful in clarifying the differences between the theoretical and experimental scaling laws.

CHAPTER III

DIRECT FLAME PHOTOGRAPHY

The decomposition of combustion noise scaling rules can be in part achieved by a direct flame photographic technique. From Equation (4),

$$P \propto \int_V dV\ (\underset{\sim}{r}_o) \int_{V_d} C(\underset{\sim}{r}_o, \underset{\sim}{d})\ dV\ (\underset{\sim}{d}) \tag{15}$$

where C is an autocorrelation of the reaction rate and V_d is a correlation volume. The second integral is over V, the reacting volume, which is of interest to this study. It is furthermore shown that the order of magnitude of Equation (15) may be expected to be given by

$$P \propto V\ V_d\ \bar{C} \tag{16}$$

where $\bar{C}$ is an order of magnitude estimate of C. The reacting volume is, therefore, a fundamental quantity in establishing the scaling laws for combustion noise. The scaling laws on reaction volume directly affect the scaling rules for combustion noise. An investigation of the parametric behavior of the flame volume is, therefore, a useful step in understanding the origin of combustion noise. A theoretical evaluation in Reference 17 deduced an analytical expression for the order of magnitude of the reacting volume based on physical reasoning. Three different models of

turbulent combustion were considered. The analytical expression developed was

$$V = K\, U^{a}\, D^{b}\, S_L^{c}\, F^{d}\, \ell_t^{e}\, \vartheta^{f} \qquad (17)$$

where V is the flame volume, U is the mean flow velocity, D the burner diameter, S_L the laminar flame speed, F the fuel mass fraction, ℓ_t the turbulence length scale and ϑ the relative intensity of turbulence. K, a, b, c, d, e and f are constants. Depending upon the model of turbulence chosen the exponents would take the values as shown in Table 5.

Table 5. Scaling Laws on Reacting Volume from Strahle's Theory

	Exponents on					
	U	D	S_L	F	ℓ_t	ϑ
Model of Turbulent Combustion	a	b	c	d	e	f
Wrinkled Flame (WF)	1	2	-1	0	1	0
Slow Distributed Reaction (SDR)	$\frac{1}{2}$	2	-2	0	$\frac{1}{2}$	$\frac{1}{2}$
Fast Distributed Reaction (FDR)	1	2	-1	0	1	0

Thus having established the importance of analyzing the flame volume in the development of the theory of combustion noise a need of an experimental study of the subject became evident. If the scaling laws could be experimentally determined for the turbulent flame volume and compared with the theoretical predictions of Reference 17 a substantial improvement in the understanding of scaling laws for combustion generated

noise would result. Also, an investigation of this kind would answer, at least partially, questions on the turbulence structure in the reaction zone.

An experimental program was therefore developed to decompose the scaling rules for the flame volume. Spectroscopic studies[28] of hydrocarbon flames have shown that the luminosity of the flame brush is due to the emission of active radicals like CH, C_2 and OH in the reaction zone. Since these active radicals are present only in the active reaction zone, the volume of the combustion region can be obtained by direct photography viewing the flame through an optical filter centered on the radiation of a particular radical. The volumes could be measured by tracing out the density curves on a microdensitometer.

The technique of direct photography is fast, direct and simple compared to methods where thermocouples are used to estimate the extent of the reaction zone. In fact, the direct photography method is free from the errors due to the presence of the probe in the flame and the positional inaccuracy of the probe caused by vibrations and deflections due to aerodynamic forces[29]. An evaluation of the accuracy of the photographic method will be done at a later stage in this chapter.

Dimensional Analysis

Dimensional analysis is based on the fundamental requirement of dimensional homogeneity in a physical equation. If it is possible to recognize all the parameters that affect a physical quantity, dimensional analysis can provide an insight into the parametric behavior. The functional form, however, cannot be determined by the dimensional analysis.

Following the arguments of Reference 17 it is reasonable that the parameters that can affect the reacting volume V are: flow velocity, U, burner diameter, D, laminar flame speed, S_L, turbulence velocity in the axial direction, u', turbulence length scale, ℓ_t, and finally the fuel mass fraction, F, which is already nondimensional. Thus over a limited range of the independent variables it is fair to assume

$$V = K\, U^{\ell}\, D^{m}\, S_L^{n}\, u'^{p}\, \ell_t^{q}\, F \tag{18}$$

Here, since the fundamental dimensions involved are only length and time and there are six unknowns to determine, there will be four nondimensional groups. By dimensional reasoning the following V dependence is obtained

$$\frac{V}{D^3} = \text{fn}\left\{\left(\frac{u'}{U}\right),\ \left(\frac{U}{S_L}\right),\ \left(\frac{\ell_t}{D}\right),\ F\right\} \tag{19}$$

Any further explanation based on Equation (19) will be deferred until after the experimental results are presented.

Experimental Procedure

The burners and flow systems used have already been explained in Chapter II. The flame is photographed using a Graflex Speed Graphic Camera and 4" x 5" black-and-white panchromatic film. An optical filter centered on the CH radiation (4315Å) is used in this work since CH is one of the predominant components in the emission spectra of these flames. More importantly, however, it is found from Reference 30 that the spectral

intensity of CH emission is much more pronounced than any other in fuel lean flames of propane-air. Thus, CH emission is more appropriate for determining the reaction volume since a majority of the experiments were planned using this fuel.

The filter used in this investigation has a half peak transmittance bandwidth of about 500 Å and a peak in the vicinity of 4300 Å. The flames are photographed inside an anechoic chamber since these experiments are done parallel with the acoustic measurements. As far as optical studies are concerned the anechoic chamber serves to prevent extraneous drafts around the flame and also eliminates stray light when photographs are being taken. A microdensitometer is used to measure the image of the flame recorded on the photographic negative.

Measurement of the Flame Volume

A turbulent premixed flame stabilized at the end of a burner tube has a luminous zone contained between fairly well-defined inner and outer cones. Although the inner and the outer cones of the flame are qualitatively simple to visualize, a quantitative study requires that certain criteria be adopted for the flame volume computation. In this study, it was decided to fix the outer boundary of the flame by defining it as the surface which has an intensity 0.1 I_{max}, where I_{max} is the maximum intensity recorded on the photograph. The definition of the inner cone presents additional difficulty since it is viewed through a part of the flame brush by the camera lens. A reasonable estimate is obtained, however, by considering the inner cone to be defined by the peaks in the densitometer trace. Figure 23 clearly explains the procedure adopted. In order to obtain the volume of the flame the densitometer traces were

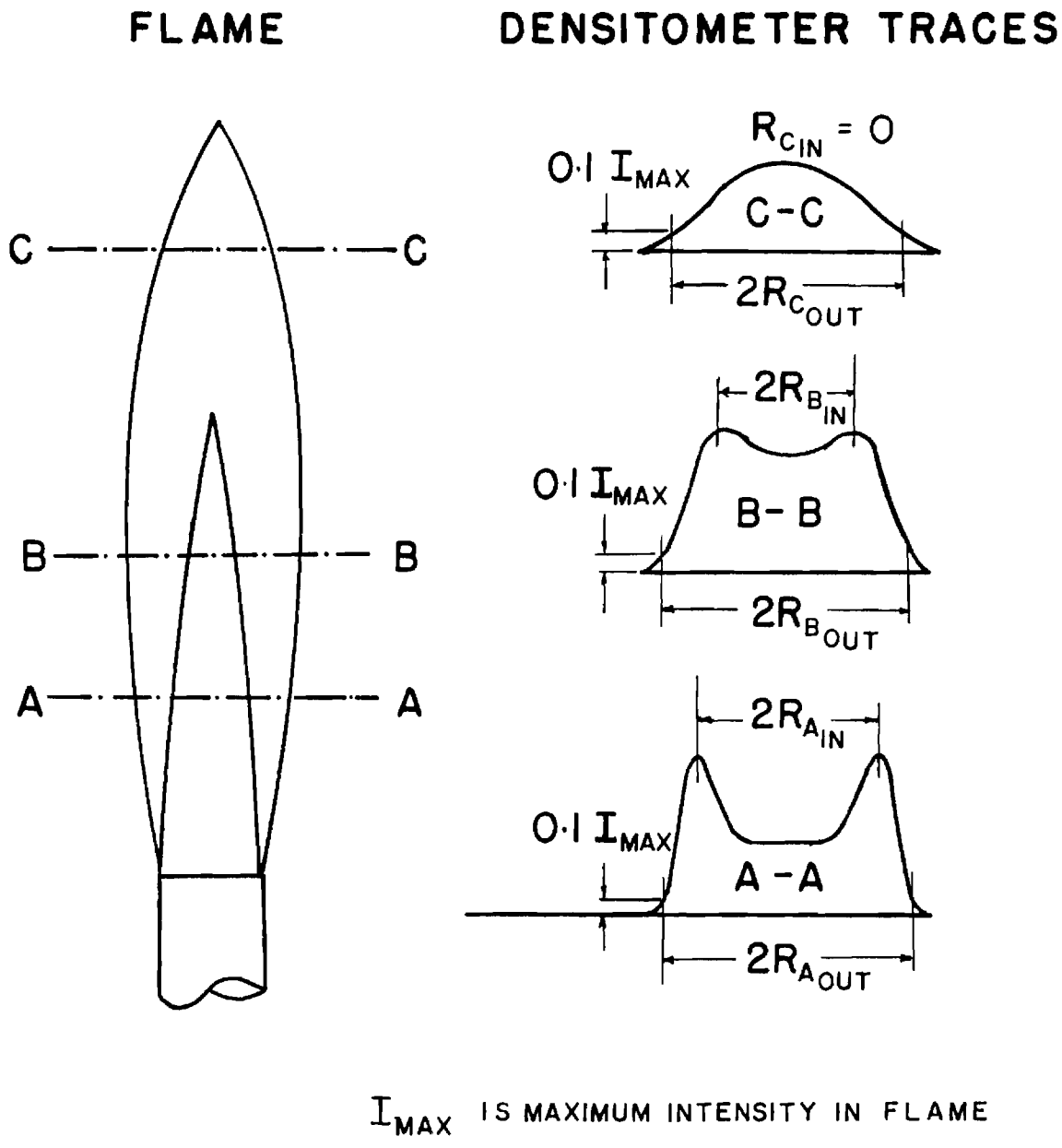

Figure 23. Flame Volume Measurement - Location of Inner and Outer Cones.

taken at various short distances along the length of the flame. From the traces the inner and outer radii were measured as shown in Figure 23. The volumes of the outer and inner cones between the adjacent sections were computed as truncated cones. The difference between their volumes gives the reaction volume between the two measurement sections. The total flame volume is then obtained as a simple sum of all such elemental volumes.

At this stage, it should be realized that an analysis of this kind does not yield the true volume of the reaction zone in a strict sense; but such an analysis is capable of furnishing acceptable scaling laws when the criteria set forth are consistently adhered to in all the tests.

Experimental Results

Acoustic Center Location

The determination of the location of the acoustic center was one of the important contributions to the acoustic measurements. Earlier it has been stated that the volume of the flame was computed as a simple arithmetical sum of the elemental volumes between various longitudinal sections. These elemental volumes were divided by the corresponding elemental length of the flame to obtain the volume per unit length which is plotted as a function of the flame length. Figure 24 shows two such plots. The acoustic center corresponds to the location of the maximum volume per unit length in the flame. The results of many experiments showed that the fraction of flame length at which the maximum volume per unit length occurred could be expressed as a function of equivalence ratio ϕ alone. This result simplified the task of determining the acoustic center to one of measuring the length of the flame. The relationship

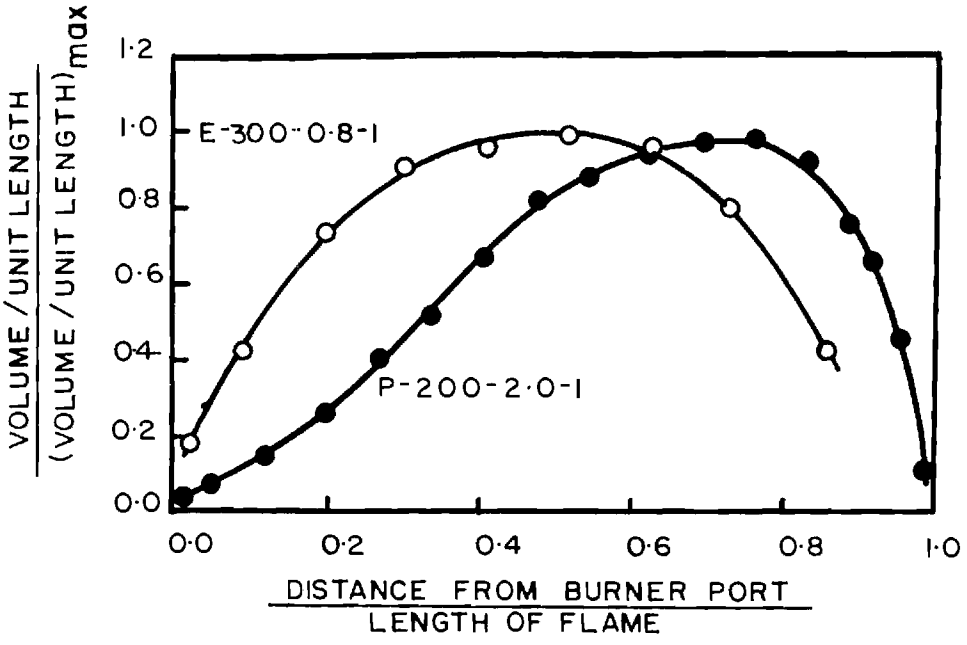

Figure 24. Flame Volume Distribution.

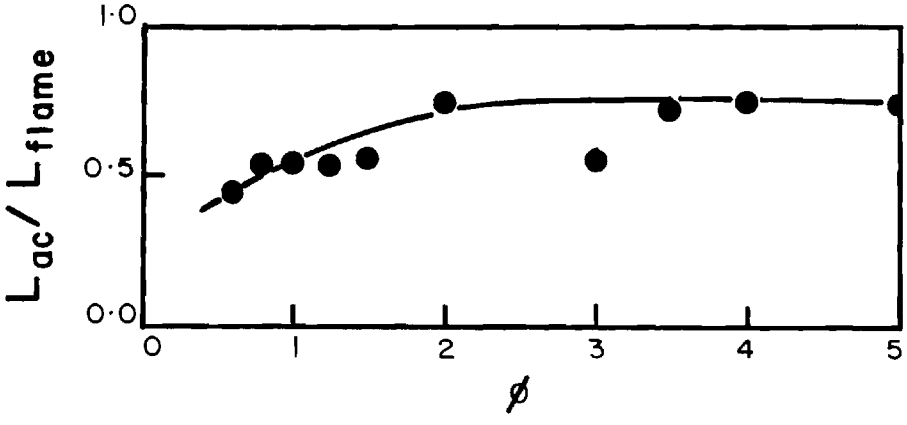

Figure 25. Distance L_{ac} from Burner Port at which Acoustic Center is Located as a Function of Equivalence Ratio.

between ϕ and fraction of flame length measured from burner port at which the acoustic center is located is shown in Figure 25. Figures 26(a), (b) and (c) present some data on the length of the flame which could be used in the determination of acoustic center. It is interesting to note that the flame length increases as only $U^{\frac{1}{2}}$ (Figure 26(a)) and as $D^{0.64}$ (Figure 26(b)). Further, the flame length achieves a minimum near stoichiometric mixtures as seen on Figure 26(c). This is simply a reflection of the fact that maximum laminar flame speed (and hence the turbulent flame speed) is obtained for conditions near stoichiometry.

Flame Volume Scaling Laws

The behavior of the flame volume with burner diameter is shown in Figure 27. It can be seen that the flame volume increases as the cube of the burner diameter. Table 5 (page 67) shows that both WF and FDR models of Strahle's theory can explain this result if the turbulence length scale ℓ_t is proportional to D. In cold jet flows it is known that the turbulence length scale is proportional to the jet diameter[31]. The result $V \propto D^3$ therefore presents a strong possibility that the turbulence length scale in the reaction zone is also proportional to the burner diameter. In Figure 27 the effect of S_L has not been eliminated from the data points.

Figure 28 presents the flame volume as a function of the mean flow velocity of the reactants in the burner tube. Based on the result of Figure 27 a D^3 correction has been applied to the flame volume so as to take care of the diameter effect and allow a simple graphical correlation. The flame volume is seen to scale linearly with flow velocity, which is in accord with the theories of Reference 17. Again on this plot the effects of S_L and F have not been considered. The tendency of the ethylene

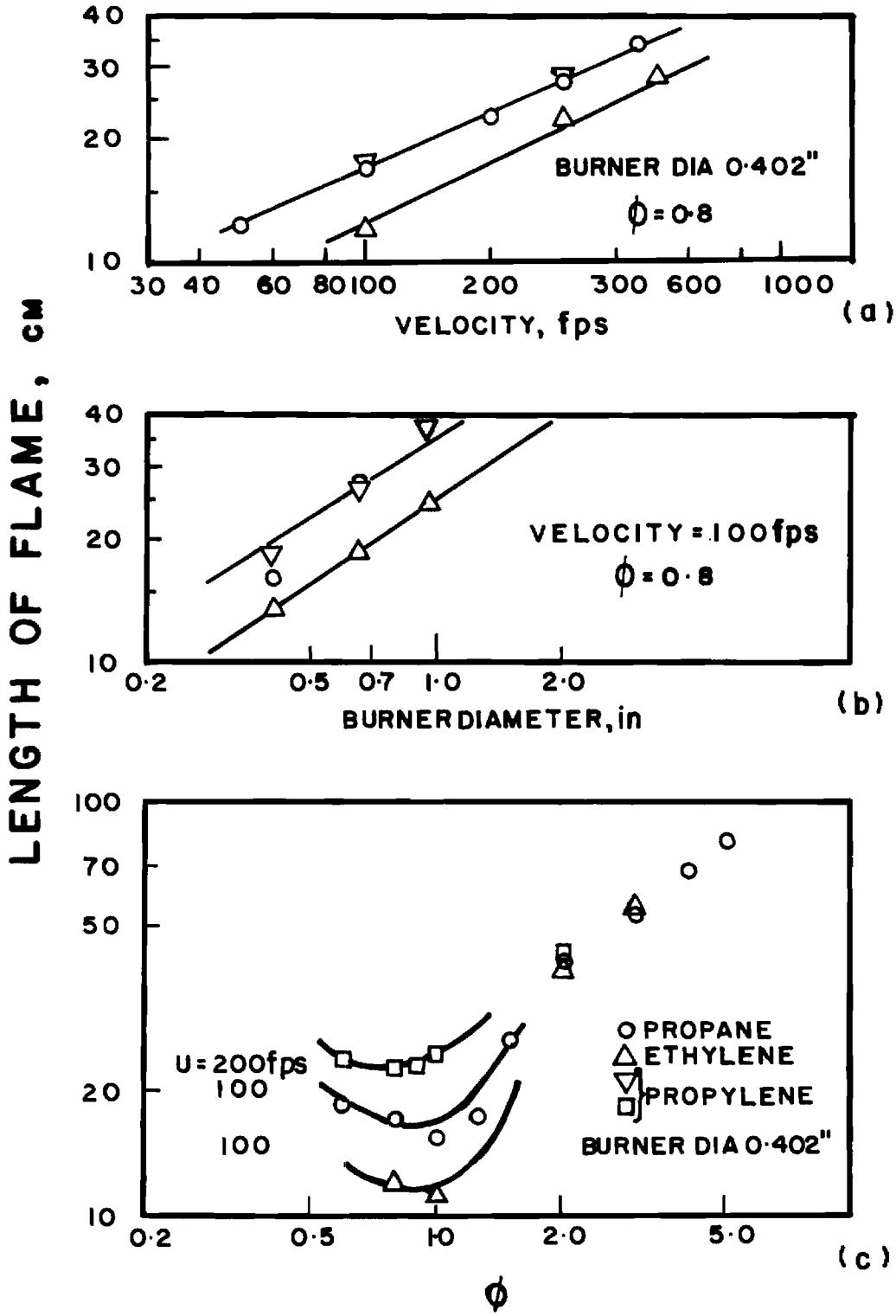

Figure 26. Length of Flame as a Function of a) Velocity, b) Burner Diameter, and c) Equivalence Ratio.

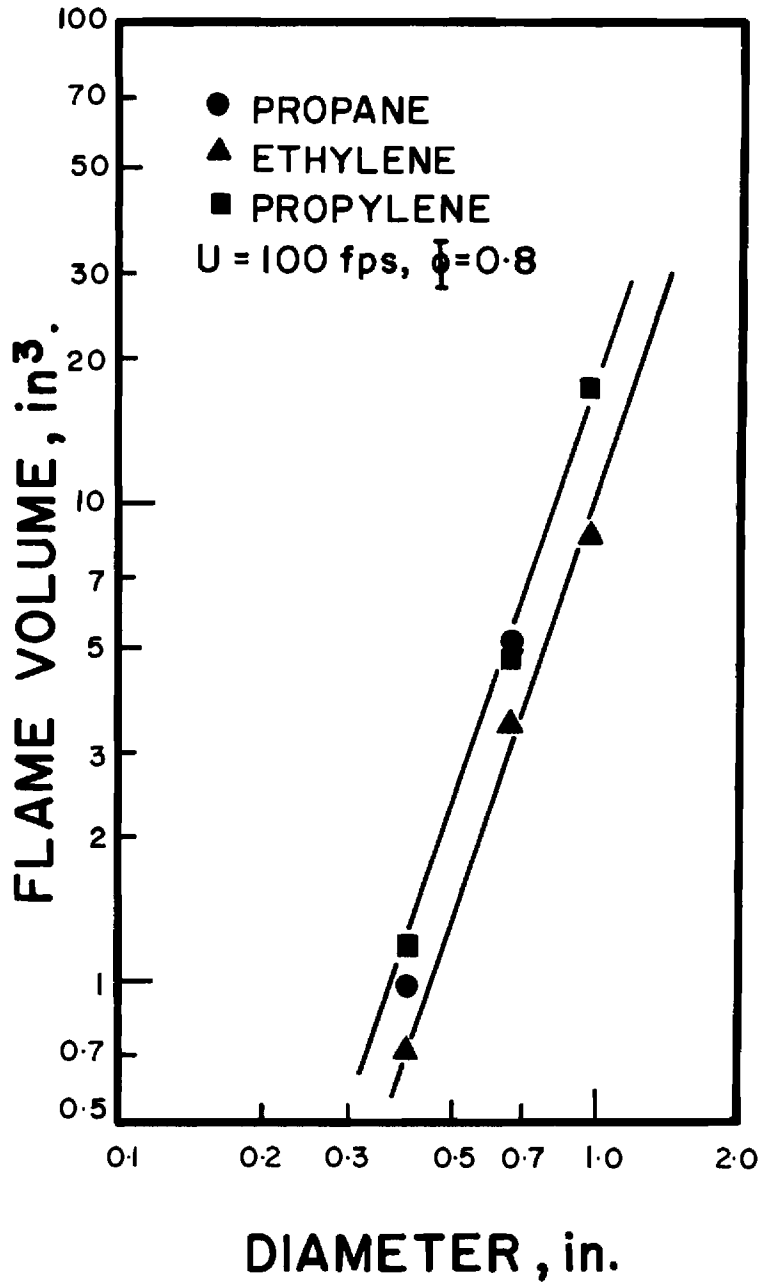

Figure 27. Flame Volume as a Function of Burner Diameter.

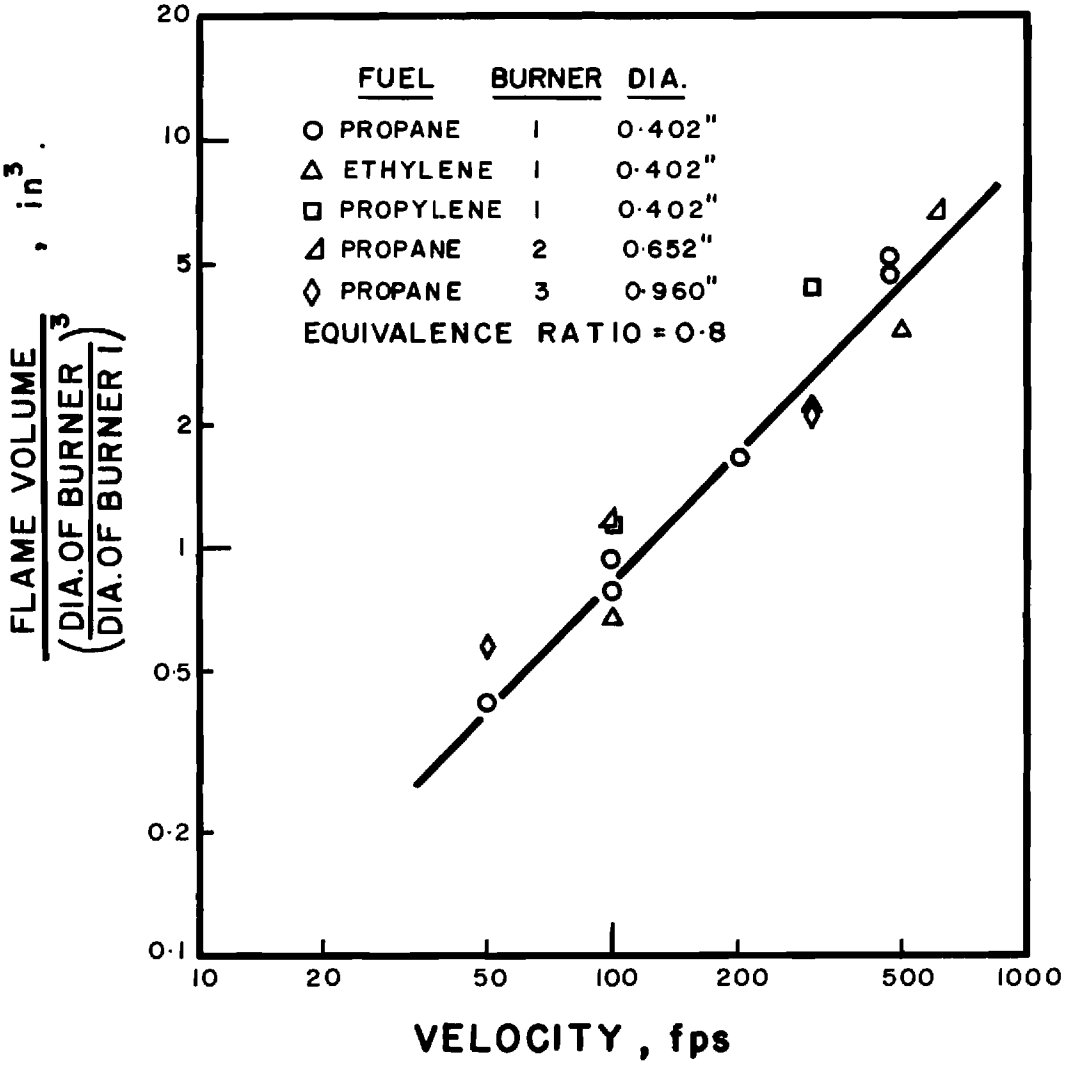

Figure 28. Flame Volume as a Function of Mean Flow Velocity of Reactants.

data points to remain below those for propane is an indication of the inverse scaling of V with S_L. Following the procedure adopted to get scaling laws for acoustic power and peak frequency by regression analysis the volume scaling laws were also deduced.

Using 39 different tests on the three burners and the three fuels at various equivalence ratios between 0.6 and 1.0 and velocities from 50 fps to 600 fps the following relation is obtained:

$$V = 40.5\ U^{0.86}\ D^{3.16}\ S_L^{-0.65}\ F^{1.34} \tag{20}$$

where V is in ft^3, U is in ft/sec, D is in ft and S_L is in ft/sec. The analysis of the errors due to the fit obtained in Equation (18) gave a mean error of 3.4% with a standard deviation of 28%. The maximum error was 78%. The rather high standard deviation of the error distribution was not unexpected. Any linear inaccuracy in linear dimensions on the photograph shows up cubed in volume computations. The important aspect of this analysis, however, is not the accuracy of measuring the reaction volume but rather obtaining the scaling laws. It has been noticed that the exponents on U, D, S_L and F obtained from the regression fit are quite stable in as much as the exponents varied very little when the number of tests used for the fit was varied from 14 to 39, the tests being picked at random. Thus, it is reasonable to assume that good statistical stability is attained for the results of the correlation of interest.

The scaling laws obtained from Equation (20) fall in line with

those deduced from Figures 28 and 29. The scaling on S_L is in favorable agreement with the estimates of Reference 17.

However, Reference 17 does not allow for any dependence upon F while experimentally there is a dependence. It may be explained on the basis of a density effect, increasing the flame thickness for a fixed input turbulence length scale. While this is speculative no other reasonable interpretation has been found.

Referring back to Equation (19) from the dimensional analysis a comparison of the experimental data with the nondimensional equation can be made. An experimental D^3 dependence can only be explained if $\ell_t \propto D$. This independently confirms the earlier deduction that the turbulent length scale should be proportional to the burner diameter. Further, the exponents on U and S_L obtained in Equation (20) are 0.86 and -0.65, respectively. This shows that the U and the S_L effects mutually balance in Equation (19). Thus, a dimensional homogeneity can only be achieved when u'/U is a constant. This result implies that the turbulence intensity in the flame is relatively independent of the other scaling parameters. Since it is known for fully developed pipe flow that u'/U is a constant[31], this analysis tends to support the statement that the turbulent intensity is not affected by the flame. The conclusion to be reached on the turbulence structure in the reaction zone is therefore that there is no major modification to the turbulence structure due to the flame.

Comparison With Acoustic Power Scaling Laws

It is now possible to compare the flame volume scaling law of $V \propto U^{0.86} D^{3.16} S_L^{-0.65} F^{1.34}$ with the acoustic power scaling law of Equation (11). As was expected in the theory, the flame volume does partially explain the scaling laws on acoustic power. Both flame volume and the acoustic power scale to about D^3 with burner diameter. This shows that almost all the diameter effect perhaps comes from the scaling of reacting volume. The reacting volume accounts only partially for the velocity scaling. This is in accord with the expectations of Reference 17. The scaling law on S_L in flame volume tends to lower the S_L exponent for acoustic power radiated.

Summarizing the comparison with Strahle's theory[17], it can be observed that the expression deduced for far field acoustic radiation in the term of Equation (3) appears to be satisfactory, considering the experimental results of References 8 and 9. Further, estimates of reaction volume are quite satisfactory except for the F scaling. Thus, the order of magnitude estimates of autocorrelation function of the time derivative of the reaction rate and the correlation volume can be suspected to be incorrect.

Concluding Remarks

A comparison of the predictions of the combustion noise theory of Strahle with the experimental results has shown that the theoretical estimates are reasonable. Summarizing the findings, the following conclusions can be drawn:

1. The direct photography technique has been shown to be a useful tool in decomposing the scaling rules of combustion noise.

2. The turbulence length scale in the reaction zone has been shown to be proportional to the burner diameter.

3. The preference for WF and FDR models has been established. Since both these theoretical models yield the same scaling laws for the flame volume, it is not possible to judge the superiority of either of the two models by this method.

4. An evaluation of the experimental findings with the results of dimensional analysis has demonstrated that the turbulence structure is determined primarily by the pipe flow process and not by the flame.

CHAPTER IV

CONCLUSIONS

A comprehensive study of the radiation of noise from open turbulent flames has been made. The study has shown that combustion noise predominates over the range of experimental results obtained and that it differs from jet noise in terms of scaling laws, directionality and spectral content. Summarizing the results of this investigation it can be concluded that:

1. Combustion noise predominates over jet noise even for flow velocities as high as 600 fps.

2. The combustion noise from open turbulent flames is weakly directional. The directionality behavior can be qualitatively explained by refraction and convection effects.

3. Combustion noise is a low frequency broad band radiation with a single peak. The peak frequency for premixed flames was obtained in the form $f_c \propto U^{0.2} S_L^{0.45} D^{-0.08} F^{0.31}$. However, for all practical purposes it may be sufficient to consider combustion noise to peak in the 250-700 Hz range for hydrocarbon fuels burning with air as the oxidizer.

4. Acoustic power has been found to follow the law $P \propto U^{2.7} D^{2.9} S_L^{1.2} F^{3.0}$. An empirical expression from which acoustic power can be directly obtained has been generated by regression analysis of the experimental data.

5. Thermo-acoustic efficiency has been shown to follow a $\eta_{ta} \propto U^{1.7} D^{0.9}$

$S_L^{1.2}$ $F^{2.0}$ law. For a 600 fps flame an η_{ta} as high as 10^{-6} has been obtained showing that noise output from high velocity flames could be appreciable.

6. A direct flame photography technique has been shown to be a useful tool in analyzing combustion noise scaling laws. The flame volume has been shown to scale as $V \propto (U/S_L)D^3$. This study has shown that turbulence in the flame is primarily decided by the pipe flow process.

7. Several discrepancies exist between the experimental findings and the theory of Reference 17. In agreement with the theory, combustion noise is monopole in nature, the noise is generated within the reacting volume and the estimates for flame volume are satisfactory. The primary deficiency appears to lie in estimation of the autocorrelation function of the time derivative of the reaction rate and in estimation of the correlation volume. However, it is noted that S_L has not been varied over a sufficiently wide range to give confidence in the S_L scaling of acoustic power or frequency. Consequently, judgment on the theoretical accuracy must be reserved until a wider S_L variation is experimentally achieved.

BIBLIOGRAPHY

1. Tucker, M., "Interaction of a Free Flame Front with a Turbulence Field," NACA Report No. 1277 (1956).

2. Bragg, S. L., "Combustion noise," Journal of the Institute of Fuel, 36, p. 12 (1963).

3. Smith, T. B. J., and Kilham, J. K., "Noise generated by open turbulent flames," Journal of the Acoustical Society of America, 35, p. 715 (1963).

4. Smith, T. B. J., "Combustion Noise," Ph.D. Thesis, University of Leeds (1961).

5. Kotake, S., and Hatta, K., "On the noise of diffusion flames," Bulletin of JSME, 8 (30), p. 211 (1965).

6. Bollinger, L. E., Fishbruke, E. S., and Edse, R., "Contribution of Combustion Noise to Overall Rocket Exhaust Jet Noise," NACA CR-463 (May 1966).

7. Thomas, A., and Williams, G. T., "Flame noise: Sound emission from spark-ignited bubbles of combustible gas," Proceedings of the Royal Society of London A294, p. 449 (1966).

8. Hurle, I. R., Price, R. B., Sugden, T. M., and Thomas, A., "Sound emission from open turbulent premixed flames," Proceedings of the Royal Society of London A303, p. 409 (1968).

9. Price, R. B., Hurle, I. R., and Sugden, T. M., "Optical studies of the generation of noise in turbulent flames," Twelfth Symposium (International) on Combustion, Pittsburg, the Combustion Institute, p. 1093 (1968).

10. Smithson, R. N., and Foster, P. J., "Combustion noise from a Meker burner," Combustion and Flame, 9, p. 426 (1965).

11. Powell, A., "Noise measurement of a turbulent gasoline vapor flame," Journal of the Acoustical Society of America, 35, p. 405 (1963).

12. Giammar, R. D., and Putnam, A. A., "Combustion roar of turbulent diffusion flames," Journal of Engineering for Power, p. 157 (April 1970).

13. Giammar, R. D., and Putnam, A. A., "Combustion roar of premix burners, singly and in pairs," Combustion and Flame, 18, p. 435 (1972).

14. Knott, P. R., "Noise generated by turbulent non-premixed flames," AIAA Paper no. 71-732 (1971).

15. Seebold, J. G., "Combustion noise and its control in process plant furnaces," ASME Paper no. 71-Pet-6 (1971).

16. Strahle, W. C., "On combustion generated noise," Journal of Fluid Mechanics, 49, p. 399 (1971).

17. Strahle, W. C., "Some results in combustion generated noise," Journal of Sound and Vibration, 23, p. 113 (1972).

18. Strahle, W. C., "Refraction, convection and diffusion flame effects in combustion generated noise," Fourteenth Symposium (International) on Combustion (to be published).

19. Lighthill, M. J., "On sound generated aerodynamically, I. General theory," Proceedings of the Royal Society of London, A211, p. 564 (1952).

20. Lighthill, M. J., "On sound generated aerodynamically, II. Turbulence as a source of sound," Proceedings of the Royal Society of London, A222, p. 1 (1954).

21. Kushida, R., and Rupe, J., "Effect on supersonic jet noise of nozzle plenum pressure fluctuations," AIAA Journal, 10, p. 946 (1972).

22. Abdelhamid, A. N., Harrje, D. T., Plett, E. G., and Summerfield, M., "Noise characteristics of combustion augmented high speed jets," AIAA Paper No. 73-189 (1973).

23. Peterson, A. P. G. and Gross, Jr., E. E., "Handbook of Noise Measurement," Seventh Ed. General Radio, Massachusetts (1972).

24. Williams, F. A., Combustion Theory, Addison-Wesley (1965).

25. "Basic Considerations in the Combustion of Hydrocarbon Fuels with Air," NACA Report No. 1300 (1957).

26. Putnam, A. A., Combustion-Driven Oscillations in Industry, American Elsevier, New York (1971).

27. Steffensen, R. J., Agnew, J. T., and Olson, R. A., "Tables for Adiabatic Flame Temperature and Equilibrium Composition of Six-Hydrocarbon Fuels (With Air and Oxygen)," Engineering Experiment Series No. 122, Purdue University (1966).

28. Gaydon, A. G., and Wolfhard, H. G., Flames: Their Structure, Radiation, and Temperature, 3rd Ed., Rev., Chapman and Hall, London (1970).

29. Fristrom, R. M., and Westenberg, A. A., Flame Structure, McGraw Hill, New York (1965).

30. John, R. R., and Summerfield, M., "Effect of turbulence on radiation intensity from propane-air flames," Jet Propulsion, 27, p. 169 (1957).

31. Schlichting, H., Boundary Layer Theory, 6th Ed., McGraw Hill, New York (1968).

Security Classification

DOCUMENT CONTROL DATA - R & D

(Security classification of title, body of abstract and indexing annotation must be entered when the overall report is classified)

1 ORIGINATING ACTIVITY (Corporate author) GEORGIA INSTITUTE OF TECHNOLOGY SCHOOL OF AEROSPACE ENGINEERING ATLANTA, GEORGIA 30332	2a. REPORT SECURITY CLASSIFICATION UNCLASSIFIED 2b. GROUP

3 REPORT TITLE

COMBUSTION GENERATED NOISE IN TURBOPROPULSION SYSTEMS

4 DESCRIPTIVE NOTES (Type of report and inclusive dates)

INTERIM

5 AUTHOR(S) (First name, middle initial, last name)

B N SHIVASHANKARA J C HANDLEY W C STRAHLE

6 REPORT DATE		7a. TOTAL NO OF PAGES 86	7b. NO OF REFS 31
8a. CONTRACT OR GRANT NO	AFOSR 72-2365	9a. ORIGINATOR'S REPORT NUMBER(S) AD768615	
b PROJECT NO	9711-02		
c.	61102F	9b. OTHER REPORT NO(S) (Any other numbers that may be assigned this report) AFOSR-TR-73-1899	
d.	681308		

10 DISTRIBUTION STATEMENT

Approved for public release; distribution unlimited.

11 SUPPLEMENTARY NOTES	12 SPONSORING MILITARY ACTIVITY AF Office of Scientific Research (NAE) 1400 Wilson Boulevard Arlington, Virginia 22209

13 ABSTRACT

Experiments on noise radiation from open turbulent premixed flames are described. Detailed directionality distributions, scaling rules for acoustic power radiated, thermo-acoustic efficiency and spectral content are presented and discussed. Scaling rules for reacting volume are generated by a direct flame photography technique; the reacting volume is shown to be directly related to the sound power output. Combustion noise is shown to be broad band noise with a single spectral peak in the range 250-700 Hz for hydrocarbon-air flames. The directionality is quite weak. The sound power output scales with flow velocity to an exponent of 2.7, with burner diameter to an exponent of 2.9, with laminar flame speed to an exponent of 1.2, and with fuel mass fraction to an exponent of 3.0. The results are examined in the light of the theory of combustion noise.

DD FORM 1 NOV 65 1473

UNCLASSIFIED
Security Classification

14. KEY WORDS	LINK A		LINK B		LINK C	
	ROLE	WT	ROLE	WT	ROLE	WT
COMBUSTION GENERATED NOISE						
ENVIRONMENTAL POLLUTION						
QUIET AIRCRAFT						
COMBUSTION NOISE SCALING						
TURBULENT COMBUSTION MECHANISMS						
TURBOPROPULSION NOISE GENERATION AND TRANSMISSION						
NOISE SUPPRESSION						

AFOSR INTERIM SCIENTIFIC REPORT

AFOSR–TR

COMBUSTION GENERATED NOISE IN TURBOPROPULSION SYSTEMS

Prepared for

Air Force Office of Scientific Research
Aerospace Sciences Directorate
Arlington, Virginia

by

W. C. Strahle
B. N. Shivashankara
J. C. Handley
M. Muthukrishnan

School of Aerospace Engineering
Georgia Institute of Technology
Atlanta, Georgia 30332

Approved for public release; distribution unlimited.

Grant No. AFOSR–72–2365 July 1974

AFOSR Interim Scientific Report

AFOSR -TR- 74-1436

COMBUSTION GENERATED NOISE IN TURBOPROPULSION SYSTEMS

Prepared for

Air Force Office of Scientific Research
Aerospace Sciences Directorate
Arlington, Virginia

by

W. C. Strahle
B. N. Shivashankara
J. C. Handley
M. Muthukrishnan

School of Aerospace Engineering
Georgia Institute of Technology
Atlanta, Georgia 30332

Approved for public release; distribution unlimited

Grant No. AFOSR-72-2365 July 1974

ABSTRACT

Continuation of experimental and theoretical work on the problem of combustion generated noise in turbopropulsion systems is presented. Tasks completed during the current period have been (a) experimental and theoretical correlation of noise power and spectra from open premixed flames of propane, propylene, ethylene and acetylene-air, (b) crosscorrelation of C_2 emission with the far field acoustic pressure, and (c) experimental and theoretical investigation of ducting effects upon the noise radiating capability of the flame. The noise radiation from simple flame types is now understood with sufficient theoretical and experimental detail that estimates may be made for combustion noise in turbopropulsion systems. It is shown that the ducting of a flame changes primarily only the radiation impedance. Feedback effects of reflected waves upon the noise source may be neglected in noise work if the system is damped heavily enough to avoid combustion instability.

TABLE OF CONTENTS

LIST OF ILLUSTRATIONS

SUMMARY

The results of the second year of the current combustion noise program are presented in this report. The objective of the program is to understand through theory and experiment the mechanism of noise radiation from turbulent combustion regions with sufficient detail to be able to deduce the relative importance of combustion noise to the overall noise radiated from turbopropulsion systems. Tasks completed during the second year have been (a) experimental and theoretical correlation of noise power and spectra from open premixed flames of propane, propylene, ethylene and acetylene-air, (b) crosscorrelation of C_2 emission with the far field acoustic pressure and (c) experimental and theoretical investigation of ducting effects upon the noise radiating capability of the flame.

In order to expand the anechoic chamber results of free flame noise radiation to include greater variation of fuel reactivity, some acetylene-air runs have been added to the results obtained during the first year. Correlations have been obtained for the thermoacoustic efficiency and Strouhal number of maximum radiated sound power as functions of Damköhler's first similarity group, Reynolds number, Mach number and fuel mass fraction. A revised, simplified theory of combustion noise has been constructed which recovers the experimental results quite nicely and which allows rather simple estimates of combustion noise.

The time derivative of the C_2 emission intensity has been shown to have a strong crosscorrelation with the far field acoustic pressure. The time derivative of this intensity is directly proportional to the time derivative of the heat production rate which directly enters the

theory of combustion noise. This work proves that the noise is directly generated in the combustion region and shows that the theory of combustion noise is basically sound.

The open flames have been ducted in a simulated cylindrical infinite tube to determine the effects of ducting on the radiated sound. The reasonable match of theoretical and experimental tube wall pressures under the theoretical assumption of no feedback interaction between the flame and wall-reflected pressure waves is significant. It shows that, at least in the case where the system is damped heavily enough to avoid combustion instability, feedback effects are unimportant in computation of the radiated noise. The primary effect of the ducting is to change the radiation impedance of the flame as compared with the free flame value. This effect is computeable.

CHAPTER I

INTRODUCTION

This interim report describes the second year's effort on a program in combustion generated noise. The first year's effort is reported in Ref. 1. In this program attention is centered on direct combustion noise - noise generated in and radiated from a region undergoing turbulent combustion. The objective of the program is to understand through theory and experiment the mechanism of noise radiation from turbulent combustion regions with sufficient detail to be able to deduce the relative importance of direct combustion noise to the overall radiated noise from turbopropulsion systems.

The first year program was devoted to a literature review of combustion noise, anechoic facility development, the measurement of reacting volume by direct flame photography and the generation of noise power output, spectra and directionality data for open turbulent premixed flames of propane, propylene and ethylene-air. The reacting volume and noise data were necessary to investigate the adequacy of a recent theory of combustion noise[2,3]. It was found that the sound power output and frequency of maximum radiated power were not adequately predicted by the theory. The reacting volume of the flame was found to scale in accordance with the theory, except for a curious scaling behavior with variations in the fuel mass fraction. In any event, further diagnostics were deemed required to investigate the adequacy of the foundation of the theory and to suggest theoretical modification to accurately reproduce observed scaling laws.

In a recent review paper[4] it was shown that the use of a non-dimensionalization procedure of Ref. 5 would yield scaling laws for acoustic power which are in accord with experiment, using either the theory of Ref. 3 or of Ref. 5. However, the scaling laws produced for the frequency of maximum radiated power were in poor agreement with experiment. Consequently, in this year's effort measurements of light emission from the C_2 radial, further free flame experiments on a more reactive fuel, and theoretical studies to modify the theory of combustion noise have been carried out to probe the foundations of the theory in more detail. The goal is to merge experiment and theory on a simple flame type so that there is confidence in applying the theory to more complex configurations.

In this year's work the problem of ducting of flame and the attendant modification of the noise output has been experimentally and theoretically investigated. Since all useful burners are enclosed and wall reflections of generated pressure waves are expected to interact with the flame, it is imperative to understand the enclosure effects.

The main body of this report deals with three areas - the additional free flame experiments and modification of the theory, C_2 radiation from flames and enclosure effects on flames. The first two items are treated with only summary statements since publications are attached as Appendices which cover this material in detail. The enclosure effects are, however, treated in detail in the body of the report, since no publication of these results has been made.

CHAPTER II

OPTICAL EMISSION STUDIES

The theory of Ref. 3 deduced that the far field acoustic pressure should be directly proportional to the Eulerian time derivative of the global reaction rate integrated over the reacting volume. This quantity can be and has been[6] measured by viewing the entire flame through an optical filter centered on C_2 and CH radiation and measuring the time derivative of the emission intensity. Indeed Ref. 6 found that the far field pressure and the measured quantity had similar spectra and behavior with a change in flow velocity and that the emission trace, if appropriately filtered, could be overlayed upon the pressure trace. Because of the crucial connection between the measurement and the deductions of the theory, it was decided to perform these measurements in this laboratory and to widen the range of flow and geometric variables over which the correlation holds. Also, a positive technique of crosscorrelation of the pressure and emission traces was used, in addition to scaling laws and spectral comparisons.

The details are located in Ref. 7, which is included as Appendix 'A' in this report. It is concluded that (a) there is a definite one-to-one correspondence between the time derivative of the emission trace and the sound pressure trace and (b) as a consequence the basic theoretical deduction appears correct and the concept of direct noise being generated in the region of active reaction is correct.

CHAPTER III

COMPLETION OF FREE FLAME EXPERIMENTS AND ANALYSIS

Guided by the results of Chapter II that the basic theory appears correct it was sought to merge theory and experiment so that the theory would be a useful tool for more complex flame types. Because of mistrust of the experimental results of the frequency behavior with fuel reactivity (laminar flame speed) runs were added with acetylene-air. The final results for the free flame correlations are presented in Appendix 'B'. A modified theory of combustion noise is also presented in Appendix 'B'. It retains the connection of reaction rate and noise as presented in Chapter II but uses different techniques for estimating magnitudes of quantities and recognizes certain changes in the turbulence structure as the reactive mixture traverses the distance from the burner tip to the flame tip. The theory is also simple and more oriented toward physical interpretation of results. The acoustic power correlations are almost exactly matched by the theory. The correlation for frequency of maximum radiated power is not as exact as one would like but it is better than had been previously derived[4]. One remaining problem is that there is some experimental uncertainty concerning the behavior of frequency with burner diameter. This will be rectified by the construction of a 2 inch diameter burner for the third year of the program so that the overall program will have varied the diameter over a 5:1 ratio. Nevertheless, it is concluded that the theory in its new form is now accurate enough to be used as a design tool for other burner type.

CHAPTER IV

ENCLOSED FLAME THEORY AND EXPERIMENTS

If flames are enclosed by any reflecting surfaces whatsoever there are at least three mechanisms by which the radiated sound characteristics may change as compared with the open flame. The first is that the radiation impedance of the flame may change causing a change in the radiated sound power. This occurs because the reflected waves alter the phase relation between pressure and velocity fluctuations. The second effect is a feedback effect between the reflected pressure waves and the combustion process resulting in either an amplification or attenuation of the wave. This phenomenon is well known through many combustion instability studies over the years. The third effect is a change in the flame aerodynamics and perhaps the turbulence structure by the presence of surfaces near the flame. The purpose of the theory and experiments of this section is to investigate the importance of the first two effects. The experiment is so designed to eliminate the third effect.

The effect of radiation impedance alteration will always occur with any sound radiator, when it is enclosed. Concerning noise measurement, however, the importance of the feedback effect, which may generally be assumed to occur, is unknown. If it is important, a large uncertainty is added in noise predictions because the amplification or attenuation effect cannot be calculated at present. Consequently, if the feedback effect is important, data on open flames cannot be used with confidence in installed configurations. The approach taken here is to construct a theory for the designed experimental apparatus <u>assuming no feedback interaction</u>. If the theory matches the experimental results (wall

sound pressure and spectra measurements), the feedback effect can be considered negligible. If not, further work in this area would be warranted.

Experimental Apparatus

The apparatus designed for these experiments is shown in Fig. 1. It consists of a 4 inch diameter tube, 4 ft. long, 1/2 of which is "Pyrex", for viewing the flame, and the other half is steel. The length is chosen to satisfy the requirement of the theory that the ratio of flame length to tube length should be small. The diameter is chosen to provide only a small aerodynamic change in the flame while being small enough to avoid excitation of transverse modes at frequencies near the frequency of maximum radiated power from the open flame. The burner used is the 3/8" burner from chapter II.

From theoretical and data reduction standpoints it would be desireable that the tube length be infinite. This is impossible from a practical standpoint, so acoustic terminations were designed to simulate as closely as possible perfectly absorbing ends. A total of 12 types of acoustic terminations, termed "mufflers," were designed, built and tested for their acoustic impedance. The main requirement was high abosrbtion at low frequency. The final design selected is shown in Fig. 2. Within the screen wire framework is an attic mineral fiber thermal insulation material. A sheet aluminum core which determins the open area vs length is shown in Fig. 3. The shape of this liner was found to be an extremely important design parameter, as compared to relatively unimportant parameters such as core length and muffler diameter. In any event the measured impedance parameters, by the traversing microphone method[8],

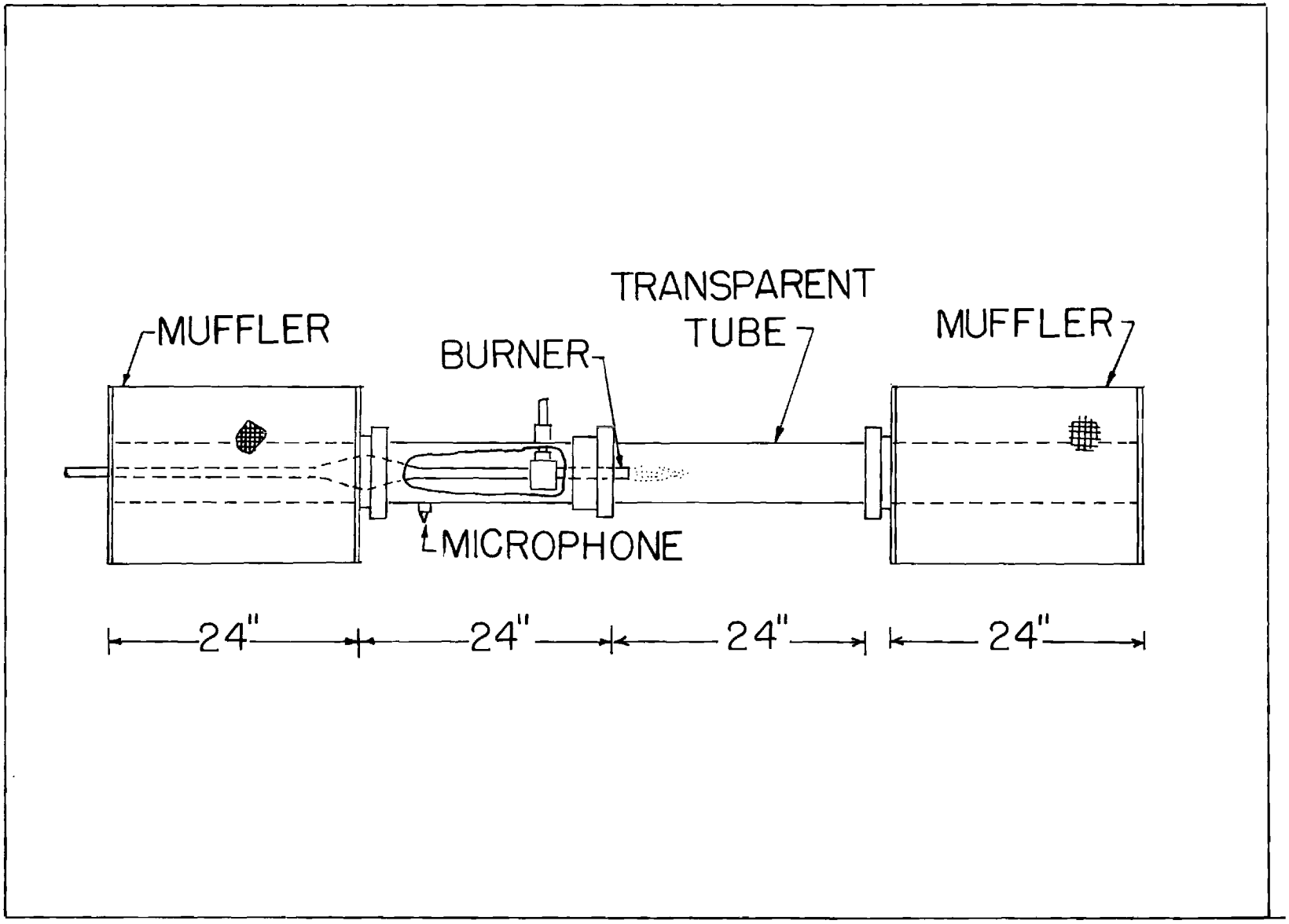

Figure 1. Drawing of the Experimental Apparatus

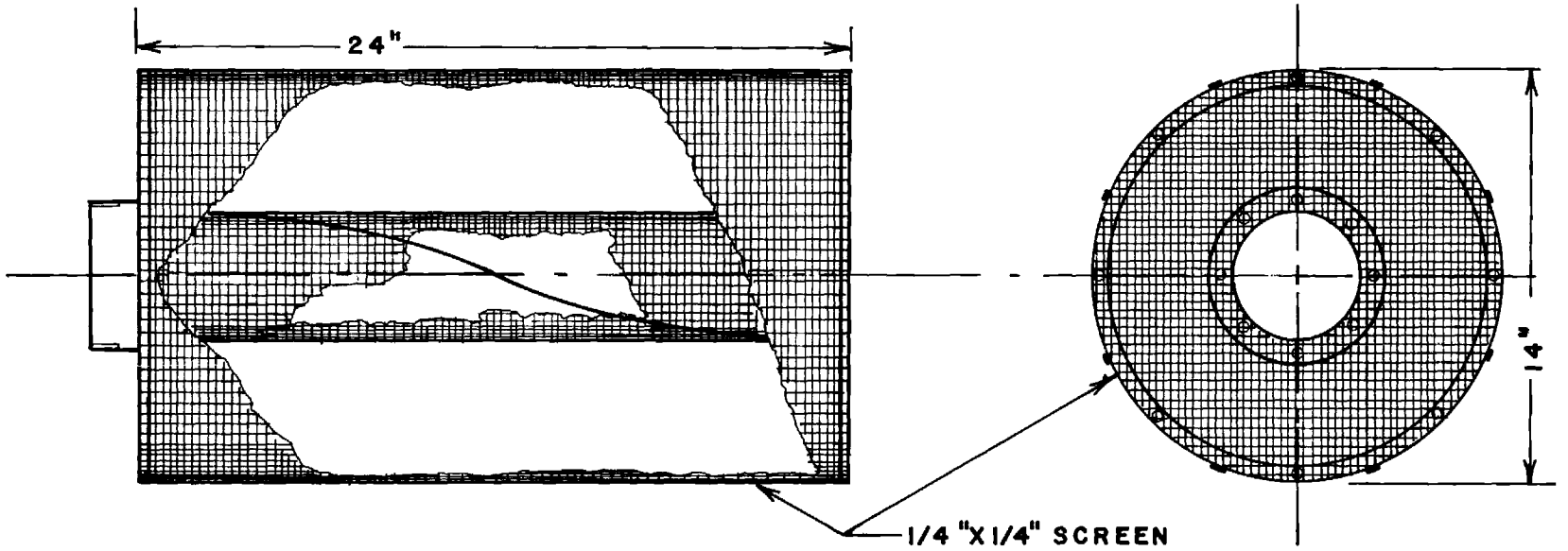

ASSEMBLED MUFFLER

Figure 2. Design of Duct Acoustic Termination

JCH
9-73
E-16-623-12

MUFFLER CORE
0.020" STAINLESS STEEL
SCALE: 3/8"=1"

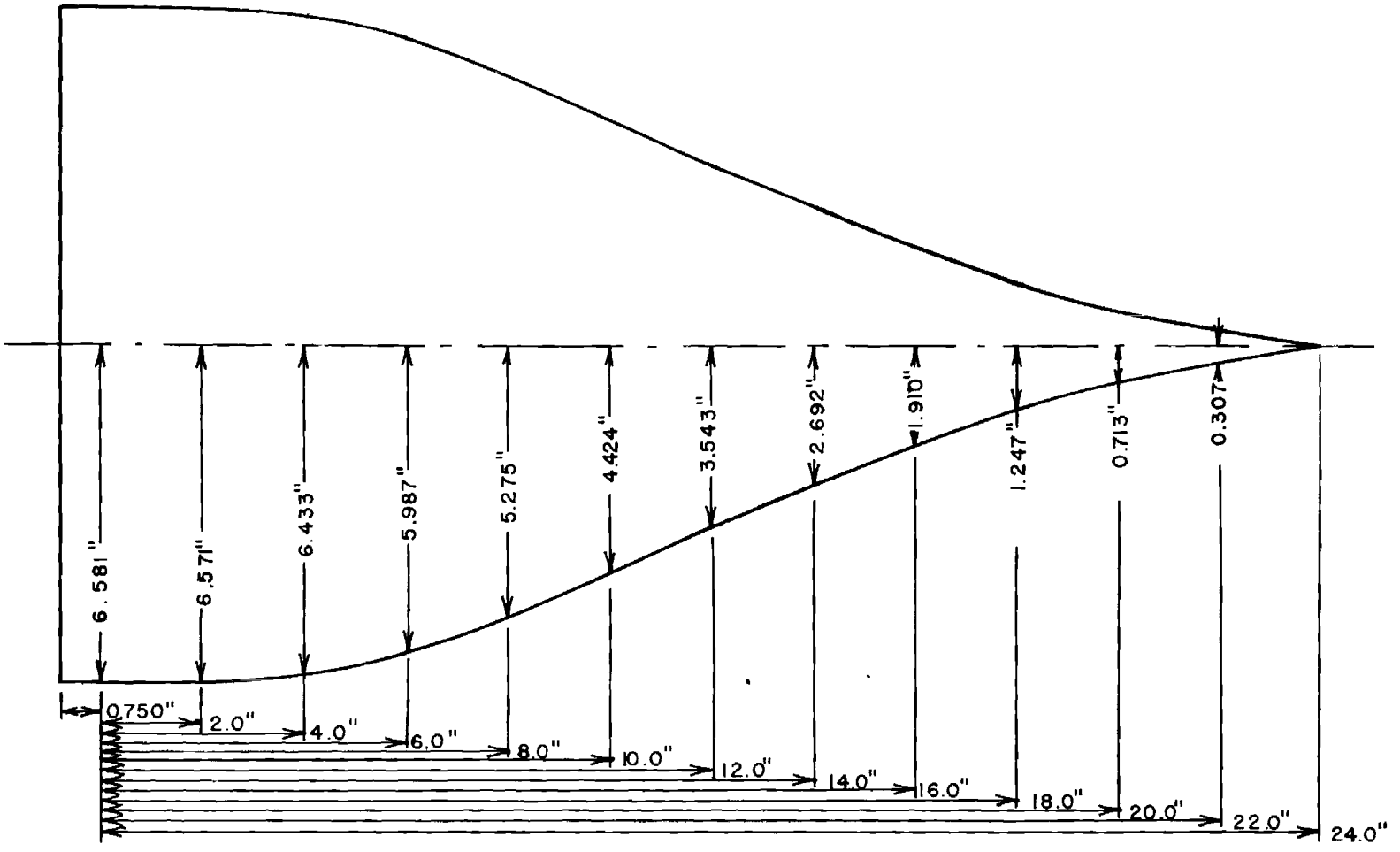

Figure 3. Design of Termination Liner

are shown in Fig. 4. The specific acoustic impedance is related to α and β by

$$\zeta = \coth[\pi(\alpha - i\beta - i/2)] = \frac{p'}{u'\bar{\rho}\bar{c}} \qquad (1)$$

where p' and u' are the acoustic pressure and velocity at the muffler entrance plane, respectively, and $\bar{\rho}$ is the steady state density and $\bar{c}$ is the steady state speed of sound. The variation of ζ with ω, the frequency, is required in the data reduction procedure outlined below.

As mentioned previously it was desired to not alter the aerodynamics or structure of the flame as compared with its structure when open. Shown in Fig. 5 is a visual comparison of the open and ducted flames. Although there is air aspiration into the tube from the flames pumping action, it is apparently weak, because the overall geometry appears preserved.

There are two effects which occur with this apparatus which are not properly accounted for in the theory. The first is the induced air flow, aspirated by the flame. Since the Mach number induced upstream and the Mach number downstream of the flame, caused by both the induced flow and burner flow, are low (< 0.1), the duct acoustics can safely neglect Mach number effects. However, the impedance of the terminations may be altered over the no flow case. The downstream muffler is expected to be most strongly affected. However, since the Mach number is low this is expected to be a weak effect. The second major effect is that there are radial and axial temperature gradients downstream of the flame and this may affect the duct acoustics and the termination impedance. Measurements of the wall temperatures downstream of the flame have shown that

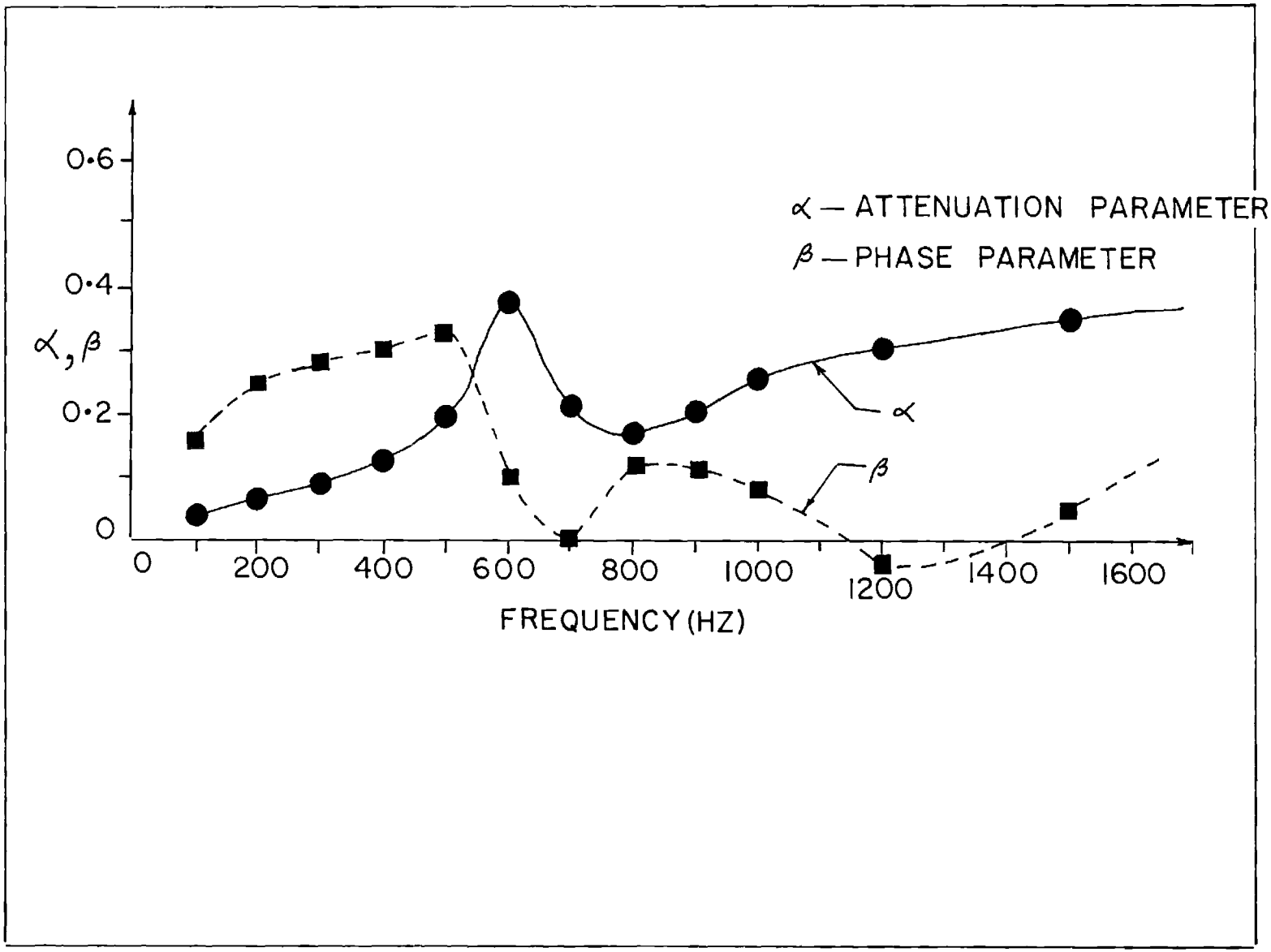

Figure 4. Acoustic Termination Impedance Parameters

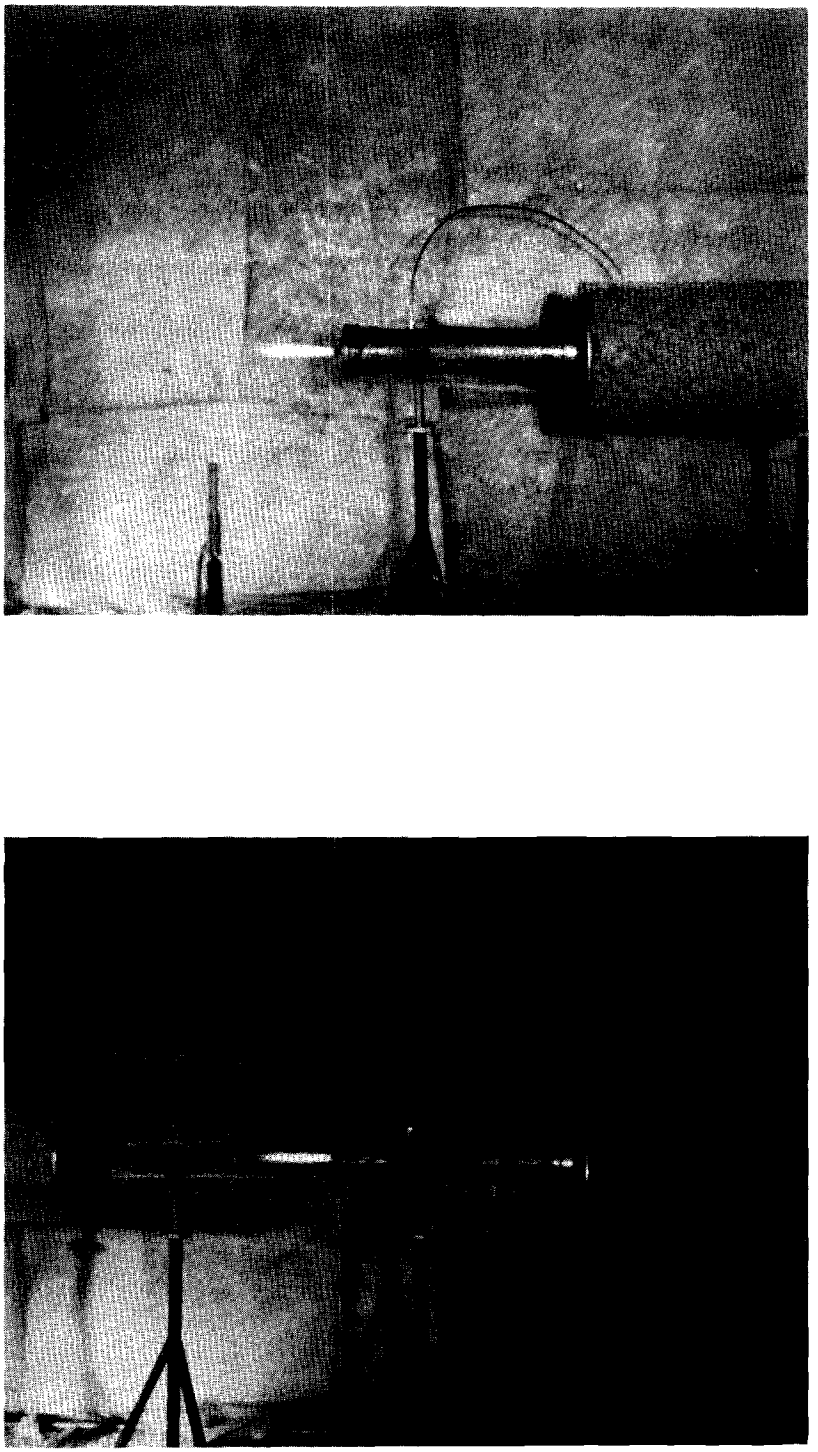

Figure 5. Comparison of Appearance of Open Flame and Free Flame

$T_{wall} \leq 500^{\circ}F$ for the highest thermal input flame tested (propane-air, $\Phi = 0.8$, U = 300 ft/sec.). Consequently, some correction could be anticipated as needed for temperature effects. These will be described below.

Two microphone positions are employed, one at 16 in. and one at 24 in. upstream of the burner mouth. The objective is to measure the sound pressure levels and the spectra and to compare with theoretical calculations using duct acoustics and the experimental data on the flame burning in the open. If the theory and experiment match, feedback effects on the flame may be concluded as negligible.

Theory

The theory is applied to the configuration of Fig. 6. All temperature effects are considered confined to the left of the origin and to the right uniform properties are considered. The mean flow velocity is assumed zero and the walls of the tube are assumed hard. At $x = \ell$ and $-\ell_2$ known impedances are assumed. The source region is assumed a monopole combustion noise source[3]. In the region containing the source

$$\nabla^2 p_w + k^2 p_w = f_w \tag{2}$$

where p_w is the Fourier transform of the pressure, k is the wave number w/c and f_w is the Fourier transform of the monopole source strength. In this region the speed of sound is a constant. In the region which contains the temperature gradients but no source

$$\nabla^2 p_w + \nabla p_w \cdot \frac{\nabla c^2}{c^2} + k^2 p_w = 0 \tag{3}$$

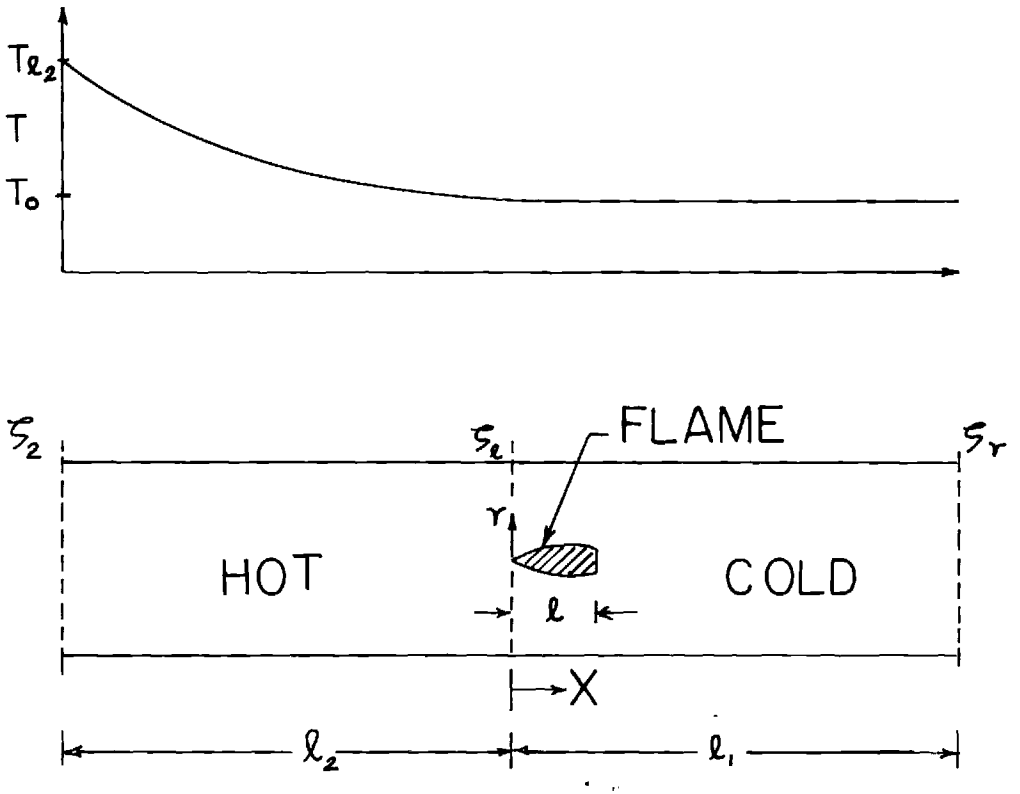

Figure 6. Nomencluture and Schematic for Theoretical Development

Assuming that c = c(x) only so that only axial temperature gradients exist, and integrating Eqs. (2) and (3) over the tube crossection,

$$\frac{d^2\bar{p}_w}{dx^2} + k^2\bar{p}_w = \bar{f}_w \equiv \int_0^{2\pi}\int_0^a f_w \, r dr d\theta \tag{4}$$

and

$$\frac{d^2\bar{p}_w}{dx^2} + \frac{d\bar{p}_w}{dx}\frac{d}{dx}\ell n\, c^2 + k^2\bar{p}_w = 0 \tag{5}$$

result from Eqs. (2) and (3), respectively. Here

$$\bar{p}_w \equiv \int_0^{2\pi}\int_0^a p_w \, r dr d\theta$$

The solution to Eq. (4) is

$$p_w = A_1 e^{ikx} + A_2 e^{-ikx} - \frac{i}{2k}\left(e^{-ikx} - e^{ikx}\right)\int_0^x \bar{f}_w \, dx \tag{6}$$

where

$$A_1 = -k\left(1 + \frac{1}{\zeta_\ell}\right)F \qquad A_2 = k\left(\frac{1}{\zeta_\ell} - 1\right)F$$

$$F = \frac{i}{2k^2}\,\frac{\left[e^{-ik\ell_1}\left(1 - \frac{1}{\zeta_r}\right) + e^{ik\ell_1}\left(1 + \frac{1}{\zeta_r}\right)\right]\int_0^{\ell_1}\bar{f}_w \, dx}{\left(\frac{1}{\zeta_\ell} - 1\right)\left(1 - \frac{1}{\zeta_r}\right)e^{-ik\ell_1} + \left(\frac{1}{\zeta_\ell} + 1\right)\left(\frac{1}{\zeta_r} + 1\right)e^{ik\ell_1}} \tag{7}$$

Here ζ_r and ζ_ℓ are the specific acoustic impedances at $x = \ell_1$ and $x = 0$, respectively. Specification of these numbers implies only plane wave motion, so attention is being restricted to frequencies below that of the

first transverse mode. Furthermore, the approximation has been made in Eq. (6) that $k\ell \ll 1$, or equivalently, that the flame length is very much less than a wavelength. Actually, however, it has been shown[3] that the much less restrictive assumption that $k\ell_e \ll 1$ will yield the same results where ℓ_e is the integral scale of turbulence.

Now an approximate soultion to Eq. (5) is desired, in order to a assess the magnitute of the temperature effect. Letting,

$$\bar{p}_w = \eta z \qquad \eta = T^{-\frac{1}{2}} \qquad c^2 = \gamma RT$$

where γ is the ratio of specific heats and R is the gas constant Eq. (5) becomes

$$\frac{d^2z}{dx^2} + \left[k^2 - \tfrac{1}{4}\left(\frac{T'}{T}\right)^2 - \tfrac{1}{2}\left(\frac{T'}{T}\right)'\right] z = 0 \tag{8}$$

If the temperature profile is chosen such that

$$T = (x-C_1)^2 C_3 \tag{9}$$

$$C_1 = \ell_2 \frac{T_o}{T_{\ell_2}} \left[\frac{1 + T_{\ell_2}/T_o}{1 - T_o/T_{\ell_2}}\right]$$

$$C_3 = T_o/C_1^2$$

Eq. (8) becomes

$$\frac{d^2z}{dx^2} + k^2 z = 0 \tag{10}$$

Since the absolute temperature variation is less than a factor of two in the experiments, k^2 varies by less than a factor of two over the length ℓ_2 and Eq. (10) is a good candidate for solution by the WKBJ method.[9] This approximate solution is

$$z = B_1 e^{-i\frac{w}{c_o} C_1 \ell n(1-\frac{x}{C_1})} + B_2 e^{i\frac{w}{C_o} C_1 \ell n(1-\frac{x}{C_1})}$$

with

$$\frac{B_2}{B_1} = e^{-2i\frac{w}{c_o} C_1 \ell n(1+\frac{\ell_2}{C_1})} \frac{1+i\frac{w}{c_o} C_1 (1-\frac{1}{\zeta_2})}{i\frac{w}{c_o} C_1(\frac{1}{\zeta_2}+1) - 1} \qquad (11)$$

Matching this solution to Eq. (7) at x = 0 yields

$$\zeta_\ell = ik \frac{\left\{1 + B_2/B_1\right\}}{\left\{\frac{1}{C_1} + i\frac{w}{c_o} + \frac{B_2}{B_1}\left[\frac{1}{C_1} - i\frac{w}{c_o}\right]\right\}} \qquad (IV\text{-}12)$$

The procedure is to use Eqs. (11) and (12) to compute ζ_ℓ, and the pressure in the cold tube may then be computed from Eqs. (6) and (7).

The only unknown in the theory arises from Eq. (7) as

$$I \equiv \int_o^{\ell_1} \bar{f}_w \, dx = \int_o^{\ell} \bar{f}_w \, dx$$

However, I is assumed known from free flame experiments, since when radiating to a free field[3]

$$p_{w_{ff}} = I \frac{e^{-ikR}}{4\pi R} \qquad (13)$$

in the far field where R is the radial distance from the source. Measurement of the free field spectrum and overall power determines II^*, where I^* is the complex conjugate of I. From Eqs. (6) and (7) $\bar{p}_w \bar{p}_w^*$ may then be computed at any axial location in the duct.

Results

Shown in Fig. 7 is a sample result of the theory and experiment. The nomenclature for the test is as follows:

E - 100 - 1 - 1 ; Ethylene, 100 ft/sec, ϕ= 1.0, 3/8" burner

where ϕ is the equivalence ratio. The pressure spectrum is shown for the flame burning unenclosed in the anechoic chamber and the overall sound pressure level at 25 inches from the source is also shown. The microphone is at a 90° azimuth with respect to the downstream axis. In the theory this measurement determines II^* as a function of frequency, from Eq. (13). This quantity is then input to compute $\bar{p}_w \bar{p}_w^*$ for the ducted flame and this result is shown on Fig. 7 as the theoretical curve. The theoretical overall sound pressure level at a particular duct location is also shown together with the measured spectrum and measured overall sound pressure level at the same duct position. It is seen that there is good agreement between theory and experiment concerning the overall sound pressure level. The spectrum appears to have the correct resonances but they are emphasised in magnitude as compared with experiment. The major resonances between 100 and 300 Hz occur due to the failure of the mufflers to be highly absorbent in this frequency range. Although data are shown to 8000 Hz, comparison of theory and experiment are only shown to 2000 Hz, since above this limit transverse modes appear. Since greater than 90% of the total sound pressure is below 1000 Hz in frequency content, this presents no error to the calculation.

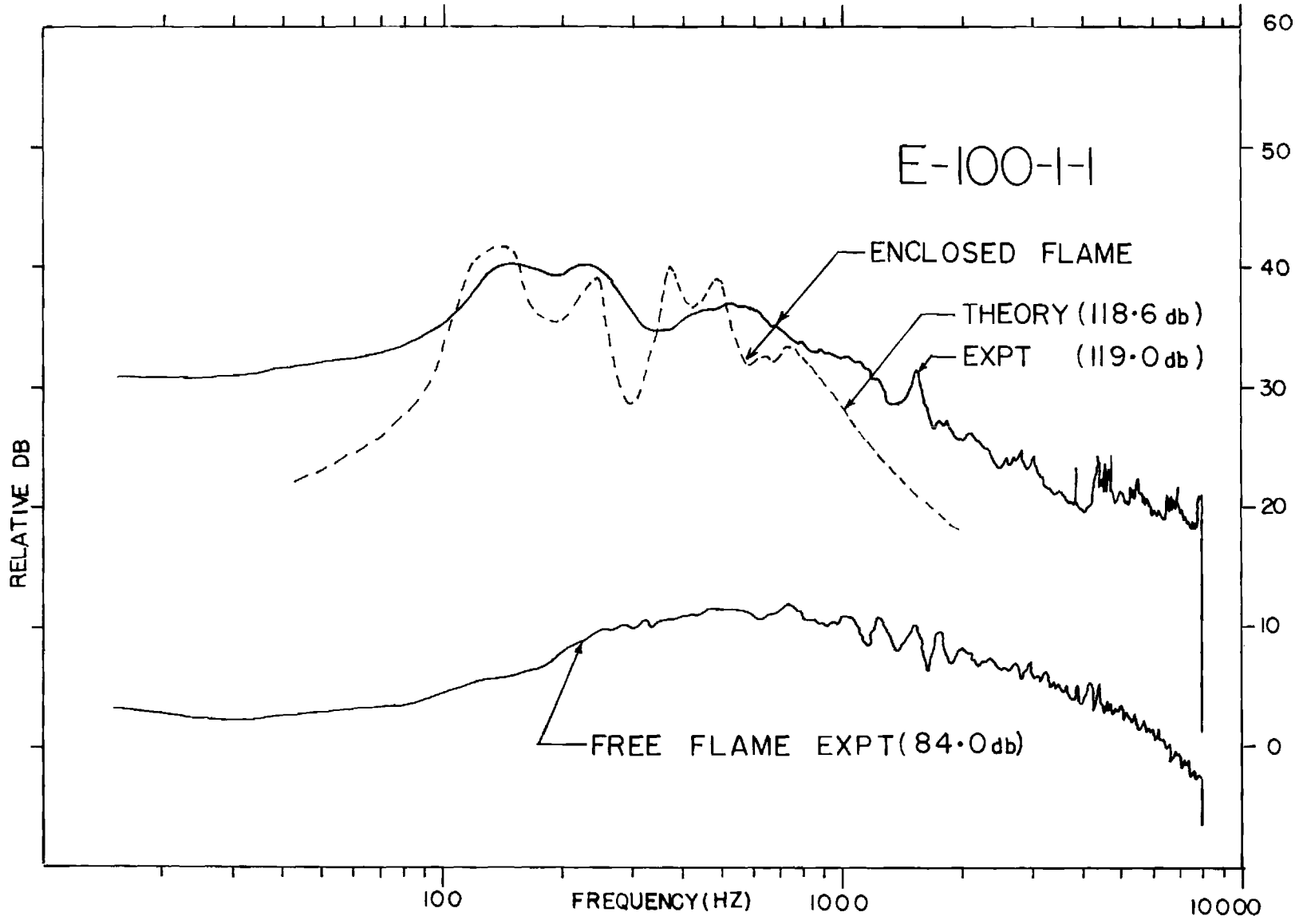

Figure 7. Typical Result of Theory and Experiment for the Open and Ducted Flame

Figure 7 does have some adjustments in the computation which will now be discussed. It has been assumed that (a) the origin of coordinates lies 6 inches to the right of the burner mouth, (b) $T_{\ell_2} = 1000^{\circ}R$ and (c) the α for the hot end muffler is twice the measured value when cold. The reasons for these inputs are described in Figs. 8-10. Viewing Fig. 8 it is seen that if one assumes the origin is at the burner mouth and that the downstream muffler behaves as it does when it is in cold, quiescent air, and that there is no temperature gradient, the spectral comparison is quite poor. The flame length here is about 8 inches and it is known that the flames radiate sound mostly from the flame tip region. Assuming that the origin is shifted downstream six inches (curve labeled offset in Fig 8), substantial improvement is achieved in the spectral comparison, although little change occurs in the overall sound pressure level. Assuming no offset but setting $T_{\ell_2} = 1000^{\circ}R$ in the computation (curve labeled C-H in Fig. 8), the spectral comparison is also improved insofar as the resonance frequencies are better predicted. One suspects, therefore, that reasonable inputs to the theory will improve the spectral shape while still allowing reasonable agreement in the overall sound pressure level.

Figure 9 shows an experimental traverse of the tube pressure level, which produces a roughly constant sound pressure level. The theory, however, assuming either offset or no offset, high temperature or the cold value, produces a variable pressure. This occurs primarily because of the mode structure at low frequencies near the reasonance peaks. The reason for the sound pressure level agreement between theory and experiment in Fig. 8 is due to the fact that the microphone location was at x = 24 inches. Assuming various multipliers on the cold and hot end α's as shown in Figs. 9 and 10, it is seen that the highter the α's the more suppressed are the resonance

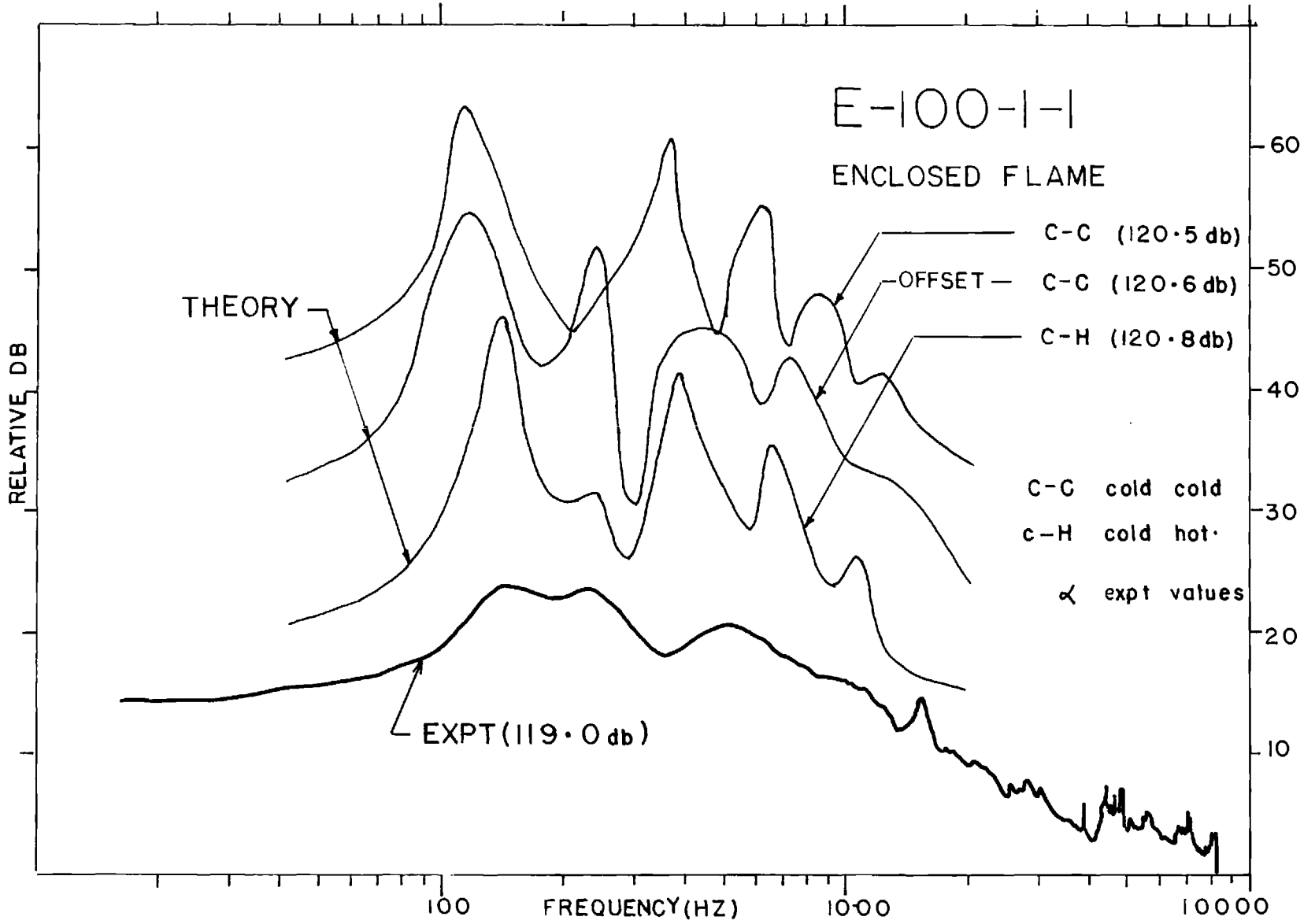

Figure 8. Comparison of Theoretical and Experimental Spectra Under

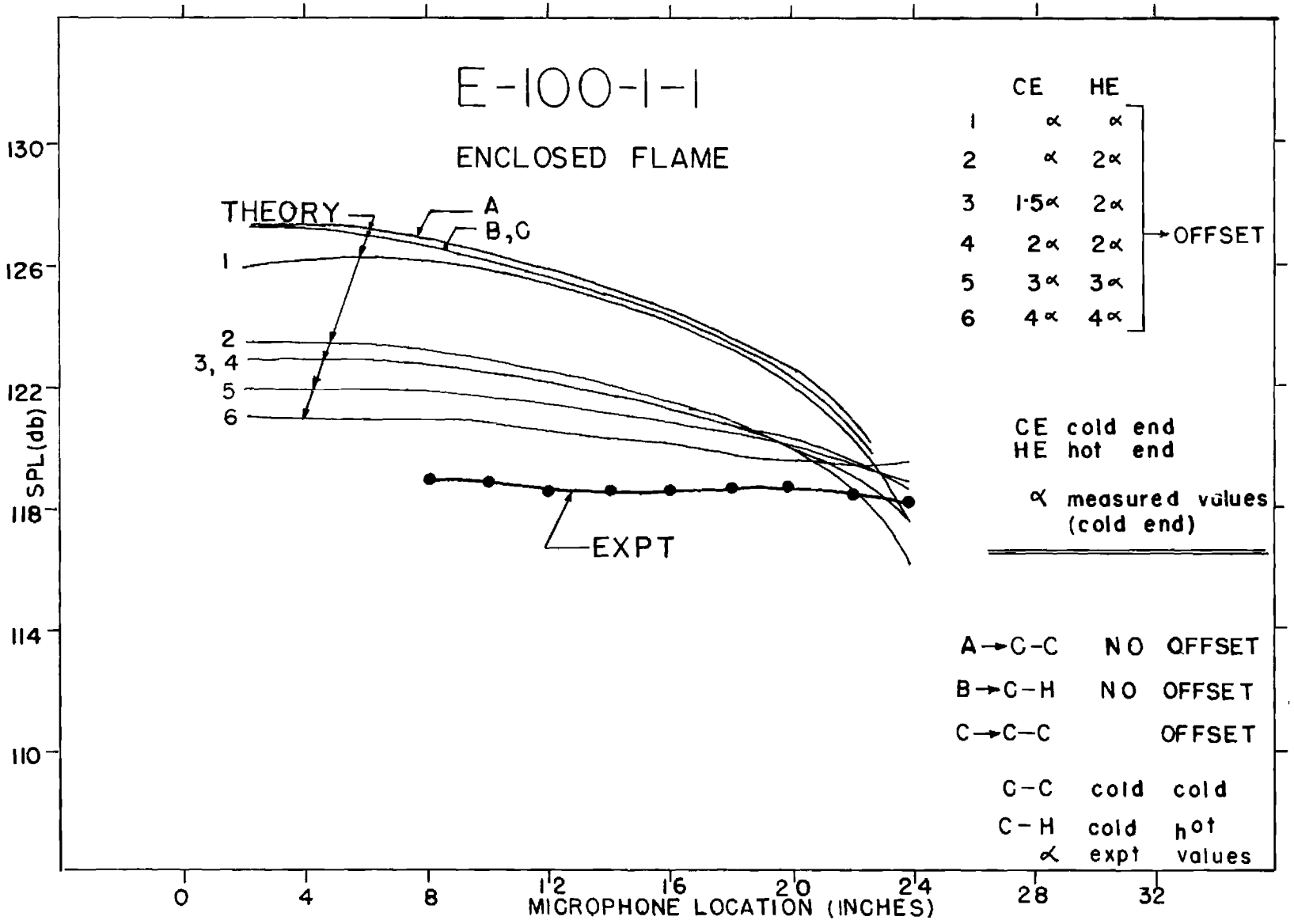

Figure 9. Comparison of Theoretical and Experimental Pressure Distribution

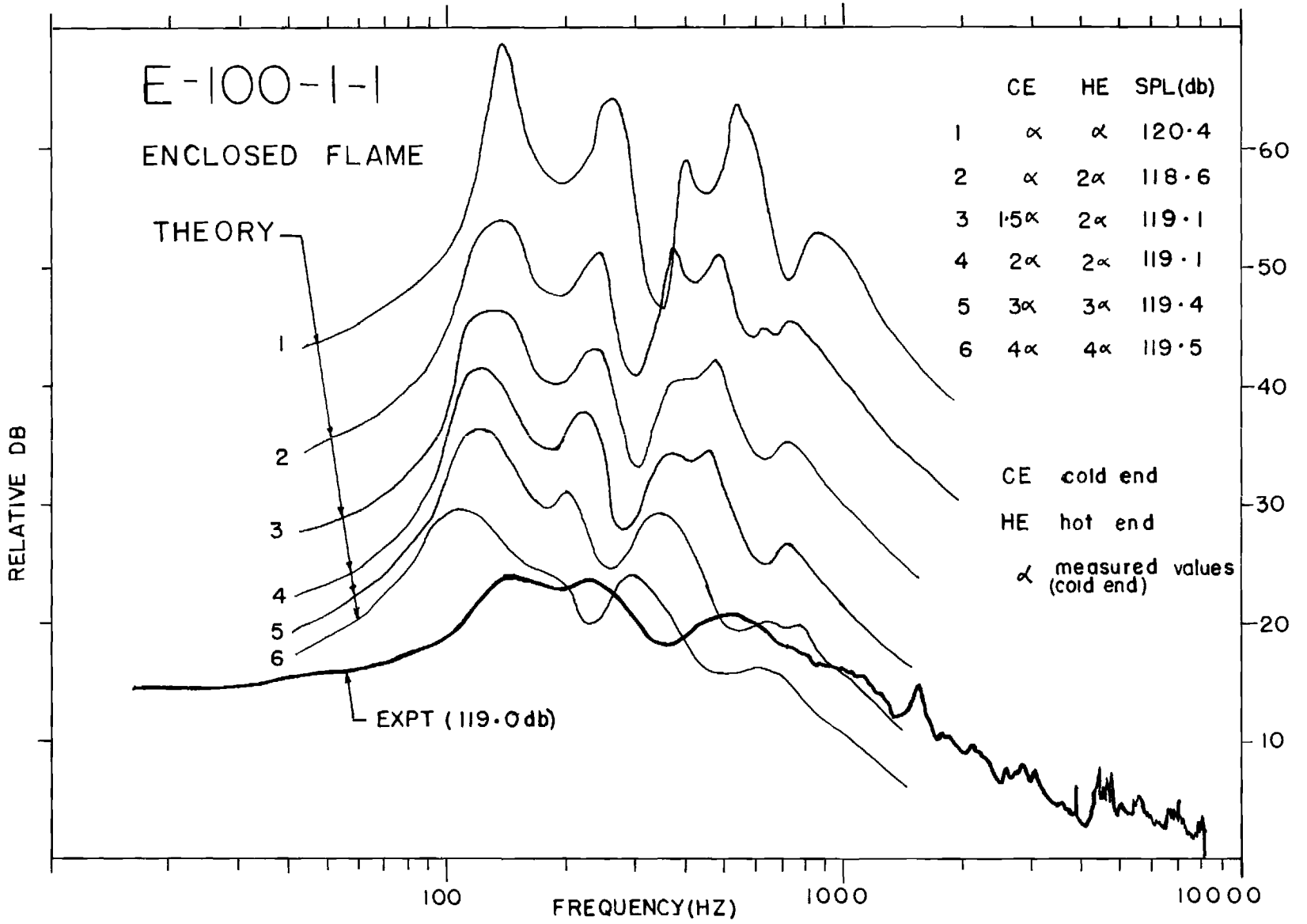

Figure 10. Spectral Comparison of Theory and Experiment Under Several Impedance Assumptions

peaks, as expected, and the flatter is the pressure vs distance curve. In Fig. 10 the offset and high temperature conditions have been used. There appears no justification for manipulating the cold end α, however. In all following computations the α in the hot end has been raised by a factor of two over the experimental value as a compromise between improving the spectral fit and the pressure vs distance while not varying α over an unreasonable range.

Using the offset, high temperature, and high α hot end assumptions, the data have been reduced for three propane-air flames. The comparisons are shown in Figs. 11-13. All sound pressure measurements in the tube are made at the 24 inch location. In all cases the spectral comparisons are fair but the overall sound pressure comparisons are good. The general agreement in pressure level is of the order of 3 db. The experimental values are always higher than the theoretical values, but this may be due to the modal pattern predicted by the theory as shown in Fig. 9.

It appears that the experimental system, either through muffler behavior or wall dissipation, is more heavily damped than would be expected from the no flow impedance measurements. Nevertheless, the predicted overall pressure levels are not sensitive to this behavior at the 24 inch microphone location (see Fig. 9). Consequently, even if the spectral comparisons are somewhat poor for some tests the overall pressure predictions appear to have a positive correlation with the experimentally achieved values, and it appears that the basic assumptions are valid. The major conclusion, therefore, is that if the characteristics of the unenclosed flame are known the enclosed noise can be predicted within about 3 db accuracy. Of course, this assumes the enclosure acoustics are perfectly known. While there are certain to be

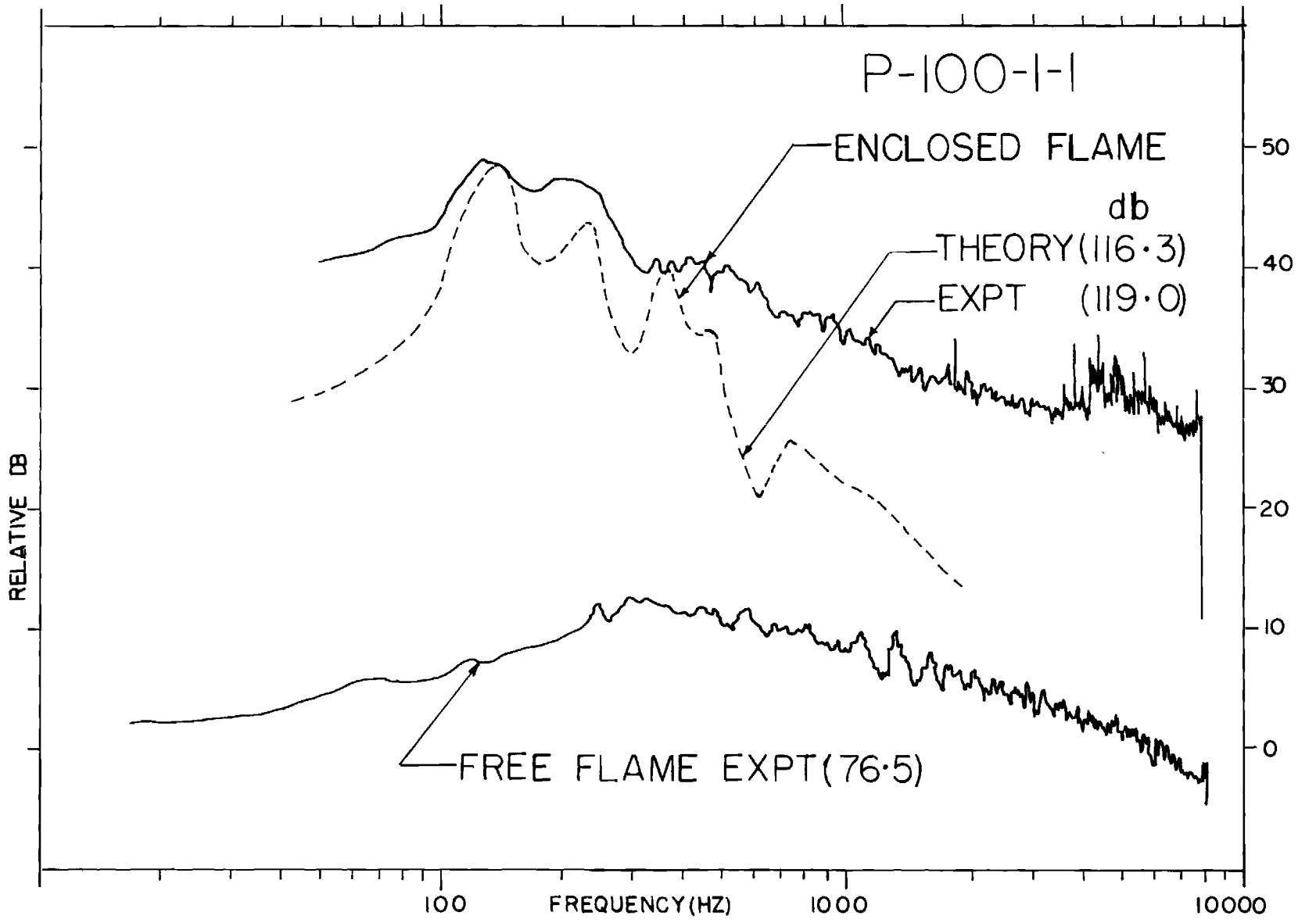

Figure 11. Comparison of Theory and Experiment for Propane-Air at 100 ft/sec, Φ= 1.0

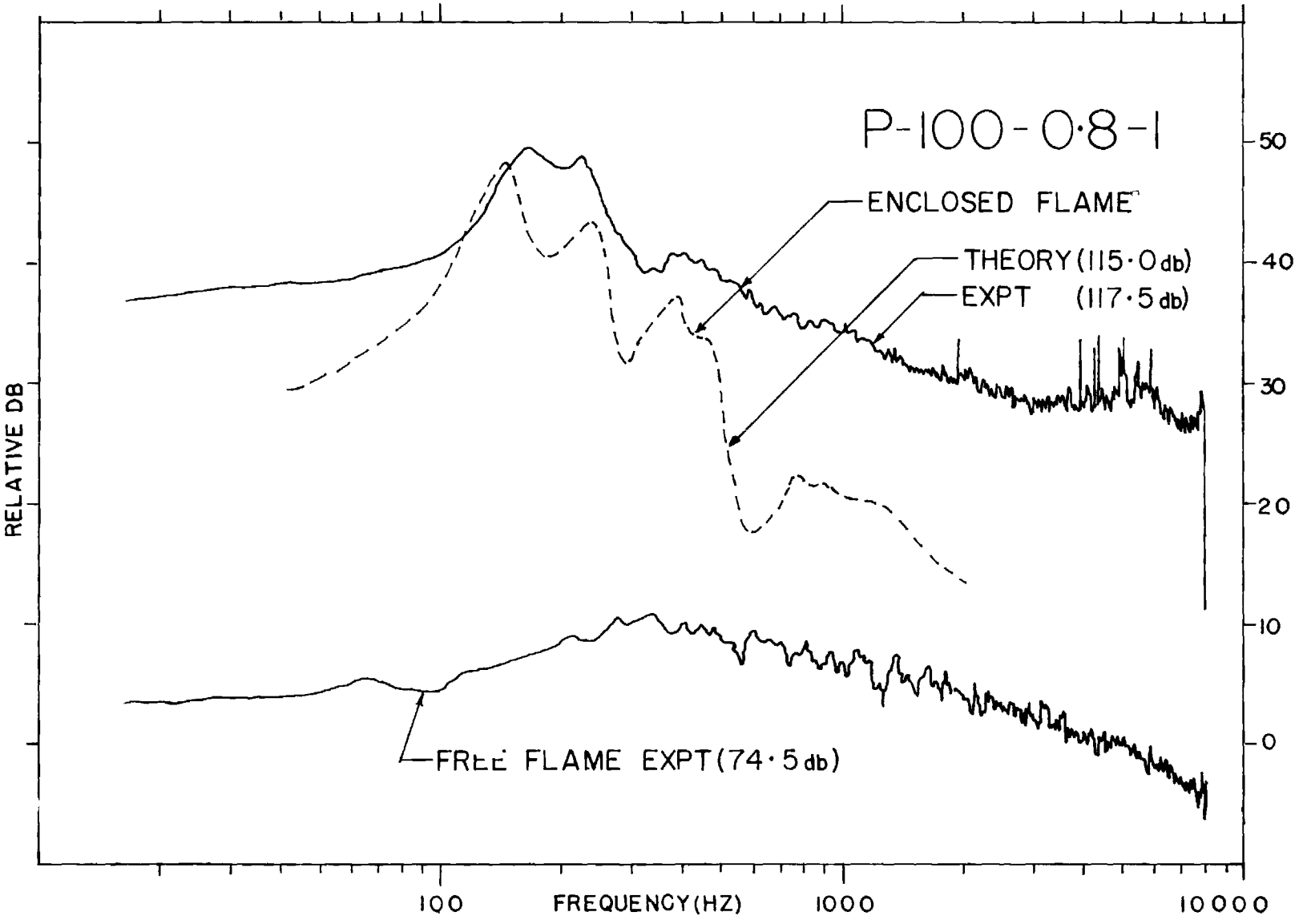

Figure 12. Comparison of Theory and Experiment for Propane-Air at 100 ft/sec, $\Phi = 0.8$

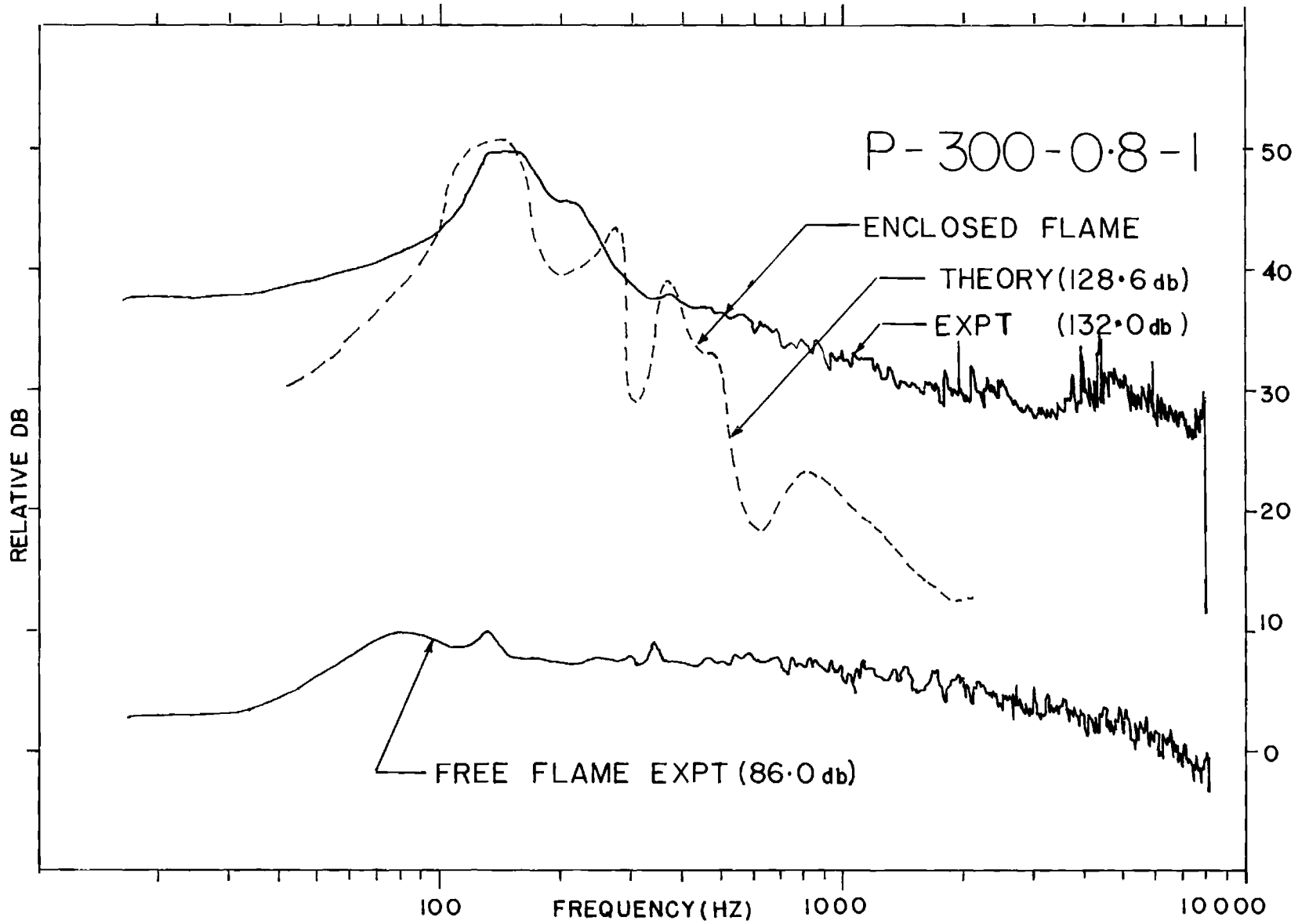

Figure 13. Comparison of Theory and Experiment for Propane-Air at 300 ft/sec, $\Phi = 0.8$

Page missing from report

CHAPTER V

CONCLUSIONS

1. There exists a direct proportionality of the far field acoustic pressure from open flames and the volume-integrated Eulerian time derivative of the heat release rate in the flame.
2. As a result of conclusion #1 the basic theory of Ref. 3 appears adequate with the major fault occurring in manipulations occurring after the pressure-reaction rate link is derived.
3. Completion of the open flame tests and modification of the theory have produced an accurate correspondence between theory and experiment on this flame type, at least as far as the radiated power is concerned.
4. One point of poor accuracy between theory and experiment is the scaling law produced on frequency of maximum radiated power. Further experiments at larger burner diameters are warranted to check the accuracy of the empirical law in this regard.
5. For systems which are damped sufficiently to avoid combustion instability the noise output of an enclosed flame may be predicted if the open flame noise radiation characteristics are known and the acoustics of the enclosure are known.
6. The theory is sufficiently accurate that it may now be used for other flame types if the turbulence parameters may be estimated. As a consequence of conclusion #5 a primary requirement for estimation of ducted flame noise behavior is a knowledge of the duct acoustics.

REFERENCES

1. Strahle, W. C., Shivashankara, B. N., and Handley, J. C., "Combustion Generated Noise in Turbopropulsion Systems," AFOSR Interim Scientific Report, AFOSR-TR-73-1899 (1973).

2. Strahle, W. C., "On combustion generated noise," Journal of Fluid Mechanics, 49, p. 399 (1971).

3. Strahle, W. C., "Some results in combustion generated noise," 23, p.113 (1972)

4. Strahle, W. C., "A review of combustion generated noise," AIAA Paper No. 73-1023 (1973)

5. Chiu, H. H. and Summerfield, M., "Theory of combustion noise," Paper presented at 4th International Colloquium on Gasdynamics of Explosions and Reactive Systems, San Diego (1973).

6. Hurle, I. R., Price, R. B., Sugden, T. M. and Thomas, A., "Optical studies of the generation of noise in turbulent flames," Twelfth Symposium (International) on Combustion, Pittsburg, The Combustion Institute, p. 1093 (1968).

7. Shivashankara, B. N., Strahle, W. C. and Handley, J. C., "An evaluation of combustion noise scaling laws by an optical technique," AIAA Paper No. 74-47 (1974).

8. Morse, P. M. and Ingard, K. U., Theoretical Acoustics, New York, McGraw-Hill, p. 469 (1968).

9. Morse, P. M. and Feshback, H., Methods of Theoretical Physics, New York, McGraw-Hill, Part II, p. 1092 (1953).

Appendix A

An Evaluation of Combustion Noise Scaling Laws by an Optical Technique

by

B. N. Shivashankara, Warren C. Strahle

and John C. Handley

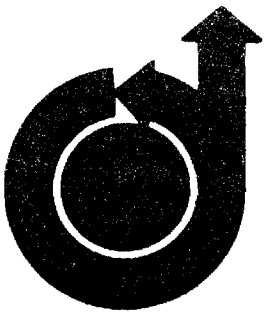

AIAA Paper No. 74-47

AN EVALUATION OF COMBUSTION NOISE SCALING LAWS BY AN OPTICAL TECHNIQUE

by
B. N. SHIVASHANKARA, WARREN C. STRAHLE,
and
JOHN C. HANDLEY
Georgia Institute of Technology
Atlanta, Georgia

AIAA 12th Aerospace Sciences Meeting

WASHINGTON, D.C. / JANUARY 30-FEBRUARY 1, 1974

AN EVALUATION OF COMBUSTION NOISE SCALING LAWS BY AN OPTICAL TECHNIQUE

B. N. Shivashankara*, Warren C. Strahle** and John C. Handley***
School of Aerospace Engineering
Georgia Institute of Technology
Atlanta, Georgia 30332

Abstract

An investigation which was conducted to verify the existence of a one-to-one correspondence between the acoustic and optical emissions from open premixed turbulent flames is described. The sound pressure and the time derivative of the emission intensity of light radiation have been compared using (a) direct time traces, (b) a cross-correlation technique and (c) spectral analysis. Further substantiation to the existence of the correlation has been provided by evaluating combustion noise scaling laws using optical measurements. These laws have been compared with existing scaling laws obtained from sound pressure measurements. Important conclusions regarding the origin of combustion noise have been drawn from these results.

Introduction

Combustion noise scaling laws have been deduced in the past by the measurement of sound pressures in the far field. Although this provides important scaling rules for the far field noise radiation, there is a clear need for additional information in order to fully understand the mechanism of noise generation. The experimental findings of Hurle et al[1] and Price et al[2] appear to be an important step in this direction. Hurle et al[1] showed that the sound pressure waveform could be deduced from the waveform of the time derivative of the emission intensity when the flame is viewed through a narrow band optical filter. Open turbulent flames and spherically expanding flame fronts were considered in this work. Price et al[2] extended the validity of such a correlation to include diffusion flames as well as liquid spray combustion. In both References 1 and 2, the one-to-one correspondence between the optical and acoustic waveforms was established over a limited band-width of the signals. The limitation of band-width was primarily necessitated by the large amount of noise in the optical circuitry. Since the band-width considered included the predominant frequencies of combustion noise, the correlation could be considered significant. In an attempt to theoretically explain the results of Hurle et al[1] and Price et al[2], Strahle[3] obtained an expression for the far field acoustic density in the form

$$\rho \propto \int_V \omega_t \left(\underset{\sim}{r}_o,\ t - \frac{r}{a_o}\right) dV \left(\underset{\sim}{r}_o\right) \qquad (1)$$

where ω_t is the time derivative of the reaction rate referred to a retarded time corresponding to the distance r between the source and the far field location at which density is measured. This result supports the findings of References 1 and 2 and states that the far field acoustic density can be expressed as a volume integral of the time derivative of the time retarded reaction rate.

A good cross-correlation between the instantaneous sound pressure p(t) and the time derivative of the emission intensity $\dot{I}(t)$ from zones of turbulent combustion would establish that the noise emitters are solely restricted to regions of active reaction thus isolating the origin of combustion noise. Further, the theoretical prediction of Reference 3 would be verified. If in fact p(t) and $\dot{I}(t)$ are correlated, it should be possible to deduce at least some of the scaling laws on the radiated sound power by the optical technique without the use of any sound measuring equipment.

The experiments on premixed turbulent flames in References 1 and 2 used burner sizes varying from 0.17" to 0.67" diameter with flow velocities up to about 100 ft/sec. An equivalence ratio of 0.9 to 1.3 was covered. The experimental study described in this paper was conducted with an aim to determine if the correlation between the acoustic and optical emissions does exist for higher velocity flames also. A 100 ft/sec to 600 ft/sec velocity range was chosen. Burners up to 0.96" in diameter were used. The mixture ratio was varied between 0.8 and 1.25. The comparison of p(t) and $\dot{I}(t)$ was accomplished by the use of (a) direct time traces and (b) spectral analysis as was done by Hurle et al[1] and Price et al[2]. In addition to these two methods, cross-correlation function analysis was also employed. Further, using $\dot{I}_{r.m.s}$ values scaling laws of radiated acoustic power with respect to flow velocity and burner diameter were deduced.

Experimental Set-Up

The experimental facility used for these experiments was the same as the one used for the noise measurements of Reference 4. The burner sizes were 0.402", 0.652" and 0.96" in diameter. Gaseous fuels propane and ethylene were used with air as the oxidizer. The open, premixed turbulent flames were stabilized using a pilot flame of hydrogen. The anechoic chamber provided a satisfactory dark enclosure for the light measurements to be made. The image of the flame was focused on the cathode of a photomultiplier tube (RCA931A or EMI9601S) using a f/4.5-50mm enlarger lens fixed to the front end of the photomultiplier tube housing. The photomultiplier tube was placed with its axis in the same horizontal plane as the burner axis and at 90° to the flow direction. In the experiments conducted, the distance between the burner and the front of the lens was 53.5 to 75 inches. At this distance, it was determined that the lens would capture the light from the entire flame brush over the complete range of experimental conditions. The light collected by the lens was filtered through a narrow

* Post Doctoral Fellow
** Professor, Member AIAA
*** Research Engineer

band optical filter centered on C_2 radiation (5165 Å). The peak transmission of the filter was at 5155 Å with a half-peak transmittance band-width of 50 Å. The selection of the filter was based on the recommendations of References 1 and 2. It is known from spectroscopic studies (e.g. see Reference 5) that radicals like CH, C_2 and OH exist only in the zone of reaction. The mean intensity of emission of any one of these active radicals should be proportional to the global reaction rate in the flame while the time derivative of the emission intensity should be proportional to the time derivative of the global reaction rate. Thus, by focusing the entire flame onto the photomultiplier tube an effective volume integration is performed over the reacting volume.

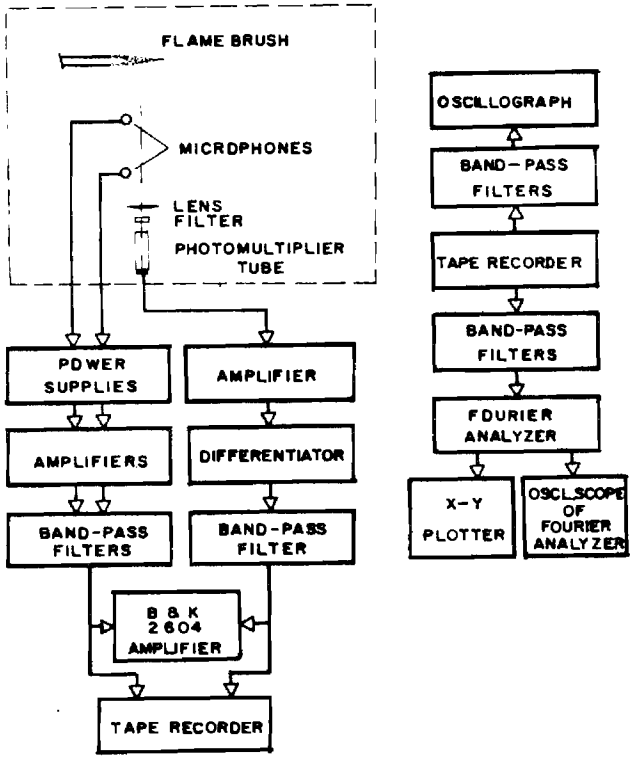

Fig. 1 Instrumentation schematic.

Figure 1 shows the instrumentation used in this study. The output of the photomultiplier tube is amplified using a NEFF type 122 d.c. amplifier. The mean emission intensity I is measured by a d.c. digital voltmeter at this stage. The output of the amplifier is then differentiated to obtain I(t). The particular differentiating circuit was known to yield -de(t)/dt when a voltage e(t) was introduced at the input. Necessary correction was applied for this in the data analysis. The differentiated signal was then passed through a Krohn-Hite Model 3202R filter and recorded on one of the channels of an Ampex 1300FR, 14 channel magnetic tape recorder using necessary amplification.

Two Brüel and Kjaer type 4134 half-inch condenser microphones, stationed at 90° to the flow direction with reference to the burner exit, were used for sound pressure measurement. The microphones were placed between 14" and 25" from the burner part.

The outputs from the microphones were also filtered by band-pass filters identical to the one used to filter $\dot{I}(t)$. The sound pressure waveforms were recorded simultaneously with $\dot{I}(t)$ on two other channels of the tape recorder. In some instances, the filtering was done at the time of reproduction of the recorded signals. The data were recorded at 30 inch/sec tape speed. The tape recorder had a flat response (± 1 db) up to 10 kHz at this tape speed setting. In order to expand the time scale of instantaneous traces on the oscillograph the tape was played back at 1-7/8 ips producing a speed reduction of 16. The reproduced signals were plotted on a paper chart using a CEC type 5-124 A oscillograph. A paper speed of 64 in/sec was used for this purpose. The spectra of p(t) and $\dot{I}(t)$ as well as the cross-correlation functions between them were obtained from the magnetic type record using a Hewlett Packard type 5465 Fourier Analyzer. This system had an analog to digital converter along with an 8K computer to perform the necessary calculations. In order to obtain stable results a 100 sample averaging technique was used.

Comparison of Instantaneous Waveforms

The instantaneous time traces of sound pressure p(t) and the time derivative of the emission intensity I(t) are compared in Figure 2. Three typical cases are presented. The following notation is used to identify the tests:

P	- 100	- 0.8	- 0.40
Fuel P = Propane E = Ethylene	Flow Velocity (ft/sec)	Equivalence Ratio	Burner Diameter (inches)

The waveforms shown are oscillograph recordings redrawn incorporating a time shift τ^*. $\tau^* = r/a_o$ is the amount of time by which the p(t) waveform is moved in the -t direction to account for the time taken by sound to travel the distance between the source (the flame) and the receiver (the microphone). The optical radiation from the flame reaches the photomultiplier almost instantaneously in comparison with τ^*. The tape recorder used is known to introduce phase differences between signals recorded on different channels. The maximum phase difference is about 20° for a signal of frequency 1000 Hz. Also, the phase difference is directly proportional to the frequency. Due to this phase difference it is possible that an error of the order of 5% (of τ^*) is introduced in the time shift τ^* on Figure 2, which is quite small since only qualitative comparisons are being made. Some similarities exist between the p(t) and $\dot{I}(t)$ waveforms over a wide range of experimental conditions. Thus, it has been demonstrated that the results of References 1 and 2 can be extended to include high velocity flames. Further, one-to-one correspondence between p(t) and $\dot{I}(t)$ has been shown to exist for different burners and mixture ratios. The most important conclusion of this correlation between optical and acoustic emissions is that sources of combustion noise are primarily located in the visible flame brush. This can be considered to support the theory of Reference 3 which recognized the value of evaluating the flame volume in studying combustion noise scaling laws.

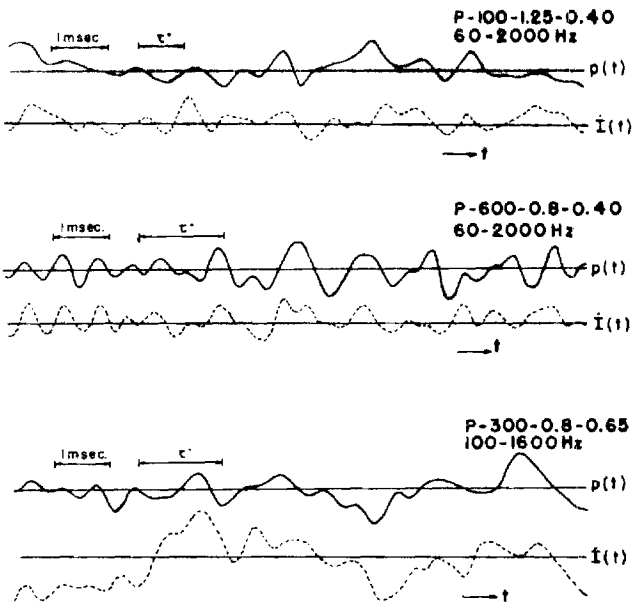

Fig. 2 Comparison between $\dot{I}(t)$ and $p(t)$ waveforms. $p(t)$ waveforms are shifted to left by τ^*.

Although comparing the instantaneous $p(t)$ and $\dot{I}(t)$ would establish a one-to-one correspondence directly, certain experimental difficulties are involved. These difficulties arise mainly due to spurious electronic noise in the instrumentation. The $p(t)$ is relatively free from spurious noise. However, the differentiator in the optical circuitry tends to magnify the relative importance of noise making the signal to noise ratio in $\dot{I}(t)$ rather low. In many cases (for example P-100-0.8-0.4) it was very difficult to compare the two waveforms and decide whether or not a reasonable similarity existed between them. Further discussion on the spurious noise has been presented later in this paper.

The foregoing discussion clearly demonstrates that more definite evidence than what was presented in Figure 2 is required before a one-to-one correspondence between optical and acoustical emissions from turbulent flames can be accepted. Therefore, further experiments aimed at obtaining cross-correlation and spectral distributions were conducted.

Cross-Correlation

The cross-correlation function[6] gives a measure of the similarity between two waveforms used in the calculation. If the same signal is used in the place of both waveforms, an auto-correlation function would result. The auto-correlation function is an extension of the concept of the root-mean-square value of a wave. The auto-correlation function is always symmetric about the point of zero delay; it has a maximum value equal to the mean square value of the wave at the point of zero delay.

The cross-correlation function, on the other hand, does not always maximize at zero delay. In fact, the point at which the maximum occurs is one of the most significant results arising from the cross-correlation function analysis of two signals. This delay time at which the maximum occurs forms an important basis in isolating the source of a disturbance.

Correlation techniques have been used extensively in aero-acoustic problems, for example, in the work of Bhatt[7] and Goff[8]. Recently, Abedlhamid et al[9] employed this technique to establish correlation between the noise from high-speed jets and combustor pressure disturbances. Mathematically, the cross-correlation function G between two waveforms $x(t)$ and $y(t)$ can be expressed as

$$G(\tau) = \lim_{T \to \infty} \frac{1}{T} \left\{ \int_{-\frac{T}{2}}^{\frac{T}{2}} x(t)\, y(t - \tau)\, dt \right\} \qquad (2)$$

For the case at hand

$$\begin{aligned} x(t) &\equiv p(t) \\ y(t) &\equiv \dot{I}(t) \end{aligned} \qquad (3)$$

Recall that the sound wave takes a time τ^* to reach the microphone. Thus, for a one-to-one correspondence between $p(t)$ and $I(t)$, we should have

$$p(t) = K\dot{I}(t - \tau^*) \qquad (4)$$

where K is some constant. The cross-correlation function, therefore, becomes

$$G(\tau) = \lim_{T \to \infty} \left\{ \int_{-\frac{T}{2}}^{\frac{T}{2}} \dot{I}(t - \tau^*)\, \dot{I}(t - \tau)\, dt \right\} \qquad (5)$$

and would maximize at $\tau = \tau^*$. Thus, the experimental cross-correlation functions should maximize at $\tau = \tau^*$ if a one-to-one correspondence exists between the optical and acoustic emissions from the turbulent flames.

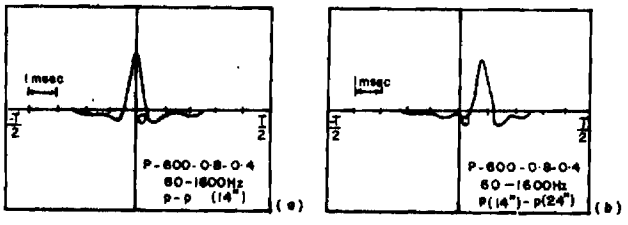

Fig. 3 Cross-correlation function between (a) $p(t)$ waveform with itself and (b) $p(t)$ at 24". Vertical scale is arbitrary.

The correlation functions are obtained using the Fourier Analyzer. The cross-correlation function displayed on the Fourier Analyzer system

oscilloscope screen is photographed. The traces shown in Figures 3 and 4 are redrawn using these photographs. Figure 3 essentially illustrates how cross-correlation works. Figure 3(a) shows an auto-correlation function for the p(t) of the P-600-0.8-0.40 case. Figure 3(b) is a display of the cross-correlation function between p(t) as measured by the microphones at 14" and 24" from the flame. Notice that the cross-correlation maximizes at $\tau \approx 0.8$ msec which corresponds to the time taken by sound waves to travel the distance between the two microphones. In Figure 3, as well as in Figure 4, trace lengths of T/4 have been cleared at both ends of the time axis. This is required in order to eliminate wrap around errors[16]. Cross-correlation functions between $\dot{I}(t)$ and p(t) waveforms over various experimental conditions are presented in Figure 4. Figure 4(a) shows the cases for which p(t)'s from the microphone at 14" have been used. The cross-correlations maximize for $\tau \approx 1.0$ msec in these cases. Figure 4(b) is for p(t)'s from microphone at 24". The time delay at which maxima occur is ≈ 1.8 msec. In Figure 4 the

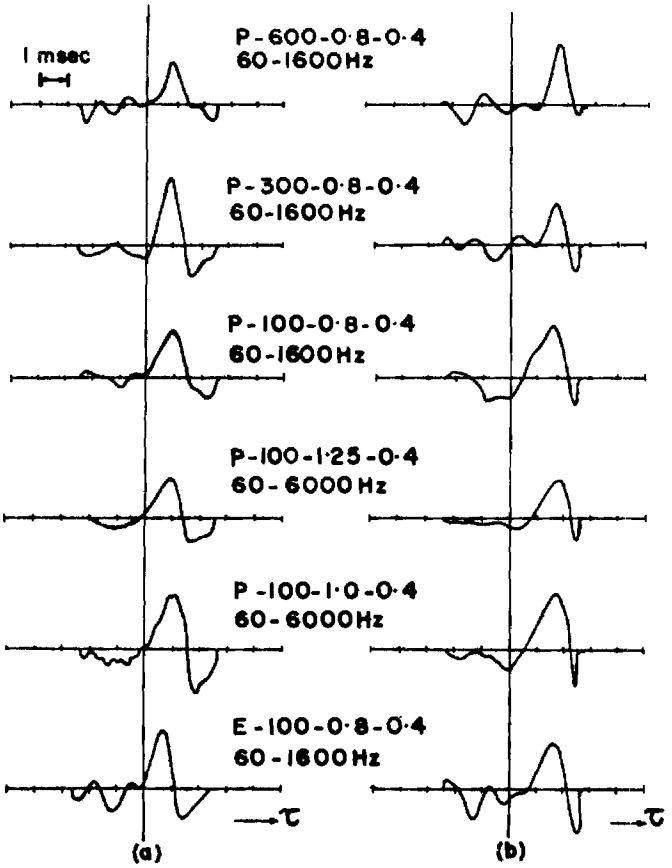

Fig. 4 Cross-correlation between p(t) and $\dot{I}(t)$ waveforms. (a) p(t) from microphone at 14". (b) p(t) from microphone at 24".

experiments include a flow velocity range of 100-600 fps. The fuels propane and ethylene are used and both fuel-lean and fuel-rich mixtures are included. Thus, over a wide range of parameters a good cross-correlation between p(t) and $\dot{I}(t)$ exists.

Frequency Spectra of Optical Emission

After having established that a good cross-correlation exists between the acoustic and optical emissions, the spectra of $\dot{I}(t)$ and p(t) were compared. These spectra should show identical frequency distributions if a one-to-one correspondence exists.

First, the P-100-1.25-0.40 case is considered. The comparison between the instantaneous p(t) and $\dot{I}(t)$ traces was shown to be quite reasonable in Figure 2(a) for this case. Figure 5(a) shows that the spectra of $\dot{I}$ and p are in excellent agreement up to 1000 Hz. The correspondence between the spectra grows progressively worse due to electronic noise at higher frequencies. Since in Figure 2(a) the waveforms were restricted to 2000 Hz, it was possible to observe a reasonable similarity.

Figure 5(b) shows the spectra for the case P-100-0.8-0.40. It has been stated earlier that an instantaneous waveform comparison was found to be extremely difficult for this case. The spectra for optical emission is almost flat over the entire frequency range showing that the I(t) signal is dominated by spurious noise. The reason for the difference in behavior between the two cases shown in Figure 5 can be explained to some extent by their mean intensities. It will be shown later, in Figure 7, that electronic noise dominates for flames with low mean intensity. The P-100-1.25 -0.40 flame, being much brighter

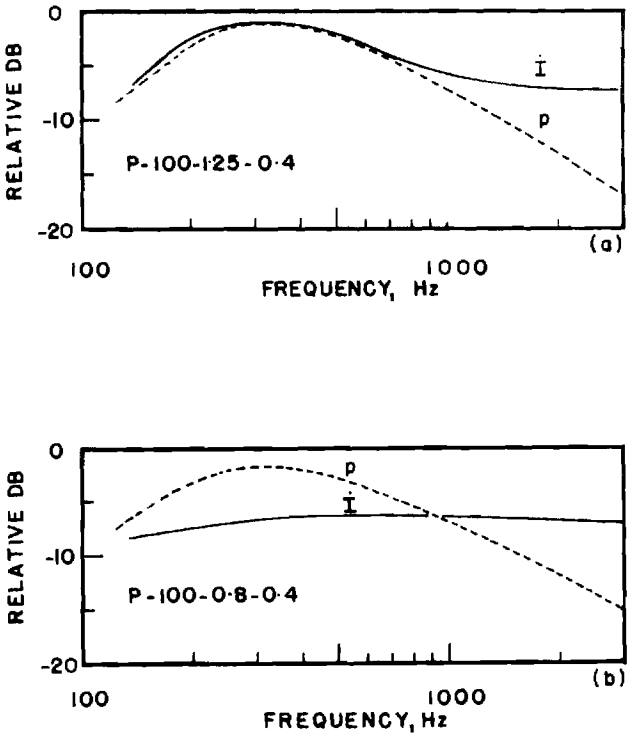

Fig. 5 Frequency spectra of $\dot{I}$ and p (a) for P-100-1.25-0.4 case and (b) for P-100-0.8-0.4 case.

than the P-100-0.8-1 flame, has a better signal to noise ratio and, therefore, shows a reasonable spectral comparison.

Similar spectral comparisons were made at various other experimental conditions. In general, it was observed that above about 1000-2000 Hz frequency electronic noise dominates $\dot{I}(t)$. Thus, any study using optical emissions from flames should exclude frequency components above 1000-2000 Hz unless

better electronics are available. Since, in Reference 4, it has been established that for hydrocarbon-air flames the combustion noise peaks in the 250-700 Hz range, this should not be a major restriction. Nevertheless, electronic noise appears to be a major problem to guard against in optical emission studies. Hurle et al[1] presented the spectra of both total $\dot{I}$ signal as well as the electronic noise. The signal to noise ratio was found to be very close to unity for frequencies below 200 Hz and above about 4000 Hz. In the range of 200-4000 Hz the signal to noise ratio was found to be about two at best. The spectrum of $\dot{I}$ corrected was compared with the spectrum for the sound pressure and moderate correspondence was observed by the authors in Reference 1. Price et al[2] state that the overall $\dot{I}_{r.m.s.}$ values were corrected for electronic noise. In the present experiments the corrections applied on the overall $\dot{I}_{r.m.s.}$ were between about 2 to 10 db (see Figure 8). Although these corrections are rather high there is reason to believe that the corrections applied for the data of References 1 and 2 must also have been of comparable magnitude.

Scaling Laws for Acoustic Power from Optical Emission Measurements

The investigation discussed in this section arises as a natural consequence of the results presented so far in this paper. If, in fact, there is a one-to-one correspondence between p(t) and I(t), then it should be possible to obtain at least the scaling laws on the flow velocity U and burner diameter D for the radiated acoustic power from the optical experiments. The scaling laws with respect to S_L and F would require the use of more than one fuel.* Since the line intensities in the optical spectra for various fuels differ, there are bound to be additional corrections required for mean intensities. Because of the presence of substantial amounts of spurious noise in the $\dot{I}$ measurements, the scaling laws by the optical technique should be considered more as a substantiation to the existence of the correlation rather than as a method for generating combustion noise scaling laws. The following paragraphs describe experiments using propane as the fuel designed to recover the velocity and diameter scaling on the radiated acoustic power.

The photo-multiplier tube output was amplified and differentiated. The differentiated signal was passed through a band-pass filter set to allow frequencies between 180-1000 Hz. This restriction on frequency was decided by the results of the spectral analysis. The filtered $\dot{I}$ was measured by the volt meter of a B & K 2604 microphone amplifier. The r.m.s. value of $\dot{I}$ was read out as db (re. $1v_{rms}$). The meter was set to the "slow" position. The gain on the amplifier was noted. The voltage supply to the photomultiplier tube, the band-width of the filters, the distance between the photomultiplier tube and the flame etc., were left undisturbed over a sequence of runs over which either velocity or the burner diameter was varied. This would ensure that changes in $\dot{I}_{r.m.s.}$ measured would be representative of the changes at the flame. The $\dot{I}_{r.m.s.}$ measured would be due to both the true signal and the electronic noise. Since it had been determined that electronic noise is appreciable it was necessary to correct the measured $\dot{I}_{r.m.s.}$ for electronic noise.

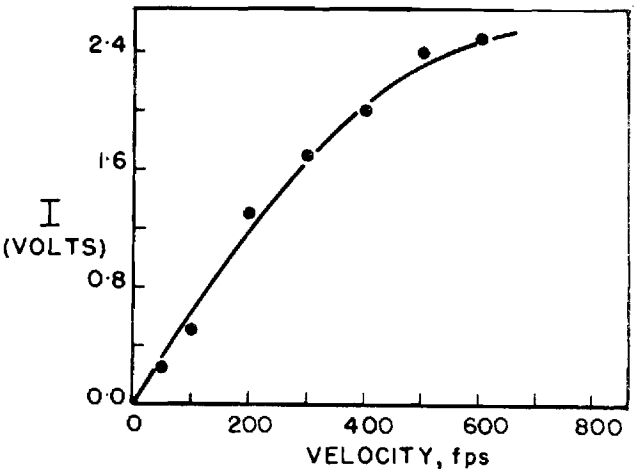

Fig. 6 Mean intensity as a function of flow velocity.

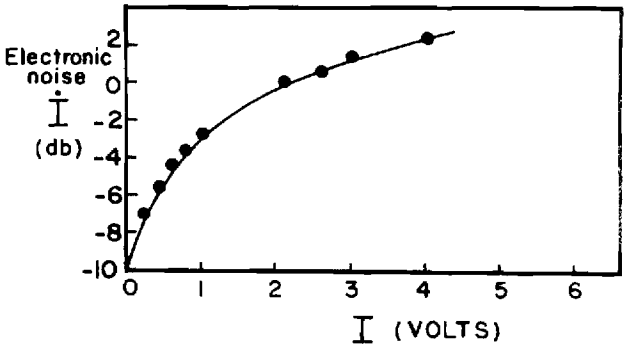

Fig. 7 Electronic noise $\dot{I}$ as a function of mean intensity.

Electronic noise in $\dot{I}$ is known to be a function of the mean intensity I received by the photomultiplier tube. Figure 6 shows the variation of mean intensity of the particular flame under consideration with flow velocity. These mean intensity values were measured by a d.c. volt meter at the input to the differentiator without disturbing any of the instrument settings. Using a standard lamp supplied with ripple-free d.c. current, a light source with negligible light flickering was obtained. The $\dot{I}_{r.m.s.}$ measured for this case should be indicative of the electronic noise. Figure 7 shows the $(\dot{I}_{r.m.s.})_{elec.\ noise}$ as a function of mean intensity I. Using Figures 6 and 7 together the values of electronic noise at various flow velocities for the particular flame could be determined. Now,

$$\left(\dot{I}_{r.m.s.}\right)_{true} = \left(\dot{I}_{r.m.s.}\right)_{measured} - \text{db correction}$$

in db in db

The values of db correction were obtained from standard background noise correction graphs[6]. Hurle et al[1] and Price et al[2] also found that corrections such as these were needed for their measurements.

*F is the fuel mass fraction and S_L is the laminar flame speed.

Figure 8 shows $(\dot{I}_{r.m.s.})_{true}$ as a function of flow velocity U. Also, values of $(\dot{I}_{r.m.s.})_{total}$ have been shown on Figure 8 to indicate that corrections applied are quite heavy. $(\dot{I})^2_{r.m.s.}$ appears to scale as $U^{2.7}$. This implies a $P \propto U^{2.7}$ scaling which is in excellent agreement with the $U^{2.7}$ law of Reference (4).* However, it should be cautioned against considering the optical method to be accurate based on the $\dot{I}^2_{r.m.s.} \propto U^{2.7}$ result. Below 200 fps, the signal to noise ratio was so low as to make it impossible to get $(\dot{I}_{r.m.s.})_{true}$. Also, recall that a rather restricted frequency range of 180-1000 Hz has been used for these experiments.

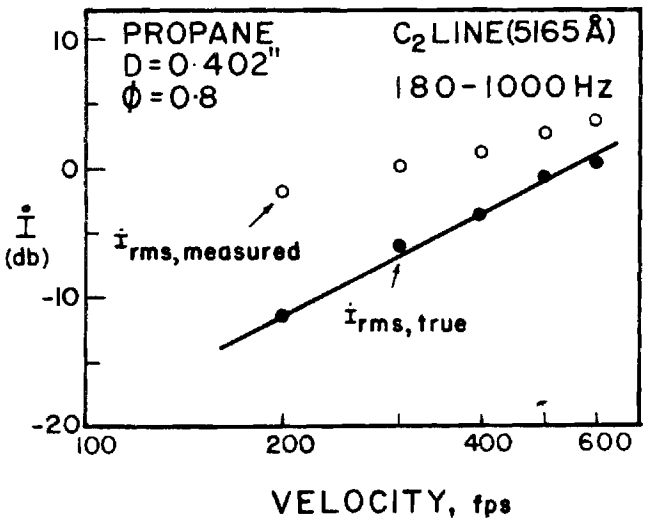

Fig. 8 Acoustic power law with flow velocity by optical technique.

An essentially same procedure was adopted to obtain the variation of $\dot{I}_{r.m.s.}$ with the burner diameter. Figure 9 shows the variation of $\dot{I}_{r.m.s.}$ with diameter. The data points have been corrected for electronic noise. It can be seen that $\dot{I}^2_{r.m.s.}$ scales with diameter to an exponent roughly between 2 and 4.5. A least square fit preferred a $\dot{I}^2_{r.m.s.} \propto D^{4.5}$ law. However, improved data are required before one can conclusively determine the scaling law. $\dot{I}_{r.m.s.} \propto D^{2\text{-}4.5}$ implies that radiated acoustic power, P, would also scale to $D^{2\text{-}4.5}$. Sound pressure measurements of these flames, in Reference 4, gave a $P \propto D^{2.9}$ scaling. In any case, the results presented in Figures 8 and 9 do show that scaling laws obtained by optical measurements reflect the proper trend as compared with those obtained from sound pressure measurements, considering the very poor signal to noise ratios encountered in $\dot{I}$ signals. This strongly supports the theoretical deduction of Reference 3 shown in Equation (1) which states that the far field sound density (or pressure) is proportional to the global integration over the reacting volume of the first Eulerian time derivative of the time retarded reaction rate.

---

* P is the radiated acoustic power.

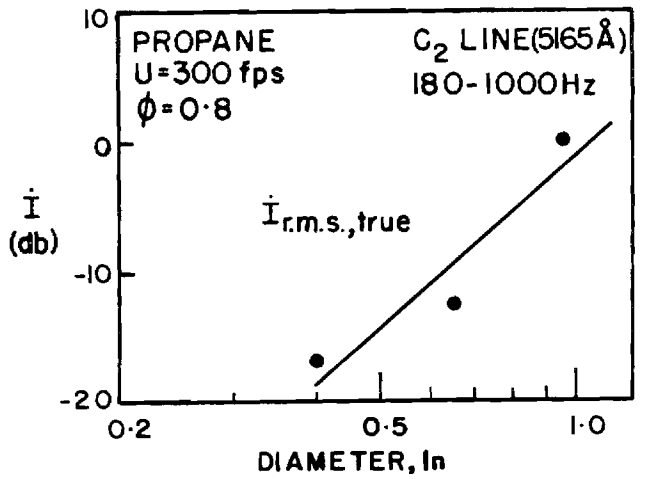

Fig. 9 Acoustic power law with burner diameter by optical technique.

Concluding Remarks

The intimate relation observed between the optical and acoustic emissions raises one important question: Is the correlation obtained because the noise generated, outside the flame zone, in the hot efflux, travels through the region of reaction and creates light fluctuations? This possibility can be ruled out because if a pressure wave p(t) passes through a flame, it creates changes in the reaction rate ω. Since $I(t) \propto \omega(t)$, this implies that $p(t) \propto I(t)$, thus, contradicting the experimental result $p(t) \propto \dot{I}(t)$.

The experiments described in this paper have shown despite the experimental difficulties due to electronic noise in the differentiated photomultiplier output, it is possible to observe one-to-one correspondence between the acoustic pressure and the time derivative of emission intensity from turbulent flames. This work supports the experimental findings of References 1 and 2 and the theoretical prediction of Reference 3 (see Equation (1)). The range of validity of the correlation has been extended to include flow velocities as high as 600 ft/sec. Whereas, Hurle et al[1] and Price et al[2] compared p(t) and $\dot{I}(t)$ directly, the present study employed cross-correlation technique in addition to direct time-trace comparisons. Further, scaling laws for radiated acoustic power were developed with respect to the flow velocity and the burner diameter. These laws compared favorably, with the ones obtained by sound pressure measurements in Reference 4, when the band-width was limited to 180-1000 Hz and necessary corrections were applied for electronic noise. This result, again, substantiates the existence of a correlation between optical and acoustic emissions. A practical implication of this result is that noise output from regions of combustion could perhaps be obtained directly without having to use an anechoic chamber. Unless better electronics are available, poor signal to noise ratio would severely restrict the use of this method. The most important conclusion of this study is that combustion noise sources are primarily located within the visible flame brush.

Acknowledgements

This work was supported by the National Science Foundation and the Air Force Office of Scientific Research under Grants No. GK 32544 and AFOSR-72-2365, respectively. The support is gratefully acknowledged.

References

1. Hurle, I. R., Price, R. B., Sugden, T. M., and Thomas, A., "Sound Emission from Open Turbulent Premixed Flames," Proceedings of the Royal Society of London A303, p. 409 (1968).

2. Price, R. B., Hurle, I. R., and Sugden, T. M., "Optical Studies of the Generation of Noise in Turbulent Flames," Twelfth Symposium (International) on Combustion, Pittsburg, the Combustion Institute, p. 1093 (1968).

3. Strahle, W. C., "Some Results in Combustion Generated Noise," Journal of Sound and Vibration, 23, p. 113 (1972).

4. Shivashankara, B. N., Strahle, W. C., and Handley, J. C., "Combustion Noise Radiation by Open Turbulent Flames," AIAA Paper No. 73-1025, 1973.

5. Gaydon, A. G., and Wolfhard, H. G., Flames: Their Structure, Radiation and Temperature, 3rd Ed., Rev., Chapman and Hall, London (1970).

6. Peterson, A. P. G. and Gross, Jr., E. E., "Handbook of Noise Measurement," Seventh Ed. General Radio, Massachusetts (1972).

7. Bhat, W. V., "Use of Correlation Technique for Estimating In-Flight Noise Radiation by Wing-Mounted Jet Engines on a Fuselage," Journal of Sound and Vibration, 17 (3), p. 349 (1971).

8. Goff, K. W., "Application of Correlation Techniques to Some Acoustic Measurements," Journal of the Acoustical Society of America, 27 (2), p. 236 (1955).

9. Abdelhamid, A. N., Harrje, D. T., Plett, E. G., and Summerfield, M., "Noise Characteristics of Combustion Augmented High Speed Jets," AIAA Paper No. 73-189 (1973).

10. Hewlett Packard Fourier Analyzer System 5450A/5452A Systems Operating Manual, Hewlett Packard (1970).

Appendix B

A Rational Correlation of Combustion Noise Results from Open Turbulent Flames

by

Warren C. Strahle and B. N. Shivashankara

Submitted for the Fifteenth International Symposium on Combustion

A RATIONAL CORRELATION OF COMBUSTION NOISE RESULTS FROM OPEN TURBULENT PREMIXED FLAMES

Warren C. Strahle
School of Aerospace Engineering, Georgia Institute of Technology
Atlanta, Georgia

B. N. Shivashankara
School of Aerospace Engineering, Georgia Institute of Technology
Atlanta, Georgia

The results are presented of 103 tests on the noise generation capability of bunsen burner type premixed hydrocarbon-air turbulent flames. The fuels used have been propane, propylene, acetylene and ethylene, all burning at 1 atmosphere in an anechoic chamber. The results for sound power output, reacting volume and spectral content are correlated with the burner diameter, flow velocity, fuel mass fraction and laminar flame speed; these variables are sufficient to produce correlations with respect to the Reynolds number, Mach number, fuel mass fraction and the first Damköhler similarity group. Introducing a new simplified version of the theory of combustion noise, known turbulent flame speed correlations, and the theory of isotropic turbulence decay downstream of the burner lip, it is shown that the correlations for frequency content and radiated sound power have a rational basis.

Introduction

Recently, experimental results have been reported on the noise generation capability of open turbulent premixed hydrocarbon-air flames anchored on burner tubes.[1] This work extended the study of Smith and Kilham[2]

to include larger burners and a wider flow velocity range and with a goal in mind to produce scaling laws with respect to the four variables F, D, S_L and U. Of primary interest were scaling laws for sound power output and the frequency of maximum radiated power. Both prior and subsequent to the cited experimental study several theories of combustion noise appeared in the literature.[3-5] In a recent review paper[6] it has been pointed out that none of these theories can adequately explain the observed scaling laws. This has been somewhat surprising since at least the theory of Reference 4 is known to contain the appropriate physics to explain the origin of combustion noise as deduced in References 7-9.

From a practical standpoint flames of this particular type are not of much use because of flashback considerations. However, the purpose of this paper is to understand the noise and to merge theory and experiment on a simple flame. It is considered imperative to understand this simple flame type in sufficient detail to match theory and experiment. If this understanding is not obtained, the use of the theory in more complex configurations would be open to severe question. Consequently, the purpose of this paper is to explain the observed free flame results on the basis of a revised theory of combustion noise.

Experimental Correlations

Experimental details are located in Reference 1 as are the results for propane, propylene and ethylene-air experiments. In order to gain better confidence in the scaling laws' behavior with respect to the fuel reactivity some acetylene runs have been added. Table 1 shows the final correlation results for the overall sound power, the frequency of maximum radiated sound power, and the reacting volume. The reacting volume is taken from Reference 10. Also shown is the turbulent flame speed correlation of Reference 11; the configuration of Reference 11 was identical to that of

the noise experiments except for the minor difference of the fuel used in an annular stabilization flame. In the turbulent flame speed correlation the effect of F was not explicitly stated in Reference 11. Review of this reference shows, however, that evidence of the insensitivity of S_L^t to F was indeed presented. The geometrical parameters such as flame length and width varied in the same manner between the sets of experiments of References 10 and 11.

Table 1

Empirical Correlations

Correlation	Equation [a]	Mean Error	Standard Deviation	Number Of Tests
Sound Power	$P = 3.7 \times 10^{-6} U^{2.67} S_L^{1.83} F^{-.40} D^{2.78}$	6%	41%	63
Reacting Volume	$V_c = 6.9 \times 10^{3}\ U^{.88}\ S_L^{-.93} F^{3.11} D^{3.22}$	3%	26%	40
Frequency of Maximum Power	$f_c = 2.3\ U^{.18} S_L^{.88} F^{-1.21} D^{-.13}$	1%	16%	62
Turbulent Flame Speed	$S_T = .44\ U^{.24} S_L F^{0} D^{.50}$	b	b	

a. U in ft/sec, D in ft, S_L in ft/sec, P in watts, V_c in ft^3, f_c in Hz, S_T in ft/sec

b. Not presented

Estimates of the uncertainties in the exponents may be obtained by comparing the predicted formula variations with the standard deviation of the fit. Although this will not be done here, it will be stated that for the noise experiments U was varied over a 12:1 ratio, D over a 2.74:1 range,

F over a 1.7:1 range and S_L (at fixed F) over a 3.8:1 range. Roughly the same variations apply to the S_T results of Reference 11.

It is, of course, conceptually more satisfying and more widely useful in an engineering sense if the results are presented in dimensionless form. If one were to write down the pertinent equations for the unsteady, turbulent combustion process and make the simplifying assumptions of a global reaction rate and $Le \approx Pr \approx 1$, it is well known that the important dimensionless groups which would arise are F, Re, M, $\omega D/U$, Da_1, and Da_2. Variation of the four parameters F, U, D, and S_L allows an independent variation of η_{ta} and $\omega_c D/U$ with respect to Re, M, F and Da_1. Consequently the results of Table 1 may be cast into the following dimensionless form:

Thermoacoustic Efficiency

$$\eta_{ta} = 5.48 \times 10^{-7}\ Da_1^{.92}\ Re^{-.14}\ F^{-1.4}\ M^{2.72}\ f_1(Da_2) \qquad (1)$$

Frequency of Maximum Radiated Power

$$\omega_c D/U = 1.91 \times 10^{-5}\ Da_1^{.44}\ Re^{.43}\ F^{-1.21}\ M^{-.82} f_2(Da_2) \qquad (2)$$

Turbulent Flame Speed

$$S_T/U = 7.23 \times 10^{-3}\ Da_1^{.50} M^{-.26}\ f_3(Da_2) \qquad (3)$$

Since Da_2 was not varied, but is quite constant for hydrocarbon-air flames, all that may be said is that $f_1(149) \approx f_2(149) \approx f_3(149) = 1$.

For low Mach number tests, as these were, one would expect only a weak M dependence for S_T, as is confirmed by Equation (3). This same expectation would hold for $\omega_c D/U$, but this is not confirmed by Equation (2).

Notice that, since the speed of sound will quite naturally enter any acoustic power computation, there is no expectation that Equation (1) will be independent of M, as it is not. This will be theoretically confirmed later.

The reason for including the S_T and V_c correlations is that the acoustic power and frequency scaling laws deduced theoretically require knowledge of the flame geometry and its variation with other flow, chemistry and geometrical parameters. For example,

$$V_c = S_f \ell_f \approx \frac{5}{2} D L_f \ell_f \approx D^2 \frac{U}{S_T} \ell_f \frac{\pi}{4} \tag{4}$$

which allows L_f to be determined from the S_T correlation and ℓ_f to be determined from the S_T and V_c correlations. Equation (4) defines the mean flame thickness, ℓ_f. The factor 5/2 in the second of Equations (4) is obtained by a best fit to the geometrical data of Reference 11, and since S_T was defined in Reference 11 as $S_T = U \pi \frac{D^2}{4 S_f}$ it follows that $L_f \approx \frac{\pi}{10} D \frac{U}{S_T}$.

In order to obtain an idea of the numerical magnitudes of various mean flow, chemistry and turbulence parameters a typical run is chosen which yields quantities close to mean values of all quantities investigated. This run is as follows

Ethylene-air at $\phi = 0.8$

$p_o = 1$ atm $\qquad T_o = 59^\circ F$

$U = 300$ ft/sec $\qquad D = 0.05433$ ft

For this case the following properties may be computed:[12,1]

$c_o = 1117$ ft/sec $\quad \rho_o = 0.0765$ lb/ft^3 $\quad F = 0.0349$

$\alpha_o \approx \nu_o = 1.564 \times 10^{-4}$ ft^2/sec $\quad S_L = 1.693$ ft/sec

$d_L \approx \alpha_o / S_L = 9.24 \times 10^{-5}$ ft $\quad P = 0.0393$ watts

$Re = 1.042 \times 10^5$ $\quad M = 0.269$ $\quad Da_1 = 3.32$

$\eta_{ta} = 5.36 \times 10^{-7}$ $\quad f_c = 495$ Hz $\quad \omega_c = 3110$ sec^{-1}

From Equation (4) and the flame volume correlation of Table 1 the following geometrical parameters may be computed:

$S_T = 5.562$ ft/sec $\quad S_f = 0.1250$ ft^2

$L_f = 0.921$ ft $\quad \ell_f = 0.0781$ ft

$V_c = 9.77 \times 10^{-3}$ ft^3

Using formulas for isotropic turbulence[13] for the nearly isotropic core of the pipe flow, it is found that at the pipe exit plane

$u' \approx 12$ ft/sec $\quad \ell_e \approx 0.3D = 0.0163$ ft

$\varepsilon \approx u'^3/\ell_e = 1.060 \times 10^5$ ft^2/sec^3 $\quad \ell_m = (\alpha_o^3/\varepsilon)^{\frac{1}{4}} = 7.75 \times 10^{-5}$ ft

$\lambda_g = \sqrt{\frac{\ell_e}{u'}}\, 15\alpha_o = 1.785 \times 10^{-3}$ ft

Comparison of the values ℓ_m and d_L shows that the thickness of a laminar flame is comparable to the Kolmogoroff microscale and comparison of ℓ_f and ℓ_e shows that the turbulent flame thickness is of the order of 5 integral scales. In the following development only u' and ℓ_e will be used in any detail. The magnitudes of ℓ_m and λ_g are presented here so that the reader may make mental comparisons for many of the following conclusions.

Using the above data to compute several different frequencies shows that only one process corresponds to a frequency commensurate with the observed f_c. This is the frequency of macroscopic mixing

$$f_e \equiv u'/\ell_e = 736^{-1} \approx f_c$$

For example, the chemical frequency $f_{chem} \equiv S_L^2/\alpha_o = 1.833 \times 10^4$ sec^{-1} is far too high to be considered representative of a process important in combustion noise. One is led therefore to a possible interpretation of combustion noise based upon inhomogeneities caused by the turbulent mixing process at the size scale represented by the energy containing eddies. Following this interpretation, it will be determined whether or not the observed scaling laws may be recovered theoretically. It shall be noted here that upon a cursory glance f_e above would normally have no apparent dependence upon F or S_L, as is indicated for f_c in Table 1. However, such a dependence does exist and it is explained later.

Theory of Combustion Noise

It has recently been rather conclusively demonstrated[9] that the far field sound pressure is related to the volume average of the time derivative of the heat release rate. This has also been shown theoretically, but by a rather tortuous argument.[3,4] A simpler method has been discovered to present this argument and it will be given here. In the configuration of Figure 1 the surface S_1 is drawn exterior to the combustion region and shear layer except that it cuts across the hot shear layer downstream of the flame tip. For frequencies whose wavelengths are long compared to a typical dimension of the volume enclosed by S_1 so that one is in the hydrodynamic field (acoustic near field) the solution to the wave equation for the far field acoustic pressure is[14]

$$p'(\underset{\rightarrow}{r},t) = \frac{1}{4\pi r} \int_{S_1} \left.\frac{\partial p'}{\partial n_o}\right|_{\underset{\rightarrow}{r}_o,\ t-\frac{r}{c_o}} dS(\underset{\rightarrow}{r}_o)$$

$$= -\frac{\rho_o}{4\pi r} \int_{S_1} \left.\frac{\partial \underset{\rightarrow}{v}'}{\partial t}\right|_{\underset{\rightarrow}{r}_o,\ t-\frac{r}{c_o}} \cdot \underset{\rightarrow}{n}_o\, dS(\underset{\rightarrow}{r}_o) \qquad (5)$$

Equation (5) represents an equivalent monopole source as is known to be characteristic of combustion noise. Other than the frequency restriction, which is experimentally valid, three assumptions have been made in deriving Equation (5). The first is that $c = c_o$ everywhere; while this is valid outside the shear layer, it is not valid as S_1 crosses the shear layer. However, this is a refraction effect which is small at low frequencies.[1,15] The second assumption is that $\rho = \rho_o$ everywhere on S_1. This approximation is necessary for simplicity and the error introduced can only be determined by comparison with experiment. The third assumption is that the Mach number is small everywhere and this is clearly justified. Now it has previously been shown[4] that in the near field

$$\int_{S_1} \frac{\partial \underset{\rightarrow}{v}'}{\partial t} \cdot \underset{\rightarrow}{n}_o\, dS(\underset{\rightarrow}{r}_o) = \frac{\gamma - 1}{\gamma p_o} H \int_{V_c} \frac{\partial w}{\partial t}\, dV(\underset{\rightarrow}{r}_o) \qquad (6)$$

which directly links the far field pressure in Equation (5) to the time derivative of the heat release rate as is experimentally known.[7,8,9] Equations (5) and (6) have an interesting physical interpretation which runs somewhat counter to physical intuition. That is, it is implied that if there were no heat release fluctuation in the total flame there would be no noise; a 100% efficient flame would not be noisy. In any event there is

strong experimental evidence for the validity of Equations (5) and (6) and they yield a rather direct interpretation of combustion noise.

In Reference 4 the volume integral of Equation (6) was estimated by several turbulent flame theories, but the scaling laws obtained for acoustic power radiated were not in close agreement with experiment.[1] The difficulty is believed to lie in the fact that quantities do not behave smoothly within V_c. That is, chemical reactions and diffusive preparation processes must take place on a molecular scale or on the scale of turbulence of the order of the Kolmogoroff microscale, which is of the order of 10^{-3} times the turbulent flame "thickness," as seen above. Estimates made of the volume integral must properly account for this disparity between the relevant scales and apparently it was not done correctly in Reference 4. The surface integral of Equations (5) and (6) may be more easily estimated, however, in the light of the observation that u'/ℓ_e appears to be the dominant frequency. The fluctuations of reaction rate appear to be caused by the large scale turbulent motions which cause variable mixture ratios and temperature. These variations become smoothed over ℓ_e downstream of the reaction region where the bulk of the reactants have indeed reacted. Velocity fluctuations on S_1, however, are caused by different parcels of fluid having been heated differently, according to Equation (6).

Accepting this explanation, it remains to estimate the acoustic power. Since

$$P = \frac{\langle p'^2 \rangle}{\rho_o c_o} 4\pi r^2 ,$$

$$P = \frac{\rho_o}{4\pi c_o} \left\langle \left[\int_{S_1} \frac{\partial \underline{v}'}{\partial t} \cdot \underline{n}_o \, dS(\underline{r}_o) \right]^2 \right\rangle \qquad (7)$$

Equation (7) has the following order of magnitude, estimated in the same manner as in References 16, 3 and 4

$$P \text{ is } O\left[\frac{\rho_o}{4\pi c_o} S_{cor} S_f u'^2 \omega_c^2 \right] \tag{8}$$

which presumes S_1 is driven toward S_f and u' is the velocity fluctuation normal to the flame front downstream of the flame. Accepting that total heating fluctuations are driving u', the fluctuation should be proportional to the normal velocity change in the steady state. That is

$$u' \propto \frac{\rho_o S_T}{\rho_1} \approx \frac{FHS_T}{c_p T_o} \tag{9}$$

ω_c has already been estimated as u'/ℓ_e and the correlation area, S_{cor}, must be taken as approximately ℓ_e^2 in accordance with the statement that the integral scale is causing the nonuniformities. Introducing these estimates and Equation (9) into Equation (8), and introducing a constant of proportionality, K_η,

$$\eta_{ta} \equiv \frac{P}{\rho_o U \frac{\pi D^2}{4} FH} = K_\eta \frac{1}{4\pi} \left(\frac{4S_f}{\pi D^2}\right) Da_2^2 F \frac{S_T^2 u'^2}{c_o HU} \tag{10}$$

It is now to be determined whether or not Equation (10) recovers the scaling laws of Table 1 and Equation (1).

Generation of the Scaling Laws

Before proceeding further with Equation (10) it is necessary to observe that L_f is sufficiently long that a substantial decay may take

place in the turbulence of the reacting core before the flame tip is reached. Since it is known[1,3] that the majority of the noise is produced near the flame tip it is most appropriate to estimate u' in Equation (10) as the value at the tip rather than at the burner exit plane. The formulas used are those of Reference 17 which are

$$u'_{FT} = \frac{u'_{BE}}{f^{\frac{1}{2}}} \qquad \ell_{e_{FT}} = \ell_{e_{BE}} f^{\frac{1}{2}}$$

$$f = p + 1$$

$$p = \frac{10\alpha_o L_f}{U_{g_{BE}}^2} \tag{11}$$

It is desired to put f in the form of a power law so that the scaling laws of Equation (10) will turn out in such a form. Letting $f = \alpha p^n$ and finding α and n such that f and df/dp match the data for the sample case above it is found that

$$n = 0.601 \qquad \alpha = 1.959$$

Then since $u'_{BE} \propto U$ and $\ell_{e_{BE}} \propto D$, it is found that

$$u'_{FT}/U = 0.01904 \frac{Da_1^{0.1502}}{M^{0.0781}}$$

$$\ell_{e_{FT}}/D = 0.630 \frac{M^{0.0781}}{Da_1^{0.1502}} \tag{12}$$

Combination of Equations (4), (10), (11) and (12) finally yields

$$\eta_{ta} = K_\eta(8.34 \times 10^{-8})\ Da_1^{0.800}\ Re^0\ F\ M^{2.584}\ Da_2\ f_3(Da_2) \tag{13}$$

Equation (13) is to be compared with Equation (1) and the agreement is considered remarkable. The behavior with Da_1, Re and M is predicted almost exactly; the behavior with respect to F is the primary deficiency, and an indication is given of the behavior with respect to Da_2 for which there is no experimental information. If the orders of magnitude of the various quantities have been correctly predicted there is the expectation that K_η should be a constant of order unity. Checking this by placing in the sample case numbers for F, Re, and Da_2, Equation (1) yields

$$\eta_{ta} = 6.33 \times 10^{-6}\ Da_1^{0.92} M^{2.72}$$

while Equation (13) yields

$$\eta_{ta} = K_\eta(6.82 \times 10^{-7})\ Da_1^{0.800}\ M^{2.584}$$

which yields a K_η with an order of magnitude of ten. This is considered quite close to the expected magnitude considering the rough estimates involved.

A final check on the validity of the approach is to check the frequency scaling law. From Equation (12)

$$\frac{f_c D}{U} = 0.0302\ \frac{Da_1^{0.300}}{M^{0.156}} \tag{14}$$

or

$$f_c \propto U^{0.54}\ S_L^{0.60}\ D^{-.70} \tag{15}$$

Comparing Equation (15) with Table 1 it is seen that the theoretical equation predicts the proper trends but is deficient with respect to the D and F scaling. It should be noted in the empirical formula that the very weak D dependence and the experimental range of 2.74:1 for the D variation does not place the f_c variation with D outside the standard deviation of the experiments. For this reason the empirical exponent on D of -0.13 is suspect. Further experiments are in order at larger sizes to check this point.

The deficiency of Equation (15) with respect to F indicates that something has been left out. Assume for the moment that the theoretical estimate for f_c is modified to account for the observed F dependence in the following manner:

$$f_c \propto \frac{u'_{FT}}{\ell_{e_{FT}} F^{-1.21}}$$

Placing this estimate in the developments leading to Equation (13) yields

$$\eta_{ta} \propto Da_1^{0.800}\ Re^{0}\ F^{-0.42}\ M^{2.584}$$

which is in almost exact agreement with Equation (1). While the strong F dependence of V_c implies through Equation (4) a strong F dependence of ℓ_f and consequently of ℓ_e, the above agreement cannot imply that $\ell_{e_{FT}} \propto F^{-1.21}$ because ℓ_e cancels out of Equation (8) as seen in Equation (10). Consequently, the only apparent way to rationalize the above result is to set $u'_{FT} \propto F^{-1.21}$. There appears no physical explanation for this result and it must be accepted as a deficiency of the theory.

If one computes the ratios $u'_{FT}/\lambda_{g_{FT}}$, $S_T/\ell_{e_{FT}}$ and $S_T/\lambda_{g_{FT}}$ one finds that they are not far removed from the numerical magnitudes observed for f_c. Furthermore, the scaling laws for frequency are at least as good as that of Equation (15). They are, however, not accepted as theoretical estimates for f_c because a) the η_{ta} equation which is produced is not as accurate as Equation (13) and b) the physical basis for using them is not as clear as when using u'/ℓ_e.

Concluding Remarks

It appears that the noise generation process from open premixed turbulent flames may be theoretically explained by downstream velocity fluctuations caused by a fluctuating heat release which is in turn caused by large scale fluctuations in the turbulence. Even this simple flame type yields rather complex scaling laws because of the distortion of the flame shape with a change in variables and the recognition that there is a substantial decay of the turbulence in traversing the distance from the burner exit to the flame tip. Empirical correlations of the turbulent flame speed and flame geometry together with theoretical acoustics and the decay behavior of isotropic turbulence have produced acoustic power and frequency scaling laws which are in close agreement with experiment. It now appears possible to use the theory with confidence to investigate other flame types for which little experimental information is available on the noise generation characteristics.

The scaling laws generated theoretically are especially satisfactory with respect to variations of Reynolds and Mach numbers and Damköhler's first similarity group. Variations with respect to Damköhler's second similarity

group have not been experimentally investigated but the theory gives an indication of the variation of acoustic power with this parameter. There are some uncertainties in the behavior of frequency and acoustic power with variations in F. Presumably more information on the turbulence structure downstream of the flame is required to resolve this uncertainty. Finally, further experiments are in order on the behavior of frequency when diameter is varied, since it has not been varied over a wide enough range to have confidence in the empirical scaling law. Experiments are currently underway in this area.

Nomenclature

c	speed of sound
c_p	specific heat at constant pressure
d_L	laminar flame thickness
D	burner diameter
Da_1	Damköhler's first similarity group, calculated by $S_L^2 D/U\alpha_o$
Da_2	Damköhler's second similarity group, $H/c_p T_o$
f	function defined by Equations (11)
f_1, f_2, f_3	undetermined functions of Da_2
f_c	frequency of maximum radiated acoustic power (Hz)
F	fuel mass fraction
H	fuel heating value
ℓ_e	integral scale of turbulence
Le	Lewis number
L_f	turbulent flame length
ℓ_f	average turbulent flame thickness

ℓ_m	Kolmogoroff microscale of turbulence
M	Mach number
$\underset{\rightarrow}{n}_o$	unit normal vector
p	function defined by Equation (11)
p	pressure
P	acoustic power
Pr	Prandtl number
r	distance from origin
Re	Reynolds number based on U and D
S_L	laminar flame speed
S_T	turbulent flame speed
S_f	mean turbulent flame area
S_1	control surface bounding the flame
S_{cor}	correlation area
t	time
T	temperature
u'	rms turbulence intensity
U	flow velocity
U'	mean estimate of the magnitude of $\underset{\rightarrow}{v}'$
$\underset{\rightarrow}{v}'$	fluctuating velocity vector
V_c	volume of region of reaction
w	fuel disappearance rate, mass per unit volume per unit time
α	thermal diffusivity
γ	ratio of specific heats
ϵ	turbulence dissipation
ρ	density

η_{ta} thermoacoustic efficiency, $P/\rho_o U \pi \frac{D^2}{4} F H$

ϕ equivalence ratio

ω circular frequency

ω_c circular frequency of maximum radiated acoustic power (rad/sec)

ν kinematic viscosity

λ_g Taylor microscale

$< >$ denotes a time average

Subscripts

o cold exterior conditions

1 conditions downstream of the flame

BE burner exit

FT flame tip

Acknowledgments

This work was supported by the Air Force Office of Scientific Research and the National Science Foundation under Grants AFOSR-72-2365 and GK 32544, respectively. This support is gratefully acknowledged.

References

1. SHIVASHANKARA, B. N.: AIAA Paper No. 73-1025 (1973).

2. SMITH, T. J. B. and KILHAM, J. S.: J. Acoust. Soc. Am. 35, 715 (1963).

3. STRAHLE, W. C.: J. Fluid Mech. 49, 399 (1971).

4. STRAHLE, W. C.: J. Sound Vib. 23, 113 (1972).

5. CHIU, H. H. and SUMMERFIELD, M.: Theory of Combustion Noise, Paper presented at 4th International Colloquium on Gasdynamics of Explosions and Reactive Systems, San Diego (1973).

6. STRAHLE, W. C.: AIAA Paper No. 73-1023 (1973).

7. HURLE, I. R., PRICE, R. B., SUGDEN, T. M. and THOMAS, A.: Proc. Roy. Soc. (London) A303, 409 (1968).

8. PRICE, R. B., HURLE, I. R. and SUGDEN, T. M.: Twelfth Symposium (International) on Combustion, p. 1093, The Combustion Institute, 1969.

9. SHIVASHANKARA, B. N., STRAHLE, W. C. and HANDLEY, J. C.: AIAA Paper No. 74-47 (1974).

10. SHIVASHANKARA, B. N., STRAHLE, W. C. and HANDLEY, J. C.: Decomposition of Combustion Noise Scaling Rules by Direct Flame Photography, Paper presented at 4th International Colloquium on Gasdynamics of Explosions and Reactive Systems, San Diego (1973).

11. BOLLINGER, L. M. and WILLIAMS, D. T.: Effect of Reynolds Number in the Turbulent Flow Range on Flame Speeds of Bunsen Burner Flames, NACA TN 1707, 1948.

12. Basic Considerations in the Combustion of Hydrocarbon Fuels with Air, NACA Report No. 1300 (1957).

13. HINZE, J. O.: Turbulence, p. 184, McGraw-Hill (1959).

14. CURLE, N.: Proc. Roy. Soc. A231, 505 (1955).

15. STRAHLE, W. C.: Fourteenth Symposium (International) on Combustion.

16. LIGHTHILL, M. J.: Proc. Roy. Soc. (London) A211, 564 (1952).

17. HINZE, J. O.: Turbulence, p. 211, McGraw-Hill (1959).

List of Captions

Figure 1. Geometry and coordinate system for open turbulent flames anchored on burner tubes.

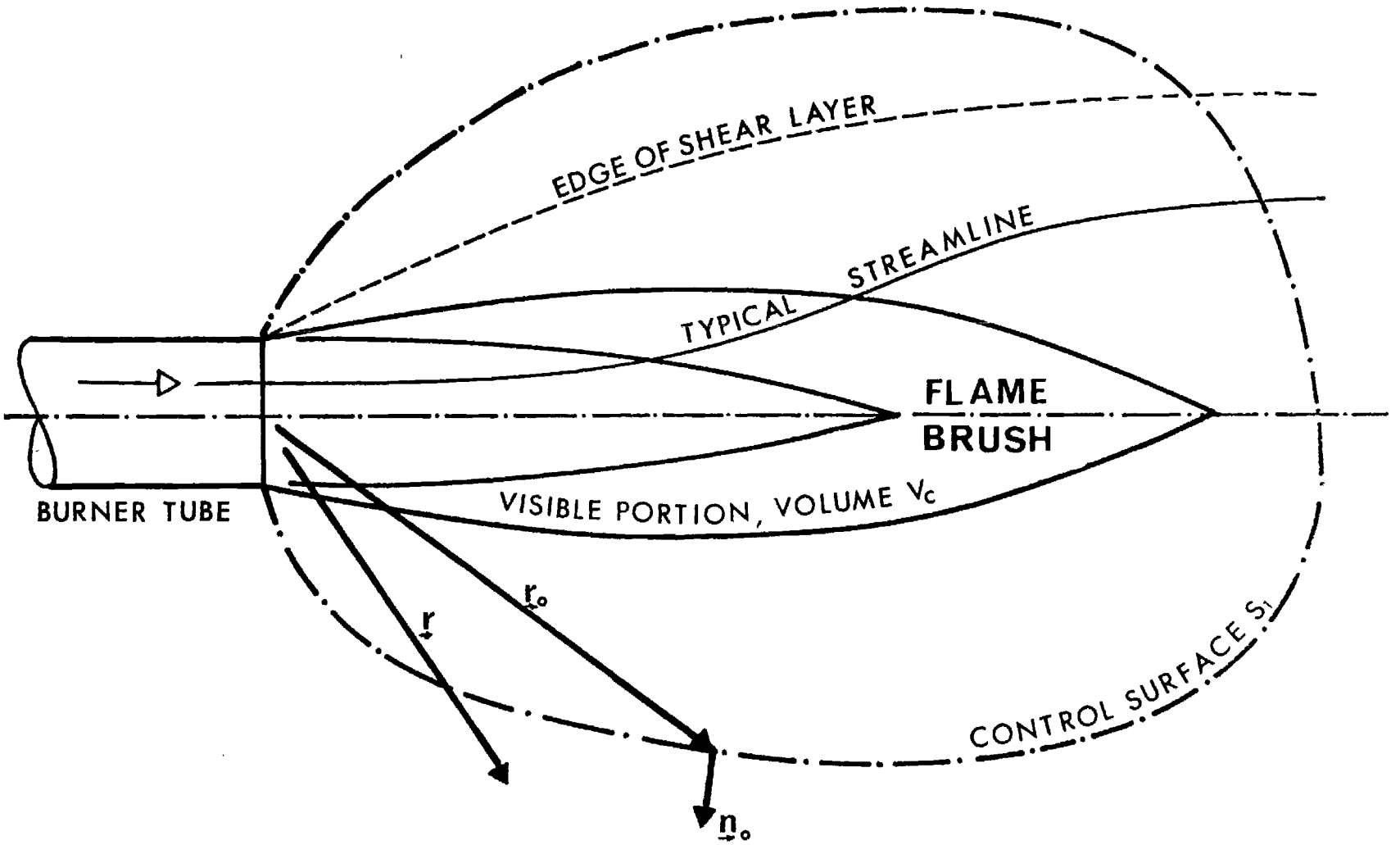
EDGE OF SHEAR LAYER
STREAMLINE
TYPICAL
FLAME
BRUSH
BURNER TUBE
VISIBLE PORTION, VOLUME V_c
r_o
r
CONTROL SURFACE S_1
n_o

REPORT DOCUMENTATION PAGE

READ INSTRUCTIONS BEFORE COMPLETING FORM

1. REPORT NUMBER: AFOSR-TR-74-1438
2. GOVT ACCESSION NO.:
3. RECIPIENT'S CATALOG NUMBER:

4. TITLE *(and Subtitle)*: COMBUSTION GENERATED NOISE IN TURBOPROPULSION SYSTEMS

5. TYPE OF REPORT & PERIOD COVERED: INTERIM Jun 1973 - May 1974

6. PERFORMING ORG. REPORT NUMBER:

7. AUTHOR(s): W C STRAHLE, M MUTHUKRISHNAN, B N SHIVASHANKARA, J C HANDLEY

8. CONTRACT OR GRANT NUMBER(s): AFOSR-72-2365

9. PERFORMING ORGANIZATION NAME AND ADDRESS: GEORGIA INSTITUTE OF TECHNOLOGY, SCHOOL OF AEROSPACE ENGINEERING, ATLANTA, GEORGIA 30332

10. PROGRAM ELEMENT, PROJECT, TASK AREA & WORK UNIT NUMBERS: 681308, 9711-02, 61102F

11. CONTROLLING OFFICE NAME AND ADDRESS: AIR FORCE OFFICE OF SCIENTIFIC RESEARCH/NA, 1400 WILSON BOULEVARD, ARLINGTON, VIRGINIA 22209

12. REPORT DATE: July 1974

13. NUMBER OF PAGES: 65

14. MONITORING AGENCY NAME & ADDRESS *(if different from Controlling Office)*:

15. SECURITY CLASS. *(of this report)*: UNCLASSIFIED

15a. DECLASSIFICATION/DOWNGRADING SCHEDULE:

16. DISTRIBUTION STATEMENT *(of this Report)*

Approved for public release; distribution unlimited

17. DISTRIBUTION STATEMENT *(of the abstract entered in Block 20, if different from Report)*:

18. SUPPLEMENTARY NOTES:

19. KEY WORDS *(Continue on reverse side if necessary and identify by block number)*

COMBUSTION GENERATED NOISE
ENVIRONMENTAL POLLUTION
QUIET AIRCRAFT
TURBULENT COMBUSTION
NOISE SUPPRESSION

20. ABSTRACT *(Continue on reverse side if necessary and identify by block number)*

Continuation of experimental and theoretical work on the problem of combustion generated noise in turbopropulsion systems is presented. Tasks completed during the current period have been (a) experimental and theoretical correlation of noise power and spectra from open premixed flames of propane, propylene, ethylene and acetylene-air, (b) crosscorrelation of C_2 emission with the far field acoustic pressure, and (c) experimental and theoretical investigation of ducting effects upon the noise radiating capability of the flame. The noise radiation from simple flame types is now understood with sufficient theoretical

and experimental detail that estimates may be made for combustion noise in turbopropulsion systems. It is shown that the ducting of a flame changes primarily only the radiation impedance. Feedback effects of reflected waves upon the noise source may be neglected in noise work if the system is damped heavily enough to avoid combustion instability.

AFOSR FINAL TECHNICAL REPORT

AFOSR–TR–

COMBUSTION GENERATED NOISE IN TURBOPROPULSION SYSTEMS

prepared for

Air Force Office of Scientific Research

Aerospace Sciences Directorate

Arlington, Virginia

by

Warren C. Strahle

M. Muthukrishnan

John C. Handley

School of Aerospace Engineering

Georgia Institute of Technology

Atlanta, Georgia 30332

Approved for Public Release; distribution unlimited

Grant No. AFOSR–72–2365

July, 1975

REPORT DOCUMENTATION PAGE

READ INSTRUCTIONS BEFORE COMPLETING FORM

1. REPORT NUMBER

2. GOVT ACCESSION NO.

3. RECIPIENT'S CATALOG NUMBER

4. TITLE (and Subtitle)
COMBUSTION GENERATED NOISE IN TURBOPROPULSION SYSTEMS

5. TYPE OF REPORT & PERIOD COVERED
FINAL
June 1972 - May 1975

6. PERFORMING ORG. REPORT NUMBER

7. AUTHOR(s)
W C STRAHLE
M MUTHUKRISHNAN
J C HANDLEY

8. CONTRACT OR GRANT NUMBER(s)
AFOSR 72-2365

9. PERFORMING ORGANIZATION NAME AND ADDRESS
GEORGIA INSTITUTE OF TECHNOLOGY
SCHOOL OF AEROSPACE ENGINEERING
ATLANTA, GEORGIA 30332

10. PROGRAM ELEMENT, PROJECT, TASK AREA & WORK UNIT NUMBERS
681308
9711-02
61102F

11. CONTROLLING OFFICE NAME AND ADDRESS
AIR FORCE OFFICE OF SCIENTIFIC RESEARCH/NA
1400 WILSON BOULEVARD
ARLINGTON, VIRGINIA 22209

12. REPORT DATE
July 1975

13. NUMBER OF PAGES
61

14. MONITORING AGENCY NAME & ADDRESS(if different from Controlling Office)

15. SECURITY CLASS. (of this report)
UNCLASSIFIED

15a. DECLASSIFICATION/DOWNGRADING SCHEDULE

16. DISTRIBUTION STATEMENT (of this Report)

Approved for public release; distribution unlimited.

17. DISTRIBUTION STATEMENT (of the abstract entered in Block 20, if different from Report)

18. SUPPLEMENTARY NOTES

19. KEY WORDS (Continue on reverse side if necessary and identify by block number)
COMBUSTION GENERATED NOISE
ENVIORNMENTAL POLLUTION
QUIET AIRCRAFT
TURBULENT COMBUSTION
NOISE SUPPRESSION

20. ABSTRACT (Continue on reverse side if necessary and identify by block number)
The results are presented of a three year program investigating direct combustion noise in hydrocarbon-air flames. Tasks completed during the final year of the program have been a) the use of an exterior facility to investigate the noise from a large, 2 inch diameter burner and b) the use of the anechoic facility to test flames stabilized by bluff body flameholders. Emphasis in the program has been on premixed, fuel lean turbulent flames using ethylene, acetylene, propane and propylene fuels with air as the oxidizer. Conclusions of practical interest are a) combustion noise can be an important contributor to the overall noise

problem from turbopropulsion systems if the system extracts high shaft power b) it is not important to the noise problem from afterburning turbopropulsion systems, c) if the noise output of a particular combustor type is known in one installation, valid predictions may be made for the noise output of the same type of combustor in a different installation and d) combustion noise may be a contributor to the afterburner instability problem.

AFOSR Final Technical Report

AFOSR-TR-

Combustion Generated Noise in Turbopropulsion Systems

prepared for

Air Force Office of Scientific Research
Aerospace Sciences Directorate
Arlington, Virginia

by

Warren C. Strahle
M. Muthukrishnan
John C. Handley

School of Aerospace Engineering
Georgia Institute of Technology
Atlanta, Georgia 30332

Approved for Public Release; distribution unlimited

Grant No. AFOSR-72-2365 July, 1975

ABSTRACT

The results are presented of a three year program investigating direct combustion noise in hydrocarbon-air flames. Tasks completed during the final year of the program have been a) the use of an exterior facility to investigate the noise from a large, 2 inch diameter burner and b) the use of the anechoic facility to test flames stabilized by bluff body flameholders. Emphasis in the program has been on premixed, fuel lean turbulent flames using ethylene, acetylene, propane and propylene fuels with air as the oxidizer. Conclusions of practical interest are a) combustion noise can be an important contributor to the overall noise problem from turbopropulsion systems if the system extracts high shaft power b) it is not important to the noise problem from afterburning turbopropulsion systems, c) if the noise output of a particular combustor type is known in one installation, valid predictions may be made for the noise output of the same type of combustor in a different installation and d) combustion noise may be a contributor to the afterburner instability problem.

TABLE OF CONTENTS

CHAPTER I

Summary of Tasks

This three year program to investigate direct combustion noise (noise generated in and radiated from a region of active turbulent combustion) was made up of four major tasks. These were a) to investigate, correlate and understand the noise generation capability of open turbulent flames anchored on the end of burner tubes, b) to investigate the origin and existence of combustion noise by instantaneous CH and C_2 emission measurements, c) to determine the scaling predictability in installed configurations by enclosing the flames with reflecting surfaces and d) to investigate the effect of the flame stabilization method on the noise generated.

The first task investigated the fuels acetylene, propylene, propane and ethylene burning with air at 1 atmosphere. The flames were anchored on the ends of burner tubes of diameters 0.402, 0.652, 0.960 and 2.063 inches, and the flames were stabilized to velocities as high as 600 ft/sec by an annular hydrogen pilot/diffusion flame. Tests on the three smallest burners were conducted inside an anechoic chamber and the largest burner was tested in an exterior facility. Equivalence ratios between 0.6 and 1.3 were used. Sound measurements and information received were overall sound power, directionality and spectra. The test variables were airflow, fuel flow, fuel type and burner diameter. These variables were sufficient to obtain a correlation of the thermoacoustic efficiency (ratio of sound power to heat input rate) and Strouhal number of maximum spectral density as a function of the following four dimensionless groups: Reynolds number, fuel mass fraction, Mach number and Damköhler's first similarity group (ratio of flow time to chemical time). The data were explainable in terms of the senior author's theory of combustion noise. The

results of this task have been reported in Refs. (1) - (3) and in Appendix A of this report.

The second task investigated the relation between optical emission fluctuations and acoustic emissions from flames. Viewing the entire flame brush, the optical signal was filtered to let in only the emission from either C_2 or CH radiation. The instantaneous signal was differentiated in time and compared with the far field acoustic pressure trace. Crosscorrelation of the traces were prepared. The purpose was to show a direct correspondence between the fluctuation in the reaction rate in the flame and the emitted sound. This was to prove that the origin of the acoustic signal lies inside the flame. The data confirmed the expectations. The results of this task have been reported in Refs. (2) and (5).

The purpose of the third task was to investigate the effects of enclosing the flames of the first task. A right circular tube was placed about the smallest burner and the tube ends were provided with acoustic terminations (mufflers) that absorbed most of the incident sound. The overall noise and noise spectra interior to the tube were measured and compared with the results of the flame burning in the anechoic chamber. Theoretical acoustics were applied to the tube configuration assuming that there was a) no feedback between wall-reflected pressure waves and the flame and b) no modification of the combustion noise source strength as compared with the open flame source strength. The measured tube noise properties were found to closely correspond to the predicted values. This task showed that if the properties of the free flame noise generation characteristics were known then the enclosed flame noise properties could be computed if the enclosure acoustics were known. Furthermore, it was demonstrated that enclosure effects may be substantial in determining the overall acoustic power output from a flame. The results of this work have been presented in Refs. (2) and (6).

The fourth task was conducted to determine if the mechanism of flame stabilization had a substantial effect on the noise generated. The burner tubes had conical flameholders mounted at the mouth of the tube, so a free jet of fuel and air impacted the flameholder at the burner mouth. For the higher speed flames (> 100 ft/sec) it was also necessary to bleed hydrogen through the base of the flameholder to stabilize the flame. The flame shape was significantly altered over the comparable free flame. The sound power output and frequency content were also altered but in a manner consistent with theory, given the flame shape change as an input to the theory. The results of this work are reported in Appendix B of this report.

CHAPTER II

Summary of Accomplishments and Conclusions

1. This program has provided experimental data over the widest range of test parameters ever obtained for simple free jet turbulent flames. In extreme cases the thermoacoustic efficiency of such flames may be as high as 10^{-5}, with 10^{-6} a more reasonable number. With thermoacoustic efficiencies in this range combustion noise will dominate jet noise until jet velocities of the order of 600-800 ft/sec, a fact directly demonstrated in this program.
2. The broad band combustion noise, for the flame types investigated here, has a single peak in the spectral level and the frequency of this peak is dominated by the frequency of the energy containing eddies of the incoming flow. There is, however, observed a dependence upon the heat release in the flame which is not yet explainable. For hydrocarbon flames combustion noise is usually low frequency noise with the majority of sound power occurring at frequencies less than 1000 Hz.
3. Direct combustion noise exists. It is generated in and radiated from a region undergoing turbulent combustion. This has been proven directly by comparing instantaneous CH-C_2 emission data with the far field pressure trace.
4. Combustion noise power output depends upon the flame type, but, given a measurement at one operating condition, combustion noise is theoretically understood to allow scaling to another operating condition. The physical mechanism of combustion noise is a velocity fluctuation downstream of the reaction zone caused by differential heating of various elements as they pass through the flame. An effective monopole source results at low fre-

quencies.

5. In damped acoustical enclosures the effect of enclosing a flame on the resultant noise output can be calculated if the flame steady state aerodynamics are not altered by the enclosure. However, most practical installations do not have high acoustical damping so the effect of feedback between wall-reflected pressure waves and the flame may be important in actual installations (as is well known from combustion instability occurrences). An example of enclosure effects without feedback is included as Appendix C of this report which shows that combustion noise alone can cause rather large pressure fluctuations in a combustion chamber with reasonably hard walls.

6. A priori prediction of combustion noise and a full understanding of the frequency content of combustion noise must await substantial progress in turbulent flame theory. Currently, however, scaling rules may be developed on a reasonable firm theoretical groundwork.

7. For afterburning turbojets or turbofans, combustion noise does not contribute to the overall noise problem because the jet velocity and consequent jet noise are too high. The jet velocity is substantially lower during taxi and ground operations and for turbopropulsion systems with high shaft power takeoff. For these systems and conditions, combustion noise should dominate jet noise. An important caveat, however, concerns the currently unknown behavior of the sound propagation process through the turbine and nozzle assembly; although the combustion process can dominate jet noise in sound power output, it is unknown if it can get out of the engine without significant attenuation.

References

1. Strahle, W.C., Shivashankara, B. N., and Handley, J.C., "Combustion Generated Noise in Turbopropulsion Systems, "AFOSR TR-73-1899, October, 1973.

2. Strahle, W.C., Shivashankara, B.N., Handley, J.C. and Muthukrishan, M., "Combustion Generated Noise in Turbopropulsion Systems, "AFOSR TR-74-1438, July, 1974.

3. Shivashankara, B.N., Strahle, W.C. and Handley, J.C., "Combustion Noise Radiation by Open Turbulent Flames, "Aeroacoustics: Jet and Combustion Noise; Duct Acoustics AIAA, New York, 1975, pp. 277-296.

4. Strahle, W.C., "The Convergence of Theory and Experiment in Direct Combustion Noise, "AIAA Paper No.75-522, 1975.

5. Shivashankara, B.N., Strahle, W.C. and Handley, J.C. "An Evaluation of Combustion Noise Scaling Laws by an Optical Technique," AIAA Paper No. 74-47, 1974.

6. Strahle, W.C. and Shivashankara, B.N., "Wall Reflection Effects in Combustion Generated Noise, " AIAA Paper No. 75-127, 1975.

7. Strahle, W.C. and Shivashankara, B.N., "A Rational Correlation of Combustion Noise Results from Open Premixed Turbulent Flames, "Fifteenth Symposium (International) on Combustion, The Combustion Instutute, Pittsburgh, 1975.

Appendix A

Results from the Large Burner Tests and Final Open Flame Data Analysis

In the open flame results of Ref. (7) there was some uncertainty regarding the dependence of frequency of maximum spectral level on the burner diameter. The variation of the frequency with diameter when diameter was varied from 0.402 in. to 0.960 in. was not outside the standard deviation of the results. Consequently, it was desired to increase the burner diameter further; however, this required tests out of doors in order to put the microphones in the far field. The facility used was built under NASA funding for combustor can tests and it was modified to receive a 2.063 in. diameter burner tube of construction identical to that described in Ref. (1). The burner tube and microphones are shown in Fig. A-1.

Six tests were conducted at a flow velocity of 200 ft/sec with either propane or ethylene and at equivalence ratios from 0.7 to 1.0. A typical spectrum is shown in Fig. A-2. There has been a noticeable shift in spectral content to low frequencies ($\approx$ 100 Hz) which was not that observeable in small burner tests but which was expected through theory.

Putting all tests of this program through the regression analysis of Ref. (1), the following results were obtained for the overall sound power output and frequency of maximum radiated power

$$P = 0.625 \times 10^{-5} U^{2.67} D^{2.81} S_L^{1.83} F^{-0.26} \text{ watts}$$

Number of tests = 68

Mean error = 6.4% Standard Deviation = 41.0% (A-1)

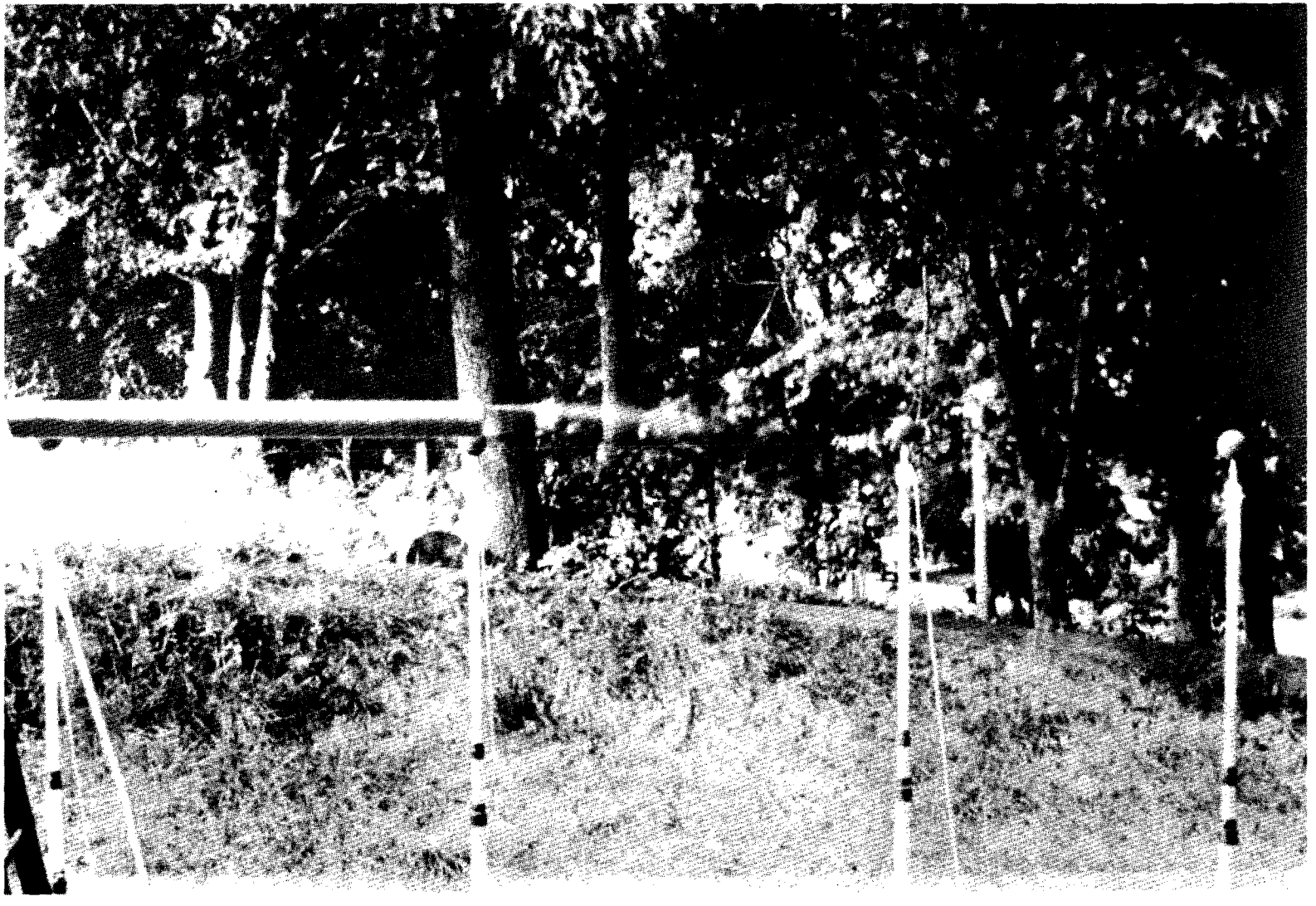

Figure A-1 Photograph of large burner in exterior facility with microphone in place.

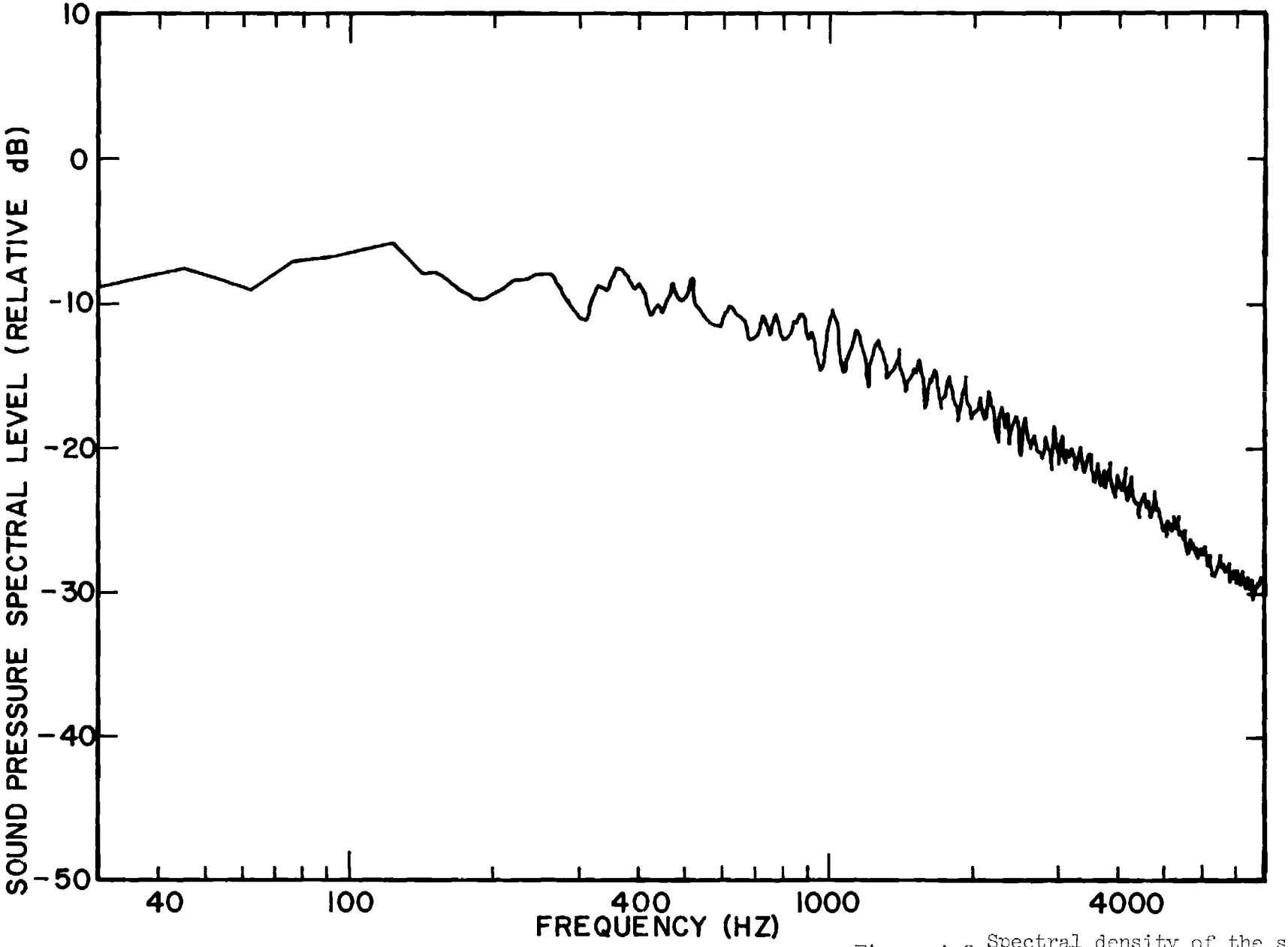

Figure A-2 Spectral density of the sound pressure for propane-air at a flow velocity of 200 ft/sec

$$f_c = 0.966\ U^{0.128}\ S_L^{0.784}\ F^{-1.09}\ D^{-.585}\ \text{Hz}$$

Number of tests = 67

Mean Error = 2.6% Standard Deviation 23.4% (A-2)

In the above P is acoustic power in watts, S_L the laminar flame speed in ft/sec, U the flow velocity in ft/sec, D the burner diameter in feet, F is the fuel mass fraction and f_c the frequency of maximum radiated power in Hz. The data have been generated for the following ranges of parameters: 0.402 inches $\leq$ D $\leq$ 2.063 inches, $0.6 \leq \phi \leq 1.0$ where ϕ is the equivalence ratio, and S_L has been varied independently of ϕ by using the fuels ethylene, acetylene, propane and propylane.

Using the methods of Ref. (7) the analytical prediction for the frequency is

$$f_c \propto U^{0.54}\ S_L^{0.60}\ D^{-.70}$$

where the fuel mass fraction does not enter theoretically because it has no influence on the upstream turbulence. Acknowledging that experimentally it does have an effect, probably because of density effects (which would imply a dependence on the fuel heating value which was not investigated in this program), the accepted form for f_c is

$$f_c \propto U^{0.54}\ S_L^{0.60}\ D^{-0.70}\ F^{-1.09} \qquad \text{(A-3)}$$

which is to be compared to Eq. (A-2).

The theoretical law for acoustic power, taken from Ref. (7) but including the empirical correction for the F-dependence of f_c is

$$P \propto U^{2.78}\ D^{2.80}\ S_L^{1.60}\ F^{-0.18} \qquad \text{(A-4)}$$

Eq. (A-4) is in remarkable agreement with Eq. (A-1) and the theory is therefore considered adequate for the generation of scaling laws.

The four variables investigated are sufficient to consider that four independent dimensionless groups have been varied. These are F itself, Damköhler's first similarity group (S_L^2 D/U α_o), Reynold's number (based on D) and Mach number. Eq. (A-1) may be cast in dimensionless form for the thermo-acoustic efficiency

$$\eta_{ta} = 3.20 \times 10^{-9} \, Re^{-.11} \, M^{2.69} \, F^{-1.26} \, Da_1^{0.92} \qquad \text{(A-5)}$$

Similarly, the frequency correlation of Eq. (A-2) may be cast in terms of a non-dimensional Strouhal number as

$$S \equiv \frac{f_c D}{U} = 7.45 \times 10^{-4} \, Da_1^{.39} \, Re^{.02} \, M^{-.50} \, F^{-1.09} \qquad \text{(A-6)}$$

To form the above dimensionless correlations the heating value assumed was 18,500 Btu/lb, the thermal diffusivity, α_o, was chosen as 1.564×10^{-4} ft^2/sec, the Prandtl number was taken as unity and the ambient density was taken as 0.0765 lb/ft^3.

Appendix B

The Effect of Flameholders on Combustion Generated Noise

The Effect of Flameholders on Combustion Generated Noise *

M. Muthukrishnan +

W. C. Strahle **

J. C. Handley ***

ABSTRACT

Experiments were conducted to study the noise characteristics of flames stabilized on bluff bodies by making far field sound pressure measurements in an anechoic chamber. Burners with internal diameters 0.402, 0.652 and 0.96 inches were used. Two cones with base diameters of 0.625 and 1 inches served the purpose of flameholders. Flow velocities were varied from 50 to 300 fps. Gaseous propane, ethylene and acetylene were used with air as the oxidizer all burning at 1 atmosphere in pressure. A hydrogen pilot flame, anchored at the flameholder base, was used to stabilize the combustible mixture at higher velocities. Detailed directionality distributions and spectral characteristics were obtained for this type of flame. Scaling laws for acoustic power radiated, frequency of maximum sound power (called the peak frequency) and surface area of the reaction gone were developed. The results show a weak directionality. Flow velocity, laminar flame speed, fuel mass fraction and burner diameter are found to be important correlating variables in the determination of various empirical relationships. Theoretical scaling laws were consistent with the empirical relationships obtained through experiments.

---

* This work was sponsored by the U.S. Air Force Office of Scientific Research under Grant Number AFOSR-72-2365. Dr. D. H. Neale also assisted in the experimentation on this program.

+ Graduate Research Assistant

** Regents' Professor

*** Research Engineer

NOMENCLATURE

a	speed of sound
B	maximum width of luminous zone in the flame
c_p	specific heat at constant pressure
C_2	correlation function defined by Eq. (3)
d	base diameter of flameholder
d_{cor}	correlation length scale
D	diameter of burner tube
Da_1	Damköhlers' first similarity group, calculated by $\frac{S_L^2 D}{U \alpha_o}$
Da_2	Damköhlers' second similarity group, $H/c_p T_o$
$f_1, f_2, f_3,$	undetermined functions of Da_2
f_c	frequency of maximum radiated power (Hz)
F	fuel mass fraction
H	heat of combustion
L	length of luminous zone in the flame
Le	Lewis number
$\dot{m}$	mass flow rate
M	Mach number
$\vec{n}, \vec{n}_o$	normal vectors
p	pressure
P	acoustic power
Pr	prandtl number
$\vec{r}$	distance from the origin
$\vec{r}_o$	coordinate vector
Re	Reynold's number
S_L	laminar flame speed
S_r	bounding area of reaction zone
S_T	turbulent flame speed

t	time
T	temperature or time interval
u'	rms turbulence intensity
U	flow velocity of reactants
V	velocity
α	thermal diffusivity
γ	ratio of specific heats
ρ	density
ω	circular frequency
ω_c	circular frequency of maximum radiated power
η_{ta}	thermo-acoustic efficiency
ϕ	equivalence ratio
$< >$	time average

Subscripts

0	cold exterior conditions
1	downstream of the flame

Superscripts

/	acoustic perturbation quantity
—	steady state quantity

INTRODUCTION

It is a common observation that flow systems become noisier once combustion is started in them. Hence, in practical situations like aircraft using turbopropulsion systems and in industrial furnaces combustion noise can contribute a significant amount to the overall noise output.

A review of combustion noise is presented in Ref. (1). Theoretical studies on combustion noise have been reported in Refs. 2-8.On the experimental front, the literature contains a majority of the experiments conducted on open premixed flames,[9,10,11] on open diffusion flames,[11,12,13] or industrial burners.[14,15] Most recently, Shivashankara et.al.[16] have conducted an extensive set of noise measurements of premixed flames anchored at the ends of burner tubes and radiating to a free field. They have reported on extensive data on the directionality patterns and acoustic spectra. Also, they have obtained unambiguous scaling laws for acoustic power radiated, frequency of maximum radiated power (called peak frequency) and reaction volume.

A question arose at this point whether or not the results of Ref. 16 are unique as far as open free flames are concerned. Stated otherwise, it was necessary to know the extent to which the method of flame retention would have influenced the noise characteristics of open free flames quoted in Ref. 16. With a view to clarify the above suspicion, a different method of flame stabilization is used in the present program. Hence, this paper discusses the experimental study carried out to investigate the noise characteristics of premixed flames stabilized through external conical flameholders. The flow velocity was varied from 50 to 300 fps. A simple burner configuration was chosen for rational interpretation of experimental results. Gaseous propane, ethylene and acetylene fuels have been used with air as the oxidise Conical flameholders of two sizes were employed to stabilize the flames.

EXPERIMENTAL APPARATUS

It is preferrable that all noise measurements should be made in free field surroundings. This ideal situation was achieved very closely by conducting the noise measurements described in this paper in an anechoic chamber which is 13 x 10 x $6\frac{1}{2}$ feet (working space) in size. The chamber has been tested for its anechoic quality and has been found satisfactory for a source to microphone distance of up to 5 feet and in the frequency range of 125 to 5000 Hz. For more details regarding this facility, the reader is referred to Ref. 17.

The burners used in the present experiments are 0.402, 0.652 and 0.96 inches in internal diameter. the conical flame holders employed have 0.625 and 1 inch diameter bases. The burners are assembled in the anechoic chamber with their axes horizontal at 3 feet above the floor and at least $2\frac{1}{2}$ feet from the walls.

Figure 1 shows the flow system. A 1000 ft^3, 125 psi air resevoir supplied air for the experiment . The fuels, hydrogen and nitrogen are supplied from gas bottles stored outside the anechoic chamber. The air flow is measured by rotameters whereas hydrogen and fuel flows are measured by orifice meters. The range of each meter was increased by using a control valve downstream of each flow meter. The flow noise has been reduced by introducing a muffler in the airline. The use of flexible rubber hoses between the muffler exit and burner entrance eliminated the flow noises, which otherwise would have been generated by abrupt flow turns.

The metered supply of fuel and air is mixed at a T-junction from whence the combustible mixture is led into the burner. A mixing chamber filled with 4mm diameter glass balls is provided in the burner tube just before 50 diameter straight lengths to ensure proper mixing of fuel and air.

Since the flames tend to blow off the flameholders at high velocities, the use of a pilot flame became essential. This pilot flame is established at the

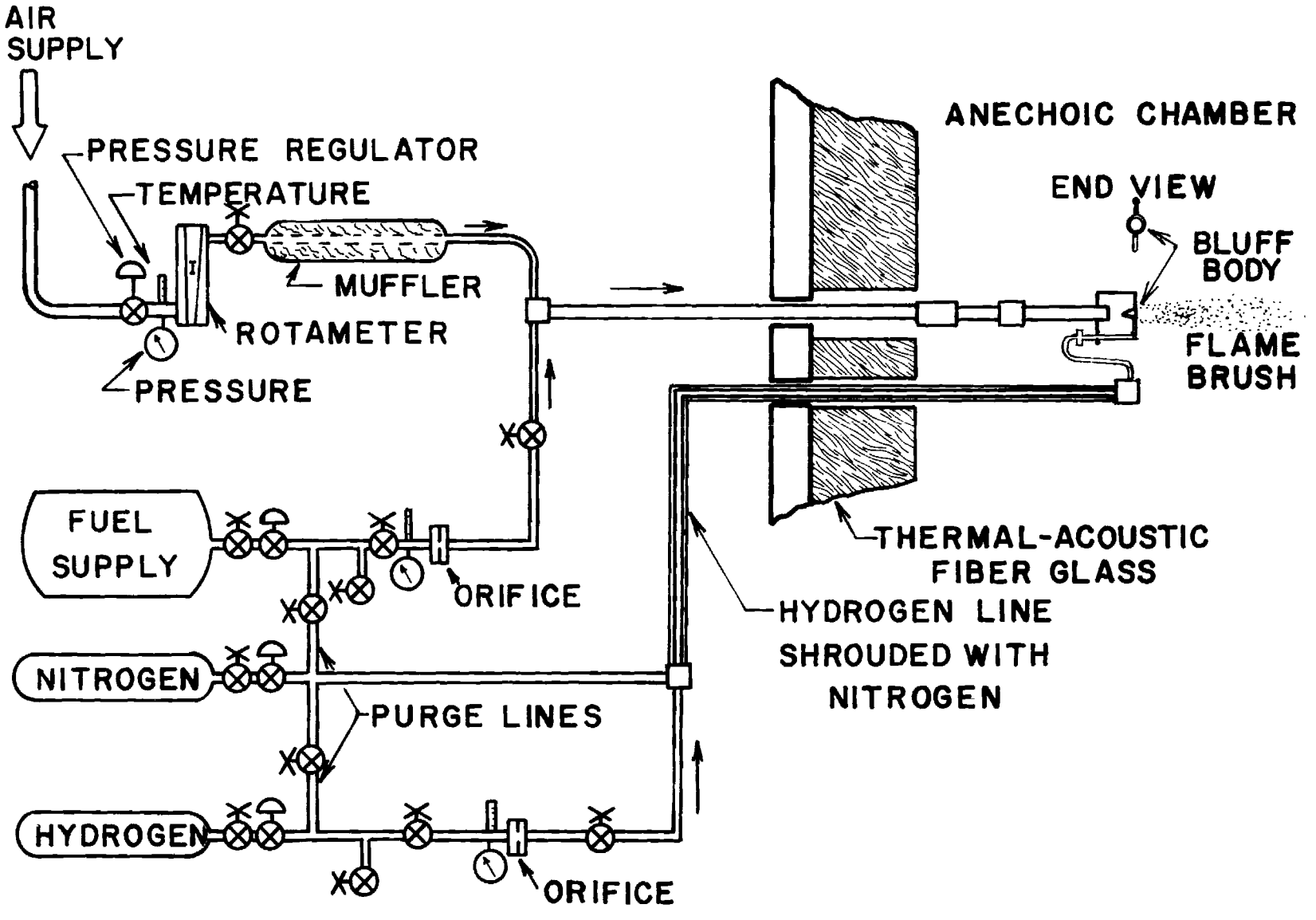

Figure 1. Flow System Schematic with Flameholder in Position.

base of conical flameholders by means of hydrogen. An enlarged view of the flameholder and hydrogen gas lines is shown in Figure 2. The hydrogen line entering the anechoic chamber is shrouded by nitrogen. Both the fuel and hydrogen lines are provided with a nitrogen purge.

The instrumentation used for the present investigation is the same as that described in Ref. 16. For the sake of completeness, however, it will be repeated here. Sound pressure levels are measured by Brüel and Kjaer type 4134 half-inch condenser microphones mounted on stands in the same horizontal plane as that of the burner. The microphones are placed at a constant radius with respect to the base of the flameholder and at angular locations between 15° and 120° to the flow direction. There is a likelihood of flow noise being introduced if microphones are located at positions closer than 15° to the flow direction. The output of the microphones is directly read out as sound pressure level on a Brüel and Kjaer type 2606 microphone amplifier, one at a time. They are also amplified by an array of five NEFF type 122 amplifiers and recorded on five channels of an AMPEX FR 1300, 14 channel magnetic tape recorder at a speed of 30 ips. A Whittaker type PC-125 acoustic calibratior was used for the direct calibration of microphones. A recording of the sound output on the tape from an acoustic driver, producing a 1000 Hz sound and located at the center of the microphones, served the purpose of calibration reference for data analysis.

The data acquisition and reduction schematic is shown in Figure 3. The apectral analysis of the noise is performed on a Hewlett Packard type 5645 Fourier analyser and associated instruments. A multi-sample averaging technique is used to obtain stable results and eliminate spurious noise from the signal. The output from the Fourier analyser is plotted on an x-y plotter.

A direct flame photography technique was developed to enable better understanding and analysis of combustion noise scaling laws. Its significance and development are discussed in the next section.

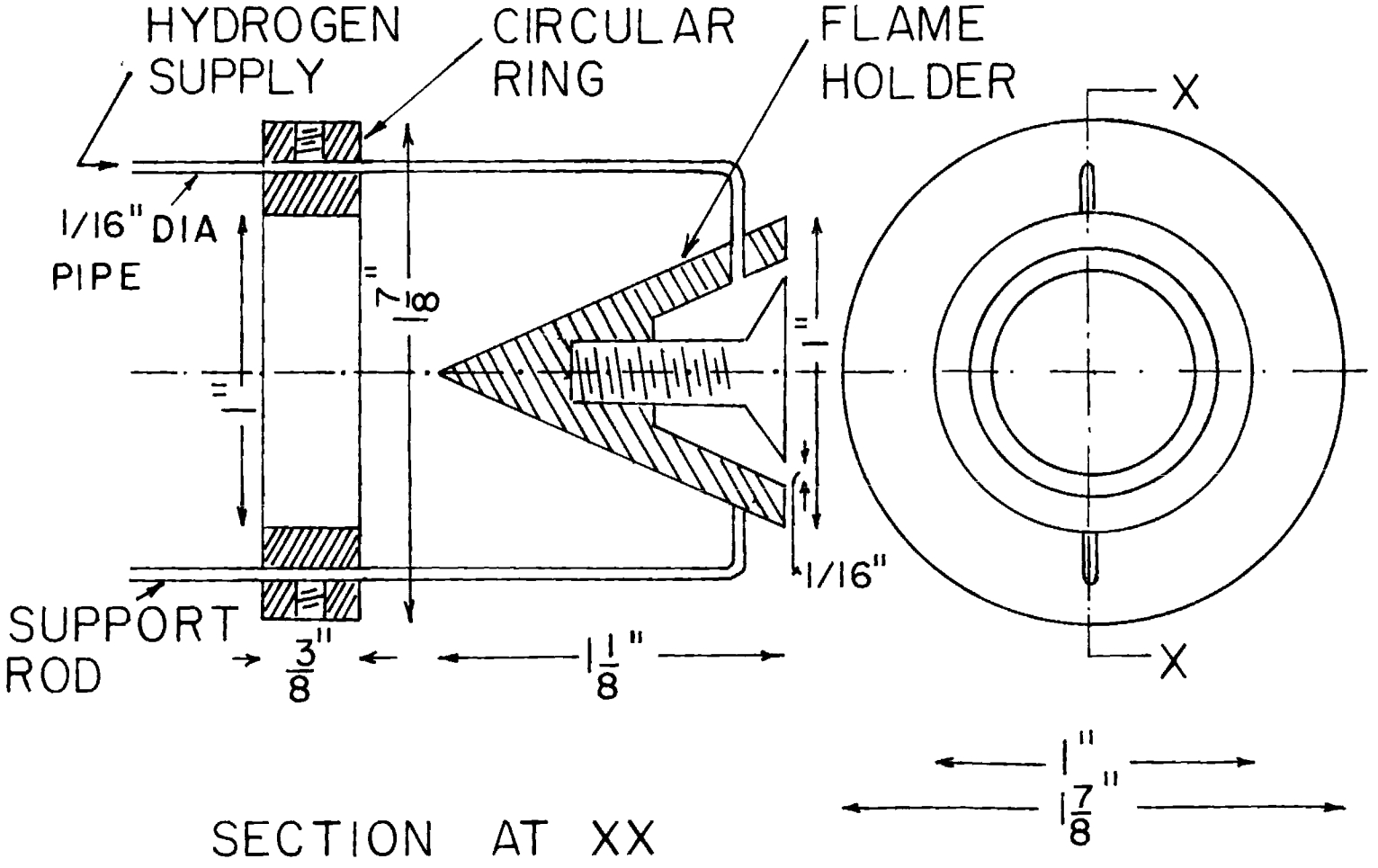

Figure 2. Flameholder Assembly.

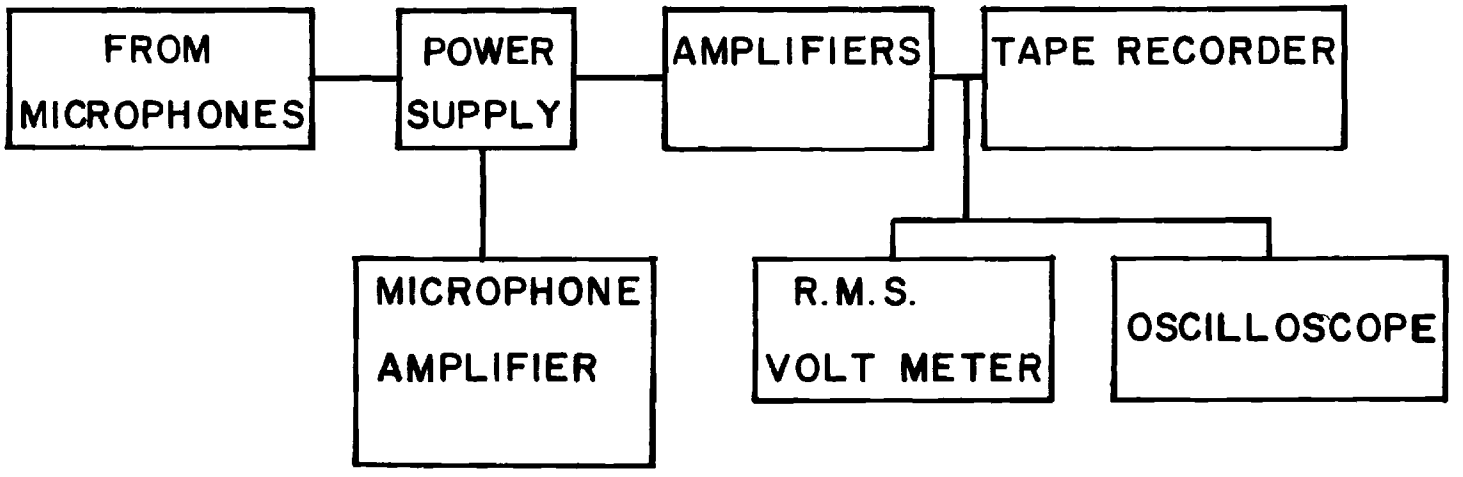

a. DATA ACQUISITION

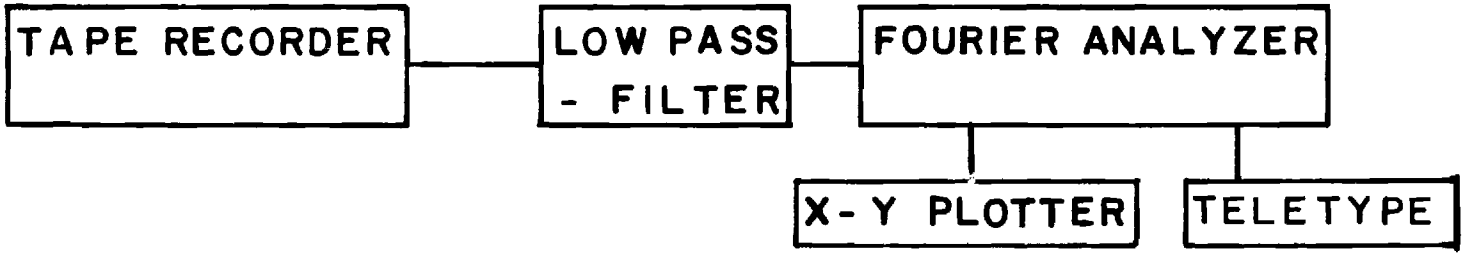

b. FREQUENCY ANALYSIS

Figure 3. Data Acquisition and Reduction Schematic for Acoustic Experiments.

EXPERIMENTAL PROCEDURE

The flames, at high velocity, were stabilized at the base of the flameholders by a diffusion flame of hydrogen. In all the present experiments, 2 to 3 percent of hydrogen by volume of main flow was found to be optimum. But for low velocity flames, below 100ft/sec, no pilot flame was necessary.

The sound pressure levels were indicated by a B & K type 2606 microphone amplifier, using 22.5 Hz to 22.5 KHz linear response with the meter adjusted to slow response. In most cases the meter oscillations were less than a dB and the arithmetic mean between maximum and minimum readings was taken as the sound pressure level.

The locations of the microphones were fixed with respect to the flameholder base and flow direction. But the computations of the acoustic power radiated and the directionality requires the measured sound pressures being referenced to the acoustic center in the flame. The acoustic center is a point within the noise generating region from which the noise would appear to originate to a far field observer. Figure 4 shows a plot of sound pressure level against axial distance at points close enough and parallel to the axis of the flameholder. It can be seen that the maximum overall noise level and, hence, the source of sound coincides with a position very near to the flameholder base. Since the shift of the origin from the flameholder base to the acoustic center leads to only a very minor change in the acoustic power radiated and directionality, the origin of measurements was retained as the flameholder base itself.

A polynomial relation,

$$p^2 = \frac{1}{r^2} \sum_{n=0}^{3} a_n \cos^n \theta \qquad (1)$$

suggested by the theory in Ref. 6, was fitted to the measured sound pressure levels by the method of least squares. The polynomial in cos θ was found to provide a very close fit to the data.

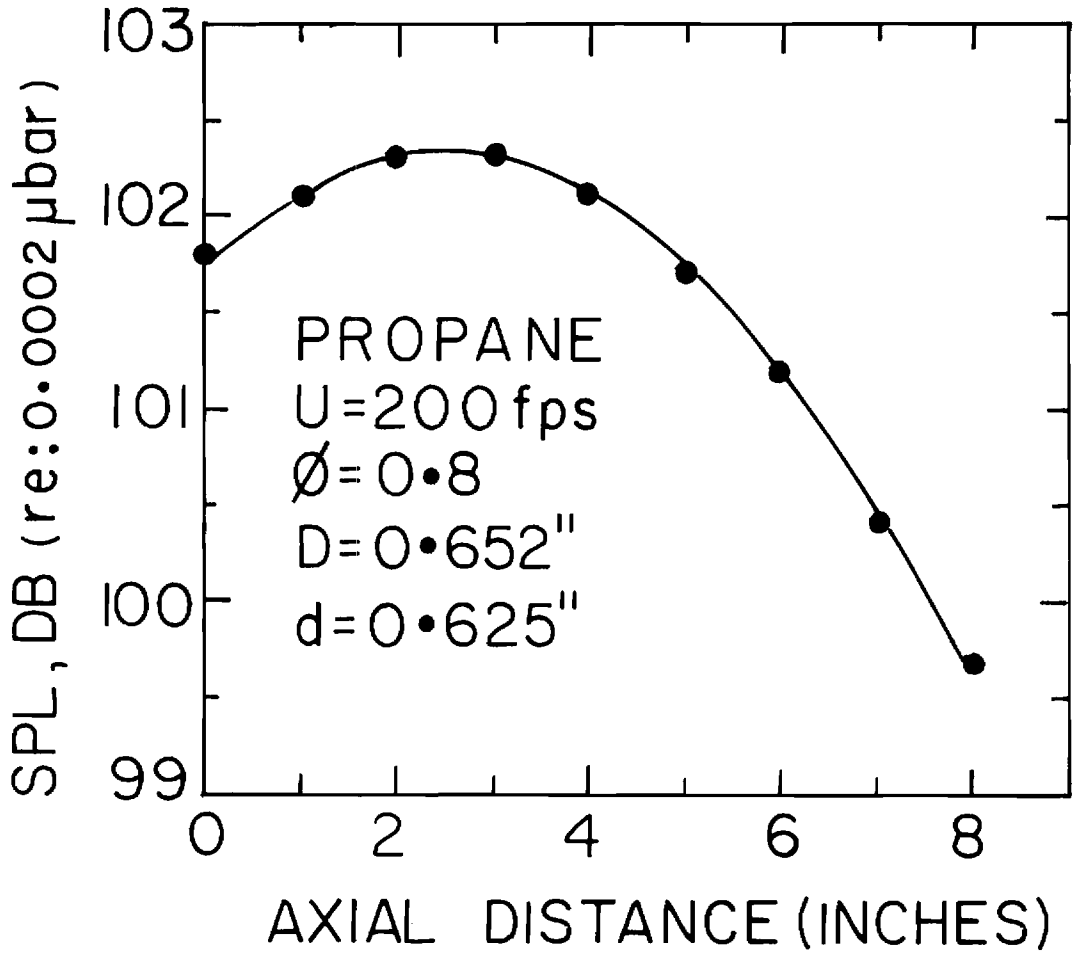

Figure 4. Variation of Sound Pressure Level along a Line Parellel to Flame Length and 8.25" below the Burner Axis.

The acoustic power radiated from the flame is calculated by integrating the polynomial relation, Eq.(1), over a sphere of some radius assuming axial symmetry. The sound pressure level at the last microphone location was used for values at other locations beyond the last microphone. The above procedure leads to the obvious question whether or not any appreciable error is introduced in directionality patterns and acoustic power calculations due to such an extrapolation. Shivashankara et.al.[16], using the same procedure as described above for their noise measurements of flames anchored on burner tubes, have concluded through detailed experiments that the error introduced due to extrapolation is insignificant.

A better understanding and analysis of combustion noise scaling laws can be achieved by a direct flame photography technique. In Ref. 8 an expression for the acoustic power radiated from a region undergoing turbulent combustion is given as

$$P \propto \int_{S_1} dS\,(\vec{r}_o) \int_{Sd} C_2\,(\vec{r}_o, \vec{d})\, dS(\vec{d}) \qquad (2)$$

where C_2 is the autocorrelation of the time derivative of normal velocity and is given by

$$C_2 = \lim_{T\to\infty} \frac{1}{T} \int_{-T/2}^{+T/2} \frac{\partial V_n(\vec{r}_o,t)}{\partial t} \frac{\partial V_n(\vec{r}_o+\vec{d},t)}{\partial t}\, dt \qquad (3)$$

Through an order of magnitude analysis it has been further shown in Ref. 8 that

$$P \propto S_1\, d_{cor}^2 < V_n'^2 > \omega_c^2 \qquad (4)$$

It is clearly seen from Eq. (4) that the surface area of reaction zone is a basic parameter in establishing scaling laws for combustion noise. This necessitates the evaluation of surface area of reaction zone.

The flame is photographed using a Graflex Speed Graphic Camera with an optical filter centered on CH radiation (4315Å). The filter used in the present investigation has a half peak transmittence bandwidth of about 680Å and a peak in the

vicinity of 4400A. The flames are photographed inside the anechoic chamber which eliminates stray light when photographs are being taken.

Figure 5 is a representative sketch of the photograph of the turbulent flame anchored at the base of the conical flameholder. The photograph of the flame revealed two distinct zones, one corresponding to an intense luminous zone followed by another zone due to afterburning glow. Since only the intense luminous zone is found to be responsible for maximum noise radiation, it is more appropriate to take into account only the area corresponding to the zone of intense luminosity, for surface area calculations. Then S_1 can be written as

$$S_1 \propto LB \tag{5}$$

where L and B are the measured quantities from the photographs.

EXPERIMENTAL RESULTS AND DISCUSSIONS

Figure 6 clearly indicates that the combustion noise dominates over the noise from a pure jet of same velocity and also the air jet plus pilot flame combination over the entire regime of experimental results obtained. Actually the tests were carried up to 600 fps. However only those tests have been considered in which the difference between combustion noise and air plus pilot flame noise was at least 3 db or more. This resulted in the elimination of tests above 300 fps.

Directionality Patterns

Quite often, the nature of the source can be guessed from the directionality of its sound radiation in the far field. The directionality results presented here are polynomials in $\cos\theta$ [Eq. (1)] fitted to experimental measurements. The flame holder base is chosen as the origin of reference and the azimuthal positions are measured from the flow direction. The directionality is determined by observing the variations in sound pressure level with the azimuthal angle θ. Figure 7 shows

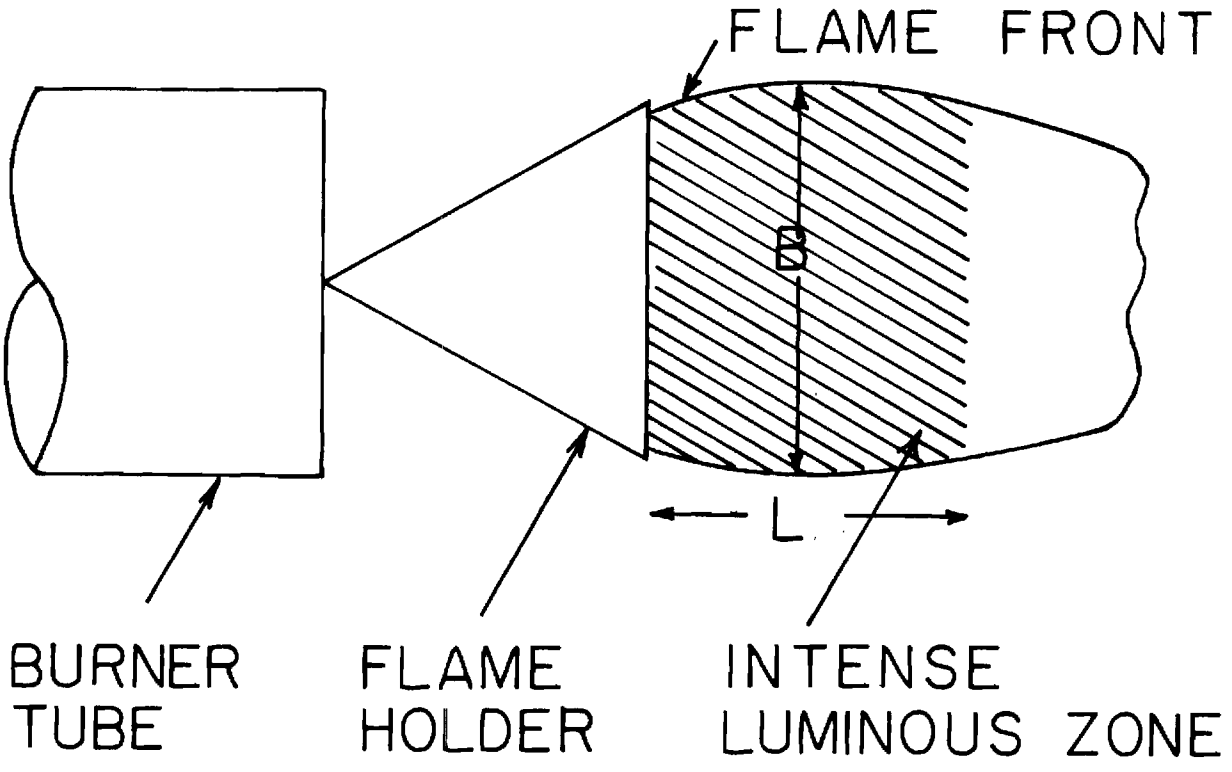

Figure 5. Flame Measurements for the Calculation of Surface Area of the Reaction Zone.

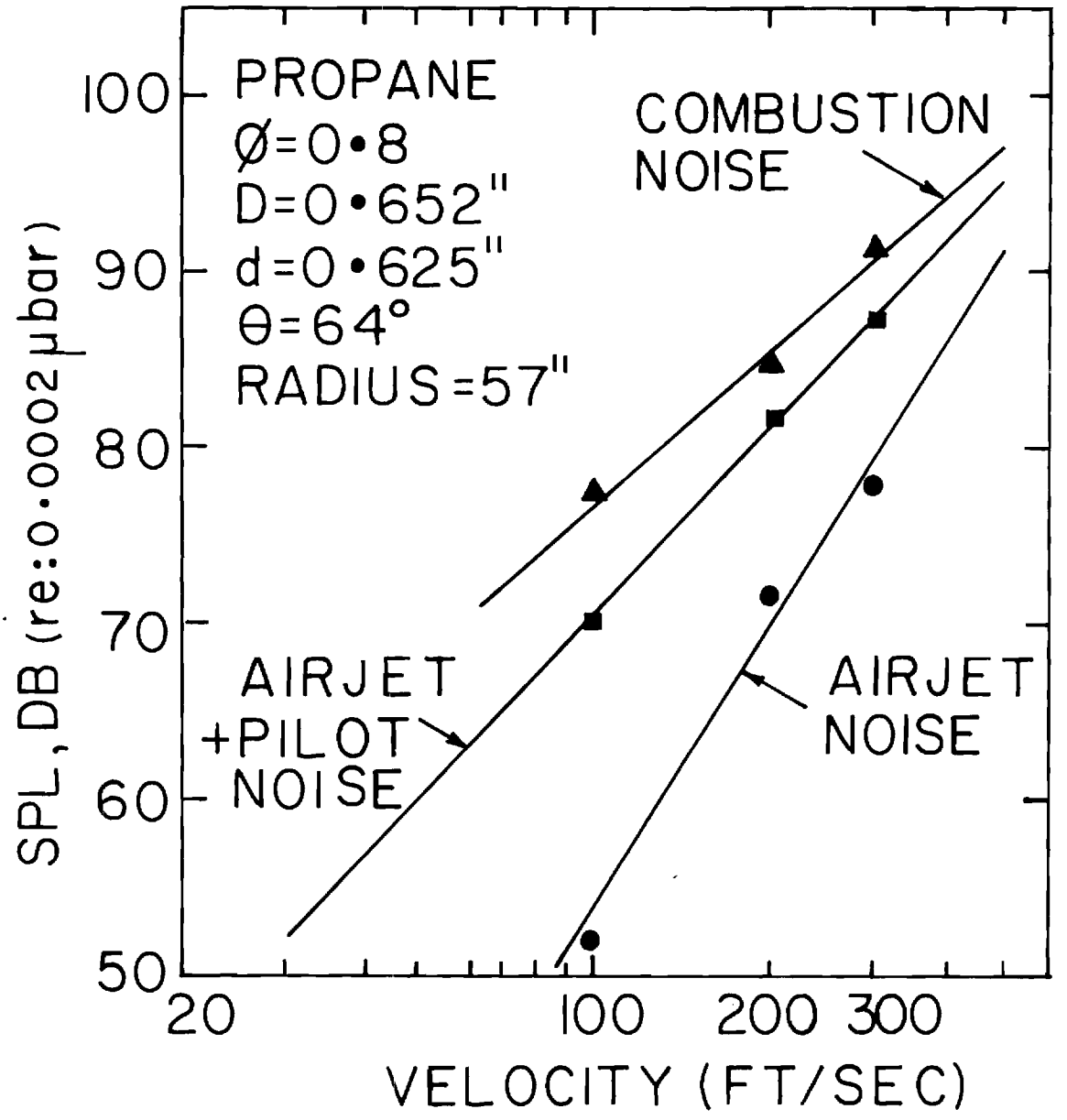

Figure 6. Relative Magnitude of the Different Noise Sources at Various Flow Velocities.

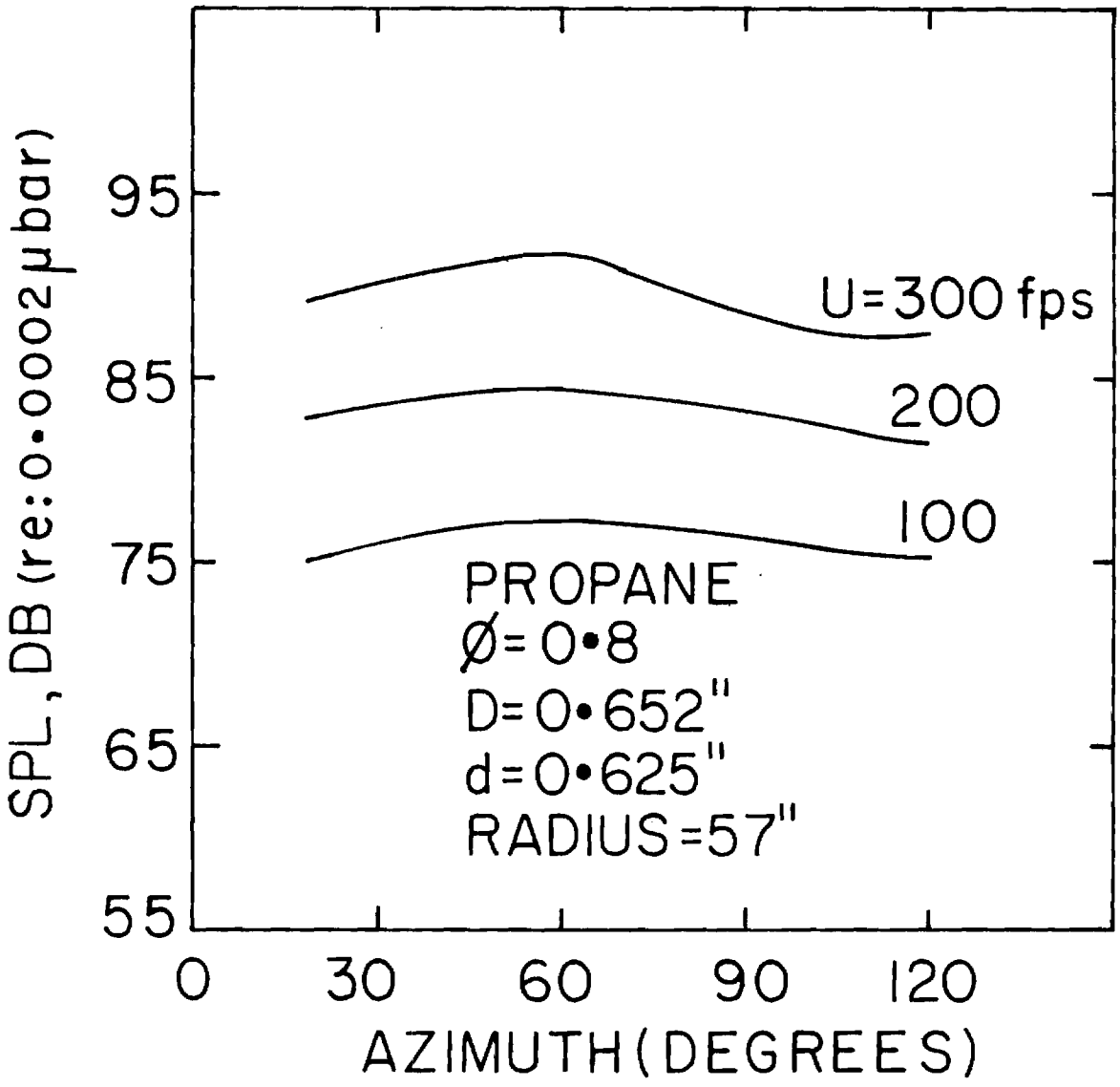

Figure 7. Directionality at Various Flow Velocities.

the directionality patterns at various flow velocities for propane-air flames of equivalence ratio 0.8. A very weak directionality is observed at all velocities.

Figure 8 shows the effect of burner diameter on the directionality of sound radiation. It can be concluded that the direction of maximum sound radiation is almost the same for all the three burners. Figure 8 also reveals that the directionality increases with an increase in diameter. In addition, Figure 8 shows the changes in the directionality patterns when the flameholder sizes are varied, keeping other parameters constant. It can be seen that the directionality is reduced when the flameholder size is changed in the case of burners with diameter 0.96 inches, whereas there is no appreciable change when using the 0.652 inches diameter burner.

The dependence of directionality on the equivalence ratio (ϕ) is brought out in Figure 9. The range of ϕ included is between 0.6 to 1.0. The effect of equivalence ratio on directionality is minor. Acetylene shows the maximum directionality. Figure 10 shows the effect of changes in the flameholder size on directionality when all the other conditions are fixed. It can be seen from Figure 10 that the direction of maximum sound radiation and the overall directionality patterns remain almost same when the flameholder size is varied.

All tests conducted in the present investigation show that combustion noise is weakly directional. The general lack of strong directionality leads to the support of the monopole theory of noise generation. For all different combinations of tests carried out, the direction of maximum noise radiation falls within 55° to 65° measured from the flow direction. One can speculate that the preferred direction of noise radiation may be partly due to the convection of individual sound sources through the zone of combustion by the gaseous flow and partly due to the refraction of acoustic radiation by temperature gradients surrounding the flame.

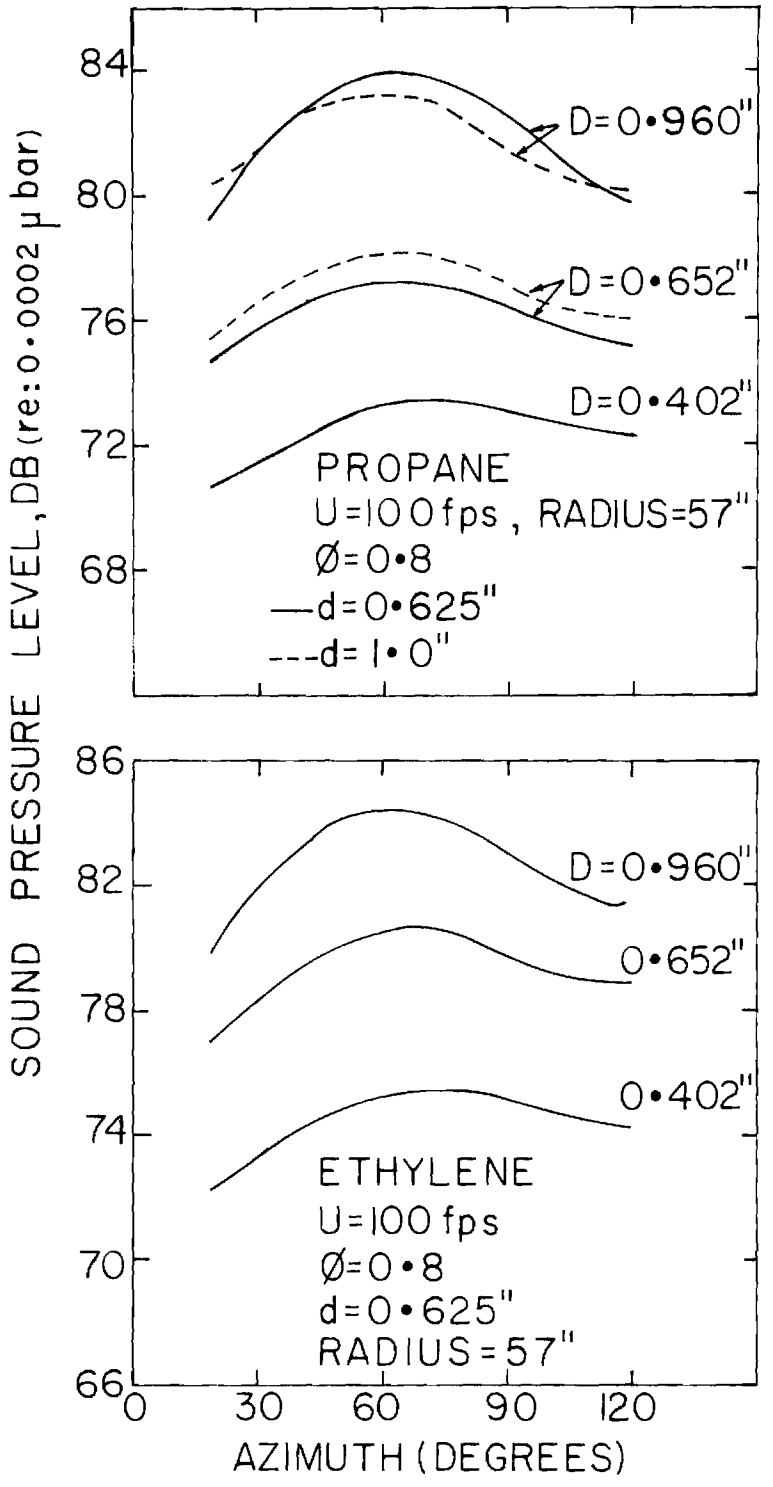

Figure 8. Dependence of Directionality on Burner Diameter.

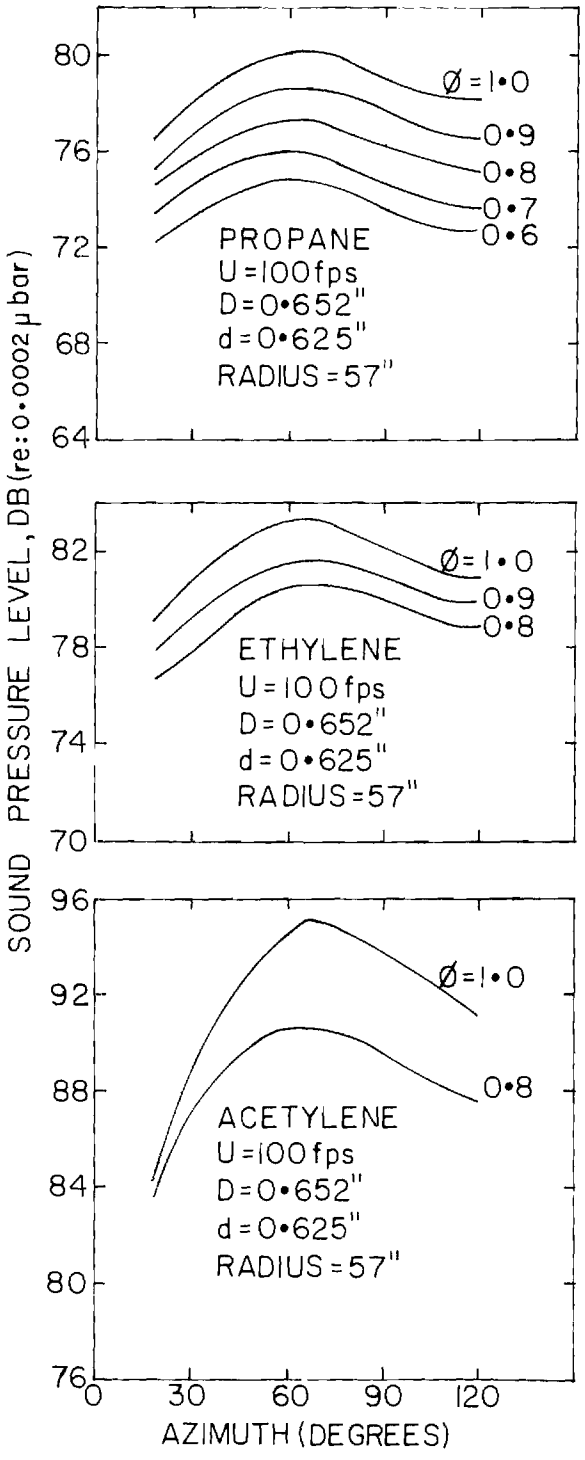

Figure 9. Effect of Equivalence Ratio on Directionality.

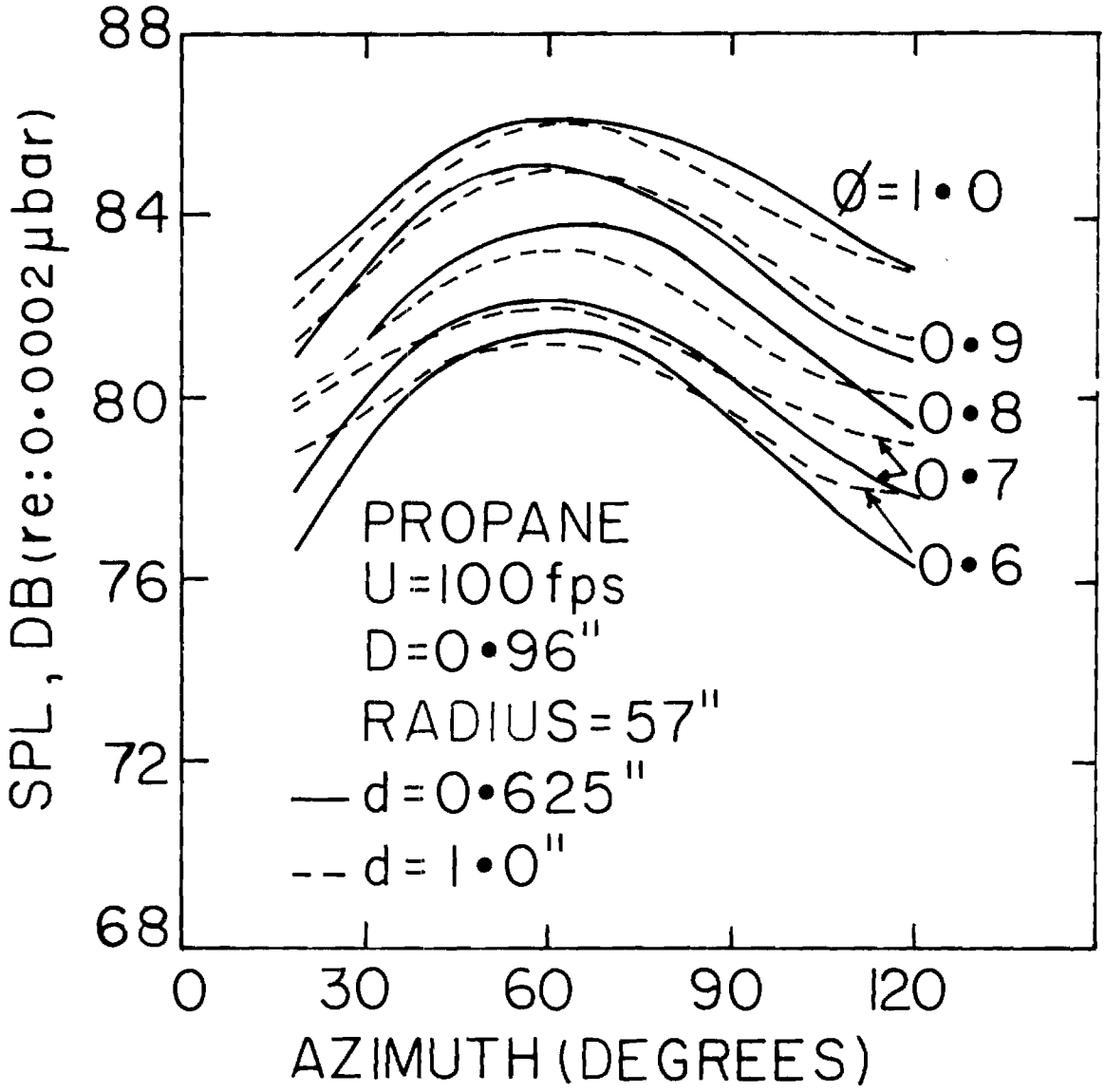

Figure 10. Effect of Flameholder Size on Directionality.

Spectral Characteristics

The frequency spectra were obtained from the tape recorded sound pressure signals using a Fourier analyser. A low pass filter, inserted between the Fourier analyser and the tape recorder, eliminated all high frequency components above a pre-selected maximum, thereby preventing aliasing. Finally, all frequency spectra were plotted on an X-Y plotter. The spectra presented in this paper are smooth lines drawn through such X-Y plots. The upper limit of the frequency was 5000 Hz.

The frequency dependence of the directionality is studied in Figure 11. It is found that the spectra at various azimuthal locations are almost parallel to each other, thereby establishing the fact that the directionality is almost independent of the frequency except for the location near the axis of the flame, which shows a decrease in the high frequency components.

SCALING LAWS ON ACOUSTIC POWER RADIATED

Following Refs. 4 and 5, it is concluded that U, D, S_L and F are the important parameters to be considered for the acoustic power computations. The behaviour of the total acoustic power output of the flame as a function of velocity is displayed in Figure 12. Over a 3:1 velocity ratio a $U^{2.25}$ law fits the acoustic power radiated. It is worth noting that the exponent on the velocity in the case of combustion noise is much smaller than the corresponding exponent in the case of subsoni jet noise.

It was shown in Figure 8 that at a given azimuthal point, the sound pressure level increased with an increase in the burner diameter when all other variables were fixed. Moreover, it is obvious from the preceding paragraph that the noise output decreases with a decrease in velocity due to a positive exponent on U. This will require the burner size to be increased to maintain the same mass flow. The above facts lead to the conclusion that the diameter D of the burner tube is yet another parameter in influencing the noise radiation and thereby warranting a

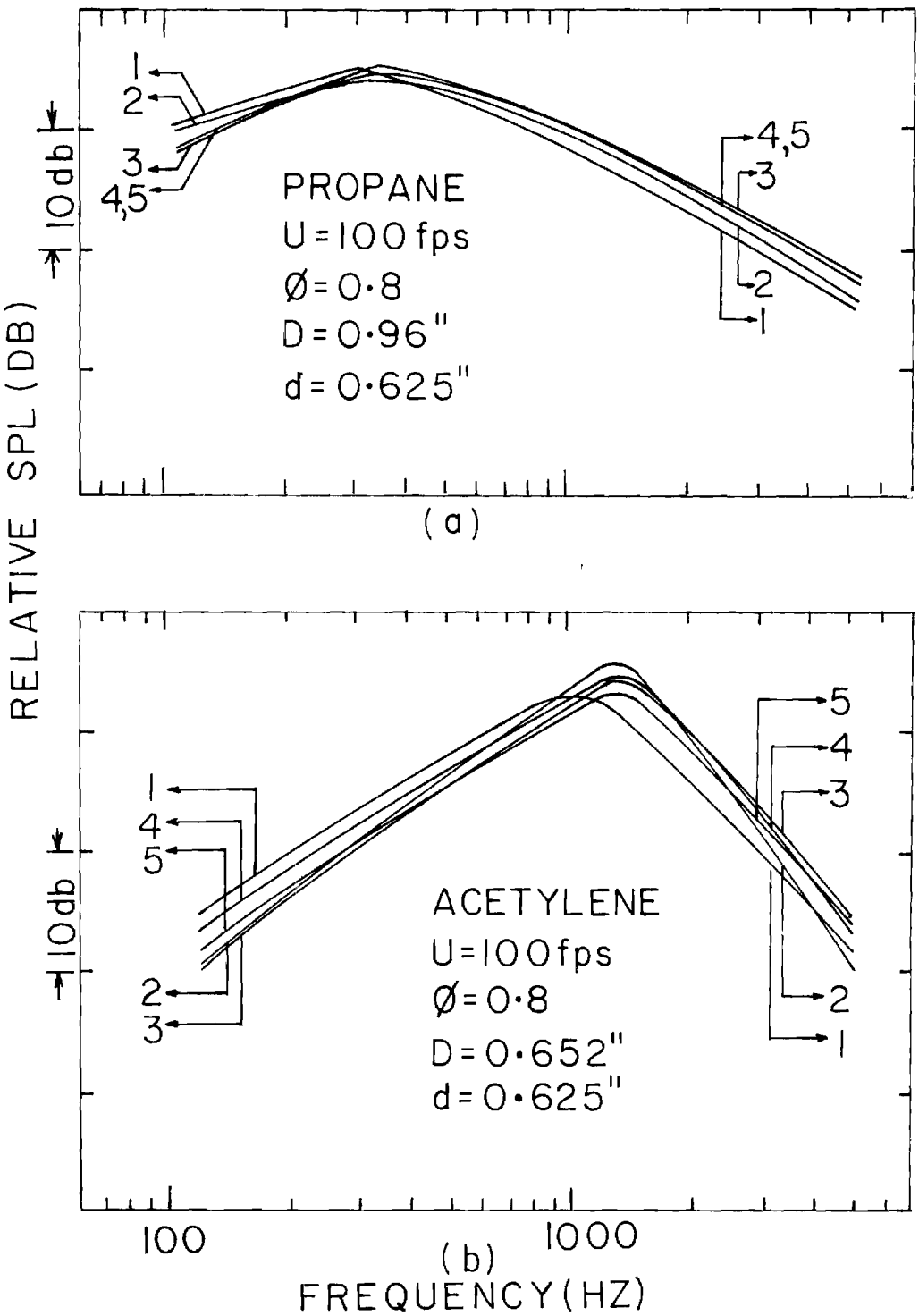

Figure 11. Frequency Dependence of Directionality. The Numbers 1 to 5 Indicate Microphone Locations between 15^{o} and 120^{o}.

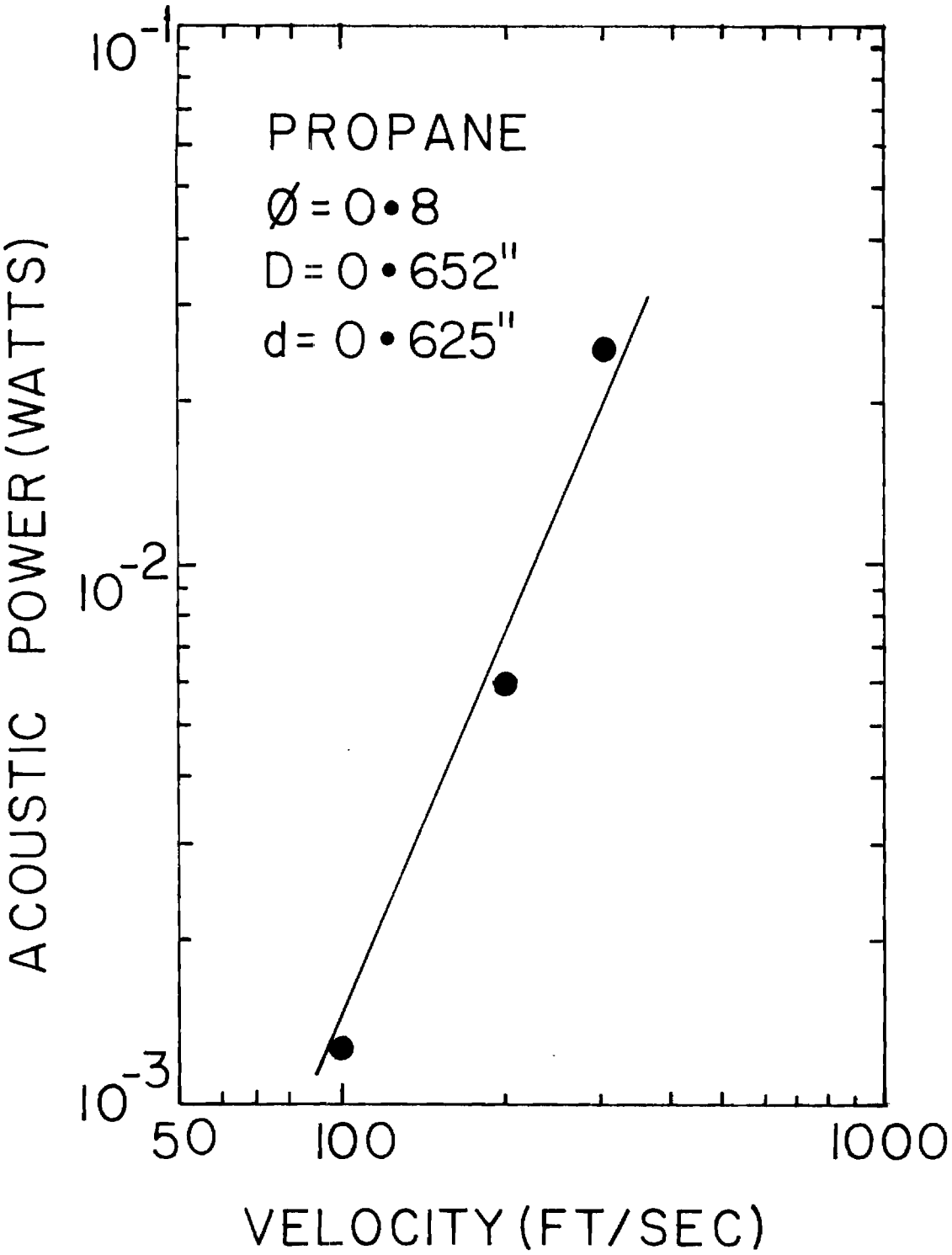

Figure 12. Variation of Acoustic Power with Flow Velocity.

study of its effect on noise output. This effect is illustrated in Figure 13. An exponent of 2.28 on D is obtained for propane-air flames and 2.00 for ethylene-air flames.

Since the laminar flame speed (S_L) happens to be a direct measure of the reaction rate, it is desirable to consider S_L as yet another parameter influencing acoustic power output. The S_L values of the fuels used in this investigation were obtained from the equation

$$\frac{S_L}{S_{L\,max}} = 2.6 \log_{10} \phi + 0.94 \quad \text{for } \phi \leq 1$$

from Ref. 18. The $S_{L\,max}$ values are chosen from Ref. 18 as 1.41, 2.46 and 5.12 ft/sec for propane, ethylene and acetylene respectively. Figure 14 shows the variation of acoustic power with laminar flame speed. S_L can be independently varied by changing the fuels with all other parameters held constant. But, even when ϕ is kept constant, there is a variation in fuel mass fraction (F) with the change of fuels because

$$F = \frac{\phi \left(\frac{F}{1-F}\right)_{Stoic}}{1 + \phi \left(\frac{F}{1-F}\right)_{Stoic}}$$

and $\left(\frac{F}{1-F}\right)_{Stoic}$ for propane, ethylene and acetylene are 0.064 , 0.0677 and 0.0755 respectively. Since the acoustic power depends on both S_L and F, it is necessary to correct the acoustic power output for F dependence. This correction was found to be very minnor because the variation in F is very small. Hence, Figure 14 exhibits the variation of corrected acoustic power with S_L values and hence should yield scaling laws on S_L. The exponent on S_L was found to vary from 2.14 to 2.28 as one approaches stoichiometric from fuel lean mixtures.

The discussions in the previous paragraphs centered around the variation of acoustic power radiated with individual parameters U, D and S_L taken one at a time. Though it would first seem to be more attractive, a large number of experiments

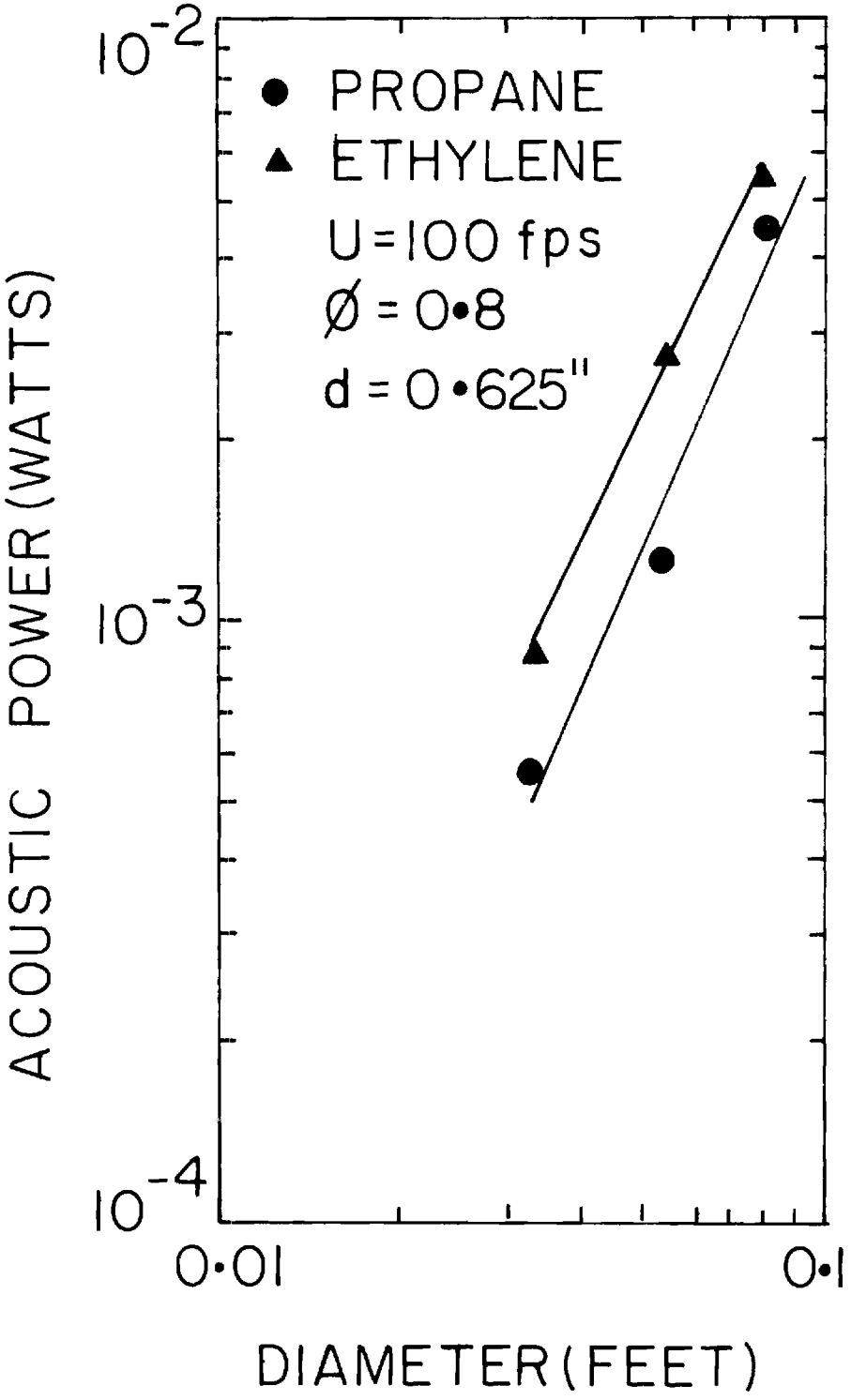

Figure 13. Diameter Dependence of Acoustic Power.

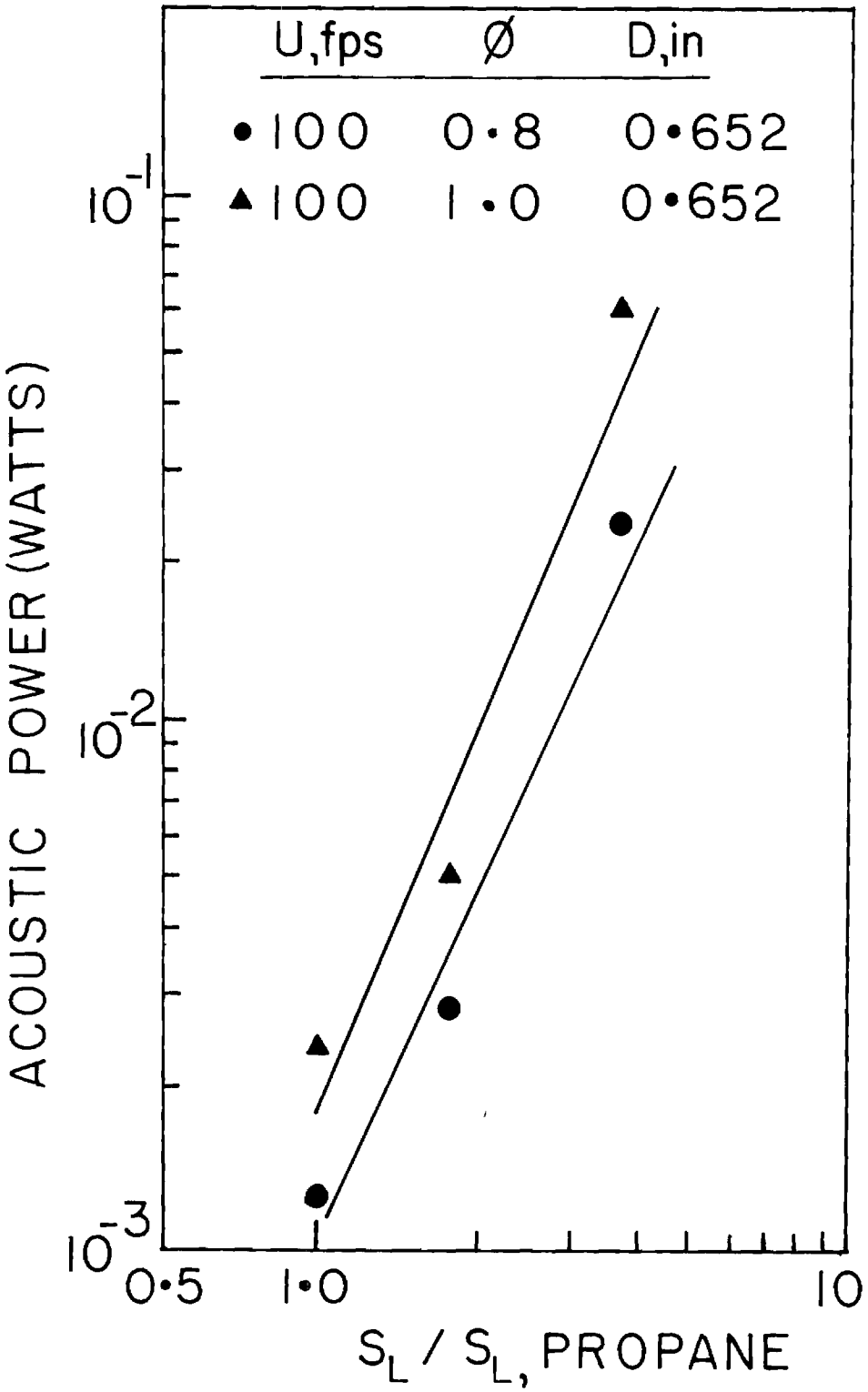

Figure 14. Effect of Laminar Flame Speed on Acoustic Power

are necessary to accomodate the variation in all the parameters. This situation can be remedied by resorting to a regression analysis which facilitates the fitting of a theoretically derived law to the experimental observations. Considering U, D, S_L and F as the important parameters influencing acoustic power computations, theory suggests a relation,

$$P = K U^a D^b S_L^c F^d, \qquad (6)$$

where the prefactor K and the exponents a,b,c and d are constants. By taking logarithms on both sides of Eq. (6) it is possible to fit a curve by the method of least squares. Using 35 different tests, the following expression was obtained for the acoustic power radiated from open turbulent flames anchored on the external conical flameholders.

$$P = 0.67 \times 10^{-6} \; U^{2.83} \; D^{2.77} \; S_L^{1.89} \; F^{-0.89} \text{ Watts} \qquad (7)$$

where $50 \leq U \text{ (fps)} \leq 300$; $0.0335 \leq D\text{(ft)} \leq 0.08$; $0.6 \leq \phi \leq 1.0$; and U and S_L are in fps and D is in ft. The mean error in the regression analysis was 9.87 % with 171.8 % and -57.6 % as the maximum and minimum errors respectively. The standard deviation was 47.6 % . Although at first sight these errors appear to be rather large, they can be justified to be acceptable because of the following reasons.

(a) A wide range of acoustic powers (from 10^{-4} to 10^{-1} watts) are included in Eq. (7),

(b) The instrumentation accuracies are of the order of a db, and the above standard deviation is only about 2 db.

At this point it is worthwhile to see the reliability of the regression fit. This is brought out through Figure 15 where the regression fit values are plotted against the measured values. It is seen that Eq. (7) fits the experimental values to a good degree and the deviations are minor. Figure 15 shows that the data points corresponding to almost all the tests with the larger size conical flame holder lie on the lower side of the regression curve indicating that the regression fit slightly underestimates the acoustic power output. But it should be noted that

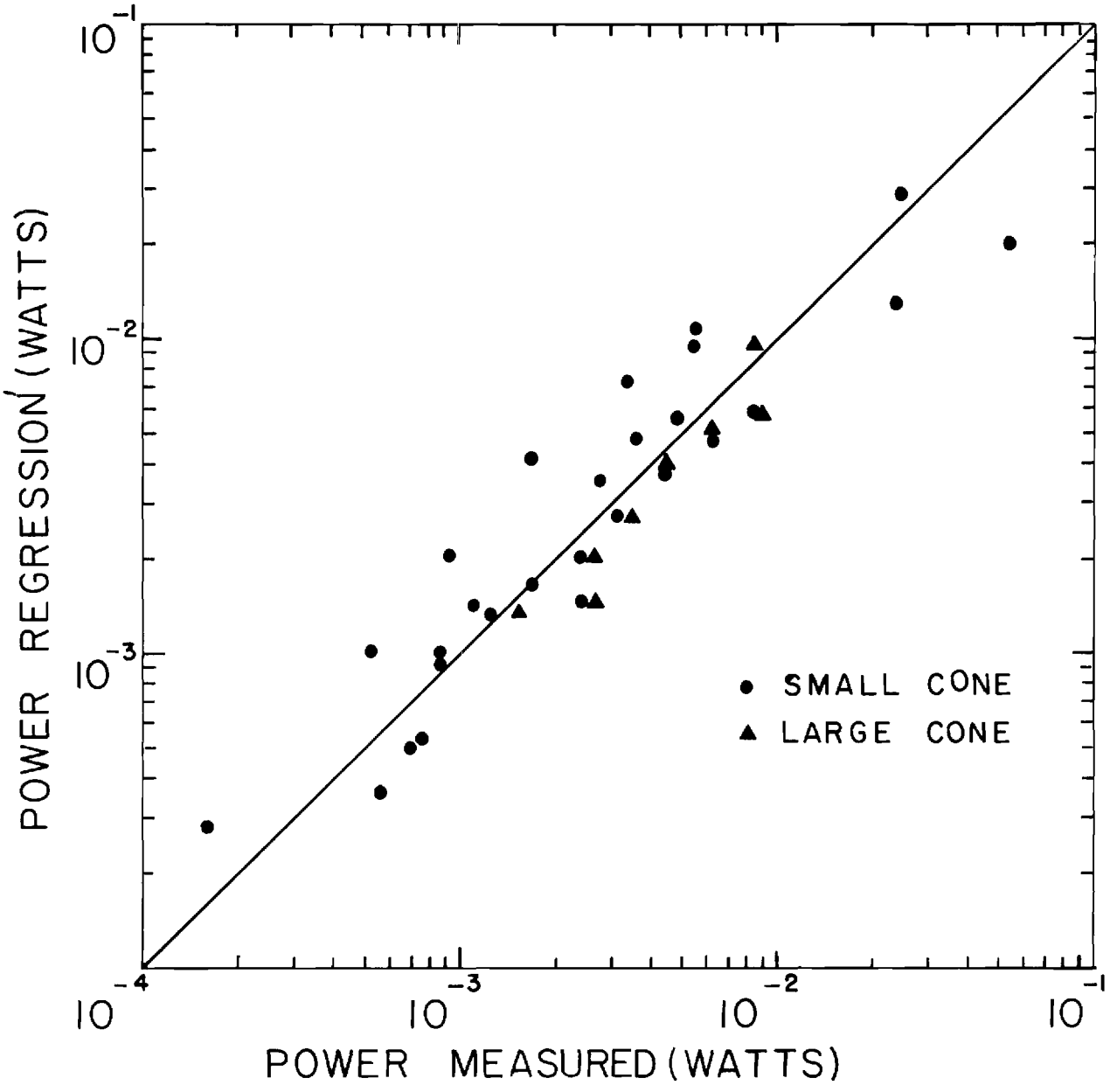

Figure 15. Significance of Regression Fit for Acoustic Power.

a change in the flameholder size almost by a factor of two, has led to only a very minor difference (less than one dB) between the regression fit and the measured values. Thus it can be finally concluded that the acoustic power can indeed be represented by a power law type with respect to the parameters U,D, S_L and F, without regard to the flameholder size. This is also shown in Figure 16.

Comparing the acoustic power output of the present investigation with the same tests of Ref. 16, it has been found that the acoustic power output from the flames anchored on the external flameholders differ from those stabilized on the burner tube ends by a factor of a maximum of two. This shows that the method of flame retention has only a minor influence on the acoustic power output.

A common term, related to the efficiency of acoustic radiation, is the thermoacoustic efficiency (η_{ta}) which is defined as

$$\eta_{ta} = \frac{\text{Acoustic Power Radiated}}{\text{Thermal Input}} \tag{8}$$

Thomas and Williams [19] have obtained values of the order of 10^{-6} for spherically expanding flames. For spherically expanding flames, one can assume equal contribution to the sound intensity in the far field from all parts of the sphere. However, since in the acoustic analysis the turbulent flame is described as a collection of randomly distributed monopole sources, one can expect some cancellation of various compressions and rarefactions to occur. So it is highly reasonable to expect a value of 10^{-6} as a likely upper limit to the thermoacoustic efficiency for hydrocarbon-air flames.

Noting that the heat input = $\dot{m}\,FH$, η_{ta} can be written as

$$\eta_{ta} = \frac{P}{\frac{\pi}{4} D^2 U \rho_o F H} \tag{9}$$

Therefore, the scaling law for η_{ta} can be written using Eqs. (7) and (9) as

$$\eta_{ta} \propto U^{1.83} D^{0.77} S_L^{1.89} F^{-1.89} \tag{10}$$

The variation of thermoacoustic efficiency with the flow velocity, with the other

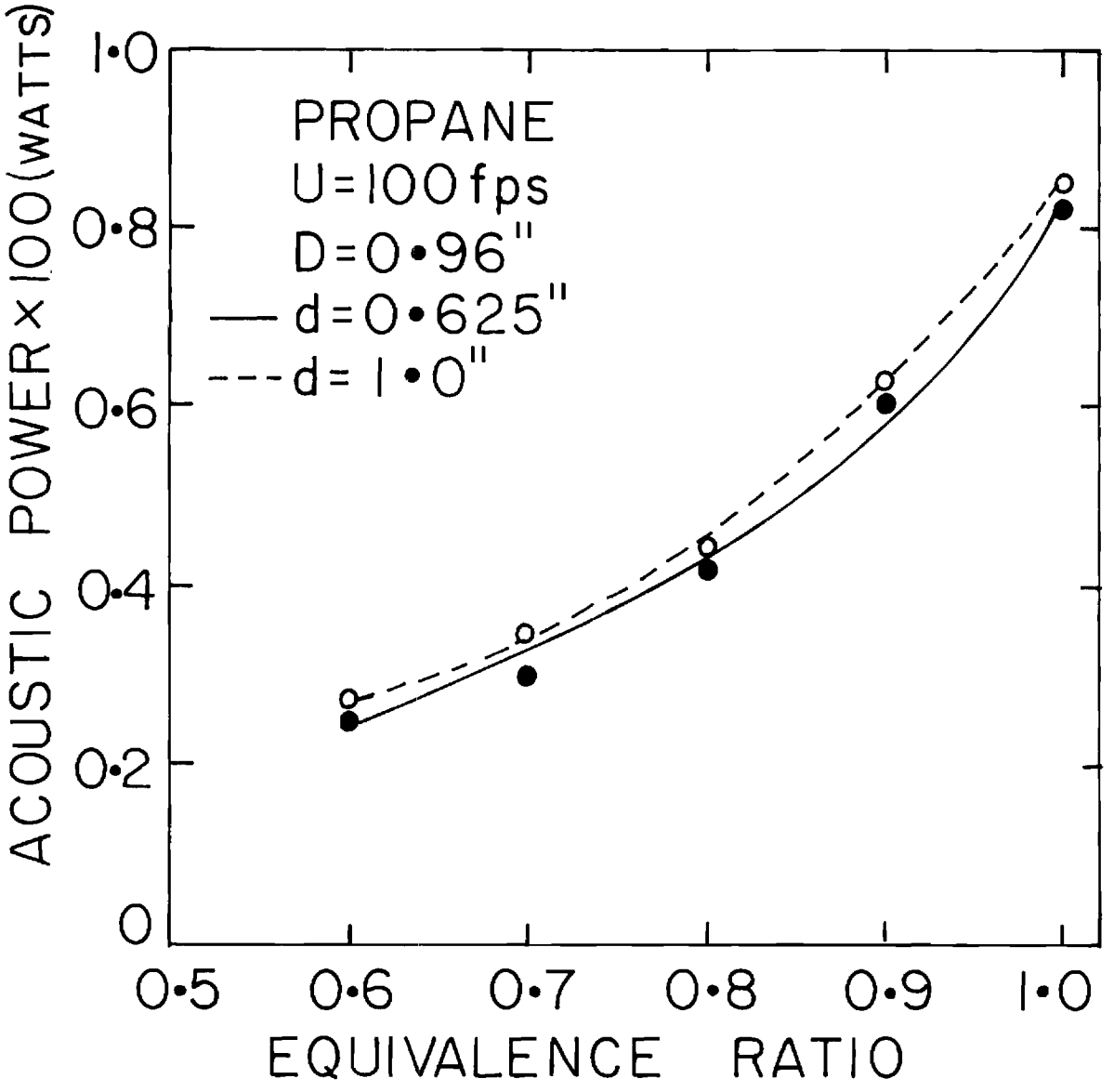

Figure 16. Effect of Flameholder Size Variation on Acoustic Power Output.

parameters fixed, is brought out through some representative values in Table 1.

Table 1. Thermoacoustic Efficiency for Propane-Air Flames of $\phi = 0.8$ on a Burner of Diameter 0.652 inches

Velocity (fps)	Power (Watts)	Thermoacoustic Efficiency
100	0.1248×10^{-2}	0.75×10^{-7}
200	0.5656×10^{-2}	0.17×10^{-6}
300	0.2551×10^{-1}	0.51×10^{-6}

In this connection it is worth mentioning that Ref. 16 quotes a highest value of 1.01×10^{-6} for thermoacoustic efficiency at a flow velocity of 600 fps.

Scaling Laws on Peak Frequency:

Figure 17 illustrates the effect of flow velocity on the frequency spectra. The peak frequency (i.e. frequency corresponding to the maximum power per unit frequency interval in the spectrum) seems to increase with an increase in the flow velocity. Over a 3:1 velocity ratio the peak frequency (f_c) changes from 380 to 1100 Hz. The variation of peak frequency with diameter is shown in Figure 18. It is found that the peak frequency decreases as the burner diameter increases. The effect of laminar flame speed (S_L) on peak frequency is brought out through Table 2 where a few representative values are presented.

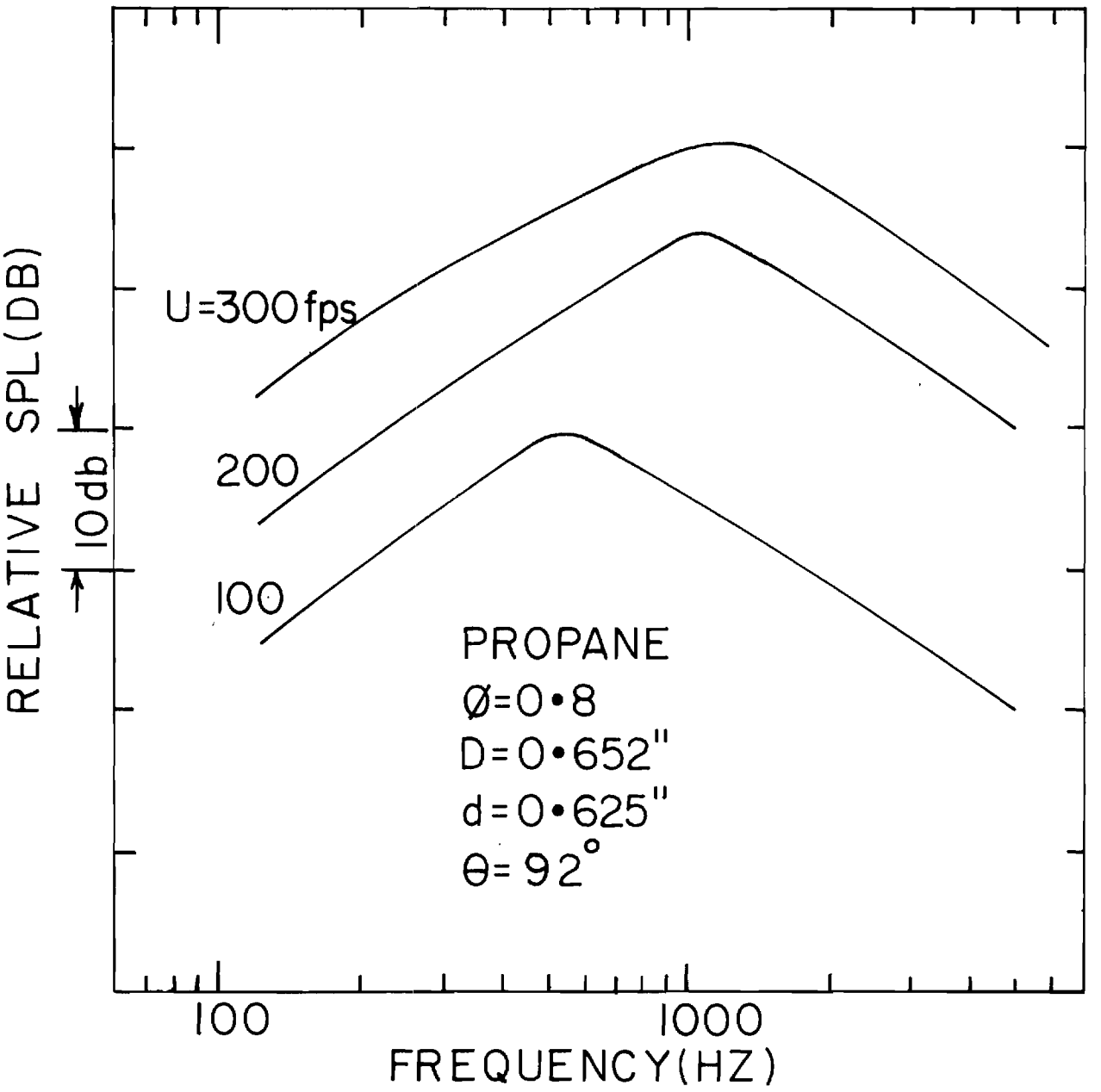

Figure 17. Effect of Flow Velocity on the Frequency Spectra.

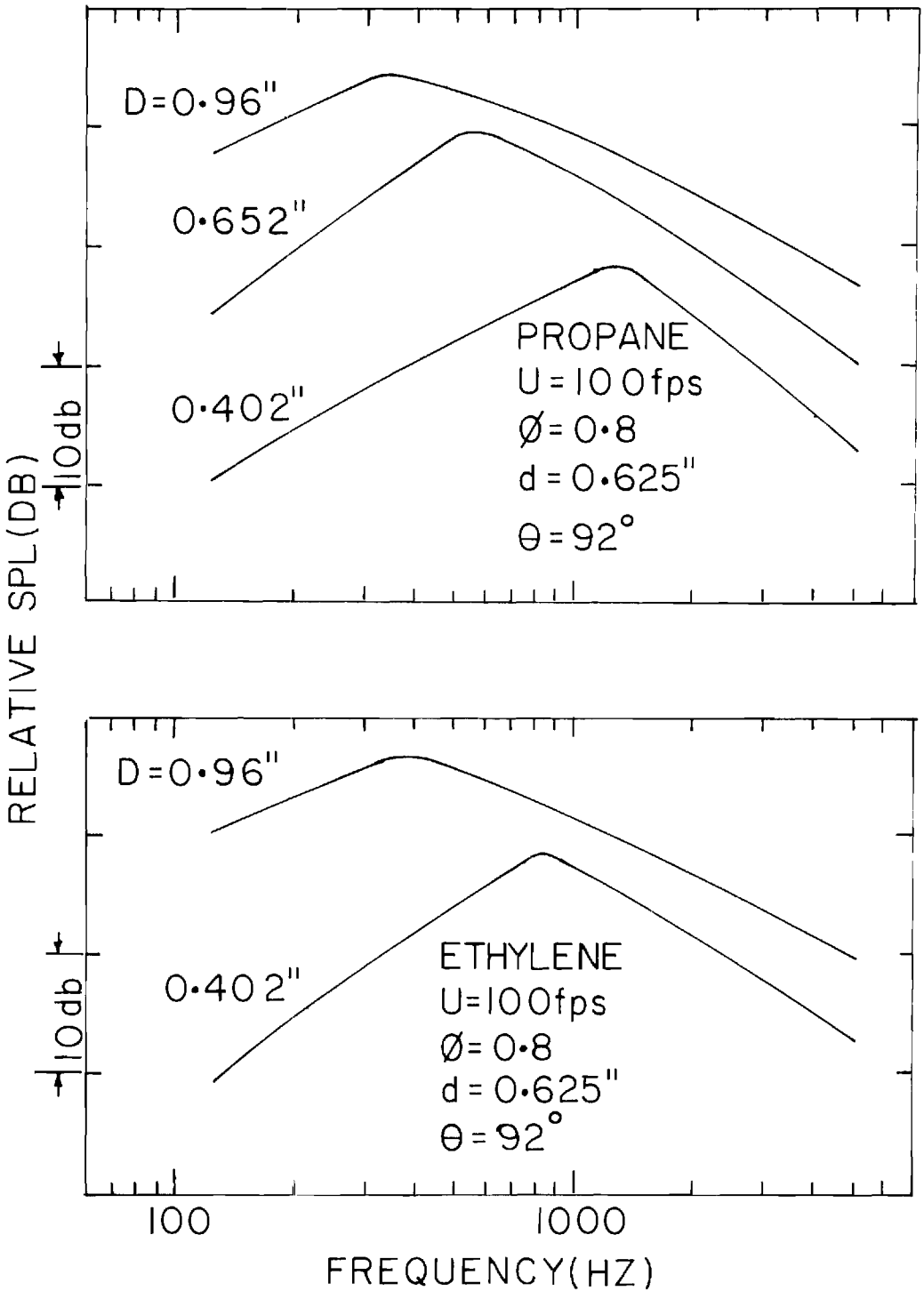

Figure 18. Dependence of the Frequency Spectra on Burner Diameter.

Table 2. Peak Frequency Values for Various Fuel Air Combinations

U = 100 fps d = 0.625 inches

Burner Diameter (inches)	Equivalence Ratio ϕ	PEAK FREQUENCY (Hz)		
		Propane-Air	Ethylene - Air	Acetylene - Air
0.96	0.8	320	350	-
	0.7	280	305	-
	0.6	275	280	-
0.652	1.0	380	-	1320
	0.8	380	-	1300
0.402	0.8	1300	1310	-

It can be seen from the above table that the peak frequency values corresponding to ethylene - air and acetylene - air combinations are higher than those of propane - air. This effect appears due to the fact that ethylene and acetylene have higher S_L values.

Lastly, the effect of the flameholder size on the frequency spectra is illustrated in Figure 19 where two cases are plotted. It is found that the variations in the flameholder size have a very little influence on the peak frequency value.

A scaling law for peak frequency (f_c) was obtained by regression analysis to the peak frequencies measured from frequency spectra. The procedure followed was similar to the one adopted for obtaining the acoustic power scaling law, Eq. (7). Thus, the peak frequency is given by

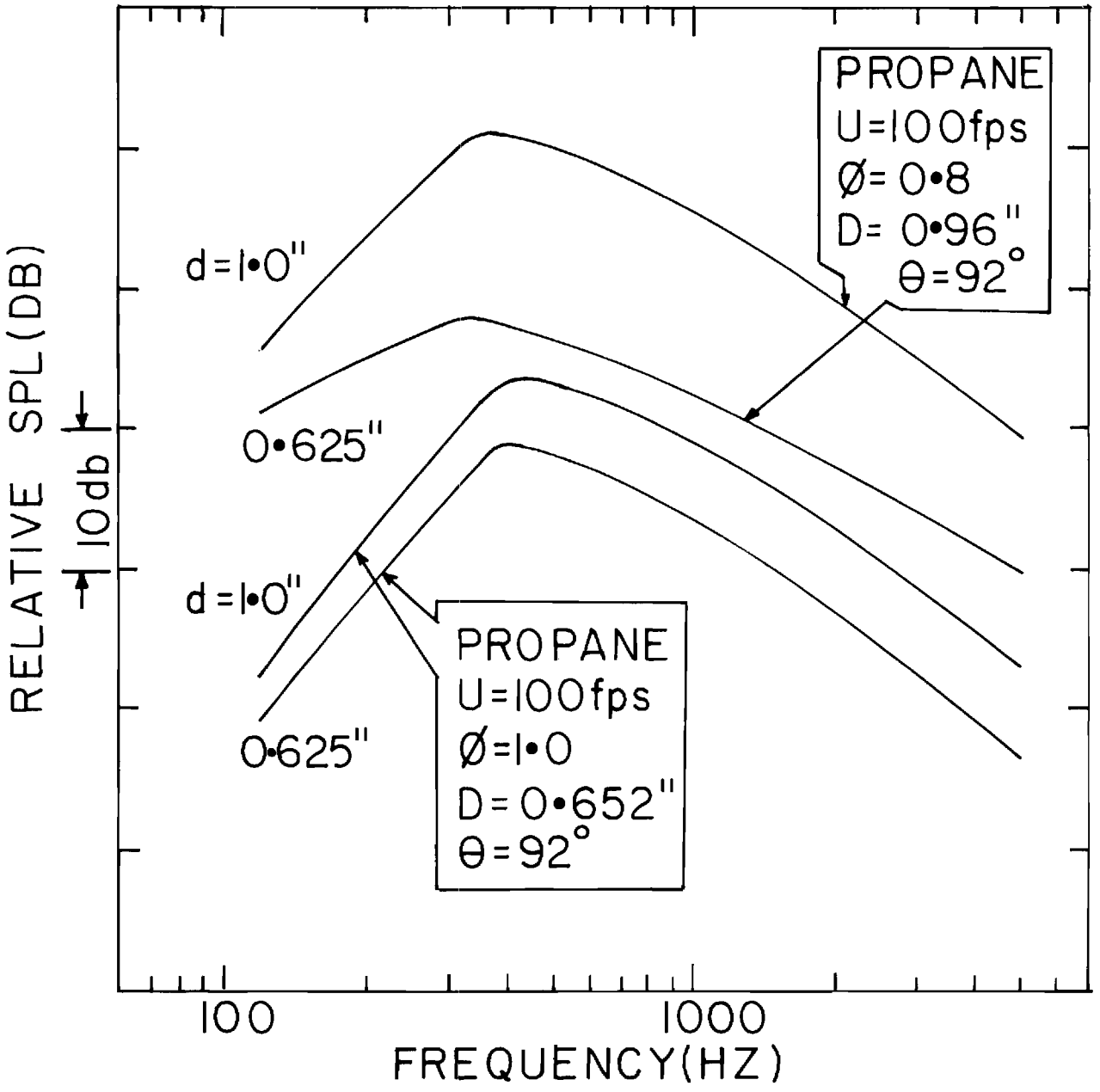

Figure 19. Effect of Flameholder Size Variation on the Frequency Spectra.

$$f_c = 0.42 \times 10^{-2} \; U^{0.58} \; D^{-1.37} \; S_L^{0.7} \; F^{-1.7} \quad \text{Hz} \qquad (11)$$

where $50 \leq U \text{ (fps)} \leq 300$; $0.0335 \leq D\text{(ft)} \leq 0.08$; $0.6 \leq \phi \leq 1$. Also U and S_L are in fps and D is in feet. The Number of tests used for the above equation was 31. The mean error was 3.63 % and the standard deviation was 27.6 %

Scaling Laws for Surface Area of Reaction Zone:

The behavior of the flame surface area with burner diameter is shown in Figure 20. It can be seen that the flame surface area increases with an exponent of 2.42 on diameter. Figure 21 shows the variation of flame surface area with the flow velocity of reactants in the burner tube. Based on the discussion in the previous paragraphs, a $D^{2.42}$ correction has been applied to take away the diameter effects from the data points. It is found that the flame surface area scales with an exponent of 0.94 for mean flow velocity.

A regression fit , similar to the ones used for obtaining scaling laws for acoustic power radiated and peak frequency, yields an empirical relation for surface area of the reaction zone as

$$S_1 = 0.6 \times 10^5 \; U^{0.97} \; D^{2.2} \; S_L^{0.86} \; F^{2.6} \; \text{in}^2 \qquad (12)$$

where $50 \leq U \text{ (fps)} \leq 300$; $0.0335 \leq D \text{ (ft)} \leq 0.08$; $0.6 \leq \phi \leq 1$. Also, U and S_L are in fps and D is in feet. Totally, 27 tests were used for the above regression analysis and the mean error in the analysis was found to be 61 %. It is important to note that any linear inaccuracy in linear dimensions on the photograph shows up squared in area computations.

Comparison of Theoretical and Experimental Results

Purely from a theoretical point of view, using order of magnitude analysis, Eq. (4) was developed by Strahle[8] for the acoustic power radiated from open turbulent flames. Eqs. (7), (11) and (12) give the correlations for acoustic power radiated, peak frequency and surface area of reaction zone, using experimental results. It will be interesting to investigate whether or not the theo-

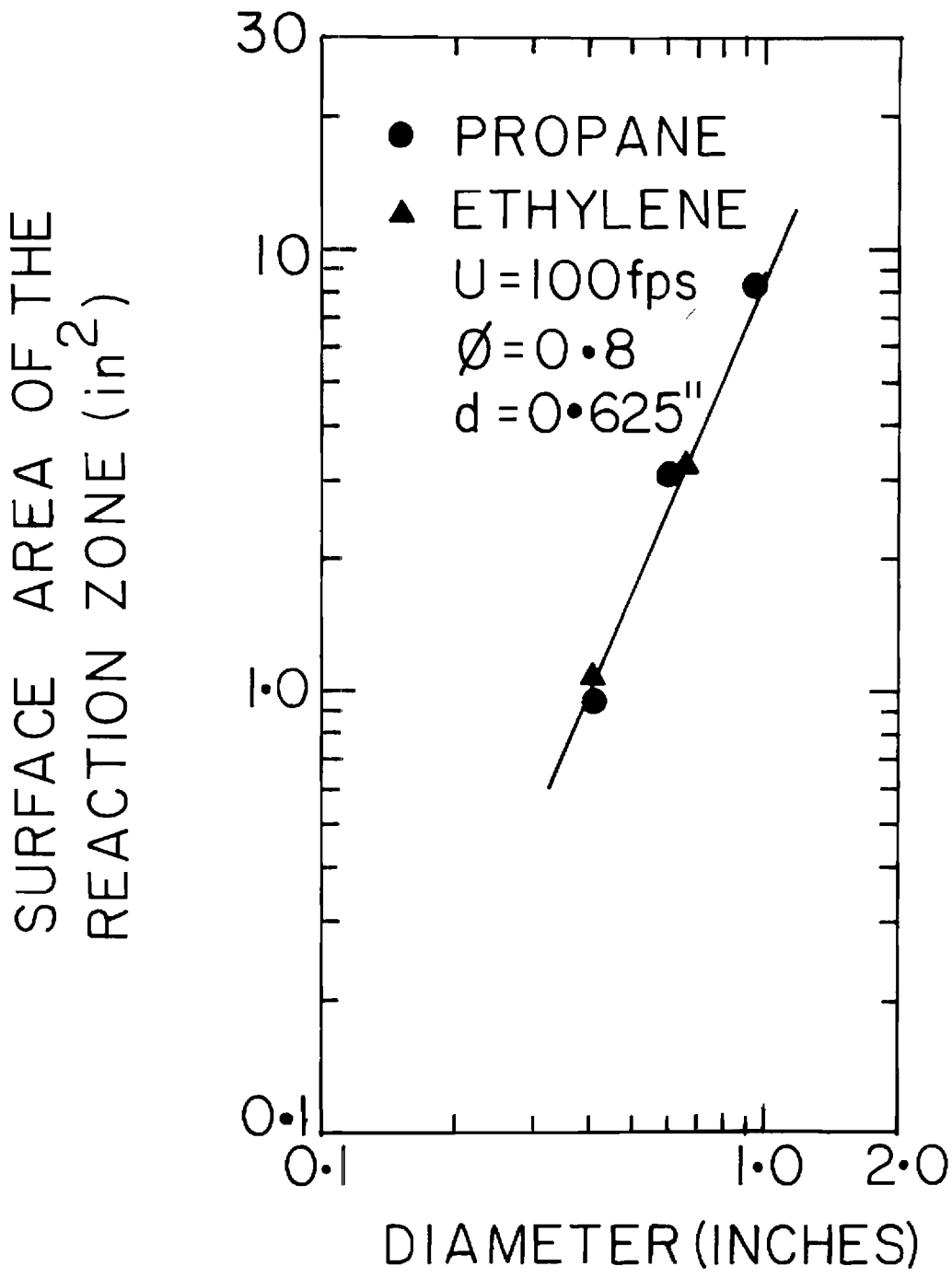

Figure 20. Variation of the Surface Area of the Reaction Zone with Burner Diameter.

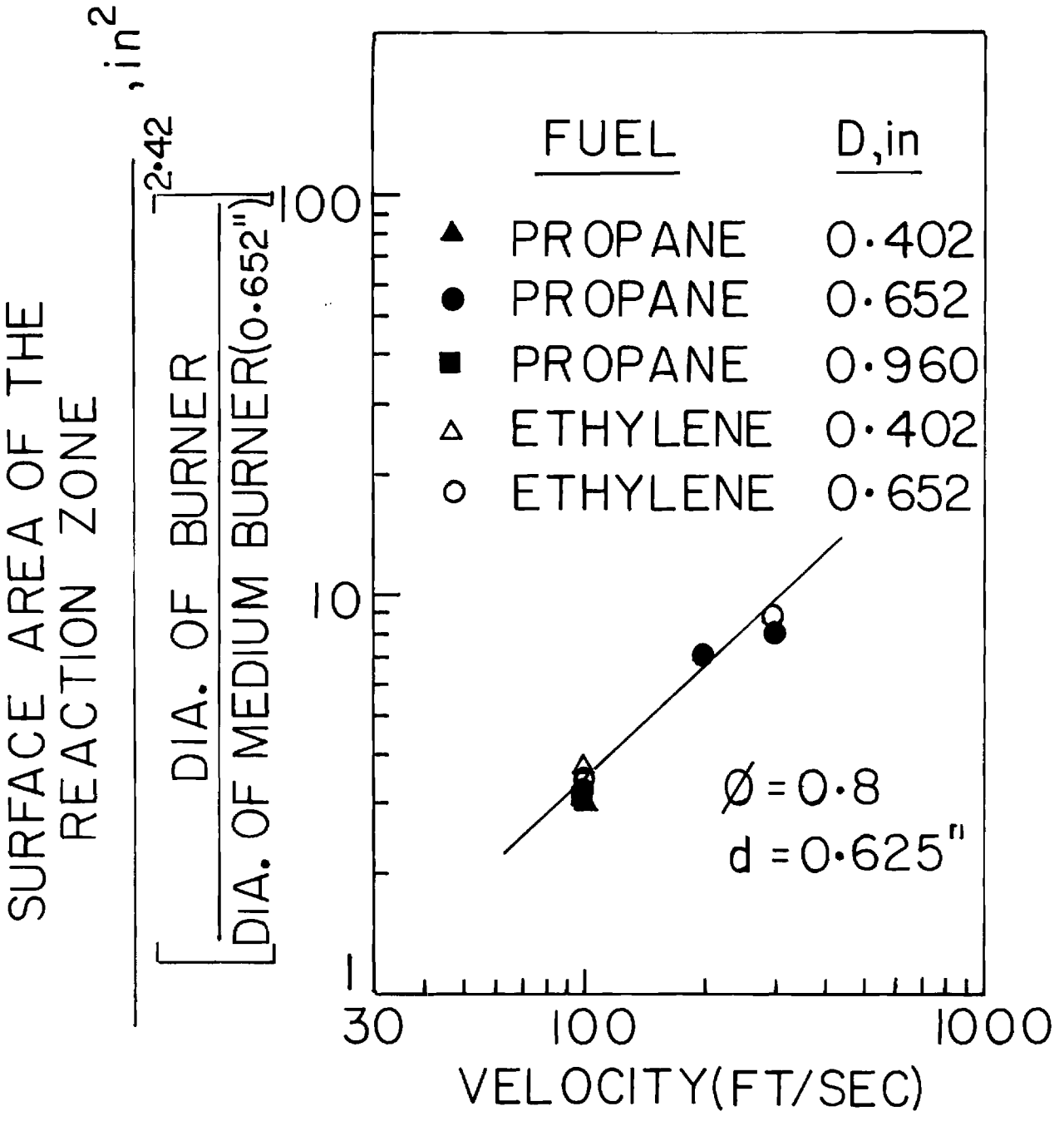

Figure 21. Effect of Flow Velocity on the Surface Area of the Reaction Zone.

retically derived Eq. (4) can be recovered from experimentally obtained relationships.

Following Ref. 8, accepting that the differential heat release rate is the cause for the normal velocity fluctations of the flame front downstream of the flame and defining the incoming normal velocity as the turbulent flame speed (S_T), it is obvious to write

$$V'_n \propto \frac{\bar{\rho}_o}{\bar{\rho}_1} S_T \approx \frac{F}{c_p} \frac{H}{T_o} S_T \qquad (13)$$

The above equation defines S_T values for the evaluation of V'_n. Using continuity the turbulent flame speed can be written as

$$S_T = \frac{\dot{m}}{\rho_o S_1} \qquad (14)$$

Using Eq. (14) , Eq. (13) can be written as

$$V'_n \approx \frac{F}{c_p} \frac{H}{T_o} \frac{\dot{m}}{\rho_o S_1} \qquad (15)$$

Further, S_1 and f_c correlations are available through Eqs. (12) and (11). Finally an estimate for d_{cor} is required so that Eq. (4) can be used to obtain acoustic power. Ref. 8 makes use of the hypothesis that the correlation distance (d_{cor}) is the integral scale of turbulence of the cold flow and arrives at a scaling law for correlation distance after taking into account the turbulence decay behavior downstream of the burner mouth.

The complex nature of turbulence interactions for the present case renders an estimate of d_{cor} more uncertain. The straight forward approach would be that all the quantities appearing on the right hand side of Eq. (4) should be substituted to get the acoustic power,P,which, in turn, would be compared with the acoustic power scaling law [Eq. (7)]. But, due to the above mentioned difficulties the acoutistic power in Eq. (4) was substituted using Eq. (7) and an empirical relation for d_{cor} was obtained. Then it was checked whether or not the estimate for

d_{cor} will recover the observed frequency law. According to the above procedure, an estimate for d_{cor} turns out to be

$$d_{cor} \propto U^{0.32} \; D^{1.85} \; S_L^{-0.19} \; F^{1.55} \qquad (16)$$

The above correlation gives an exponent of 1.85 on D. This value seems to be a little high. Since both the burner tube and the flameholder are of comparable sizes, one would expect d_{cor} to scale like D. Following Ref. 7, the frequency of macroscopic mixing (f_m) can be written as

$$f_m \equiv \frac{u'}{l_e} = \frac{u'}{d_{cor}} \qquad (17)$$

Assuming $u' \propto U$ and substituting for d_{cor} from Eq. (16), f_m scales like

$$f_m \propto U^{0.68} \; D^{-1.85} \; S_L^{0.19} \; F^{-1.55}$$

The above scaling law for f_m is close to the one for peak frequency given by Eq. (11). This leads to the conclusion that frequency is determined by the turbulence in the incoming flow.

Non-dimensional Analysis of Scaling Laws:

The scaling laws developed in the last sections [Eqs. (7), (11) and (12)] for acoustic power, peak frequency and surface area of reaction zone contain dimensional quantities like U, D and S_L. In engineering applications, it will be more widely useful if the results are presented in dimensionless form. Following Ref. 7, for an unsteady trubulent combustion process, making the simplifying assumptions of a global reaction rate and $Le \approx Pr \approx 1$, the important dimensionless groups turn out to be F, Re, M, $\frac{\omega D}{U}$, Da_1 and Da_2. An independent variation of η_{ta} and $\omega_c D/U$ can be achieved by varying the four parameter U, D, S_L and F. Therefore, the scaling laws previously developed can be cast into the following dimensionless form:

Thermoacoustic Efficiency

$$\eta_{ta} \propto Re^{-0.18} \; M^{2.96} \; F^{-1.89} \; Da_1^{0.95} \; f_1(Da_2) \qquad (19)$$

Peak Frequency

$$\frac{\omega_c D}{U} \propto Re^{-0.72} M^{0.65} F^{-1.7} Da_1^{0.35} f_2 (Da_2) \qquad (20)$$

Since Da_2 has a quite constant value for hydrocarbon-air flames, $f_1 = f_2 = 1$, but their functional forms are unknown.

CONCLUSIONS

An experimental study was carried out to investigate the noise characteristics of flames stabilized on external flameholders. A simple burner configuration was chosen for rational interpretation of the results. The burner sizes have been 0.402, 0.652 and 0.96 inches in diameter. Two cones with base diameters of 0.625 and 1 inches served the purpose of external flameholders. The flow velocities have been varied from 50 to 300 fps. Gaseous propane, ethylene and acetylene were used with air as the oxidizer. A summary of the results of the present investigation and conclusions drawn therefrom are presented below:

1. Combustion noise is found to dominate over jet noise over the entire range of experimental variables studied.
2. Only a weak directionality of the combustion noise is observed in the present investigation. Since the same facts are reported in Ref. 16 also, one can conclude that the variations in flame retention techniques do not influence the directionality patterns of the noise radiation from open turbulent flames and that combustion noise is a monopole noise source regardless of the retention technique.
3. Acoustic power output scales like $P \propto U^{2.83} D^{2.77} S_L^{1.89} F^{-0.89}$ Ref. 16 also quotes an almost identical expression for flames stabilized at the burner tube ends. Moreover, for identical conditions the acoustic power output of the present investigations differs from that of the flames stabilized on burner tubes by a maximum factor of two only. This leads to the conclusion that although different types of flame stabilization

techniques have been used the variations in acoustic power output are not significant. However, the theoretical breakdown of the scaling laws, when compared with experiment, shows that different mechanisms are operative for the bluff body stabilized flames and the agreement may be fortuitous. It is also observed that a change in the flameholder size seems to have little influence on the acoustic power radiated.

4. A maximum value of 0.5×10^{-6} has been obtained for thermoacoustic efficiency in the present investigation.

5. Frequency spectra display the usual combustion noise spectral characteristics, having a broad-band noise with a single peak in the frequency range of 250-1500 Hz. A scaling law for peak frequency turns out to be $f_c \propto U^{0.58} D^{-1.37} S_L^{0.7} F^{-1.7}$. Here again the variations in flameholder size are found to have a minor effect on peak frequency values.

6. The present experimental investigation supports the theory developed in Ref. 8 because there is a consistency between the theoretical and experimental results. The concept that the frequency is set by the frequency of the energy containing eddies of the incoming flow appears to be valid in this configuration, as it has been in others.

REFERENCES

1. Strahle, W.C., "A Review of Combustion Generated Noise," AIAA Paper No. 73-1023, 1973.
2. Bragg, S.L., "Combustion Noise, "Journal of the Institute of Fuel, Vol. 36, No. 1, January 1963, pp, 12-16.
3. Chiu, H.H. and Summerfield, M., "Theory of Combustion Noise," Acta Astronautica, Vol. 1, Nos. 7-8, July-August 1974, pp. 967-984.
4. Strahle, W.C., "On Combustion Generated Noise," Journal of Fluid Mechanics, Vol. 49, No. 1, September 1971, pp. 339-414.
5. Strahle, W.C., "Some Results in Combustion Generated Noise," Journal of Sound and Vibration, Vol. 23, No. 1, July 1972, pp. 113-125.
6. Strahle, W.C., "Refraction, Convection and Diffusion Flame Effects in Combustion Generated $N_o$ise, " Fourteenth Symposium (International) on Combustion, The Combustion Institute, Pittsburg, 1973.
7. Strahle, W.C. and Shivashankara, B.N., "A Rational Correlation of Combustion Noise Results from Open Premixed Turbulent Flames," Fifteenth Symposium (International) on Combustion, The Combustion Institute, Pittsburg, 1975.
8. Strahle, W.C., "The Convergence of Theory and Experiment in Direct Combustion Generated Noise," AIAA Paper No. 75-522, 1975.
9. Smith, T. B.J., and Kilham, J.K., "Noise Generated by Open Turbulent Flames," The Journal of the Acoustical Society of America, Vol. 35, No. 5, May 1963, pp. 715-724.
10. Kotake, S., and Hatta, K., "On the Noise of Diffusion Flames," Bulletin of JSME, Vol. 8, No. 30, May 1965, pp. 211-219.
11. Kumar, R.N., "Further Experimental Results on the Structure and Acoustics of Turbulent Jet Flames," AIAA Paper No. 75-523, 1975.

12. Giammar, R.D., and Putnam, A.A., "Combustion Roar of Turbulent Diffusion Flames," Journal of Engineering for Power, Vol. 1, No. 1, April 1970, pp. 157-165.

13. Knott, P.R., "Noise Generated by Turbulent Non-premixed Flames," AIAA Paper No. 71-732, 1971.

14. Seebold, J.G., "Combustion Noise and its Control in Process Plant Furnaces," ASME Paper No. 71-Pet-6, 1971.

15. Giammar, R.D., and Putnam, A.A., "Combustion Roar of Premix Burners, Singly and in Pairs," Combustion and Flame,Vol. 18, No. 3, June 1972, pp. 435-438.

16. Shivashankara, B.N., Strahle, W.C., and Handley, J.C., "Combustion Noise Radiation by Open Turbulent Flames," AIAA Paper No. 73-1025, 1973.

17. Shivashankara, B.N., "An Experimental Study of Noise Radiated by Open Turbulent Flames," Ph.D. Thesis, Georgia Institute of Technology, August, 1973.

18. "Basic Considerations in the Combustion of Hydrocarbon Fuels with Air," NACA Report No. 1300, 1957.

19. Thomas, A., and Williams, G.T., "Sound Emission from Spark-ignited Bubbles of Combustion Gas," Proceedings of the Royal Society of London, Vol. A294, 1966, pp. 449-466.

Appendix C
Noise Generation in an Afterburner Compartment

An interesting question which arises as a consequence of this research is whether or not combustion noise is responsible for the chamber pressure roughness levels in combustors. In particular, the issue of afterburner pressure roughness levels is of concern here. It was proven in Ref. (2) that feedback between the flame and reflected pressure waves could be neglected if the system were highly damped. While that is not the case in an afterburner enclosure, it is believed that a lower limit to the roughness level may be computed assuming that feedback interaction are absent.

Figure A-1 summarizes the computation. The dashed line shows the spectral shape assumed for the combustion noise if the flame were burning in a free field. This shape is typical of results obtained in this program. Also, typical of results obtained, the thermoacoustic efficiency assumed for the after burner flame is 10^{-6}. These two inputs are used in the theory of Ref. (2) with the afterburner size and temperature inputs shown on Fig. A-1. Also needed are the acoustic impedances at the turbine outlet and the nozzle inlet. It is assumed that the nozzle behaves as a quasi-static nozzle with an inlet Mach number of 0.3. There is no information on the acoustic behavior of the turbine outlet, but it is clear that it will behave as a hard termination. For lack of better information, the nozzle impedance is also used as the turbine outlet impedance, since a quasi-steady nozzle behaves as a quite-hard termination.

The theory used is a plane wave theory so that results are not to be trusted above the frequency of the first transverse mode, or, in this case, above about 400 Hz. As will be seen, this does not limit the usefulness of

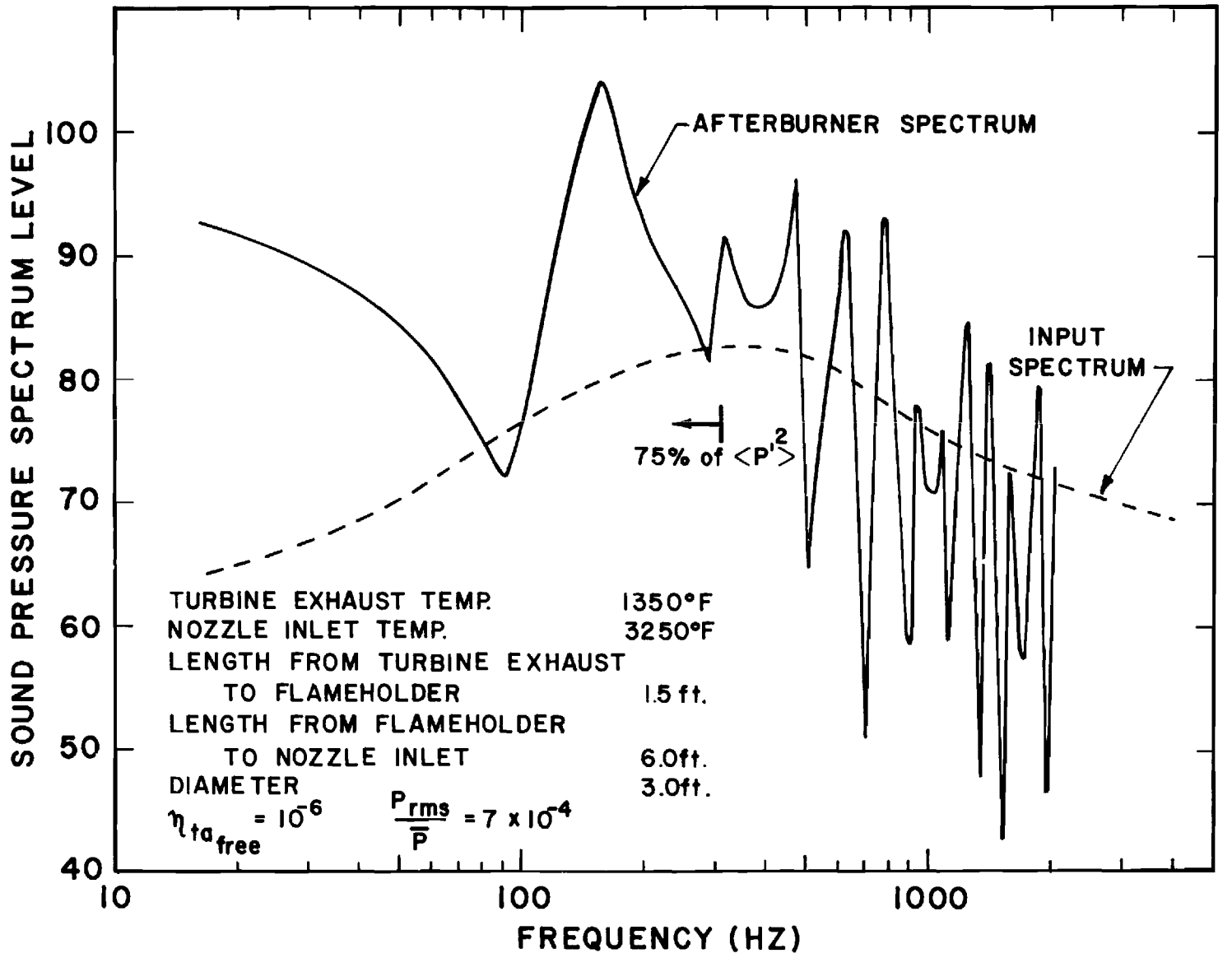

Figure C-1 Computed pressure spectrum at turbine outlet for a given set of flame noise assumptions

the computation.

The pressure spectrum which would be observed at the turbine outlet is shown as the solid line. As is shown, 75% of the area under the curve is below the frequency of the first transverse mode. This area is directly proportional to the mean square pressure so that the transverse modes do not have to be considered. The majority of the mean square pressure comes from the pumping up of the first longitudinal mode and the general augmentation of the low frequency portion of the noise. The chamber is acting as a filter and the observed pressure vs. time would look very much like an instability in the neighborhood of 150 Hz. The ratio of the root-mean-square pressure to the steady-state pressure which results from this computation is 7×10^{-4} or roughly 0.1%. This is lower than usually observed, but recall that this is a lower limit computation.

Any feedback between the pressure waves and the combustion process could augment the pressure oscillation magnitude. Furthermore, the mean square pressure result is directly proportional to the thermoacoustic efficiency which was taken somewhat low in this computation. There is also the phenomenon of entropy noise which would add to the computed pressure level. It is concluded that more work is required in this area since it appears that chamber roughness level and apparent instabilities may be caused by noise processes in some instances; however, recognition of this fact is not widespread.